University of Nottingham
UK | CHINA | MALAYSIA

Comparison of soilless and soil-based selenium biofortification methods in *Allium* genus and identification of selenium uptake genes in *Brassica* and *Arabidopsis* using associative transcriptomics

Thesis submitted to the University of Nottingham for the degree of Doctor of Philosophy.

Sahar Sheikhalivand

20151985

Supervisors: Dr Neil Graham, Dr Peter Rose

School of Bioscience, Faculty of Plant Science

University of Nottingham

Abstract

Malnutrition is a global problem underlying many of the health crises of today. Nutrient deficiency is a type of malnutrition commonly caused by undereating or an imbalanced diet. Insufficient uptake of essential nutrients can lead to a large number of health complications.

Selenium (Se) is one such nutrient, involved in antioxidant defence mechanisms via its appearance in defensive enzymes as a component of the 21 amino acid selenocysteine. These enzymes scavenge free radicals and prevent DNA and protein damage.

Se deficiency is associated with cardiovascular disease, diabetes, inflammatory disease, a decline in male fertility, a weakened immune system and many cancers. A major source of Se uptake in humans is through dietary plant consumption. Increasing Se levels in plants may thus be a useful strategy for combatting Se deficiency.

There are two ways to achieve this: the selection of crops with a greater propensity for high Se uptake and active Se biofortification. It is thus important to find genes involved in plant Se regulation and explore the best methods for plant biofortification in order to achieve an optimal outcome.

This thesis identified an *Arabidopsis Thaliana* gene (*Desi1*) involved in Se uptake and found hydroponics to be the most efficient biofortification method for Se in glasshouse plants. Extracts from Se biofortified crops were active antioxidant agents and induced cell death in HepG2 cancerous cell lines.

Future research should explore which *Desi1* alleles result in the highest levels of Se uptake and whether the high Se content in these

biofortified crops translate to higher Se levels in humans when consumed regularly.

Declaration

I declare that this is my own research and was written by myself, and that it has not been submitted for any kind of professional award or degree.

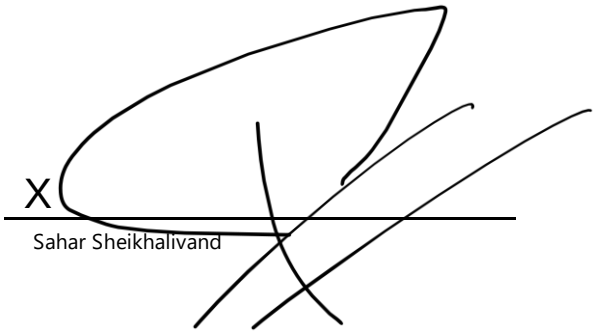

Acknowledgements

I would like to thank my supervisors Dr Neil Graham and Dr Peter Rose for the invaluable guidance and feedback during the course of my PhD. I would also like to thank Miss Lolita Wilson for her support, training and mentorship as well as all the staff at the Nutrition, Plant Science and Getaway labs. I am also very thankful to Miss Charlotte Kirk for her friendliness and support throughout my transition to the Nutrition lab.

More personally, I would like to thank my two daughters, Soutiam and Setia for their patience and encouragement, without whom I couldn't have done this without. And my mother, whose beautiful soul has now parted with this world, for the emotional support, motherly worry and faith even in her final months on this Earth.

Covid-19 Impact Statement

As the pandemic coincided with my time carrying out this research, various elements were impacted by lab closures and lockdowns. Namely, I lost one of my samples following the announcement of the first lockdown as I could not go in to collect them for analysis. I was originally planning on carrying out some experiments on potatoes, but these died due to the glasshouse shutting down for the pandemic. All three labs used were mostly closed to students (or allowed very few) during the first year of the pandemic causing some delays to my experiments.

Table of contents

List of Abbreviations

AA: Amino Acids

ABTS: 2,2′-Azino-bis(3-ethylbenzothiazoline-6-sulfonic acid)

AIDS: Acquired Immune Deficiency Syndrome

ANOVA: Analysis of Variance

APS: Ammonium Persulfate

ATP: Adenosine Triphosphate

CAT: Catalase

CV: Crystal Violet

DPPH: 2,2-Diphenyl-1-picrylhydrazyl

DW: Dry Weight

EDTA: Ethylenediaminetetraacetic Acid

GPX: Glutathione Peroxidase

HPLC: High-Performance Liquid Chromatography

ICP-MS: Inductively Coupled Plasma Mass Spectrometry

MDA: Malondialdehyde

MS: Mass Spectrometry

NIP: Nodulin 26-like Intrinsic Protein

PCR: Polymerase Chain Reaction

PMF: Proton Motive Force

ROS: Reactive Oxygen Species

RT-PCR: Reverse Transcription Polymerase Chain Reaction

SOD: Superoxide Dismutase

SULTR: Sulfate Transporter

Se: Selenium

SeNPs: Selenium Nanoparticles

SNP: Single Nucleotide Polymorphism

TCA: Trichloroacetic Acid

UV: Ultraviolet

WHO: World Health Organization

List of Figures

transporter improves SeMet translocation to the seeds. (Figure from Zhou et al., 2020).

Figure 6: According to their capacity to accumulate Se, plants are categorised as hyperaccumulators, secondary accumulators, or non-accumulators.

Figure 7: An overview of biofortification strategies that can be used to increase selenium levels in crops. Genetic tools can be used to accomplish Se biofortification (1) using conventional or aided breeding and genetic engineering, either through foliar application of Se-fertilizers (2) or soil amendment (3) the utilisation of rhizosphere or endophytic microbes, either inoculated into plants (4) or applied to soil, can be used to incorporate agronomic biofortification (5) green manure can also be made from plant material enriched with Seorganic compounds from hyperaccumulators or accumulators employed in phytoremediation, or crops cultivated in naturally enriched soils (6). SeNPs are used to accomplish nanoscale biofortification on leaves or soil (7). Se-hyperaccumulators are used in co-cropping and intercropping strategies to enrich soil with Se-organic compounds that are readily available for uptake by surrounding plants or following crops (8). (Figure from Schiavon et al., 2020)

Figure 8: Symptoms of Selenium deficiency. (Figure from iStock)

Figure 9: In the genetic code, UGA codons have two functions. (Figure from Labunskyy et al., 2014)

Figure 10: Mammalian selenium metabolism. (Figure from Kang et al., 2020).

Figure 11: An imbalance between free radicals and antioxidants leads to oxidative stress. (Figure from Ighodaro and Akinloye, 2019)

Figure 12: Selenium and carcinogenesis: cellular mechanisms (Figured adapted from Björnstedt and Fernandes, 2010).

Figure 13: It is shown that selenium is taken up and accumulated in plants. ST are Sulfur transport channels. Purples illustrated SeO4 selenate, APSe adenosine phosposelenate, PAPSe phospho adenosine phospho selenite, OASO-acetyl serine, OPHO-phospho hemoserine, DMSe dimethylselenid. Orang ones represents Metabolites. (Figure from Hariharan and Dharmaraj, 2020).

Figure 14: Human selenium intake and metabolism. SPS2 refers to selenophosphate synthase 2, tRNASec refers to tRNA for selenocysteine, EMT refers to epithelial-tomesenchymal transition. (Figure from Hariharan and Dharmaraj, 2020).

Figure 15: Selenoprotein synthesis and translational decoding. *tRNASec* refers to tRNA for selenocysteine, *SARS* refers to Seryl-tRNA sythetase, *PSTK* refers to phosphoseryl-tRNA kinase, *PSer* refers to phosphoserine, *SPS2* refers to selenophosphate synthase 2, *SeCysS* refers to selenocysteine synthase, *SeCys* refers to selenocysteine, *SBP2* refers to selenocysteine incorporation sequence binding protein 2, *SECIS* refers to selenocysteine insertion sequence, *EFsec* refers to specialized elongation factor, *HSe* is hydrogen selenide. (Figure from Hariharan and Dharmaraj, 2020).

Figure 24: Bars and Anova analysis which show effect of selenium biofortification on Iron content in the leaf and bulb of onions grown hydroponically for 77 and 140 days old (A and B respectively). Bars show Mean ± SD. n=4.

Figure 25: Bars and Anova analyse which show effect of selenium biofortification on Magnesium content in the leaf and bulb of onions grown hydroponically for 77 and 140 days old (A and B respectively). Bars show Mean ± SD. n=4.

Figure 26: Bars and ANOVA analysis which show effect of selenium biofortification on Potassium content in the leaf and bulb of onions grown hydroponically for 77 and 140 days (A and B respectively). Bars show Mean ± SD. n=4.

Figure 27: Bars and ANOVA analysis which show effect of selenium biofortification on Calcium content in the leaf and bulb of onions grown hydroponically for 77 and 140 days (A and B respectively). Bars show Mean ± SD. n=4.

Figure 28: Bars and ANOVA analysis which show effect of selenium treatments on the Se content in the leaf and bulb of two onion varieties grew hydroponically for 77 and on just bulbs for 140 days (A and B respectively). Bars show Mean ± SD. n=4

Figure 29: Bars and ANOVA analysis which show effect of selenium treatments on the S content in the leaf and bulb of two onion varieties grew hydroponically for 77 days and on just bulbs for 140 days (A and B respectively). Bars show Mean ± SD. n=4

Figure 30: Bars and ANOVA analysis which show effect of selenium treatments on the Fe content in the leaf and bulb of two onion varieties grew hydroponically for 77 and on just bulbs for 140 days (A and B respectively). Bars show Mean ± SD. n=4

Figure 31: Bars and ANOVA analysis which shows the effect of selenium treatments on the Mg content in the leaf and bulb of two onion varieties grew hydroponically for 77 and on just bulbs for 140 days (A and B respectively). Bars show Mean ± SD. n=4

Figure 32: Bars and ANOVA analysis which show the effect of selenium treatments on the K content in the leaf and bulb of two onion varieties grew hydroponically for 77 and on just bulbs for 140 days (A and B respectively). Bars show Mean ± SD. n=4

Figure 33: Bars and Anova which show effect of selenium treatments on the Ca content in the leaf and bulb of two onion varieties grew hydroponically for 77 and on just bulbs for 140 days (A and B respectively). Bars show Mean ± SD. n=4

Figure 34: Graphs showing the weights of onion bulbs over time in weeks at different concentrations of selenium treatments, for red onions and yellow onions respectively. Plotted points indicate Mn, n=4.

Figure 35: Effect of selenium treatments on the Se content of bulb of two onion varieties grew Hydroponically and stored for three months. Bars show Mean ± SD. n=4

Figure 36: Bars and ANOVA analysis which show effect of selenium treatments on Se content on bulb of two onion varieties and spring onion grown hydroponically, harvest time. Bars show Mean ± SD. n=4.

Figure 37: Bars and ANOVA analysis which show effect of selenium treatments on S content on bulb of two onion varieties and spring

onion grown hydroponically, harvest time. Bars show Mean ± SD. n=4

Figure 38: Bars and ANOVA analysis which show effect of selenium treatments on Fe content on bulb of two onion varieties and spring onion grown hydroponically, harvest time. Bars show Mean ± SD. n=4.

Figure 39: Bars and ANOVA analysis which show effect of selenium treatments on Mg content on bulb of two onion varieties and spring onion grown hydroponically, harvest time. Bars show Mean ± SD. n=4.

Figure 40: Bars and ANOVA analysis which show effect of selenium treatments on K content on bulb of two onion varieties and spring onion grown hydroponically, harvest time. Bars show Mean ± SD. n=4.

Figure 41: Bars and ANOVA analysis which show effect of selenium treatments on Ca content on bulb of two onion varieties and spring onion grown hydroponically, harvest time. Bars show Mean ± SD. n=4.

Figure 42: The spring onions were grown in pots and treated with selenium using foliar spray (yellow labels) and soil (red labels) application. (A) Early stage growing after germination. (B) Plants by transferred to the pots. (C and D) Plants were labelled depending on selenium application methods. (E) The spring onions were treated with selenium by foliar spray method in developmental phase. (F) The spring onion soak soil application method in developmental phase. (G) The plants by foliar method in last stage of growth phase. (H) The plants by soak soil application in final growth stage.

Figure 43: Spring onion plants measurements. (A, B, C) Selenium foliar spray application. (D) Harvesting. (E) Measuring width and length leaf. (F) Sample collecting. (G) Estimating leaf area.

Figure 44: Cell culture stages. (A) Culturing HepG2 cells. (B) Cancer cells as white cells after centrifuging. (C) Seeding the well plates. (D) Treatment process like dilution samples and treating the cells. (E) Looking the plates under the microscope after treatment. (F) Crystal violet viability assay.

Figure 45: Antioxidant assays. (A) Spring onion samples. (B) Sample mixed with water. (C) Mixer machine. (D) Pipetting the samples with DPPH solution. (E) Samples ready to plate reader at 517 nm in DPPH assay. (F) Samples ready to read by plate reader at 734 nm in ABTS assay.

Figure 46: Effect of selenium on the spring onion lea area (cm^2). ANOVA shows Selenium does not affect leaf area, based on the p value > 0.05. Bars indicate SD (n=30)

Figure 47: Effect of selenium on the spring onion lea length (cm). Selenium has no impact on leaf area, according to the p value > 0.05. Bars indicate SD (n=30).

Figure 48: Effect of selenium on the spring onion width (cm). According to the p value > 0.05, selenium has virtually no impact on leaf area. Bars indicate SD (n=30).

Figure 49: Effect of selenium on the spring onion Ration leaf width to length. The p value indicates that only the interaction between Se concentration and application (P = 0.002) is significant. Bars indicate SD (n=30).

Figure 50: Effect of selenium on the spring onion Ration chlorophyl. Considering the p value > 0.05, selenium has practically no effect on leaf area. Bars indicate SD (n=30).

Figure 51: Effect of selenium on the spring onion yield (kg/ha). Se concentration and application only interact significantly (P = 0.03), as indicated by the p value. Bars indicate SD (n=30).

Figure 52: Effect of selenium on uptake selenium element. Based on all p value > 0.05, the ANOVA shows Selenium has no effect on selenium content. Bars indicate Mn±SD. (n=30).

Figure 53: Effect of selenium on uptake sulfur element. In terms of ANOVA, application methods and concentration-application interaction differ significantly when P values are lower than 0.05 (0.03 and 0.003 respectively). Bars indicate Mn±SD (n=30).

Figure 54: Effect of selenium on uptake Fe element. The ANOVA demonstrates that selenium has no influence on selenium content due to all the p value > 0.05. Bars indicate Mn±SD. (n=30).

Figure 55: Effect of selenium on uptake Mg element. Based on p = 0.001 in ANOVA, application methods approach indicates significant differences. Bars indicate Mn±SD. (n=30).

Figure 56: Effect of selenium on uptake K element. As indicated by p = 0.005 in the ANOVA, significant differences are observed in the application methods approach. Bars indicate mn±SD. (n=30).

Figure 57: Effect of selenium on uptake K element. The selenium concentrations differ significantly in ANOVA with p = 0. 0001. Bars indicate mn±SD. (n=30).

Figure 58: Images of HepG2 cells. (A, B) After seeding and before treatment. (A) Control. (B) Se0 NFT with extract concentration

50mg/ml. (C) Se5 NFT with extract concentration 50 mg/ml. (D) Se50 NFT with extract concentration 50 mg/ml. Scale bar = 1000 μm.

Figure 59: Images of HepG2 cells. (A) Control. (B) Se0 Spray with extract concentration 50mg/ml. (C) Se5 Spray with extract concentration 50 mg/ml. (D) Se50 Spray with extract concentration 50mg/ml. Scale. bar = 1000 μm.

Figure 60: IC50 drug (Selenium biofortified spring onion) with Spray application method. (A) IC50 drug with Se0 concentration. (B) IC50 drug with Se5 concentration. (C) IC50 drug with Se50 concentration.

Figure 61: IC50 drug (Selenium biofortified spring onion) with Soaked soil application method. (A) IC50 drug with Se0 concentration. (B) IC50 drug with Se5 concentration. (C) IC50 drug with Se50 concentration.

Figure 62: IC50 drug (Selenium biofortified spring onion) with NFT method. (A) IC50 drug with Se0 concentration. (B) IC50 drug with Se5 concentration. (C) IC50 drug with Se50 concentration.

Figure 63: Viability% of HepG2 cells after treatment with selenium biofortified extractions. Bars indicate Mn+SD (n=12).

Figure 64: These bars show the radical scavenge% in ABTS (A) and DPPH (B) assays. For the control (0 mg/ml) these percentages are zero due to no antioxidant's activity in them (just free radicals + ethanol). In others, the results depends on the level of antioxidants and the ability to scavenge free radicals. Bars indicate mn±SD. (n=3).

Figure 65: Phases of *Arabidopsis* growth. (A) Sowing of seeds. (B) Growing phase. (C) Using an automatic irrigation system. (D) Developmental phase. (E) Flowering. (F). Harvest time.

Figure 66: GAPIT Manhattan plot. An orderly list of markers in the B. napus pan-transcriptome that are associated with Selenium accumulation in terms of their -log10P values. A Bonferroni correct significance threshold is indicated by the dashed line (Alcock et al., 2017). 'A' represents genome in B.rapa (A genome) and 'C' represents genome in B.oleracea.

Figure 67: Regress Manhattan Plot. The GEMs markers are associated with Selenium accumulation to B.napus pan-transcriptome (Alcock et al., 2017). 'A' represents genome in B.rapa (A genome) and 'C' represents genome (C genome) in B.oleracea.

Figure 68: Gel electrophoresis result: (A) Right+Left primers of AT2G35800.1 gene. (B) Right+Left primers of AT2G41170.1 gene. (C) Right+Left primers of AT3G04950.1 gene. (D) Right+Left primers of AT3G07090.1 gene. (E) Left+SALK B primers of AT3G07090.1 gene. (F) Right+SALK A primers of AT3G07090.1 gene. Each line was represented by a plant number based on the PCR results.

Figure 69: Seleium uptake in untreated *Arabidopsis* plants. An untreated selenium basis trial showed 2 homozygous lines (AT3G07090 plants 3, 7) exhibited accumulation phenotypes as gene knock out mutants compared with Colombia wild type control. Bars indicate Mn± SD. (n=3).

Figure 70: Selenium uptake in treated *Arabidopsis* plants. The selenium treated trial showed no significant differences between the homozygous line and the Colombia wildtype control in terms of accumulation phenotypes. Bars indicate Mn± SD. (n=3).

Figure 71: Elemental uptake in untreated AT3G07090 homozygous and Colombia wild type lines. The homozygous line does not differ

from the control line in terms of uptake of other elements. Bars indicate Mn± SD. (n=3).

Figure 72: Elemental uptake in untreated AT3G07090 homozygous and Colombia wild type lines. No difference was observed between the homozygous line and control in the uptake of other elements. Bars indicate Mn± SD. (n=3).

Figure 73: Elemental uptake in untreated AT2G35800 homozygous and Colombia wild type lines. No difference was observed between the homozygous line and control in the uptake of other elements. Bars indicate Mn± SD. (n=3).

Figure 74: Elemental uptake in untreated AT2G35800 wild type and Colombia wild type lines. There were no observed differences in accumulation of other elements between this line and the Colombia control. Bars indicate Mn± SD. (n=3).

Figure 75: Elemental uptake in untreated AT4G12120 homozygous and Colombia wild type lines. In terms of accumulation of other elements, we found no difference between this line and the Colombia control. Bars indicate Mn± SD. (n=3).

Figure 76: Elemental uptake in untreated AT4G12120 wild type and Colombia wild type lines. There is no difference between this line and the Colombia control in regard to the accumulation of other elements. Bars indicate Mn± SD. (n=3).

Figure 77: AT3G07090.1 loci in *Arabidopsis thaliana* in ENSEMBL PLANTS. In databases, this gene contains Exons: 5, Coding exons: 4, Transcript length: 1,054 bps, Translation length: 265 residues, and is a protein coding. (Figure from ENSEMBL Plants)

Figure 78: As the SUMO cycle proceeds, immature SUMO is first maturated by cleaving off the C-terminus with a SUMO peptidase. In a conjugation step, mature SUMOs are activated by ATP and a heterodimer of SAE1 and SAE2, then SUMOylated on the substrate with SUMO ligases where it can form polySUMO chains. To generate free SUMO, SUMO isopeptidases remove SUMO from the substrate in the deSUMOylation step (Figure from Morrell and Sadanandom, 2019).

List of Tables

Right+Left genes primers. LA: Left gene primer+SalkA primer, LB: Left gene primer+SalkB primer, RA: Right gene priemr+SalkA priemer, RB: Right gene priemer+SalkB priemer.

Table 12: A PCR analysis of the *AT3G04950.1* gene was performed to determine whether each plant was homozygous or heterozygous, and to identify the wild type representative of each plant. . LR: Right+Left genes primers. LA: Left gene primer+SalkA primer, LB: Left gene primer+SalkB primer, RA: Right gene primer+SalkA primer, RB: Right gene primer+SalkB primer.

Table 13: To identify whether each plant had a homo, hetero, or wild type line, the *AT3G07090.1* gene was evaluated by PCR analysis. . LR: Right+Left genes primers. LA: Left gene primer+SalkA primer, LB: Left gene primer+SalkB primer, RA: Right gene primer+SalkA primer, RB: Right gene primer+SalkB primer.

Table 14: Analysing the *AT4G12120.1* gene by PCR helped identify whether each plant was homozygous, heterozygous, or wild type.

Table 15: Through PCR analysis, the *AT2G41170.1* gene was evaluated for each plant to determine whether it was homo, hetero, or wild type. primer, RA: Right gene primer+SalkA primer, RB: Right gene primer+SalkB primer.

Table 16: Gene summary in the National Library of Medicine.

Table 17: Identification of SUMO proteases in yeast and *Arabidopsis*, with their known names, TAIR accession

numbers, cysteine protease classification, and tissues expressed (Table from Morrell and Sadanandom, 2019).

Table 18: A map showing the location and length of the active sites of several different SUMO proteases: the orange box represents the SIM site in ULP1, the blue oval depicts the active site for C48, the green oval represents C97, and the purple oval represents C98 (Figure from Morrell and Sadanandom, 2019).

Chapter 1: Introduction

Se was first discovered by Jöns Jacob Berzelius in 1817 while analysing sludge from a sulfuric acid chamber (Akl et al., 2006 and Watts, 1994). He initially mistook this sludge for tellurium, but with further analysis realised that it was a previously unknown element (Bodnar et al., 2012). Since this discovery, Se has contributed to various technological advancements owing to its photoconductive properties.

The most notable of these was the initial version of ‘real’ television in 1926 by an investigator named Baird. Our earliest records of television systems matching light values to electrical values date back to 1884. Here, light values were replicated by a lamp based on input from a receiver. During his training, Baird was reported to have improved the Se cell, which ultimately led to his 1926 demonstration of the electric transmission of moving pictures in half-tones (Smith-Rose, 1926). This was an incredible milestone in the development of what we know as television today.

The natural abundances of Se isotopes are as follows: 74, ~0.89%; 76, ~9.37%; 77, ~7.63%; 78, ~23.77%; 80, ~49.61%; 82, ~8.73%. Thus, isotopes 80 and 78 are the most common, with their abundances being approximately 50% and 24%, respectively. Se is a semimetal belonging to the chalcogen family (group 16). It sits between sulfur and tellurium in that column of the periodic table, and thus shares many properties with them, explaining Jöns Jacob Berzelius’ initial mistake. In nature, however, Se rarely exists as a pure element and usually appears only in minerals (Boyd, 2011).

Moreover, Se appears in both organic and inorganic forms in plants (Bodnar et al., 2012) and is an important component of a wide range of biomolecules essential to humans and animals, including selenoproteins and glutathione peroxidase (GPX) (Tinggi, 2003).

1.1 Selenium in Plants

Although selenium is not considered an essential element for plants, it has been found to be beneficial (Figure 1) in plants at moderate levels (Combs, 2001; Joy, 2014; Fairweather – Tait et al, 2011; Stoffaneller, 2015).

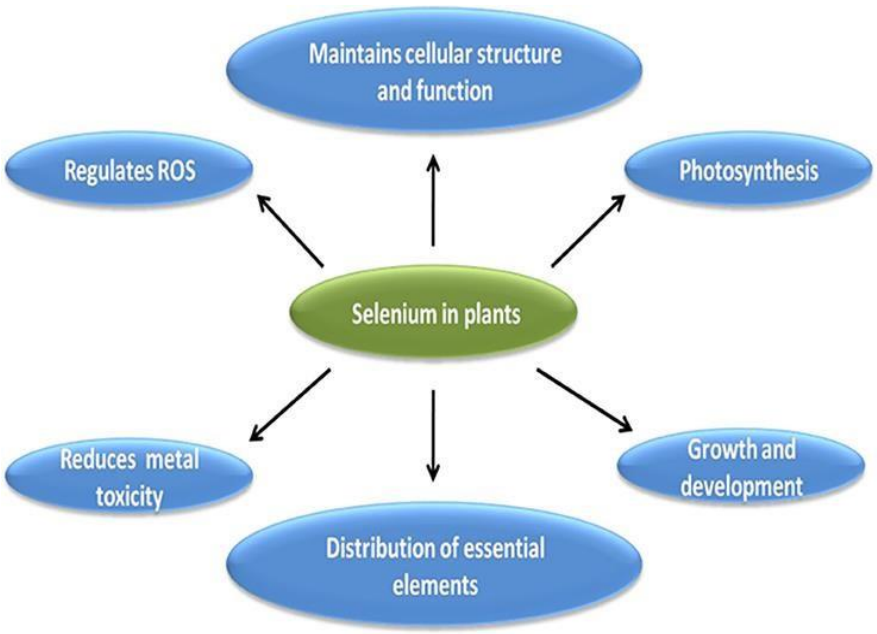

Figure 1: Plant benefits associated with selenium. *Figure from Gupta, 2017*

Several studies have demonstrated the beneficial effects of Se in protecting plants against reactive oxygen species (ROS). These protective mechanisms reduce oxidative stress on chloroplasts, contribute to plant defence against abiotic stress (e.g. cold,

drought, desiccation and metal toxicity), and also protect against biotic stress, including fungal disease and phloem-eating pests like caterpillars and aphids (Hansen et al., 2004; Rouached, 2013; Seppänen et al., 2003; Hartikainene and Xue, 1999; Chuet at al., 2010; Pukacka et al., 2011; Kumal et al., 2012; Pandey and Kupta, 2015; Hasanuzzaman and Fujita, 2012).

Plants generate ROS when under stress. ROS can be harmful to the plants, disturbing cell membranes and cellular proteins and resulting in cell death when produced in excess. However, they are also an integral part of plant defence systems against other stressors, such as aluminium (Al). Thus, ROS must be carefully regulated, produced in sufficient quantities to counter stressors, whilst appropriately neutralised to prevent self-inflicted harm to the plant.

Cartes el all. (2010) demonstrated a reduction in Al toxicity in rye grass by converting the superoxide radical to hydrogen peroxide (H2O2). This led to the accumulation of H2O2 in the shoots and leaves of ryegrass, coincidentally the tissues with higher metabolic activity and photosynthetic and respiratory burden – both contributors to increased ROS production. These tissues sit above the ground and are thus exposed to greater levels of environmental stress, leading to increased ROS production and robust antioxidant defences which can detoxify these ROS. Shoots and leaves are therefore well-adapted for ROS regulation to allow for the management of local stressors, making them good sites for systemic oxidative stress responses as well.

It would follow that above-ground tissues are generally sites of increased antioxidant defence, including increased levels of

antioxidant Se species, and thus sites for systemic stress responses. However, as noted by Zayed et al. (1998), there are exceptions to this general trend, depending on the plant species, Se form, and environmental conditions, which can influence the distribution and accumulation of Se within the plant.

1.2 Selenium intake and metabolism in plants

The amount of Se in soil is influenced by a variety of factors, including the geological parent material. Sandy soils are known to have lower Se content than organic and calcareous soils (Kabata – Pedias, 2011; El – Ramady et al., 2014). Se can be found in a variety of oxidation states, including selenate (Se^{6+}), selenite(Se^{4+}), elemental selenium (Se^{0}), and selenide (Se^{2-}). Plant roots may take up selenite, selenite compounds, and organoselenium compounds like selenocysteine (Secys) and selenomethionine (SeMet), but not colloidal Se or metal selenides (White et al., 2004).

Aside from clay and organic matter control, there are a few more aspects to consider. The state of Se and its availability for uptake also depends on the pH and redox potential of the soil (Eh) (El – Ramady et al., 2014). Selenate and selenite (Figure 2) are the most common inorganic Se forms found in natural soils. In alkaline soils, selenate is more mobile than selenite, which is found in neutral or acidic soils and is easily absorbed by oxyhydroxides (Kabata – Pendias, 2011). Plant species, stages of growth, form and concentration of Se, physiological circumstances (salinity and soil pH), presence of other chemicals, activity of membrane transporters, and plant translocation mechanisms all influence Se uptake, translocation,

and distribution (Zhao and Mc Grath, 2009; Li et al., 2010; Renkema et al., 2012).

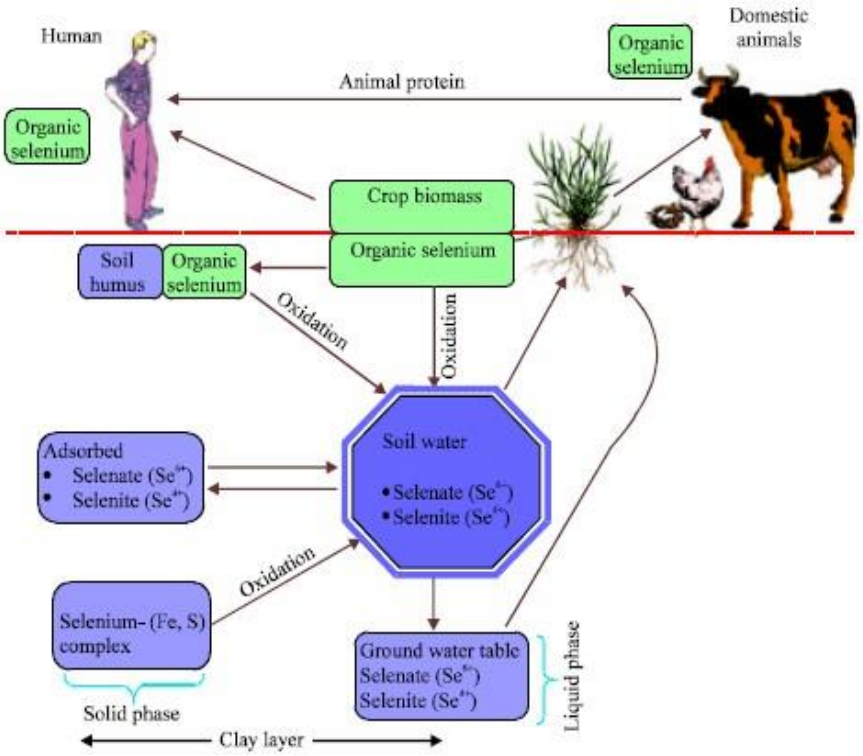

Figure 2: Soil-plant-water consumption of selenium. Se from soil water is absorbed by plant roots in selenate or selenite form. Based on the solubility of each Se form and the biological conversion of organic forms, Se concentration in soil solutions depends on both. (Figure from Burau, 1985).

The acquisition of mineral nutrients is mechanistically linked to the accumulation of Se by roots. Because selenium is not considered to be a vital nutrient in non-accumulators, isolated mechanisms for its accumulation or metabolism seem unlikely to exist in these species. As a result, the root systems foraging for mineral nutrients like N, P, K, and S, as well as how they respond to the availability or shortage of these nutrients, may

have an impact on Se uptake. The length of roots, their effective diameter (including root hairs), and their rate of growth, for example, are all factors that influence nutrient uptake (Clarkson, 1985; Yanai, 1994). A phosphate deficit that lowers any of these factors would also lower Se intake. Furthermore, as a result of this deficit, the rhizosphere may become acidic, or roots may release ligands, increasing the availability of selenite in the soil solution (Clarkson, 1985).

Selenium has chemical characteristics comparable to sulfur; it is taken up by plants via sulphate transporters and is also absorbed via the same routes (Soumen et al., 2013). High affinity sulphate transporters convey selenate throughout the plasma membrane of root cells, whereas phosphate transporters are considered to transport selenite (Terry et al., 2000; White et al., 2004; Soumen et al., 2006; Broadley et al., 2006; Hawkesford and Zhao, 2007; Li et al., 2010). Inducible sulphate transporters demonstrated better selectivity for sulphate over selenate than constitutive active sulphate transporters when external sulphate concentrations were high (White et al., 2004). Sulfate transporters SULTR1, 2 and SULTR1 were discovered to transport selenate inside *Arabidopsis thaliana* (El Kassis et al., 2007).

Selenate is primarily transported into chloroplasts, where sulfur assimilation occurs to process it after uptake (Leustek, 2002; Leustek et al., 2000). ATP sulfurylase is expected to activate Se by generating adenosine 5-phosphoselenate (Apse) (Shaw and Anderson, 1972; Shaw and Anderson, 1999). It has been shown that overexpression of ATP sulfurylase in Indian mustard *(Brassica juncea*) activates selenate to Apse, a rate-limiting step for selenate uptake in plants (Pilon – Smits et al., 1999). This

conclusion supports prior research that found the rate-limiting step in the production of organic Se compounds in Indian mustard is the conversion of SeO_4^{-2} to SeO_3^{-2} (De Souza et al., 1998). Bound Apse is nonenzymatically converted to selenite in the presence of glutathione *in vitro* (Dilworht and Bandurski, 1977). However, in *Escherichia coli*, 3-phosphoadenosine 5-phosphosulfate (PAPS) reductase is certainly required for Apse reduction (Muller et al., 1997). In plants, selenate is most likely converted to APSe by ATP sulfurylase and then reduced to selenite by adenosine 5-phosphosulfate (APS) reductase.

There is substantial evidence that glutathione reduces selenate to selenite non-enzymatically once it is reduced by selenite (Ng and Anderson, 1978). The synthesis of selenocysteine (from OAS) and selenite in glutathione and NADPH has only been observed by Ng and Anderson (1978). Selenocysteine can be synthesised by cysteine synthase when S is replaced with Se, leading Ng and Anderson to believe that the non-enzymatic reduction of selenite by glutathione was the only source of selenide in this experiment (Ng and Anderson, 1978). Because of the non-enzymatic mechanism for reducing selenite to selenide, selenite is more readily absorbed by plants than selenate. Seleno amino acids, such as selenocysteine and selenomethionine, are produced when selenite is reduced. Se toxicity is caused by the non-specific incorporation of seleno amino acids into proteins (De souza et al., 1998; Brown and Shrift, 1981).

Selenomethionine can be methylated and transformed to dimethyl selenide (DMSe). It is then volatilized after being generated by the methionine biosynthetic pathway (Brown and

Shrift, 1981). The methylation of selenomethionine is the initial step in the production of dimethyl selenide. Methionine S-methyl transferase catalyses this process. The methylation of selenomethionine is the initial step in the production of dimethyl selenide. Methionine S-methyl transferase catalyses this process. Se volatilisation is considerably reduced when this enzyme's expression is suppressed in *A. thaliana* (Tagmount et al., 2002).

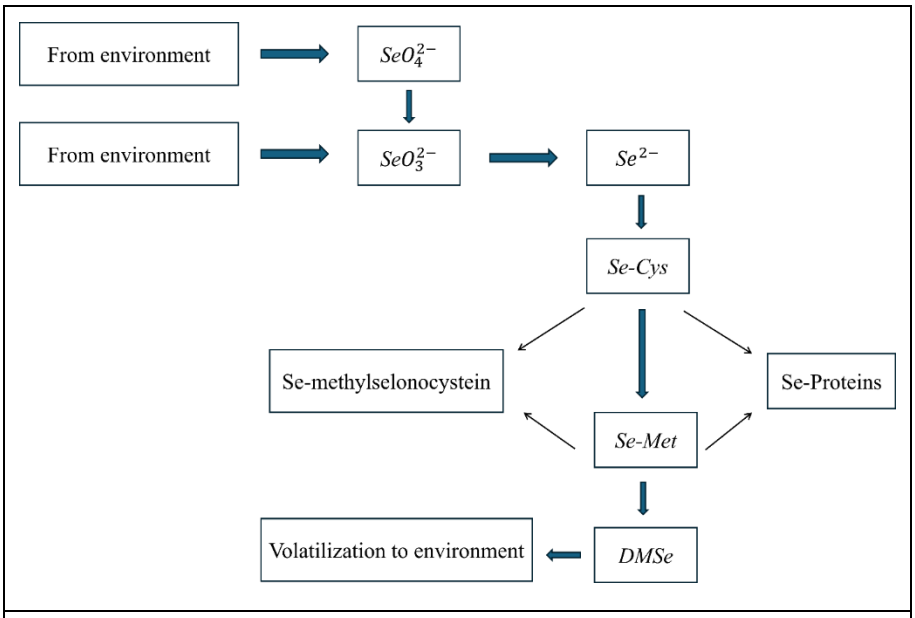

Figure 3: The main steps in the metabolism of Se in plants. (Figure recreated from Dumont et al., 2006).

The volatilization of DMSe is restored when methylselenomethionine is added to the growth medium (Figure 3). S-methylmethionine hydrolase, which normally converts Smethylmethionine (SMM) to DMS, is thought to be involved in the conversion of SeMM to DMSe (Mudd and Datko, 1990). DMSe can also be formed in the chloroplast by converting SeMM to dimethylselenoiopropionate (DMSeP) (De Souza et al., 2000). SMM provided only two enzymes: a transaminase

and a decarboxyl sulfonipropionate (DMSP) decarboxylase. These enzymes are most likely also involved in the conversion of SeMM to DMSeP (Kocsis et al., 1998). The conversion of DMSP and DMSeP to DMS and DMSe, respectively, is thought to be carried out by DMSPlyase. Plants, on the other hand, have yet to be found with DMSPlyase. DMSe volatilisation was much higher in DMSe-supplied Indian mustard plants than in selenomethionine-supplied plants, indicating that DMSeP can be converted to DMSe in plant shoots. In plants, both routes for the formation of DMS/DMSe may present (De Souza et al., 2000) (Figure 4, 5).

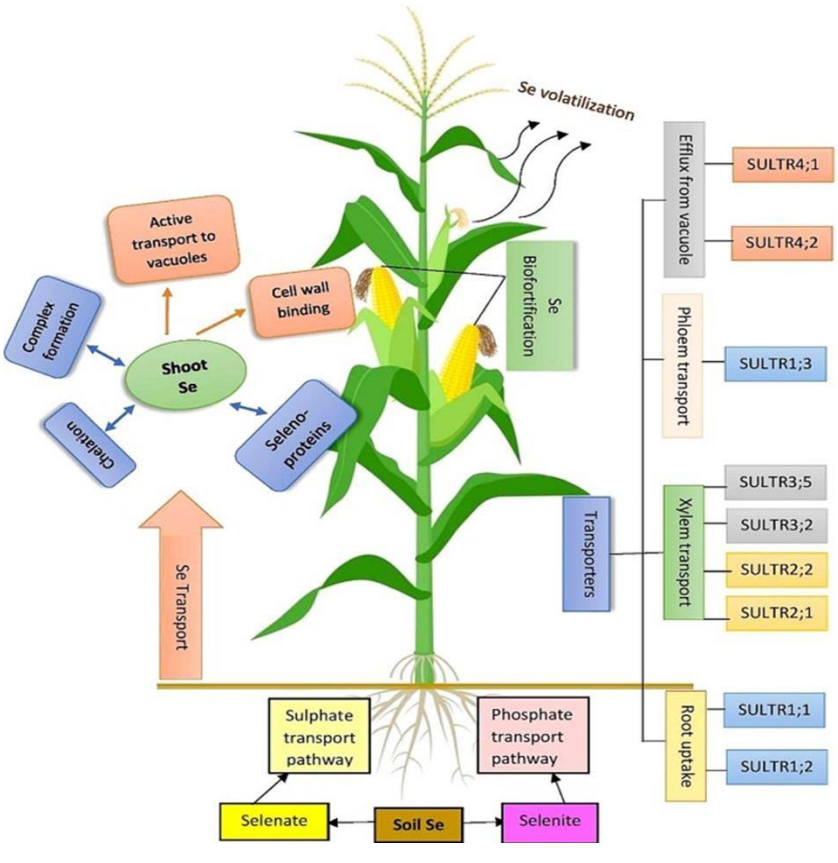

Figure 4: A potential method by which Se (selenium) may be absorbed, translocated, and assimilates in food crops, in which SULTR1;1,

SULTR1;2, SULTR1;3, SULTR2;1, SULTR2;2, SULTR3;2, SULTR3;5, SULTR4;1, and SULTR4;2 could be utilised as sulfur transporters for Se (selenium) uptake. (Figure from Sarwar et al., 2020).

Figure 4 provides an overview of various strategies for biofortifying grains with Se, an essential micronutrient for humans. Biofortification involves increasing the nutrient content of crops through agronomic practices, breeding, or genetic engineering. One approach is genetic biofortification, which involves breeding or genetically modifying plants to enhance their Se content. Another method includes Se foliar fertilization, where Se-containing fertilizers are applied directly to the leaves to improve uptake. Additionally, incorporating inorganic Se compounds into the soil through fertilizers can enhance its availability to plants.

Microbial inoculation plays a significant role in this process, as beneficial microorganisms in the soil can convert inorganic Se into plant-available forms. Furthermore, microbial activity can lead to the production of Se nanoparticles (SeNPs) and organic Se compounds, which plants can absorb more efficiently. The addition of organic Se-rich plant material, such as green manure, to the soil also contributes to improved Se availability. Se nanoparticles can be applied directly through foliar fertilization or soil irrigation to enhance plant uptake.

Intercropping or co-cropping with other plant species can also improve Se absorption in certain crops. Some plants, known as Se-hyperaccumulators, naturally take up high levels of Se, and they can contribute to the biofortification of other crops through natural processes. Additionally, crops grown in Se-rich soils can undergo natural biofortification, increasing their Se content. Se-hyperaccumulators can also be used in soil phytoremediation, helping to remove contaminants from the soil. However, it is essential to

assess the presence of other harmful substances before utilizing this approach.

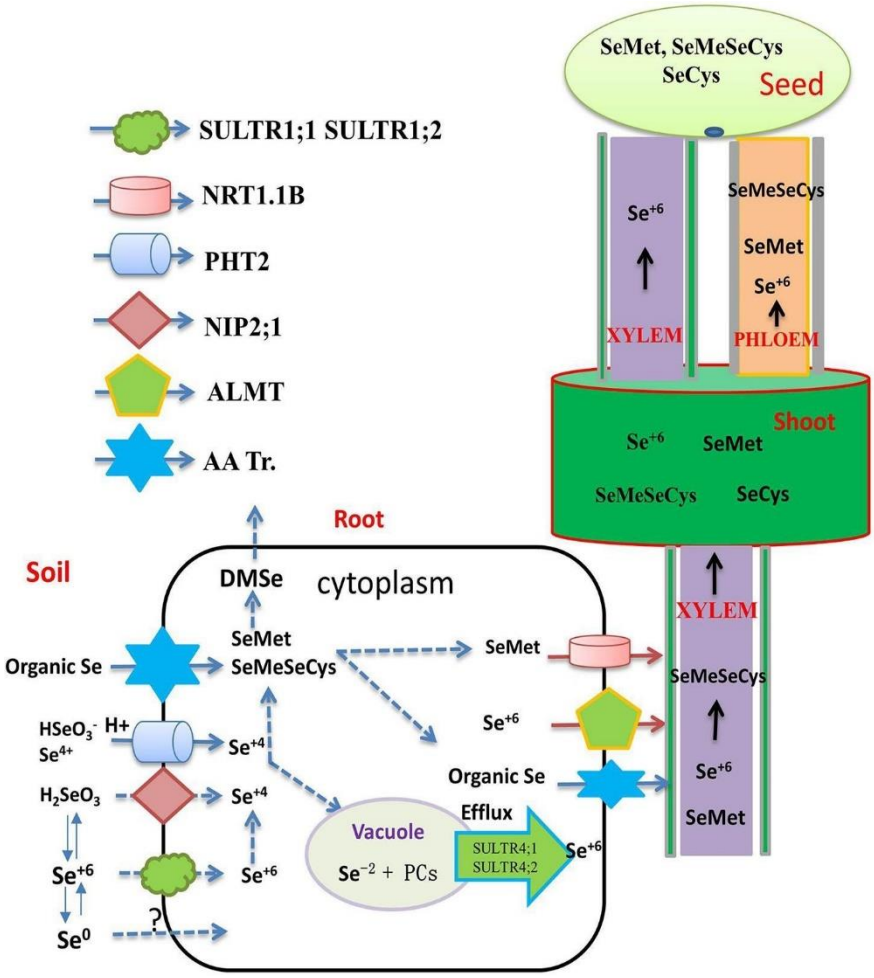

Figure 5: Schematic diagram showing the transporters responsible for bringing selenium into the grain through xylem and phloem. SULTR1; 1, SULTR1;2 for selenate, NIP2;1, PT2 and PT8 for selenite, AA Tr. for amino acids) are the primary transporters involved in inorganic Se uptake by plants. Amino acid permeases (AA Tr.) transfer organic Se forms into the xylem, where they are supplied to the shoots. The primary Se species found in the xylem is selenium, which is loaded into the xylem via SULTR2;1. Organic-Se compounds are carried into the seed by the phloem, whereas selenate is carried by both the xylem and the phloem. Overexpression of the NRT1;1B transporter improves SeMet translocation to the seeds. (Figure from Zhou et al., 2020).

1.3 Selenium Accumulation in Plants

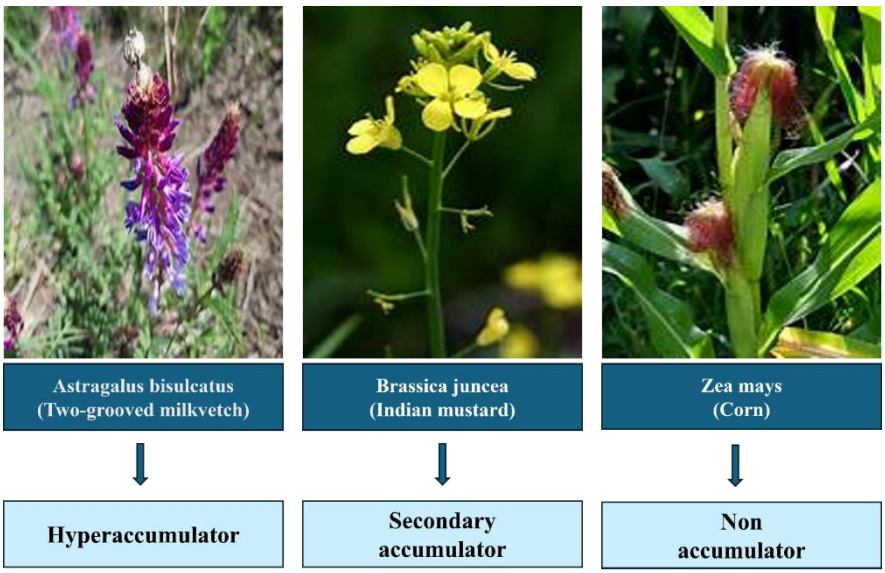

Figure 6: According to their capacity to accumulate Se, plants are categorised as hyperaccumulators, secondary accumulators, or non-accumulators.

Certain vegetables, particularly garlic (*Allium sativum*) and onion (*Allium cepa*), have been shown to accumulate higher levels of Se while also containing high concentrations of sulfur and its derivatives in their tissues (Ellis & Salt, 2003). Based on their ability to accumulate Se, plants are classified into three categories: hyperaccumulators (>1000 mg Se/kg DW), secondary accumulators (100-1000 mg Se/kg DW), and non-accumulators (<100 mg Se/kg DW) (Galeas et al., 2007; Bodnar et al., 2012).

Hyperaccumulators can absorb and concentrate exceptionally high levels of Se in their tissues, often thousands of times

more than other plants. An example of a hyperaccumulator is *Astragalus bisulcatus* (two-grooved milkvetch) (Figure 6), which can accumulate Se in its leaves at concentrations as high as 0.5–1% of its dry weight (Banuelos & Meek, 1990). These plants typically grow in Se-rich soils, often in regions with seleniferous shale (White & Broadley, 2009). Hyperaccumulators have practical applications in remediating Se-contaminated soils and are also studied for their potential role in biogeochemical prospecting (Banuelos & Meek, 1990).

Secondary accumulators, in contrast, absorb Se at higher levels than normal plants but do not reach the concentrations observed in hyperaccumulators (Terry et al., 2000). *Brassica juncea* (Indian mustard) (Figure 6) is an example of a secondary accumulator, as it can tolerate and accumulate moderate levels of Se (Pilon-Smits & Quinn, 2010). This characteristic makes secondary accumulators useful for phytoremediation in areas with moderate Se contamination, where they help reduce Se dispersion and prevent its entry into the food chain (Terry et al., 2000).

Non-accumulators, on the other hand, absorb only minimal amounts of Se and do not store significant levels in their tissues (Galeas et al., 2007). For instance, *Zea mays* (corn) (Figure 6) is typically non-tolerant to high selenium concentrations in soil and accumulates only trace amounts (Dhillon & Dhillon, 2003). Due to this characteristic, non-accumulators pose a smaller risk of Se accumulation in crops, regardless of soil type and its natural Se content, making them widely cultivated in agriculture (Galeas et al., 2007).

The variation in Se accumulation across different plant species is influenced by genetic factors, soil composition, and selective breeding practices (White et al., 2007). Non-accumulator plants generally exhibit lower Se levels due to evolutionary and selective pressures that favour other traits over Se accumulation (Zhu et al., 2014). Some plant species may have evolved to avoid the potential toxicity of Se, while others allocate resources to traits that enhance survival and reproduction in specific environments (White et al., 2007). Selective breeding has further influenced Se accumulation, as agricultural practices often prioritize crop yield and disease resistance over nutrient enrichment, leading to reduced Se content in certain cultivars (Zhu et al., 2014).

Genotypic differences also play a critical role in Se accumulation, as some plant genotypes exhibit greater efficiency in absorbing and incorporating Se from soil (Terry et al., 2000). Similar trends have been observed with sulfur accumulation, where genetic variation influences sulfur uptake and distribution, ultimately affecting plant growth and nutrient quality (Hawkesford & De Kok, 2006). Studies on sulfur metabolism have revealed that different plant genotypes display varying capacities to accumulate and utilize sulfur due to both genetic and environmental factors (Schnug & Silva, 1991). Although research on genotype-specific differences in Se accumulation remains limited, parallels with sulfur studies suggest that genetic variation significantly impacts Se uptake and distribution in plants (Zhao et al., 2002).

1.4 Biofortification

The term 'biofortification' refers to the process of increasing the levels of specific nutrients, such as Se, in agricultural food by plant breeding, genetic engineering, and agronomic methods (Rouached, 2013). Biofortified agricultural products have been presented as a possible functional agricultural technique for increasing human dietary nutrient intake (Banuelos and Lin, 2009; Zhu et al., 2009; Kieliszek and Blazejak, 2013; Borill et al., 2014) and have been successfully used to enhance intake of a number of elements. Se biofortification significantly enhances the Se content of agricultural food products and may aid in the relief of Se deficiency, which affects more than one billion people worldwide (WHO, 2009).

Researchers from all over the world are working to develop Se-enriched food products in order to reduce the number of people who suffer from illnesses associated with Se deficiency. The production of amino acids, proteins, and phenolic substances are also influenced by Se fertilisation. The nutritional content of food products can be improved by the biofortification of crops and animal feeding, which may assist to alleviate malnourishment (Schiavon et al., 2013; Dinkova – Kostova, 2013).

In many places, plants are the most plentiful source of Se, followed by meat and seafood. To ameliorate Se deficiency-induced human illnesses, it is necessary to increase Se uptake by plants and, as a result, Se concentration in the human diet. Se biofortification is the most efficient way of increasing Se levels in agriculture. As a result of soil application of Se fertilizers, edible part of plants do not become enriched with Se, and long-term use of Se fertilizers can be toxic to nearby environments, so use of Se

fertilizers should be done with caution (Winkel et al., 2015). The use of organic acids (Morgan et al., 2005; Lynch, 2007), organic forms of Se (Schiavon et al., 2013; Pezzarossa et al., 2014), or microbes (Duran et al., 2013, 2014) that increase the possibilities of Se availability to plants can improve the efficiency of Se fertilisers for Se-biofortification strategies. A useful technique for obtaining Se-biofortified food products is genetic engineering, which focuses on manipulating Se-related enzymes for Se absorption, assimilation, and volatilization (Figure 7).

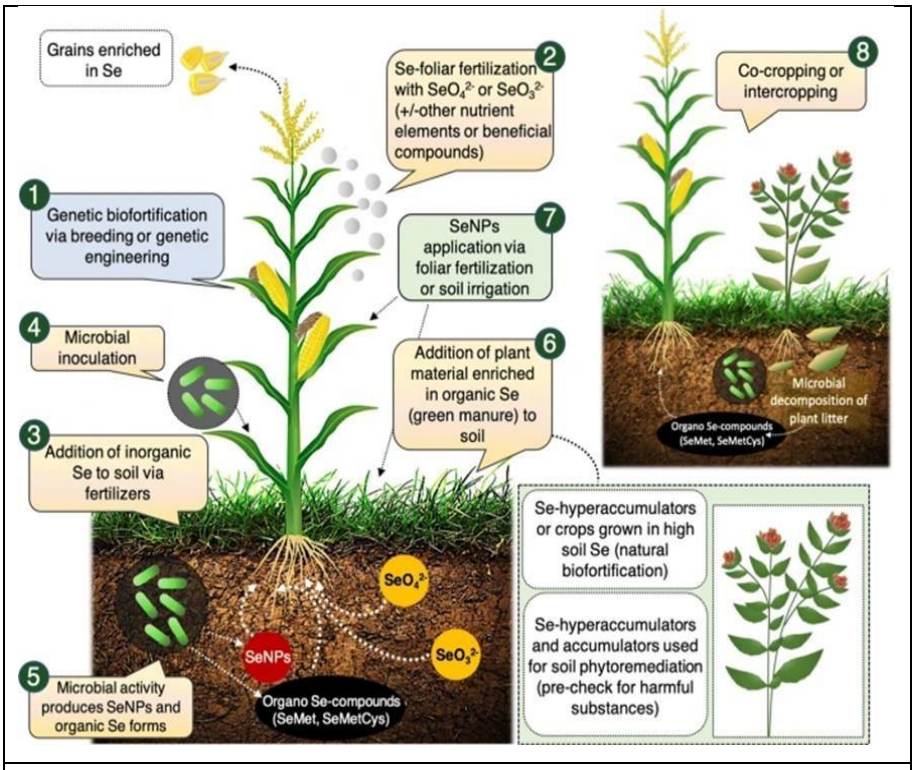

Figure 7: An overview of biofortification strategies that can be used to increase selenium levels in crops. Genetic tools can be used to accomplish Se biofortification (1) using conventional or aided breeding and genetic engineering, either through foliar application of Se-fertilizers (2) or soil amendment (3) the utilisation of rhizosphere or endophytic microbes, either inoculated into plants (4) or applied to soil, can be used to incorporate agronomic biofortification (5) green manure can also be made from plant material enriched with Seorganic compounds from hyperaccumulators or accumulators employed in phytoremediation, or crops cultivated in naturally enriched soils (6). SeNPs are used to

accomplish nanoscale biofortification on leaves or soil (7). Se-hyperaccumulators are used in co-cropping and intercropping strategies to enrich soil with Se-organic compounds that are readily available for uptake by surrounding plants or following crops (8). (Figure from Schiavon et al., 2020)

Biofortification methods include genetic modification (GM) or, more specifically, genetic engineering (GE). GM includes any and all means of altering the genetic makeup of an organism, whereas GE refers to the direct introduction/removal of or silencing/overexpressing genes. GE has been successfully applied to improve the content of essential elements beyond just vitamins and minerals. One prominent example is iron biofortification, particularly in rice, where researchers have genetically engineered rice varieties to produce higher levels of iron by introducing genes involved in iron metabolism from other plants (Yoshida et al., 2014). These genetically modified rice varieties have been shown to significantly increase iron content and improve iron absorption in human populations that rely on rice as a staple food (Zhang et al., 2021).

Another successful application of biofortification is zinc enhancement in wheat and maize, where scientists have utilized genetic engineering to increase the expression of zinc transporter proteins, thereby improving the crop's ability to accumulate zinc (Cakmak et al., 2010). Field trials and human consumption studies have demonstrated that these biofortified crops can provide higher levels of zinc, potentially reducing zinc deficiency in vulnerable populations (Bouis et al., 2011).

Calcium biofortification has also been explored, with researchers genetically modifying crops such as lettuce and other leafy greens to enhance calcium levels (Penney et al., 2012). This method typically involves introducing or overexpressing genes associated with calcium uptake and accumulation, and studies have shown that these modifications can effectively increase calcium content and improve its bioavailability in the human diet (Penney et al., 2012).

Se biofortification has similarly been pursued through genetic engineering, particularly in crops like wheat and rice, where researchers have introduced genes from yeast and other organisms to enhance Se uptake and incorporation into plant tissues (White et al., 2004). Studies indicate that these Se-enriched crops can contribute to addressing selenium deficiencies in populations where dietary intake is insufficient (Bonifacio et al., 2018).

These biofortification strategies hold significant promise in addressing global nutritional deficiencies and improving public health. However, their success depends not only on the effectiveness of genetic modifications but also on regulatory considerations and public acceptance in different regions (White et al., 2004).

1.5 Selenium and human health

Se plays a crucial role in human health, serving as an essential nutrient in preventing the progression of HIV to AIDS (Kabata-Pendias & Mukherjee, 2007). Additionally, Se functions as an

antioxidant and plays a stimulatory role in the production of thyroid hormones and their bioavailability, for example through the conversion of inactive thyroid hormone (T4) to active thyroid hormone (T3) at target organs by the selenoenzyme type 2 iodothyronine deiodinase (DOI2) (Kohrle, J et al. 2005). Thyroid hormones are vital for metabolic regulation, especially the basic metabolic rate, with excess and deficiency both resulting in illness (Kabata-Pendias & Mukherjee, 2007). Se is also integral to immune system function and is associated with fertility, cardiovascular health, diabetes, and inflammatory diseases, while supranutritional Se intake has been linked to a reduced risk of cancer (Kabata-Pendias & Mukherjee, 2007).

Se deficiency represents a significant global health concern due to its essential function in antioxidant defense mechanisms and thyroid hormone metabolism (Rayman, 2008). The primary treatment for Se deficiency involves oral supplementation with selenomethionine or sodium selenite, both of which are effective in restoring adequate Se levels and alleviating symptoms related to deficiency (Gupta et al., 2016). In addition to supplementation, biofortification strategies, including the incorporation of Se into staple crops such as rice and wheat, are increasingly being explored as a sustainable approach to improve dietary Se intake at the population level (White & Broadley, 2009). These interventions aim to enhance Se status in vulnerable populations and mitigate associated health risks, including cardiovascular diseases and impaired immune function (Thomson, 2004).

Unlike other micronutrients, Se intake varies considerably worldwide, with levels ranging from deficiency-associated disease to toxic effects such as garlic breath, hair loss, nerve damage, dental

issues, and paralysis (Johnson et al., 2010). The recommended daily Se intake for adults is 55 μg, as established by the Institute of Medicine (2000). Se in the human diet primarily originates from plants, and inadequate Se content or poor phytoavailability in plants contributes to Se deficiency in food sources (Broadley et al., 2006). Several factors, including soil Se levels, pH, organic matter content, and the ability of Se to form complexes with ions, influence Se' bioavailability in the food chain (Johnson et al., 2010). The primary dietary sources of Se include organic forms such as selenite and selenate, as well as inorganic forms such as selenomethionine (SeMet) and selenocysteine (SeC) (Hill et al., 1991). At present, Se deficiency is relatively common and a pressing nutritional concern (Combs, 2001; Joy et al., 2014; Fairweather-Tait et al., 2011; Surai, 1999).

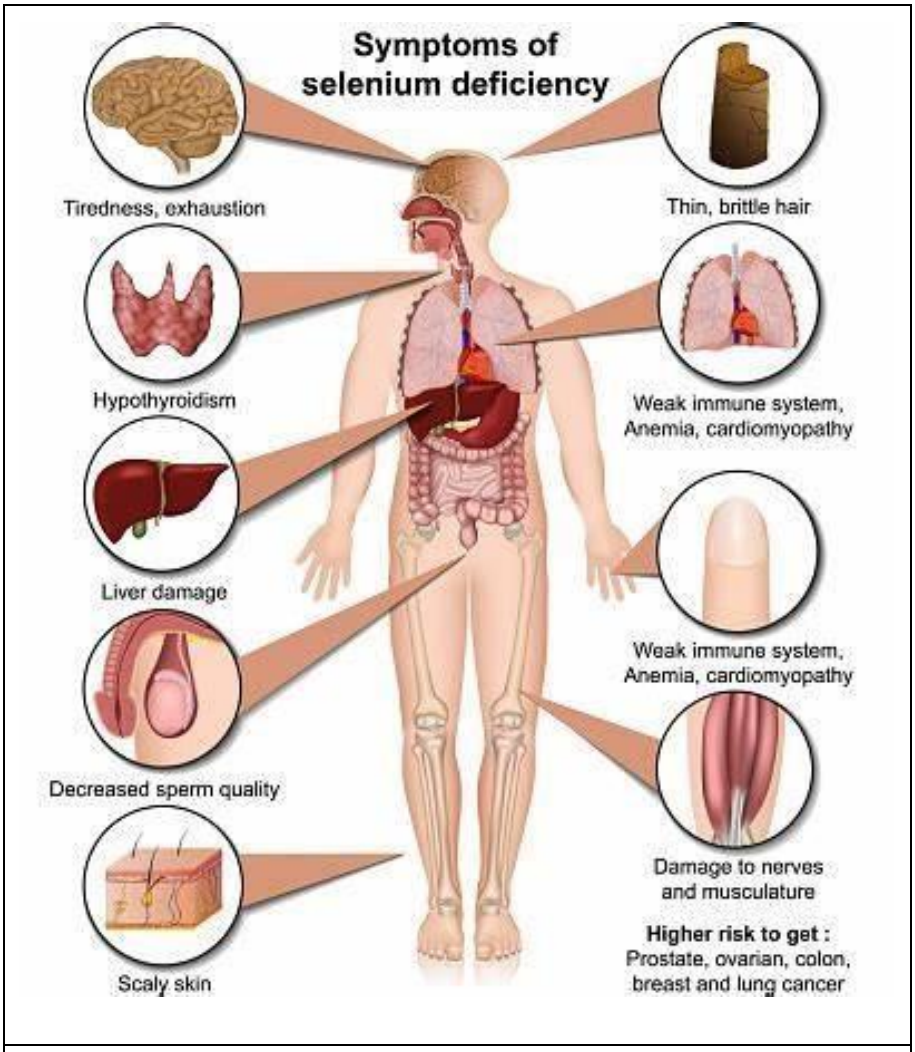

Figure 8: Symptoms of Selenium deficiency. (Figure from iStock)

1.6 Human metabolism of selenium

Since the discovery that selenium is incorporated into proteins as selenocysteine, which is encoded by the codon UAG (Figure 9), research into selenium's physiological roles and health benefits has advanced significantly. This essential nutrient plays a crucial role in immune system function, fertility, cardiovascular health, diabetes management, inflammatory diseases, and cancer prevention. The health benefits of selenium are largely attributed to its role in

selenoproteins, where selenocysteine (Sec), the 21st amino acid in the genetic code, is integral. Since the identification of Sec, our understanding of selenium's integration into selenoproteins has greatly improved. Moreover, the identities of selenoproteins that constitute the human selenoproteome—comprising of 25 genes which encode selenoproteins—have been elucidated (Labunskyy et al., 2014).

Selenocysteine, often referred to as the 21st amino acid, is crucial for human health due to its role in selenoproteins, which are essential for various biological processes (Gladyshev, 2007). It is a key component of several important antioxidant enzymes, such as glutathione peroxidases, which protect cells from oxidative damage (Combs, 2001). Additionally, selenocysteine plays a critical role in thyroid hormone metabolism by participating in the activity of deiodinases, which convert thyroid hormones to their active forms (Rayman, 2012). The incorporation of selenocysteine into selenoproteins is necessary for proper immune function and may influence inflammation and cancer prevention (Labunskyy et al., 2014). Understanding the function of selenocysteine enhances our knowledge of selenium's impact on health and disease, emphasizing its importance in maintaining overall physiological balance (Zhang et al., 2016).

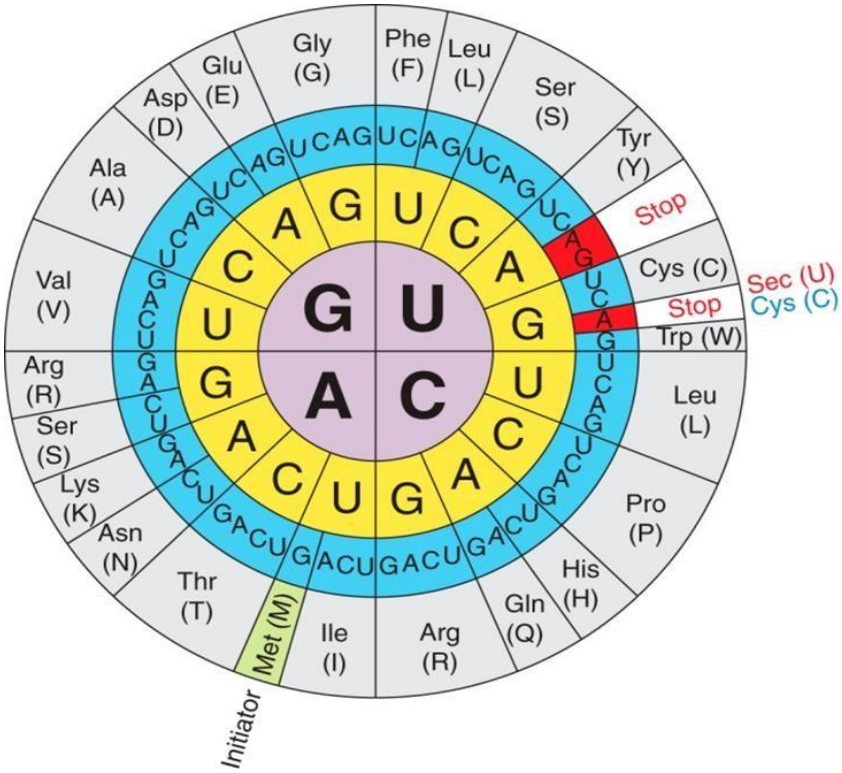

Figure 9: In the genetic code, UGA codons have two functions. (Figure from Labunskyy et al., 2014)

Selenoproteins are produced by the selenium metabolic system. Glutathione (GSH) and thioredoxin (TXN) systems convert ingested inorganic selenium to hydrogen selenide (H2Se). Selenide is then transformed to Sec amino acids, which are then incorporated into specified places of selenoproteins, such as a selenoenzyme's catalytic sites. Selenophosphate synthase2 (SEPHS2) is a catalytic enzyme that catalyses the formation of selenophosphate by reducing hydrogen selenite. Sec-$tRNA^{[ser]Sec}$ is produced by reacting phosphoseryl-tRNA (Pser-$tRNA^{[ser]Sec}$) with Sec. The machinery that uses the UGA codon incorporates Sec amino acids into polypeptide chains. Selenocysteine insertion

sequence binding protein 2 (SBP2) binds to the SECIS element in the 3untranslated region (3UTR) of selenoprotein mRNA and enables the transfer of Sec-$tRNA^{[ser]Sec}$ to the A-site of the ribosome, which identifies the UGA codon as the Sec incorporation codon (Figure 10) (Kang et al., 2020).

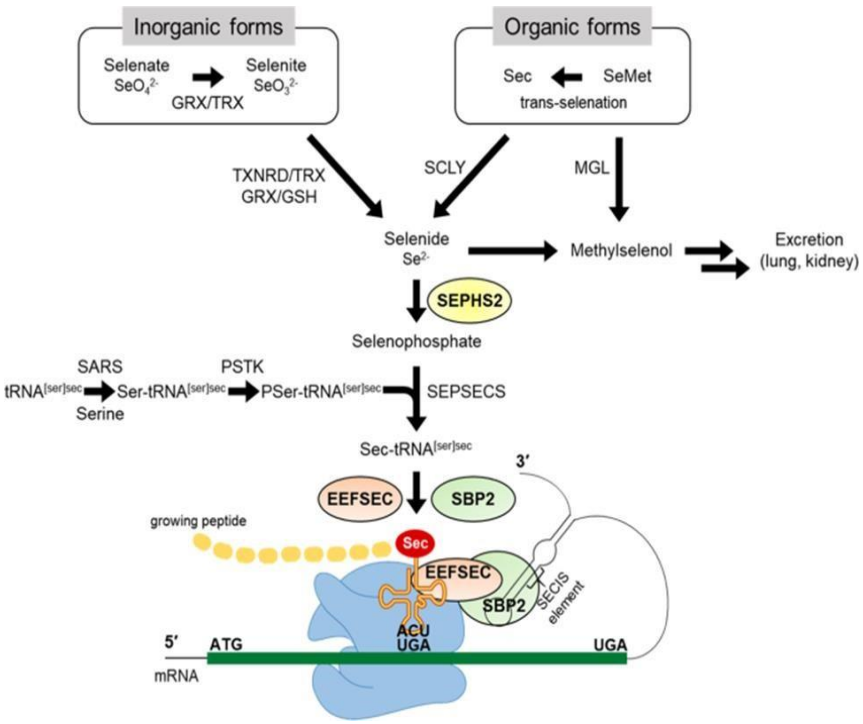

Figure 10: Mammalian selenium metabolism. (Figure from Kang et al., 2020).

1.7 Role of selenium in antioxidant defence

Free radicals, including reactive oxygen species (ROS) and reactive nitrogen species (RNS), are byproducts of cellular redox processes in the human body, primarily generated in mitochondria during ATP production (Valko et al., 2006; Chatterjee et al., 2007). While free radicals can exhibit both beneficial and harmful properties, maintaining a balance between these opposing effects is essential for health (Valko et al., 2006; Chatterjee et al., 2007). Research has

demonstrated that antioxidants play a crucial role in mitigating the risks of severe diseases by neutralizing free radicals (Valko et al., 2006; Chatterjee et al., 2007). These antioxidants are either synthesized naturally within the body or acquired externally through dietary sources and supplements (Valko et al., 2006; Chatterjee et al., 2007).

Both enzymatic and non-enzymatic antioxidants contribute to reducing the harmful effects of ROS and RNS (Valko et al., 2006; Chatterjee et al., 2007). Non-enzymatic antioxidants such as vitamin C, vitamin E, carotenoids, thiols, and natural flavonoids are among the most effective in combating oxidative stress (Valko et al., 2006; Chatterjee et al., 2007). On the other hand, enzymatic antioxidants, including glutathione peroxidase (GPx), catalase, and superoxide dismutase (SOD), serve as critical defense mechanisms against oxidative damage (Halliwell and Gutteridge, 1999; Avanzo et al., 2001; Valko et al., 2006). Certain micronutrients influence the activity of these antioxidant enzymes, with minerals such as copper (Cu), manganese (Mn), zinc (Zn), selenium (Se), and iron (Fe) playing essential roles as cofactors in their regulation (Halliwell and Gutteridge, 1999; Avanzo et al., 2001; Valko et al., 2006).

Glutathione peroxidase (GPx), an enzymatic antioxidant, exists in two forms: selenium-independent and selenium-dependent (Halliwell and Gutteridge, 1999; Avanzo et al., 2001; Valko et al., 2006). Regardless of the form, GPx prevents peroxidases from serving as potential substrates for the Fenton reaction, which could otherwise generate highly reactive hydroxyl radicals (Halliwell and Gutteridge, 1999; Avanzo et al., 2001; Valko et al., 2006).

An imbalance between free radicals and antioxidants leads to oxidative stress, a condition in which excessive ROS and RNS

overwhelm the body's antioxidant defenses (Halliwell, 2007). Oxidative stress damages essential cellular components, including lipids, proteins, and DNA, contributing to the pathogenesis of various diseases such as cardiovascular disorders, cancer, and neurodegenerative conditions (Sies, 2015). By neutralizing free radicals, antioxidants help sustain cellular homeostasis and protect against oxidative damage (Packer et al., 2017). When this balance is disrupted, it can result in chronic inflammation, accelerated aging, and an increased risk of disease (Schmidt et al., 2016). Therefore, understanding and controlling oxidative stress is vital for preventing and managing numerous health conditions (Bjelakovic et al., 2007).

The antioxidant defense system operates through three primary stages (Brezezinska-Slebodzinska, 1995; Surai, 1999; Kagan et al., 2002; Surai, 2002; Peooas et al., 2008). The first stage (prevention) involves antioxidant enzymes such as GPx, SOD, and catalase, which neutralize catalysts or remove precursor molecules of free radicals (Brezezinska-Slebodzinska, 1995; Surai, 1999; Kagan et al., 2002; Surai, 2002; Peooas et al., 2008). However, as these enzymes cannot entirely eliminate free radicals, some radicals persist and induce lipid peroxidation, protein modification, and DNA damage (Brezezinska-Slebodzinska, 1995; Surai, 1999; Kagan et al., 2002; Surai, 2002; Peooas et al., 2008).

The second stage (interception) relies on thioredoxin reductase, an enzyme that reduces oxidized thioredoxin and its homologs through nicotinamide adenine dinucleotide phosphate (Brezezinska-Slebodzinska, 1995; Surai, 1999; Kagan et al., 2002; Surai, 2002; Peooas et al., 2008). Selenium, as a crucial component of selenoproteins, plays a role in both the first and second antioxidant defense stages (Brezezinska-Slebodzinska, 1995; Surai, 1999; Kagan

et al., 2002; Surai, 2002; Peooas et al., 2008). Despite these protective mechanisms, oxidative stress may still cause irreversible damage to proteins and DNA (Brezezinska-Slebodzinska, 1995; Surai, 1999; Kagan et al., 2002; Surai, 2002; Peooas et al., 2008).

The third and final stage of antioxidant defense focuses on repairing or removing damaged biomolecules (Brezezinska-Slebodzinska, 1995; Surai, 1999; Kagan et al., 2002; Surai, 2002; Peooas et al., 2008). This phase involves proteolytic enzymes (peptidases and proteases), lipolytic enzymes (lipases), and other repair enzymes, such as proteinases, phospholipases, nucleases, DNA repair enzymes, polymerases, ligases, and various transferases (Brezezinska-Slebodzinska, 1995; Surai, 1999; Kagan et al., 2002; Surai, 2002; Peooas et al., 2008). Nevertheless, these repair mechanisms are not always sufficient to completely restore DNA integrity, potentially leading to cell cycle arrest and cell death (Sies, 1993; Buttke and Sandstrom, 1994; Surai, 2006). To preserve genetic stability, multicellular organisms initiate apoptosis (programmed cell death) to eliminate cells that have undergone genetic alterations (Sies, 1993; Buttke and Sandstrom, 1994; Surai, 2006).

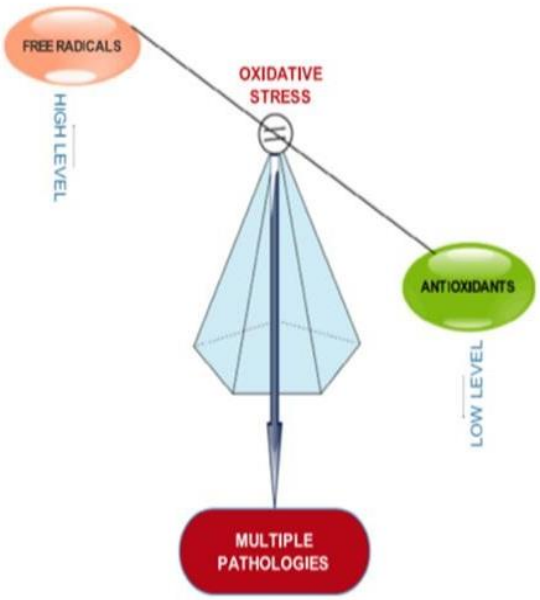

Figure 11: An imbalance between free radicals and antioxidants leads to oxidative stress. (Figure from Ighodaro and Akinloye, 2019)

1.8 Selenium anti-carcinogenicity

Se intake above the recommended daily allowance (RDA) appears to prevent certain types of cancer, indicating that higher intakes of selenium are advantageous (Zeng, 2009). Based on this inverse association between Se intake and the incidence of some types of cancer, it was first postulated in the late 1960s that selenium be anticarcinogenic. Since then, a large body of convincing evidence has emerged, including epidemiological evidence, cell and animal studies, and human intervention findings, all indicating that Se can play a role in cancer prevention (Schamberger and Frost, 1969; Schrauzer and Rhead, 1971; Combs, 2005; Whanger, 2004; Ip, 1998; Zeng and Combs, 2008; Rayman, 2005; Combs, 2004).

To maintain tissue homeostasis in humans and animals, cell proliferation and death must be controlled. The eukaryotic cell cycle is divided into four primary phases: the G1 phase, which occurs before DNA replication; the S phase, which occurs during DNA synthesis; the G2 phase, which occurs before cell division; and cell division itself (M phase). The cell cycle is a well-studied method by which eukaryotic cells proliferate, while apoptosis is a well-studied mechanism by which eukaryotic cells undergo the process of programmed death. During normal development, turnover, and pathological situations, apoptosis allows an organism to destroy undesired or faulty cells.

According to a recent study, the efficacy of Se compounds as micronutrients and chemopreventive agents is related to the chemical form and dosages of Se (Pucci et al., 2000; Zeng, 2009). Se is a micronutrient, and its most predominant forms in foods are SeMet and SeCys, with smaller quantities of methylated selenides. Among the many supplements available to consumers is inorganic Se-salts, such as selenite and selenate. A primary way by which Se exerts its biological activities is through cell cycle and apoptosis control. When Se is administered at nutritional doses, Se is incorporated into SeCys in selenoproteins and promotes the progression of the cell cycle and prevents cell death by inhibiting apoptosis. At supranutritional but sub-toxic doses, however, Se results in cell cycle arrest and cell death.

Anticarcinogenic activity, protection against oxidant damage or ageing, and even a role in reproduction and detoxicity are just a few of the benefits of Se (Zeng, 2009). For cancer protection, it is well established that Se is most effective at elevated levels,

commonly referred to as supranutritional or pharmacological levels. Se's effects on programmed cell death, DNA repair, its role in selenoenzymes, its impact on carcinogen metabolism, its effects on the immune system, its role an antiangiogenic agent, and its specific suppression of tumour cell growth through certain Se metabolites are all suggested mechanisms for cancer prevention (Combs & Gray, 1998).

The mechanism behind the inverse relationship between Se levels and cancer risk must be elucidated. It may be that Se-deficiency heightens cancer risk, for example due to inadequate antioxidation, or that higher Se levels actively reduce cancer risk, for example by reducing the cellular threshold for apoptosis, or – more likely -- a mixture of both. This is relevant for public health considerations as it determines the target levels for public Se intake – whether, for example, supranutritional Se intake may be helpful in reducing cancer rates.

The known functions of selenoenzymes in antioxidant protection (glutathione peroxidases, GPXs) and redox control (thioredoxin reductases, TRs), and thus in the metabolic defence against carcinogenic free radicals, suggest that Se deficiency could raise cancer risk. Because the electron-rich DNA bases are susceptible to electrophilic attack by reactive oxygen species (ROS) such as superoxide radicals, hydrogen peroxide, singlet oxygen, hydroxyl radicals, and electrophilic metabolites of xenobiotics and other reactive intermediary metabolites, mutagenic oxidative stress is generally thought to be a major factor in the initiation of human carcinogenesis. These can result in genetic damage, the generation of mutant oncogenes and tumour suppressor genes, and epigenetic modifications that impact expression. In animal

models, the induction of skin tumours by ultraviolet irradiation or phorbol esters varied inversely with skin GPX activity, and protection by selenite against (2-oxoproy) amine-induced intrahepatic cholangiocarcinomas in Syrian golden hamsters correlates with the restoration of hepatic GPX activity (Burke et al., 1992; Pence et al., 1994; Diamond et al., 1996; Perchellet et al., 1987; Kise et al., 1991).

In summary, several mechanisms contribute to the anticancer effects of selenium (Table 1), including its role in enhancing antioxidant defense systems, modulating immune responses, and influencing cell cycle regulation. Selenium, through its incorporation into selenoproteins, boosts the activity of antioxidant enzymes such as glutathione peroxidases, which help protect cells from oxidative damage that can lead to cancer (Rayman, 2005). Additionally, selenium modulates immune responses by enhancing the activity of immune cells and cytokines, thereby improving the body's ability to target and eliminate cancerous cells (Rayman, 2005). Furthermore, selenium has been shown to influence cell cycle regulation and apoptosis, promoting the elimination of damaged cells and reducing the likelihood of tumor development (Rayman, 2005). These multifaceted mechanisms highlight selenium's potential as a chemopreventive agent.

Table 1: These are some of the possible mechanisms that contribute to the anticancer effect of selenium. (Table redrawn from Rayman, 2005).

Anti-cancer processes or pathways	Selected evidence for Se involvement	Reference
Seleno-enzyme mechanisms Reduction of DNA damage	Se intake or status affects DNA damage in both human and animal studies	Karunasinghe et al. (2004), Kowalska et al. (2005), Waters et al. (2005)
Reduction of oxidative stress	Levels of dietary antioxidant vitamins an carotenoids and SNP that	Rayman (2005)

	affect antioxidant and selenoproteins modify the effect of Se on cancer risk	
Reduction of inflammation: inflammation promotes tumour growth (Caruso et al. 2004)	Selenoenzymes can reduce hydroperoxide intermediates in the cyclooxygenase and lipoxygenase pathways preventing the production of pro-inflammatory prostaglandins and leukotrienes	Rayman (2000)
Induction of phase II conjugating enzymes: detoxify carcinogens and reduce DNA adduct formation	Some selenocompounds e.g. methyl selenol (CH3SeH), can upregulate phase II conjugating enzymes such as glutathione-S-transferase, increasing detoxification of carcinogens	Ip & List (1997)
Enhancement of immune response: cytotoxic lymphocytes and natural killer cells are able to destroy tumour cells	Se supplementation (Na2SeO3) enhanced the immune response of volunteers and cancer patients by increasing the numbers of cytotoxic lymphocytes and natural killer cells	Kiremidjian-Schumacher et al. (1994, 2000)
Increase in tumour-suppressor protein p53: inhibits proliferation, stimulates DNA repair and promotes apoptotic death by acting as a ransciption factor for several genes, including the damage – inducible gadd genes	SeMet can activate p53 through redox regulation of key p53 cysteine residues. Methyl seleninic acid (CH3SeO2H) and Na2SeO3 modulate p53 activity by phosphorylation Selenodiglutathione also induces p53 Se compounds induced specific patterns of gadd genes	Smith et al. (2004) Lanfear et al. (1994) Kaeck et al. (1997)
Inactivation of protein kinase C (PKC), a signalling receptor that plays a crucial role in	Selective inactivation of PKC results from reaction of its catalytic domain with selenometabolites such	Gopalakrishna & Gumimeda (2002)

tumour promotion by oxidants	as CH3SeO2H (formed from membrane-bound CH3SeH and fatty acid hydroperoxides), inhibiting tumour promotion and cell growth	
Alteration in DNA methylation: abnormal methylation patterns ae associated with neoplasia and inactivation of tumour-suppressor genes	Se affects the extent of DNA methylation and the activity of DNA methyl-transferase	Davis et al. (2000), Davis & Uthus (2003), Fiala et al. (1998)

Selenium can affect the progression of carcinogenesis at distinct stages in different ways depending on its form (Figure 12).

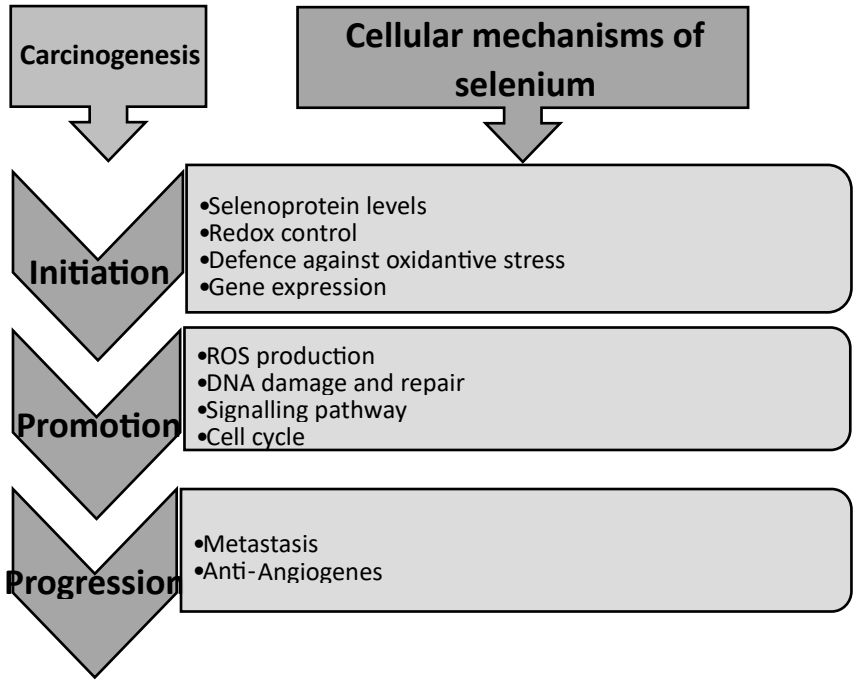

Figure 12: Selenium and carcinogenesis: cellular mechanisms (Figured adapted from Björnstedt and Fernandes, 2010).

1.9 An overview of selenium from uptake to human metabolism

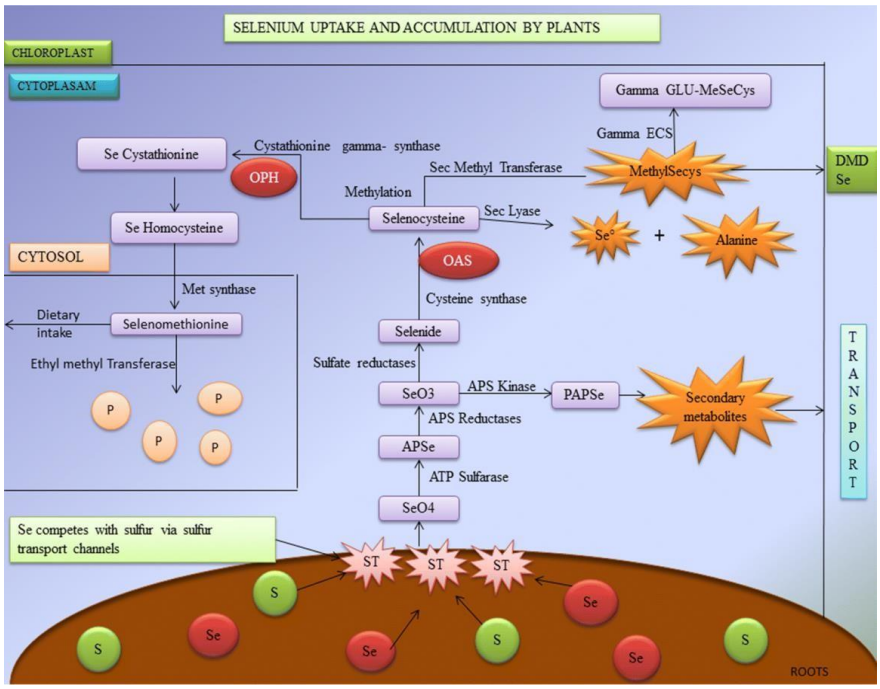

Figure 13: It is shown that selenium is taken up and accumulated in plants. ST are Sulfur transport channels. Purples illustrated SeO4 selenate, APSe adenosine phosposelenate, PAPSe phospho adenosine phospho selenite, OASO-acetyl serine, OPHO-phospho hemoserine, DMSe dimethylselenid. Orang ones represents Metabolites. (Figure from Hariharan and Dharmaraj, 2020).

Selenium uptake in plants is a complicated process. Figure 13 provides a detailed schematic illustrating the complex pathways by which plants absorb and metabolise Se. It highlights key interactions between selenium and sulfur, the role of various enzymes, and the formation of a number of compounds throughout these processes.

As shown in the diagram, selenium primarily enters the plant from the soil in the forms of selenate (SeO_4) and selenite (SeO_3). Once inside the plant, these inorganic selenium forms are reduced to selenide (Se_2^-

) which is then incorporated various organic compounds like selenocysteine, selenomethionine, and secondary metabolites.

The schematic also illustrates several metabolic pathways involving key enzymes such as methyltransferase and sec lyase, which lead to the formation of a number of selenium-containing compounds. It shows the transport of selenium within the plant, starting with uptake by the roots and subsequent movement to different tissues.

An important aspect of the diagram is the competition between selenium and sulfur for uptake and transport within the plant, as these two elements share similar pathways. The presence of phosphate groups in these pathways suggests that the involved steps are energy dependent.

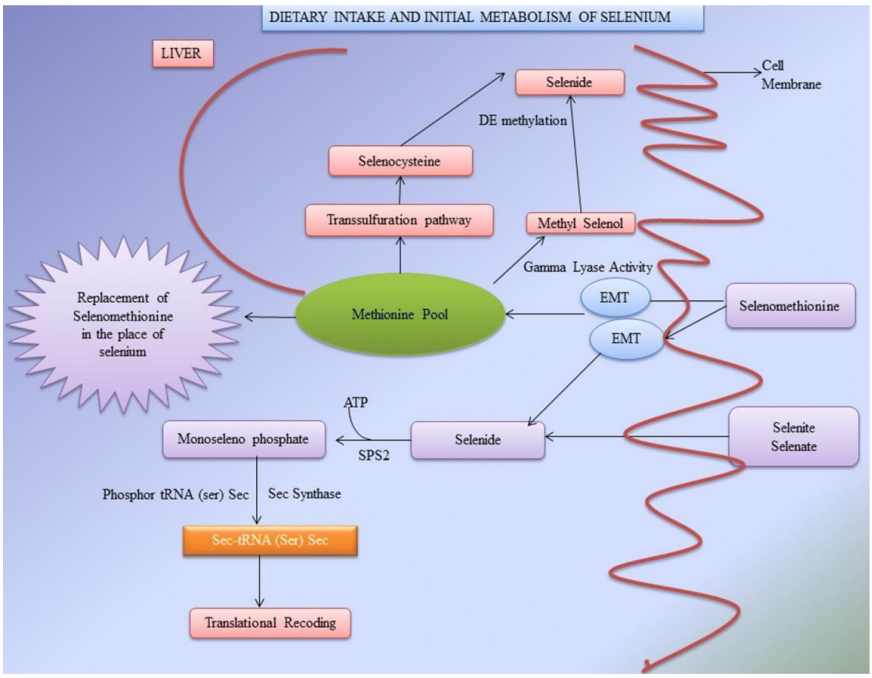

Figure 14: Human selenium intake and metabolism. SPS2 refers to selenophosphate synthase 2, tRNASec refers to tRNA for selenocysteine, EMT refers to epithelial-tomesenchymal transition. (Figure from Hariharan and Dharmaraj, 2020).

After ingestion, selenium compounds need to be metabolised by the human body into useful forms. Figure 14 provides an overview of the dietary intake and initial metabolism of selenium in the human body, illustrating a complex network of interconnected pathways and molecules involved in transforming selenium into various forms.

Selenium is primarily acquired through food consumption. The liver is highlighted as a central organ in selenium metabolism, playing a crucial role in processing and converting selenium into different compounds.

The diagram shows selenium-containing molecules such as selenide, selenocysteine, and selenomethionine – each connected by arrows representing the biochemical processes involved in their conversion. These pathways are catalysed by specific enzymes, for example, selenophosphase synthase 2 (SPS2)

As shown in the diagram, individual cellular components – such as the membrane – are crucial to selenium transport and thus its eventual utilisation within the body.

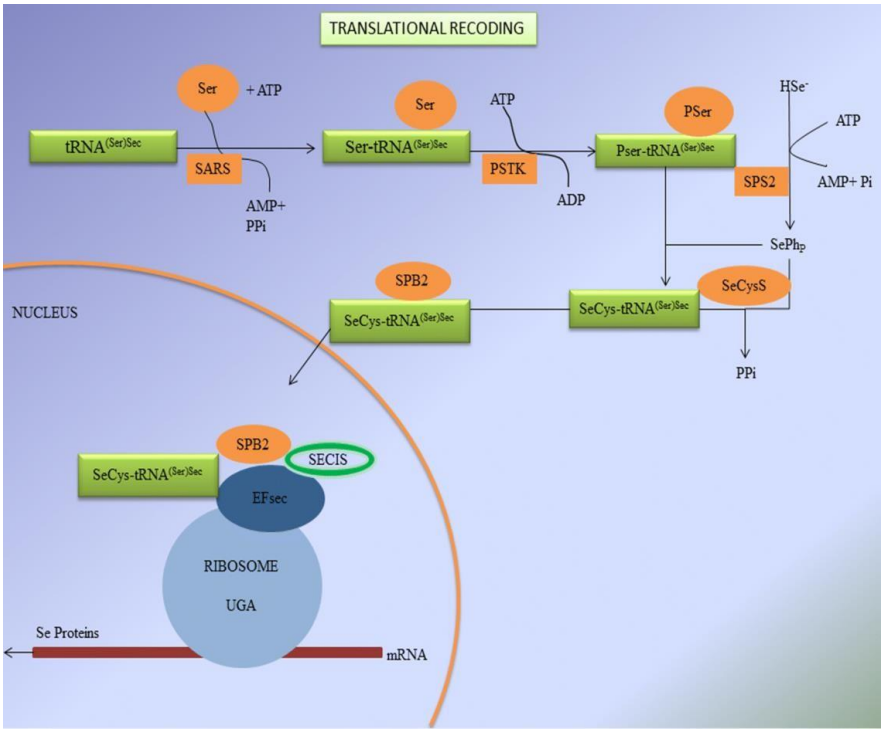

Figure 15: Selenoprotein synthesis and translational decoding. *tRNASec* refers to tRNA for selenocysteine, *SARS* refers to Seryl-tRNA sythetase, *PSTK* refers to phosphoseryl-tRNA kinase, *PSer* refers to phosphoserine, *SPS2* refers to selenophosphate synthase 2, *SeCysS* refers to selenocysteine synthase, *SeCys* refers to selenocysteine, *SBP2* refers to selenocysteine incorporation sequence binding protein 2, *SECIS* refers to selenocysteine insertion sequence, *EFsec* refers to specialized elongation factor, *HSe* is hydrogen selenide. (Figure from Hariharan and Dharmaraj, 2020).

Selenium (in the form of selenocysteine) is then incorporated into proteins. Figure 15 shows this process, through which Sec is incorporated into proteins during translation. This is a unique process known as translational coding. The UGA stop codon is reinterpreted as a sense codon for Sec, allowing its integration into proteins.

The process begins in the nucleus, where tRNA specific for Sec, known as tRNA(Ser)Sec, is synthesised. The diagram otulines the maturation of this tRNA, emphasising steps such as the attachment of

serine (Ser) and subsequent modifications that convert it into selenocysteine-tRNA(Ser)Sec.

A key regulatory component in this process is the SECIS element, found in the mRNA. This element signals the ribosome, the protein-synthesizing machinery, to incorporate Sec at the UGA codon, which is normally a stop codon. Translation factors, including EFsec, play crucial roles in facilitating this process.

As the ribosome reads the mRNA, the UGA codon, guided by the SECIS element, directs the incorporation of Sec into the growing protein chain, resulting in the formation of selenium-containing proteins. The final products are proteins with selenocysteine integrated into their structure.

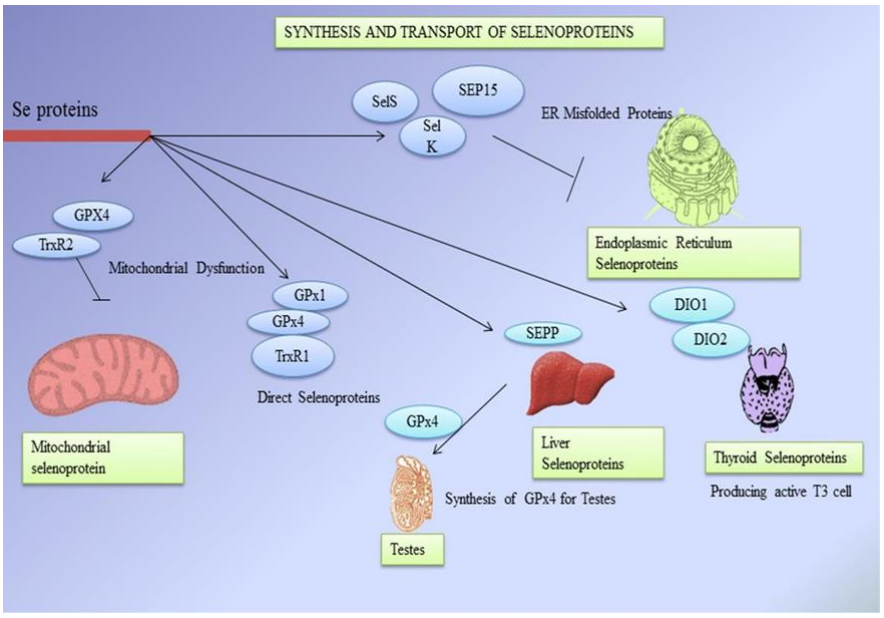

Figure 16: Selenoprotein synthesis and transportation. *GPX* refers to Glutathioneperoxidases, *TXR* refers to thioredoxin reductases, *SEPP* refers to selenoprotein P, *SEP15* refers to 15-kDa selenoprotein, *SelK* refers to selenoprotein K, *SelS* refers to selenoprotein S, *DIOs* refers to iodothyronine deiodinases, *T3* refers to 3,5,3'-triiodothyronine. (Figure from Hariharan and Dharmaraj, 2020)

Figure 16 illustrates the synthesis and transport of selenoproteins within the human body, offering a visual representation of the complex pathways involved in creating and distributing these vital proteins.

The liver is portrayed as the central hub for selenoprotein synthesis and distribution, underscoring its crucial role in this process. The diagram features various types of selenoproteins, such as glutathione peroxidase (GPX), thioredoxin reductase (TrxR), and selenoprotein P (SEPP), among others, each playing important roles in cellular function and overall health.

These selenoproteins are depicted in different cellular compartments, including the endoplasmic reticulum, mitochondria, and specific organs like the thyroid and testes, highlighting their widespread presence and diverse functions within the body. The diagram also shows the movement of selenoproteins between different parts of the body, emphasizing the dynamic nature of their transport and utilization.

1.10 Bioinformatics

> (Molecular) **bio** – informatics: bioinformatics is conceptualising biology in terms of molecules (in the sense of physical chemistry) and applying **"informatics techniques"** (derived from disciplines such as applied maths, computer science and statistics) to **understand** and **organise** the **information** associated with these molecules on a **large scale**. In short, bioinformatics is a management information system for molecular biology and has many **practical applications**.
>
> *An Oxford English Dictionary submission*

The initial definition of bioinformatics was the investigation of informatics techniques in biotic systems. This is effectively computational analysis of biological data. So, according to molecular

biologists, bioinformatics is the field of computer-aided processing of fata pertaining to genes, genomes and their byproducts (Choudhuri, 2014). Another way to describe bioinformatics is computational molecular biology. These computational approaches are used to investigate the structure, function, regulation and interacting connectivity of genes and proteins. The ultimate objective is to examine and make predictions about the entire genome of an organism's structure, organisation, regulation and dynamics (Choudhury, 2014).

Gene mapping

Understanding the genetic architecture of complex traits in both agricultural and evolutionary contexts is a fundamental aspect of biology, as these traits are influenced by multiple genetic loci, environmental conditions, and their interactions (Mackay, Stone, & Ayroles, 2009). The first wave of association mapping studies in model crops was driven not only by advances in genomic technology and methodological developments but also by the need to examine trait variation across different genetic backgrounds (Zhu, Gore, Buckler, & Yu, 2008).

With improvements in sequencing technologies and coordinated community efforts, genome-wide association studies (GWAS) have emerged as a widely used method, particularly when resequencing follows the assembly of a reference genome or when high-density genotyping arrays become available (Michael & Jackson, 2013). The development of diversity panels and genetic populations has facilitated the phenotyping of an increasing number of crops for GWAS, providing researchers with essential genetic material, phenotyping protocols, genotyping and sequencing technologies,

analysis tools, and comprehensive datasets (Lin et al., 2014; Zhao et al., 2019).

The recent advancements in GWAS have enabled researchers to establish causal links between genetic sequence variants and phenotypic trait measurements, significantly enhancing our understanding of genotype-phenotype relationships (Lin et al., 2014; Zhao et al., 2019). The completion of the *Arabidopsis thaliana* 1001 Genomes Project has further expanded access to extensive genetic data, facilitating highly resolved association mapping between chromosomal locations and complex traits, while improvements in statistical techniques have effectively mitigated population structure confounding effects (Lee, 2021).

Among the approximately 3500 species of the monophyletic *Brassica*ceae family, *Arabidopsis thaliana* is one of the most widely studied species (Price et al., 1994). *Arabidopsis* shares evolutionary ancestry with several economically significant plants, including *Brassica* species that are cultivated for vegetables and oils (Price et al., 1994). As a model system for *Brassica*ceae plants, *Arabidopsis* provides researchers with extensive genetic and genomic information, benefiting from its completely sequenced genome, efficient transformation protocols, and small, easily interpretable genome size (*Arabidopsis* Genome Initiative, 2000).

Genetic markers serve as essential tools in plant genetics and genomics for mapping traits and understanding genetic variation (Mackay et al., 2009). Single nucleotide polymorphisms (SNPs) are the most common form of genetic variation, characterized by a single nucleotide change at a specific genome position, and are widely used due to their abundance and stability (Mackay et al., 2009). Simple

sequence repeats (SSRs), also referred to as microsatellites, consist of 2-6 base pair repetitive sequences that vary in length among individuals, making them highly polymorphic and useful for genetic diversity studies and linkage mapping (Schlötterer, 2004). Insertion and deletion polymorphisms (Indels) represent variations in DNA where small sequences are inserted or deleted, which can impact gene function and are frequently employed in genetic mapping (Huang et al., 2012). Restriction fragment length polymorphisms (RFLPs) involve variations in DNA sequences that can be detected by the presence or absence of restriction enzyme cut sites, making them valuable for genetic linkage analysis and constructing genetic maps (Botstein et al., 1980). Copy number variations (CNVs) are alterations in the number of copies of a specific gene or genomic region, which can significantly affect gene expression and phenotype (Redon et al., 2006).

As mentioned above, *Arabidopsis thaliana* has been widely used in GWAS due to its small genome size and well-characterized genetic background, allowing researchers to identify genetic loci associated with key traits such as flowering time and stress responses (Alonso-Blanco et al., 2016). The GWAS approach in *Arabidopsis* involves assembling a diverse population of accessions to capture genetic variation (Kim et al., 2007). These accessions undergo genotyping using SNP arrays and are phenotyped under controlled conditions to collect trait data (Atwell et al., 2010). Advanced statistical methods are then applied to establish associations between genetic variants and phenotypic traits (Tiffin & Hufford, 2013). Candidate genes identified through GWAS are subsequently investigated to determine their functional roles in the observed traits (Mackay et al., 2012).

Mapping studies aim to identify the genomic locations of genes or genetic elements associated with specific traits (Lander & Botstein, 1989). Linkage mapping involves crossing two genetically distinct parents and analysing marker and trait segregation patterns in their offspring to locate genes responsible for trait variation (Lander & Botstein, 1989). Quantitative trait locus (QTL) mapping is employed to pinpoint genomic regions linked to quantitative traits, further refining our understanding of complex trait inheritance (Mackay, 2001). Association mapping, similar to GWAS, identifies genetic markers correlated with traits by analysing natural genetic variation within populations, offering a powerful approach for dissecting complex genetic traits in plants (Flint-Garcia et al., 2003).

1.11 Hypotheses

1. Biofortification of onion varieties and spring onions with selenium in hydroponics

Hypothesis 1.1: Increasing selenium concentrations in the hydroponic solution will lead to a significant accumulation of selenium in various tissues of both onion varieties and spring onions. Specifically, it is hypothesized that the distribution of selenium among the roots, stems, and bulbs will vary between onion varieties and spring onions.

Hypothesis 1.2: Elevated selenium concentrations in the hydroponic medium will affect the uptake of other essential elements (e.g., nitrogen, phosphorus, potassium) in onion plants, potentially leading to imbalances in their concentrations within the plant tissues.

Hypothesis 1.3: Selenium biofortification will have a measurable impact on the storage quality of onions, including factors such as

firmness, decay resistance, and shelf life, with the extent of impact varying depending on selenium concentration and onion variety.

1.2 Biofortification of spring onions with selenium through foliar spray and soil soak applications

Hypothesis 2.1: Different application methods (foliar spray vs. soil soak) and selenium concentrations will result in varying levels of selenium accumulation in spring onion tissues, with specific concentrations and methods proving more effective.

Hypothesis 2.2: Increasing selenium concentrations in spring onions will influence the uptake of other essential nutrients (e.g., nitrogen, phosphorus, potassium) and may alter their concentration patterns in the plant tissues.

Hypothesis 2.3: Selenium biofortification will affect agronomic parameters of spring onions, such as growth rate, leaf size, and bulb weight, with variations depending on selenium concentration and application method.

1.3 Effects of selenium on HepG2 liver cancer cell line:

Hypothesis 3.1: Selenium concentrations in the tissue extracts of spring onions will correlate with their effectiveness in scavenging free radicals and inducing cell death in HepG2 liver cancer cells, with certain selenium concentrations proving more potent.

1.4 Analysis of associative transcriptomics data for selenium uptake regulation

Hypothesis 4.1: Specific genes associated with single-nucleotide polymorphisms (SNPs) and gene expression markers (GEMs) will be

identified as key regulators of selenium uptake in *Brassica* napus and *Arabidopsis thaliana*. These genes are expected to show differential expression patterns related to selenium concentrations and uptake efficiency.

Hypothesis 4.2: Associative transcriptomics analysis will reveal that certain regulatory pathways and gene networks are crucial for optimizing selenium uptake and accumulation in plants, providing insights into how genetic variation influences selenium metabolism.

1.12 Objectives

Objective 1: Focuses on the impact of selenium biofortification on selenium accumulation in onion tissues, nutrient uptake, and storage quality in hydroponics.

Objective 2: Investigates the effects of selenium application methods on nutrient uptake and agronomic parameters in spring onions, with a separate hypothesis addressing the effectiveness of selenium in scavenging free radicals and inducing cell death in HepG2 liver cancer cells.

Objective 3: Aims to identify genes and regulatory pathways involved in selenium uptake in plants through transcriptomics analysis.

Chapter 2: Enhancing Nutrient Uptake in Onion and Spring Onion Via Se Biofortification in a Hydroponic System

2.1 Introduction

The deficiency of selenium is a global concern for humans and animals alike. Because crop plants provide the primary source of selenium for consumers, it is crucial to understand how selenium accumulates and distributes in plant tissues as well as how it interacts with other elements (Xinbin et al., 2020). Furthermore, biofortification of plants could be an effective way of increasing the consumption of selenium by humans. Biofortification of crops should be carefully investigated and evaluated in the context of creating enriched sources of Se for human consumption since researchers are employing a variety of methods to increase Se content in edible parts of crops (Ofori et al., 2023). Biofortification strategies contain many variables, including the mode of Se application (soil fertilization, foliar spraying, or hydroponics), Se dose, species and form of fertilizer, crop variety, and growth stage, among others (Eiche, 2019).

When growing soilless vegetables or microscale vegetables in hydroponic systems, Se can be added to the water or nutrient solution (Longchamp, 2013). Furthermore, hydroponics has the potential to be one of the most efficient methods for addressing the nutrition deficiencies caused by the declining quantity of agricultural land along with the change in climate that contributes to crop failures. Aerated water with an abundance of

nutrients and a static support system are used in hydroponics to grow plants without soil. The history of soilless cultivation has been documented as far back as the 18th century, though it may have existed earlier. Nutrient film technique (NFThydr) is one of the methods used in hydroponics. With the NFT approach, plant roots are submerged in a thin layer of water which transfers nutrients. This technique controls plant growth more easily (Saaid et al., 2013; Jones, 1997; Benton and Jones, 1982 and 2005). There is a possibility to reduce dietary deficiencies and increase health benefits by consuming selenium-enriched vegetables and crops, but it is crucial to identify plants capable of absorbing and converting selenium; there seems to be a good source in the *Allium* and *Brassica* genera (Broadly et al., 2006). These selenised vegetables contain large amounts of selenium in the form of S-methylselenocysteine and its derivates, which are known to be very effective forms of selenium for health protection (Ip et al., 2000; Hama et al., 2008; Abdulah et al., 2009).

The aim of this study was to examine the effect of selenium on uptake of other essential elements such as S, Fe, Mg, K and Ca in *Allium* (Onion and Spring onion) by using biofortification and NFT techniques.

The objectives of this study are:

1. Do different varieties of onions affect the biofortification of selenium?

2. Does the amount of selenium in onion shoots tissue or bulb tissue vary?

3. Does increasing selenium concentration on onion and spring onions affect the uptake of other elements in either a positive or negative way?

4. In terms of onion storage quality, does selenium biofortification have a positive effect?

Hypotheses:

1. Selenium biofortification will increase selenium content in onion shoots and bulbs without negatively impacting the uptake of other essential nutrients such as sulfur (S), magnesium (Mg), and calcium (Ca).

2. Different onion varieties will exhibit varying selenium uptake efficiencies, influenced by genetic and physiological factors.

3. Selenium biofortification will enhance onion storage quality by reducing oxidative stress and delaying spoilage.

4. Increased selenium concentration in the nutrient solution will correlate positively with selenium levels in onion tissues.

Selenium biofortification has been extensively studied for its potential to improve human health via plant-based dietary sources. Research by Broadley et al. (2006) emphasizes the importance of selenium-enriched vegetables in combating selenium deficiency. Additionally, selenium's role in mitigating oxidative stress and its synergistic relationship with

sulfur uptake have been documented by Zhao and McGrath (2009).

2.2 Materials and Methods

A series of experiments were conducted at the University of Nottingham's Plant Science Department to investigate the effects of selenium biofortification on the uptake of other essential elements in onions and spring onions. This study utilized a hydroponic Nutrient Film Technique (NFT) system, a method commonly employed to grow plants without soil by providing a continuous or intermittent flow of nutrient-rich water over their roots. This thin film of water ensures optimal nutrient absorption and aeration by simultaneously supplying essential nutrients and oxygen directly to the roots.

In the NFT system, plants are supported in sloped channels where nutrient solutions flow from one end to the other before being collected in a reservoir for recirculation, enhancing water efficiency. Widely used in both agricultural production and research, NFT allows precise control of nutrient delivery, making it particularly valuable for examining nutrient interactions and enhancing biofortification processes. Previous studies have demonstrated the effectiveness of NFT in investigating selenium biofortification in crops such as onions and spring onions under controlled experimental conditions.

These experiments were conducted in a glasshouse environment where additional heating was applied to maintain a constant temperature of 20°C. The ventilation system was regulated to maintain a temperature of 22°C, while

supplementary lighting provided a 16-hour illumination cycle to optimize plant growth conditions.

From 2019 to 2021, three trials were conducted in the glasshouse (Table 2).

Table 2: Selenium biofortification experiments in NFT system.

Trial	Plant	Date
Experiment1	Onion Rijnsburger (Red Onion)	August 2019
Experiment2	Onion Bedfordshire Champion (White Onion)	January 2021
	Onion Rijnsburger (Red Onion)	
Experiment3	Onion Bedfordshire Champion (White Onion)	June 2021
	Onion Rijnsburger (Red Onion)	
	Spring onion (White Lisbon)	

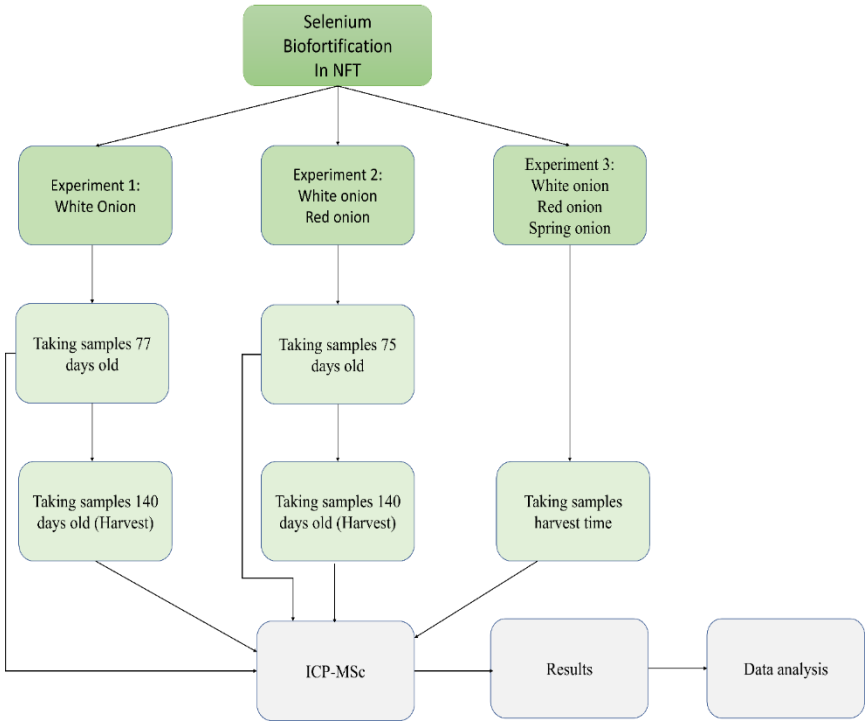

Figure 17: Diagram showing selenium biofortification experiments in NFT system.

2.2.1 Experiment 1

Seeds of white onion were sown near the end of August 2019 (Figure 18A), and grown onions were transferred (10 plants for each lane) after three weeks to NFT systems consisting of three lanes with plastic guttering sloped at a 5-degree angle, and four medium containers per lane. It consisted of four lanes that were fed by containers with nutrient solutions that were pumped to one end and collected at the other (Picture 18B). A Hortimix standard solution (Horifeeds, Lincoln, UK) was used to feed the plants every other week, and simple measurements (height) were taken to check on their growth. From 1st of October (five weeks after seeds were sown), selenium treatment was carried out until harvesting (March) (Figure 18C, D).

A concentration of sodium selenate (Na_2SeO_4) solution was added to the nutrient solution in the following order: (1) Control, (2) 5 µg ml^{-1}, and (3) 50 µg ml^{-1}. In the onion growing season, samples were taken two times at 11 weeks, 20 weeks and Selenium was added for about **20 weeks** in total. In this case, harvesting the bulbs occurred when they were ripe (Figure 18E), which coincided with the last collection. In Experiment 1, samples were collected at 11 weeks and 20 weeks during the onion growing season. Both leaves and bulbs were sampled separately, with four onions randomly selected from each line, resulting in a total of 24 samples. The collected samples were processed by drying in a freezer dryer, and the leaves and bulbs were prepared separately for ICP-MS analysis. This method allowed for detailed assessment of selenium uptake in different plant parts throughout the growth stages.

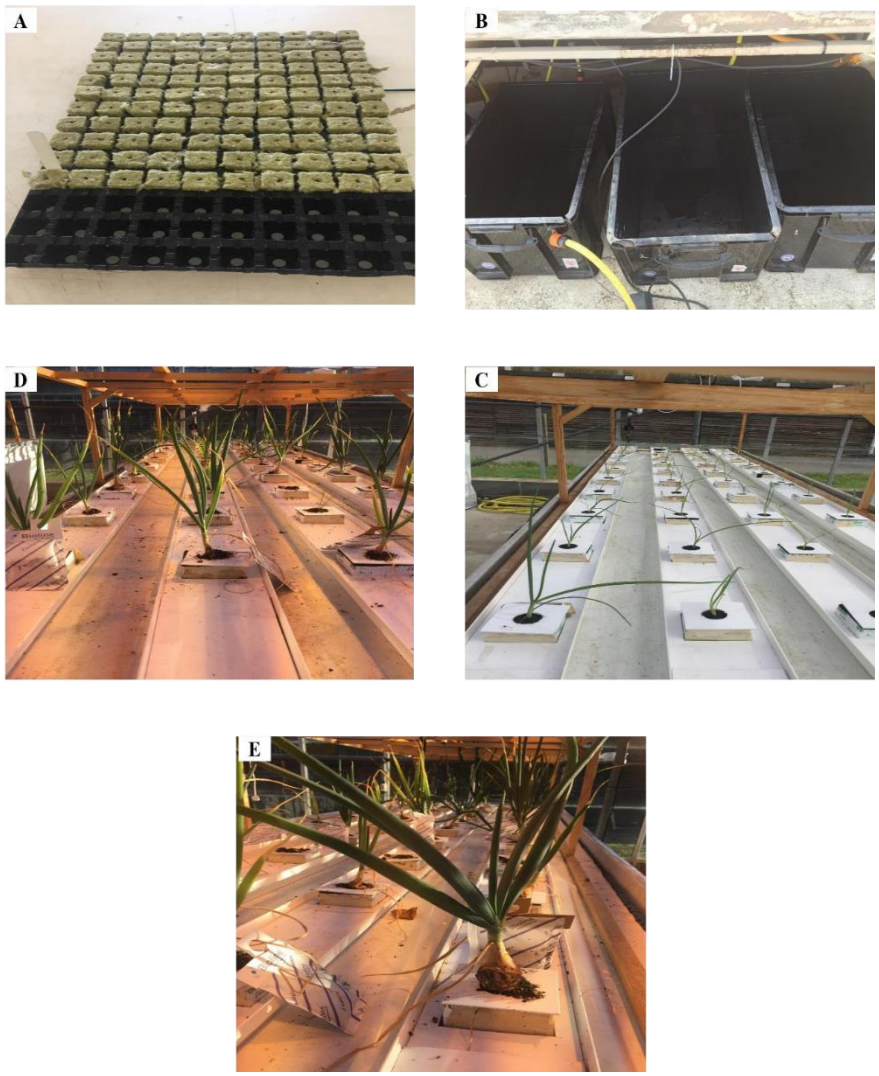

Figure 18: Steps for onion growth in the NFT system. (A) Onion seed sowing. (B) NFT containers. (C) Growing onions in NFT. (D) Onion's development phase. (E) Harvest time.

2.2.2 Experiment 2

After planting two onion varieties (*Rijnsburger, Bedfordshire Champion*) in January 2021, the onions were transferred to three-line NFT systems, each lane had ten onions (five onions for each variety). Se treatment was carried out every other week since 14/02/2021 until harvest time. For the purpose of

element analysis, a sample was collected on 02/03/2021 during the growing stage (Figure 19A) before harvest; on May 18th, onions were harvested (Figure 19B), and the leaves and bulbs were dried out in the freezer dryer before being kept in the freezer for future use. To study whether Selenium affects onion bulb storage, the remaining bulbs were stored in at room temperature for three months.

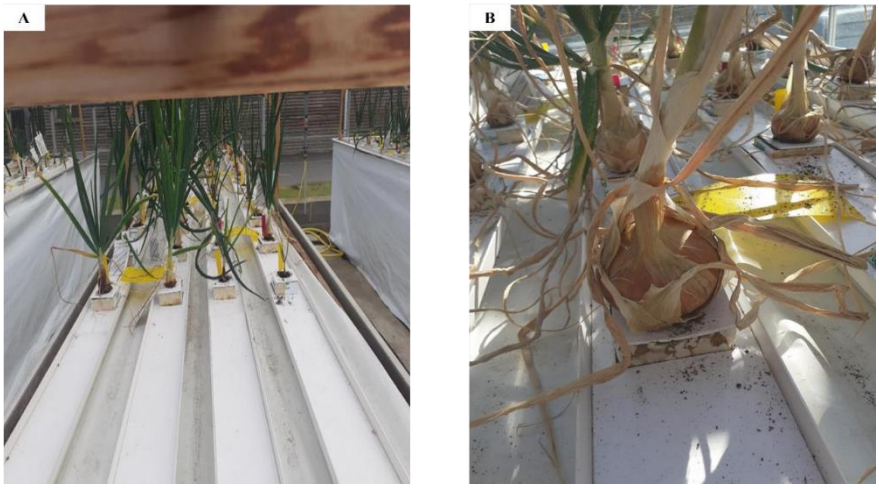

Figure 19: The two onion varieties growing in NFT. (A) Onions in the development phase. (B) Immediately prior to harvest.

2.2.3 Experiment 3

In the last NFT study, two onion varieties (*Rijnsburger and Bedfordshire Champion*) and a Spring onion (White Lisbon) (This is not the same species as the onions used in the other experiments (Rijnsburger and Bedfordshire Champion), as it belongs to ***Allium fistulosum L.***, commonly known as Welsh onion, scallion, or Japanese bunching onion, whereas the other onions are varieties of ***Allium cepa***) were grown in the NFT system according to the previous timeframe (Figure 20A, B). In

this case, the plants only received a single application of Se on 7 weeks old due to poor growth of onions, so they were harvested three weeks after the Se application. Hence, entire Spring onion plants and bulb onions were dried in a freezer dryer before being stored in a freezer for future studies (ICP-MS and biological experiments).

As a note, in both experiments 2 and 3, Sodium Selenate solution was added at the following concentrations: (1) Control; (2) 5 µg ml^{-1}; (3) 50 µg ml^{-1}.

Figure 20: (A, B) Spring onions growing in NFT.

2.2.4 ICP-MS of samples

Methodology:

Inductively Coupled Plasma Mass Spectrometry (ICP-MS) Analysis

The elemental content of onions and spring onions was measured at various growth stages using Inductively Coupled Plasma Mass Spectrometry (ICP-MS), an advanced analytical technique known for its precision and sensitivity in detecting and quantifying trace elements and isotopes. This technique is particularly suitable for selenium biofortification studies due to its capability to measure elemental concentrations at trace levels (Huang et al., 2021; Matusiewicz & Barnes, 1985). The methodology varied slightly across experiments, but the overall process ensured consistent and accurate preparation of samples for ICP-MS analysis.

Sample Collection and Preparation

Samples were collected at specific growth stages depending on the experiment. For Experiment 1, samples were taken at 11, 20, and 26 weeks during the onion growing season. At each time point, four onions were randomly selected from each line, totalling 24 samples per stage. Fresh leaves and bulbs were weighed separately, frozen, and then placed in a freezer dryer to remove moisture while preserving structural and chemical integrity. After drying, the samples were ground using liquid nitrogen to create a fine, homogenous powder suitable for digestion and analysis (Jones & Case, 1990).

Digestion Process

The digestion process differed across experiments.

Microwave Digestion (Experiment 1):
Microwave digestion involved carefully weighing 0.2–0.5 g of powdered samples into digestion tubes, followed by the addition of concentrated nitric acid (HNO_3). The tubes were sealed and subjected to controlled heating and pressure in a microwave digestion system,

ensuring uniform digestion and minimizing contamination (Kingston & Haswell, 1997).

Hot Plate Acid Digestion (Experiments 2 and 3):

For Experiments 2 and 3, the hot plate acid digestion method was used, where powdered samples were combined with concentrated nitric acid (HNO_3) and hydrogen peroxide (H_2O_2) in open digestion systems. This process was performed on a hot plate until the samples were fully digested, ensuring thorough breakdown of organic material (Jones & Case, 1990).

ICP-MS Analysis

Once digestion was completed, the samples were filtered, diluted, and introduced into the ICP-MS system. During the ICP-MS process, the digested samples were converted into a fine aerosol and introduced into a high-temperature argon plasma, which ionized the samples into constituent atoms and charged ions. These ions were then passed through a mass spectrometer, where they were separated based on their mass-to-charge ratio. The ions were subsequently detected, and their intensities were converted into quantitative data in parts per billion (ppb) (Matusiewicz & Barnes, 1985; Thomas, 2004).

ICP-MS allows for the simultaneous detection of multiple elements, offering a comprehensive elemental profile, which was critical for measuring selenium concentrations in leaves and bulbs and assessing its interaction with other trace elements (Jarvis & Gray, 1989).

Data Analysis

A two-factor ANOVA was used to evaluate the effects of selenium treatment and sampling time on elemental concentrations. The statistical results provided insights into selenium distribution and uptake dynamics between leaves and bulbs across different selenium

treatments, including control, 5 µg/ml, and 50 µg/ml. By employing both microwave and hot plate digestion techniques, the methodology ensured consistent and accurate preparation of samples, while the use of a freezer dryer and liquid nitrogen preserved the structural and chemical integrity of the samples. The ICP-MS analysis, with its precision and ability to measure multiple elements simultaneously, was helpful in understanding selenium uptake and biofortification effectiveness in onion plants (Huang et al., 2021).

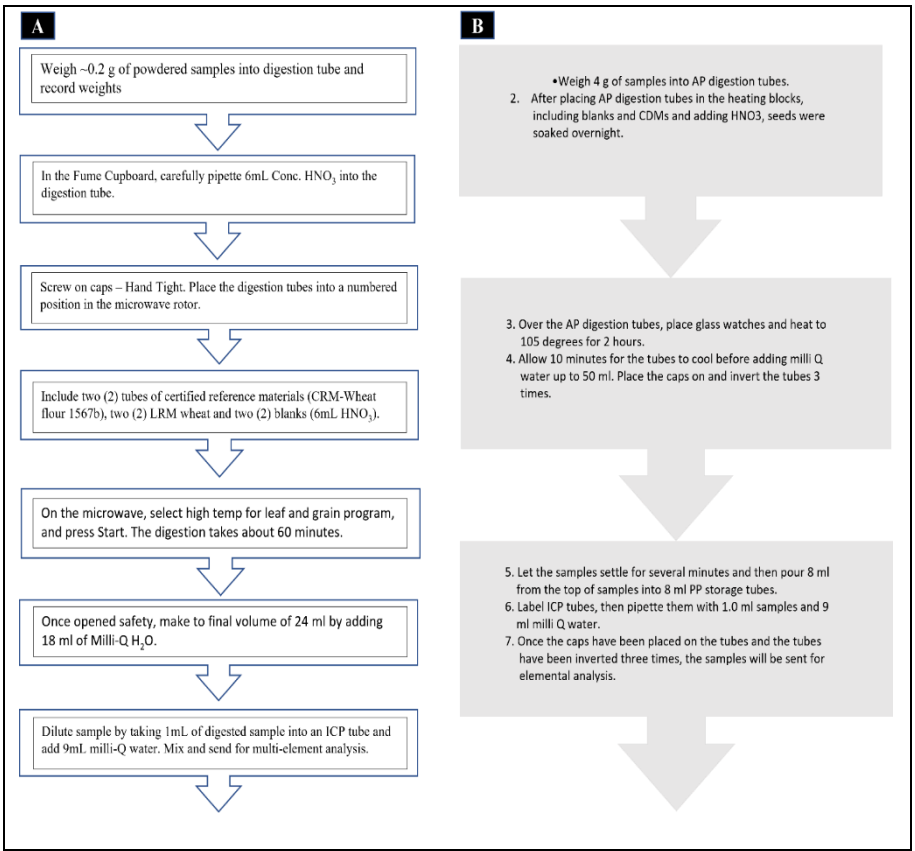

Figure 21: Microwave Digestion and Hot Plate Acid Digestion Method.

The fold changes between the leaves and bulbs of two samples after ICP-MS results were determined by applying the following formulas:

Se5 leaf: $\frac{\text{Average Se content in leaf with Se5}}{\text{Average Se content in leaf with Se0}}$

Se50 leaf: $\frac{\text{Average Se content in leaf with Se50}}{\text{Average Se content in leaf with Se0}}$

Se5 bulb: $\frac{\text{Average Se content in bulb with Se5}}{\text{Average Se content in bulb with Se0}}$

Se50 bulb: $\frac{\text{Average Se content in bulb with Se50}}{\text{Average Se content in bulb with Se0}}$

2.3 Results

Experiment 1 (White Onion – Rijnsburger):

Selenium (Se) biofortification positively correlates with most elements in onion plants, with concentrations generally higher in leaf tissues than in bulbs. During the first experiment, increased Se concentrations resulted in elevated Se levels in both leaves and bulbs. However, as onions matured, selenium content in bulbs decreased compared to earlier developmental stages. Throughout all growth stages, Se50 treatment significantly enhanced selenium levels in leaves (150.96 mg kg^{-1} DW) and bulbs (119.8 mg kg^{-1} DW) compared to the control (leaves: 0.26 mg kg^{-1} DW, bulbs: 0.72 mg kg^{-1} DW). Selenium content consistently remained higher in leaves than in bulbs. The statistical significance of these findings (p-values: 0.0002 and 0.002) confirms that Se levels differ across growth stages ($p < 0.05$), while no significant differences were found in tissue factors or their interactions ($p > 0.05$) with 95% confidence. Sulfur concentrations generally increased with selenium biofortification, suggesting a positive interaction between Se and S uptake mechanisms.

However, during bulb maturation, S levels declined compared to earlier stages, indicating possible nutrient redistribution or allocation towards physiological processes necessary for maturation. This reduction in sulfur content within bulbs may reflect a trade-off, where sulfur is redirected to other tissues or functions. Notably, the tissue factor exhibited a statistically significant difference during maturation ($p = 0.04 < 0.05$), whereas Se levels and interactions between factors did not exhibit significant differences. Iron concentrations were influenced by selenium treatments and growth stages. In Se5-treated plants, Fe content was lowest during the development phase, both in leaves (55.99 mg kg^{-1} DW) and bulbs (15.19 mg kg^{-1} DW), compared to control and Se50 treatments. During maturation, slight increases in Fe content were observed under Se50 treatment, aligning closer to control values. ANOVA analysis revealed significant differences in Fe content based on tissue factors during development ($p = 0.026$), but no significant differences were detected for Se levels or interactions.

Magnesium content exhibited tissue-specific responses to selenium treatments. In leaves, Mg levels remained stable during the development phase but increased significantly under Se5 treatment during maturation, peaking at 4780.90 mg kg^{-1} DW. In bulbs, Mg concentrations declined under Se50 treatment during the development phase but reached their highest concentration of 1264.96 mg kg^{-1} DW during maturation, suggesting that Se50 promotes delayed Mg accumulation in bulbs. In the development phase, all p-values for Mg were below 0.05, indicating significant effects of all factors and their interactions. During the maturation phase, the Se levels factor and interactions also

showed statistical significance ($p = 0.001$ and 0.027, respectively).

Potassium content demonstrated variable responses depending on the growth stage and tissue type. Increasing selenium concentrations had no significant effect on K content during the development phase. However, during maturation, K content decreased in bulbs, particularly under Se5 treatment, while leaves maintained higher K levels across all treatments. Calcium exhibited distinct trends between leaf and bulb tissues. In leaves, Ca levels increased with rising selenium concentrations, especially under Se5 treatment during maturation, reaching 13255.44 mg kg^{-1} DW. Conversely, Ca content in bulbs declined as Se concentration increased, with Se50 treatment resulting in the lowest Ca levels (2012.14 mg kg^{-1} DW) during maturation. These findings suggest divergent nutrient allocation strategies influenced by selenium biofortification. ANOVA results indicated statistically significant differences in tissue factors for Ca during the maturation stage ($p = 0.0004$), but no significant differences were observed for Se levels or interactions.

Selenium biofortification significantly influences elemental composition in onions, with marked differences between leaves and bulbs. Higher selenium concentrations consistently result in greater Se accumulation in leaves than in bulbs. While sulfur uptake increases with selenium treatments, it declines during bulb maturation, indicating possible nutrient redistribution. Iron content shows minor fluctuations, with Se50 treatment mitigating inhibitory effects observed at lower Se levels. Magnesium content reveals delayed accumulation in bulbs under high selenium conditions. Potassium and calcium display

opposing trends, with leaves retaining higher levels of both elements while bulbs show reduced concentrations under increasing selenium treatments. These results highlight complex nutrient interactions and redistribution patterns influenced by selenium biofortification, suggesting potential trade-offs in nutrient storage and utilization during different growth stages.

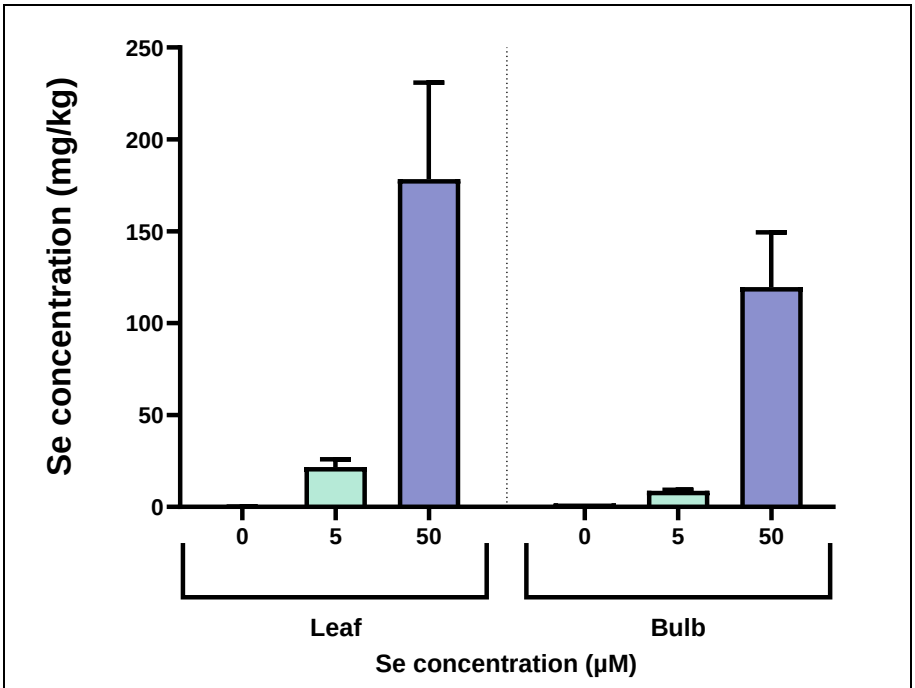

Source of Variation	*SS*	*df*	*MS*	*F*	*P-value*	*F crit*
Sample	182308.1	2	91154.04	13.53398	0.000259	3.554557
Columns	4859.056	1	4859.056	0.721442	0.406827	4.413873
Interaction	7948.636	2	3974.318	0.590082	0.564653	3.554557
Within	121233.6	18	6735.198			
Total	316349.3	23				

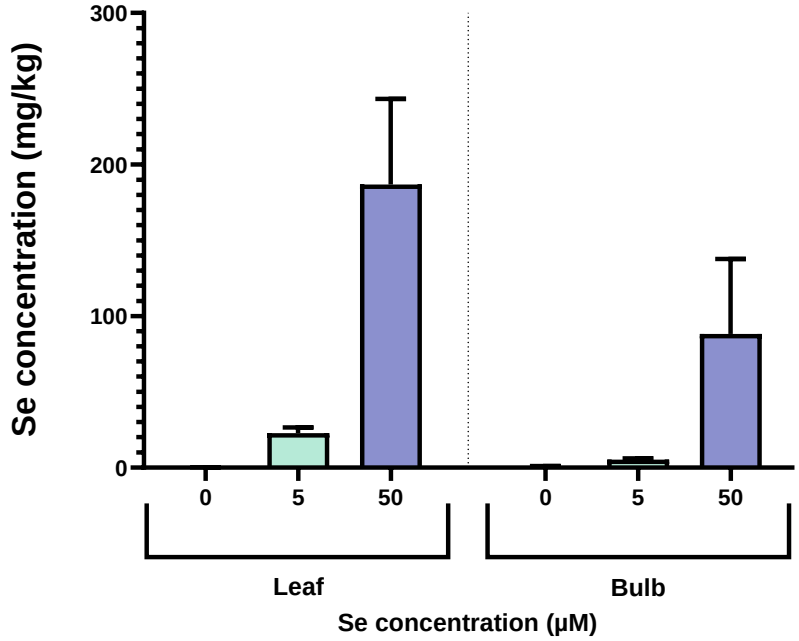

Source of Variation	*SS*	*df*	*MS*	*F*	*P-value*	*F crit*
Sample	274907.4	2	137453.7	8.369326	0.002692	3.554557
Columns	11309.39	1	11309.39	0.68861	0.417508	4.413873
Interaction	6713.677	2	3356.839	0.204392	0.817008	3.554557
Within	295623.2	18	16423.51			
Total	588553.7	23				

Figure 22: Bars and Anova analyse which show effect of selenium biofortification on **Selenium** content in the leaf and bulb of onions grown hydroponically for 77 and 140 days old (A and B respectively). Bars show Mean ± SD. n=4.

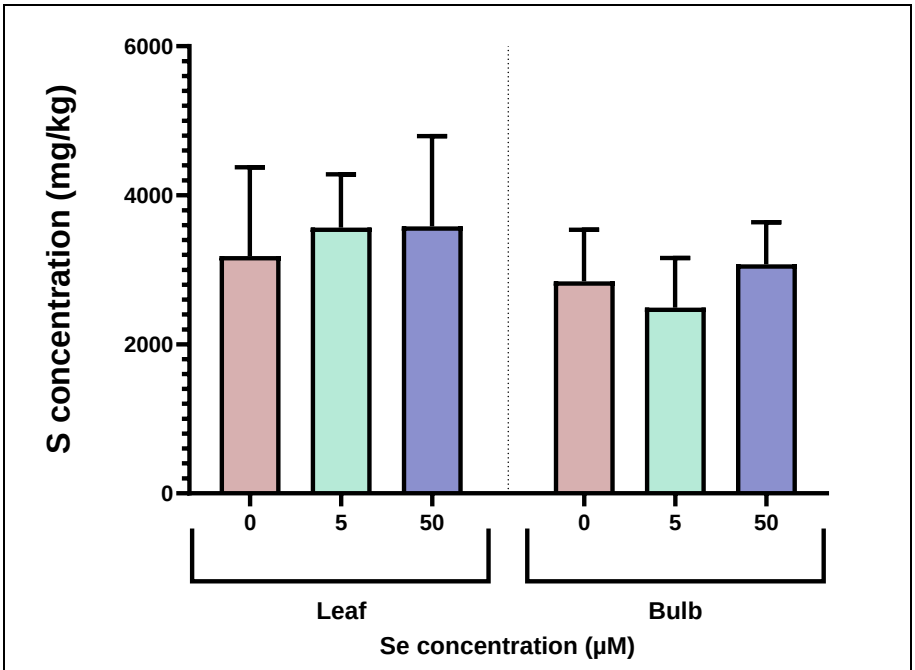

Source of Variation	*SS*	*df*	*MS*	*F*	*P-value*	*F crit*
Sample	6825417	2	3412709	1.468221	0.256641	3.554557
Columns	8901795	1	8901795	3.829746	0.066044	4.413873
Interaction	3011614	2	1505807	0.647831	0.534953	3.554557
Within	41838891	18	2324383			
Total	60577718	23				

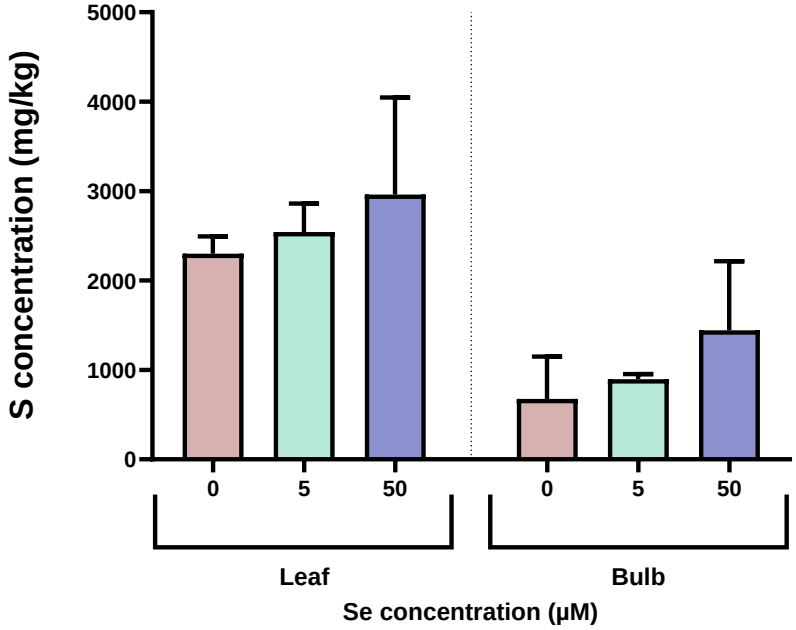

Sample	19888786	2	9944393	1.83354	0.188473	3.554557
Columns	25618849	1	25618849	4.723584	0.043343	4.413873
Interaction	4922630	2	2461315	0.453815	0.642271	3.554557
Within	97624867	18	5423604			
Total	1.48E+08	23				

Figure 23: Bars and ANOVA analysis which show effect of selenium biofortification on Sulfur content in the leaf and bulb of onions grown hydroponically for 77 and 140 days old (A and B respectively). Bars show Mean ± SD. n=4.

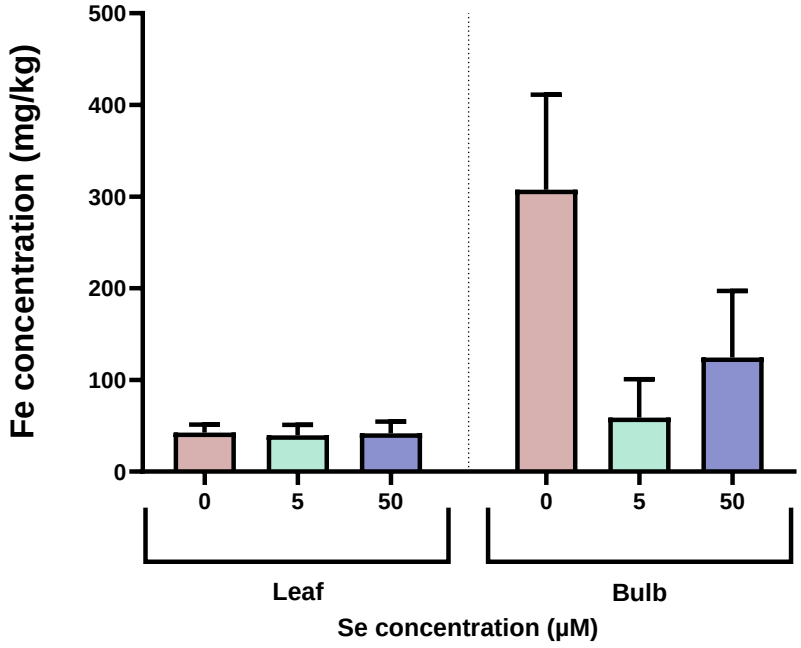

Source of Variation	*SS*	*df*	*MS*	*F*	*P-value*	*F crit*
Sample	15786.3	2	7893.15	0.345374	0.712545	3.554557
Columns	133822.2	1	133822.2	5.85555	0.026332	4.413873
Interaction	14825.35	2	7412.673	0.32435	0.727135	3.554557
Within	411370.4	18	22853.91			
Total	575804.2	23				

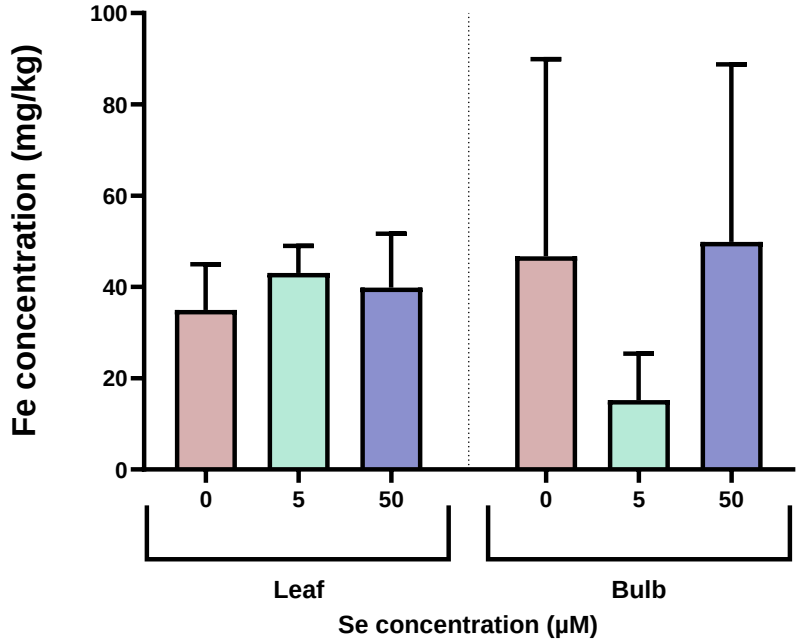

Source of Variation	*SS*	*df*	*MS*	*F*	*P-value*	*F crit*
Sample	99112.53	2	49556.26	0.816563	0.457665	3.554557
Columns	88325.55	1	88325.55	1.455384	0.243283	4.413873
Interaction	112379.3	2	56189.64	0.925864	0.414255	3.554557
Within	1092399	18	60688.84			
Total	1392217	23				

Figure 24: Bars and Anova analysis which show effect of selenium biofortification on Iron content in the leaf and bulb of onions grown hydroponically for 77 and 140 days old (A and B respectively). Bars show Mean ± SD. n=4.

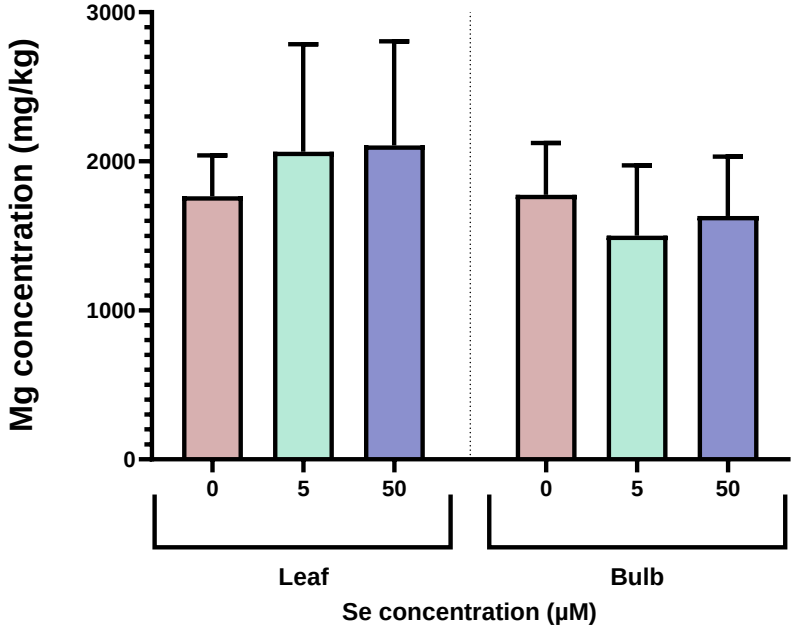

Source of Variation	*SS*	*df*	*MS*	*F*	*P-value*	*F crit*
Sample	22209.88	2	11104.94	0.059115	0.942781	3.554557
Columns	613138.7	1	613138.7	3.263899	0.087568	4.413873
Interaction	314715.1	2	157357.6	0.837656	0.448909	3.554557
Within	3381385	18	187854.7			
Total	4331448	23				

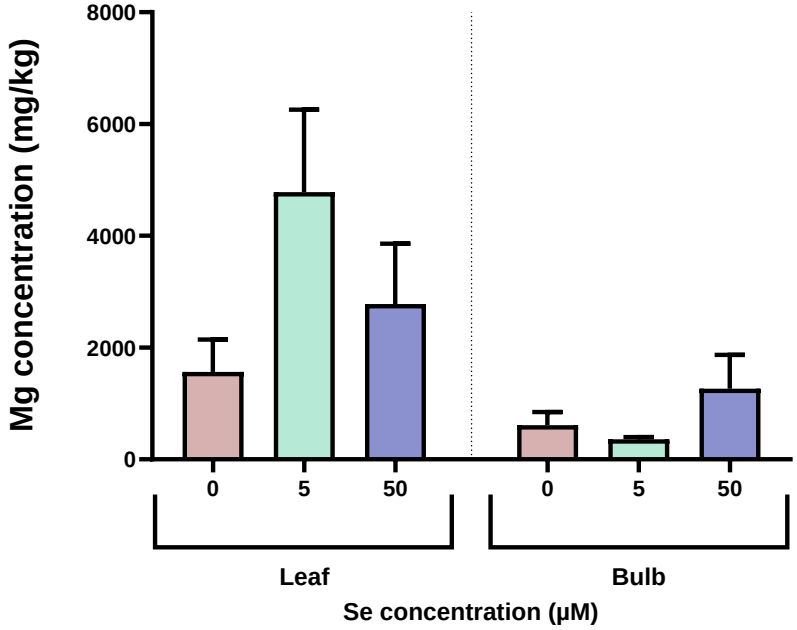

Source of Variation	*SS*	*df*	*MS*	*F*	*P-value*	*F crit*
Sample	3321677	2	1660839	1.293034	0.298739	3.554557
Columns	18150269	1	18150269	14.13076	0.001437	4.413873
Interaction	11282660	2	5641330	4.392016	0.027962	3.554557
Within	23120121	18	1284451			
Total	55874727	23				

Figure 25: Bars and Anova analyse which show effect of selenium biofortification on Magnesium content in the leaf and bulb of onions grown hydroponically for 77 and 140 days old (A and B respectively). Bars show Mean ± SD. n=4.

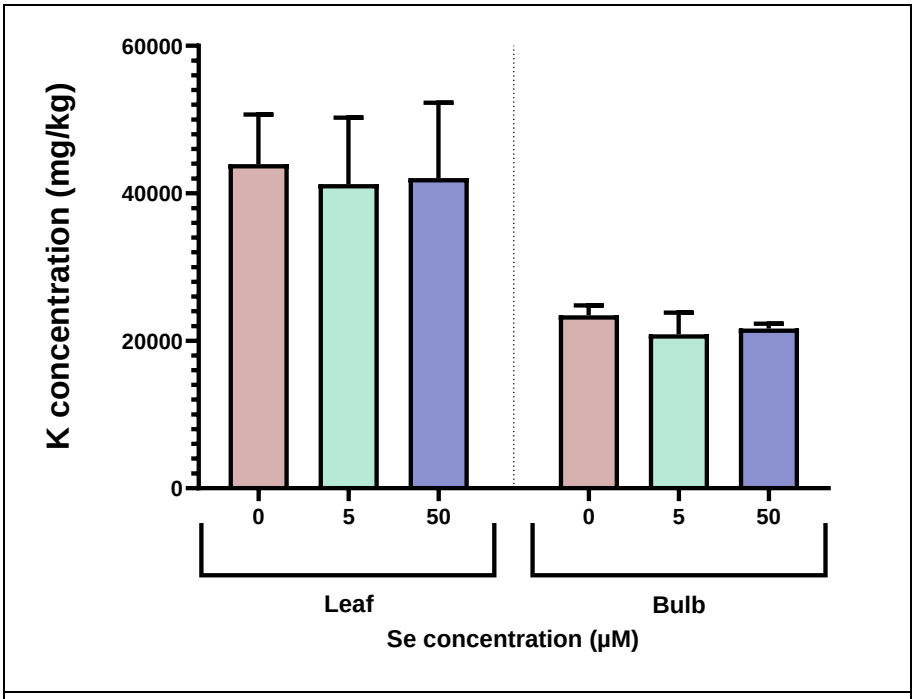

Source of Variation	*SS*	*df*	*MS*	*F*	*P-value*	*F crit*
Sample	26081150	2	13040575	0.304407	0.741284	3.554557
Columns	2.55E+09	1	2.55E+09	59.50911	4.1E-07	4.413873
Interaction	546932.8	2	273466.4	0.006384	0.993639	3.554557
Within	7.71E+08	18	42839290			
Total	3.35E+09	23				

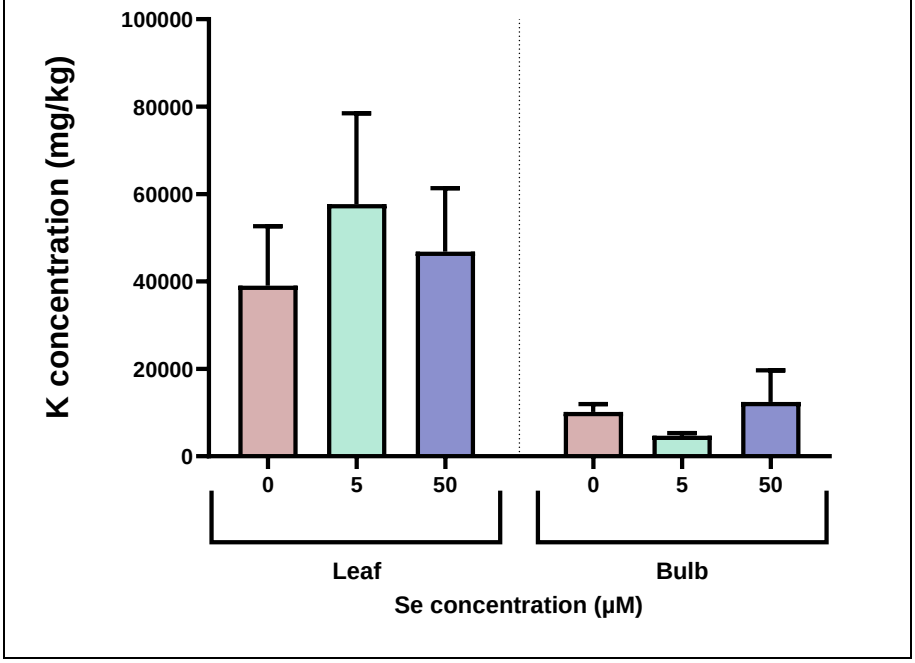

Source of Variation	*SS*	*df*	*MS*	*F*	*P-value*	*F crit*
Sample	2.41E+08	2	1.21E+08	0.636123	0.540831	3.554557
Columns	7.98E+09	1	7.98E+09	42.07189	4.23E-06	4.413873
Interaction	8.42E+08	2	4.21E+08	2.220163	0.137464	3.554557
Within	3.41E+09	18	1.9E+08			
Total	1.25E+10	23				

Figure 26: Bars and ANOVA analysis which show effect of selenium biofortification on Potassium content in the leaf and bulb of onions grown hydroponically for 77 and 140 days (A and B respectively). Bars show Mean ± SD. n=4.

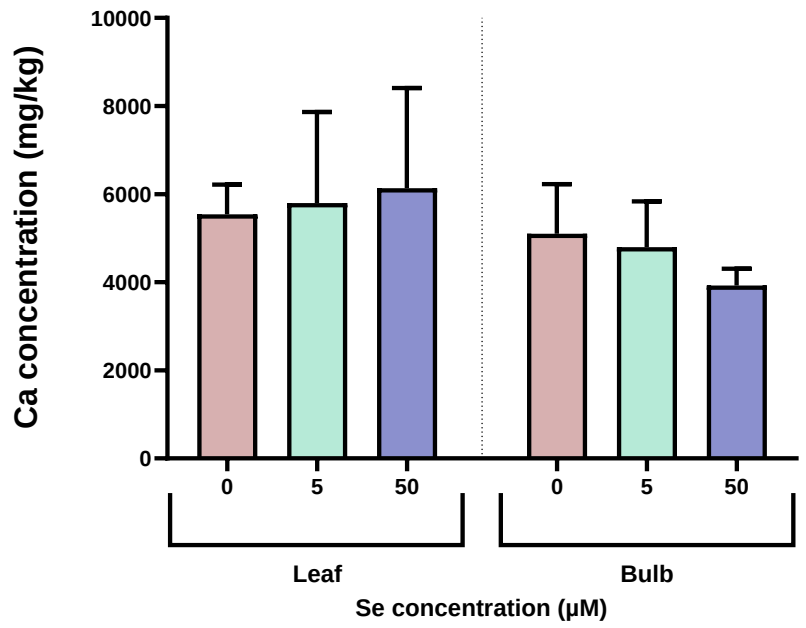

Source of Variation	*SS*	*df*	*MS*	*F*	*P-value*	*F crit*
Sample	294888.1	2	147444.1	0.069614	0.933004	3.554557
Columns	8029580	1	8029580	3.791057	0.067302	4.413873
Interaction	3947114	2	1973557	0.931788	0.412036	3.554557
Within	38124573	18	2118032			
Total	50396155	23				

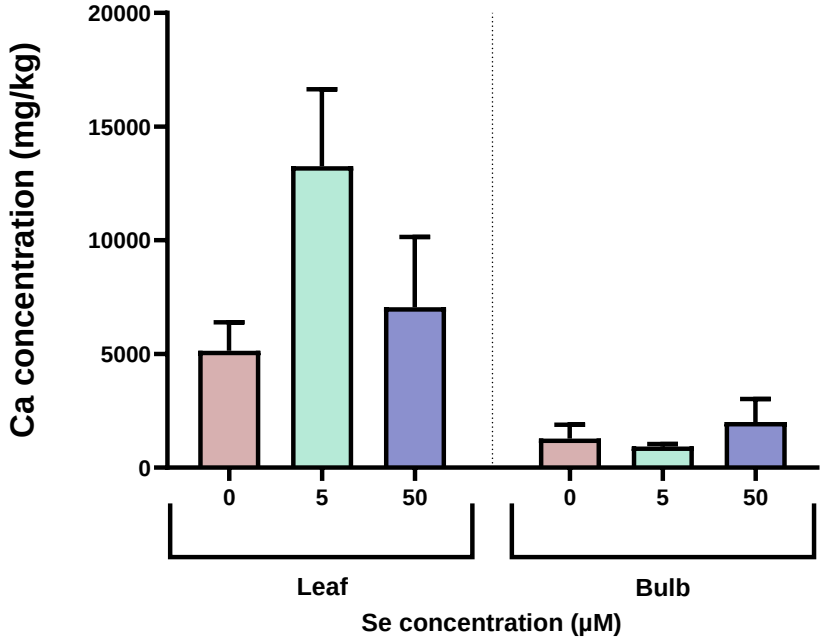

Source of Variation	SS	df	MS	F	P-value	F crit
Sample	19170242	2	9585121	0.898808	0.424557	3.554557
Columns	1.91E+08	1	1.91E+08	17.93526	0.000498	4.413873
Interaction	66670570	2	33335285	3.125888	0.068353	3.554557
Within	1.92E+08	18	10664259			
Total	4.69E+08	23				

Figure 27: Bars and ANOVA analysis which show effect of selenium biofortification on Calcium content in the leaf and bulb of onions grown hydroponically for 77 and 140 days (A and B respectively). Bars show Mean ± SD. n=4.

2.3.1 Fold change of Se at two time points:

The results of Table 3 show the fold change of Se in the first and second samples at two time points. The table shows that the rate of growth is different at each time point for both leaf and bulb at Se5 and Se50. From development to the final phase of growth, the fold change increased in all selenium concentration treatments as well as both

tissue types (leaf and bulb). Additionally, bulb fold change is lower than leaf fold change. Conclusively, due to the results showing that Se concentrations increase over time, we can conclude that tissue saturation is not occurring.

Table 3: Fold change of Se content mg/kg DW at two time points, Experiment1.

Tissue	Se levels	Average Sample 1	Average Sample 2	Fold change Sample 1	Fold change Sample 2
Leaf	0	0.26	0.14		
Leaf	5	15.01	22.75	57.05	161.84
Leaf	50	230.76	186.74	876.58	1328.08
Bulb	0	0.72	0.67		
Bulb	5	8.97	5.36	12.33	7.89
Bulb	50	150.96	88.14	207.51	129.69

Experiment 2 (Rijnsburger and Bedfordshire Champion Varieties):

There was variable correlation between selenium biofortification and other elements, either positively or negatively. In most cases, onion bulbs showed higher selenium content compared to leaves, with red onions demonstrating better selenium accumulation properties than yellow onions in both leaves and bulbs. Following Se50 treatment, selenium content in the leaves of red and yellow onion varieties, as well as their bulbs, increased to 65.54 mg kg-1DW and 52.79 mg kg-

1DW, respectively. The red variety of leaves contained significantly more selenium than the yellow variety under Se50 treatment. As the onions matured, selenium uptake increased, with the Se50 treatment resulting in substantial increases in selenium accumulation for both yellow and red varieties (107.5313 mg kg-1DW and 93.4454 mg kg-1DW, respectively), with the red variety demonstrating superior uptake (Figure 28 A, B). ANOVA analysis indicated that selenium levels significantly affected selenium content (P-value = 1.56E-07, F = 42.34), while onion variety (P = 0.598443) and interaction (P = 0.814126) were not significant. This suggests that selenium biofortification mainly depends on applied Se levels rather than variety type or their interaction.

For sulfur (S), Se50 significantly increased S levels in red onion leaves and bulbs, whereas yellow onion leaves showed an antagonistic relationship between selenium and sulfur, where increasing selenium levels reduced sulfur content. The sulfur content in bulbs decreased slightly over time, especially in yellow varieties, which had the lowest S level (3488.8576 mg kg-1DW) under Se50 treatment. During the maturation phase, the highest S absorption occurred in untreated red onions (4410.1576 mg kg-1DW) (Figure 29 A, B). However, ANOVA analysis indicated that selenium levels, onion variety, and their interactions were not significant for sulfur (P-values > 0.05).

Iron (Fe) content was not affected by selenium treatment in leaves, but bulbs showed antagonistic behaviour, with higher Fe contents observed in the control. The highest and lowest Fe concentrations in yellow bulbs were found under Se0 and Se50 treatments (27.8174 mg kg-1DW and 16.8372 mg kg-1DW, respectively). In contrast, red onions did not show a significant effect on Fe uptake according to Se levels (Figure 30 A, B). ANOVA analysis showed that selenium levels

were borderline significant (P = 0.050258), but onion variety (P = 0.45908) and interaction (P = 0.10161) were not.

Magnesium (Mg) content displayed differing responses to Se levels depending on onion variety. For red leaves, Mg content decreased with increasing selenium, whereas for yellow leaves, Mg content increased. Se5 treatment had a substantial effect on Mg accumulation in yellow bulbs compared to the other Se levels (1583.46 mg kg-1DW and 1521.86 mg kg-1DW). During the last growth stage, yellow varieties exhibited antagonistic relationships between selenium and magnesium, where higher selenium levels reduced magnesium content (Figure 31 A, B). ANOVA results indicated that selenium levels (P = 0.024006, F = 4.620921) and the interaction between selenium levels and onion variety (P = 0.038529, F = 3.923418) were significant, while onion variety alone was not (P = 0.945597).

For potassium (K), an antagonistic relationship between selenium levels and K accumulation was observed for both varieties' bulbs, with increased selenium levels resulting in decreased K content. At maturation, the lowest K content was seen in Se5 for both varieties. The highest K content for red varieties was recorded under Se50 (24825.8991 mg kg-1DW), while the yellow variety showed the highest K content under control conditions (27887.0766 mg kg-1DW) (Figure 32 A, B). ANOVA analysis indicated no significant effects of selenium levels, onion variety, or their interactions (P-values > 0.05).

Calcium (Ca) content decreased with increasing Se levels in red leaves, indicating an antagonistic relationship. In contrast, the highest Ca content (9327.36 mg kg-1DW) was found under Se50 treatment in yellow leaves. The highest Ca content in yellow bulbs occurred under control conditions (6544.57 mg kg-1DW), while Se5 treatment

resulted in the most substantial Ca accumulation in red bulbs (4886.37 mg kg-1DW). ANOVA analysis showed no significant effects for Se levels, onion variety, or their interaction with Ca content (P-values > 0.05) (Figure 33 A, B).

Overall, selenium biofortification significantly affects selenium and magnesium content, particularly when interacting with onion variety, while the influence on sulfur, iron, potassium, and calcium appears to be negligible. The lack of significant differences during the maturation phase for most elements suggests that selenium biofortification practices may be more effective during developmental stages rather than at maturity. Future research should focus on understanding the mechanisms behind selenium's interaction with magnesium to enhance nutritional value and stress resistance in onions.

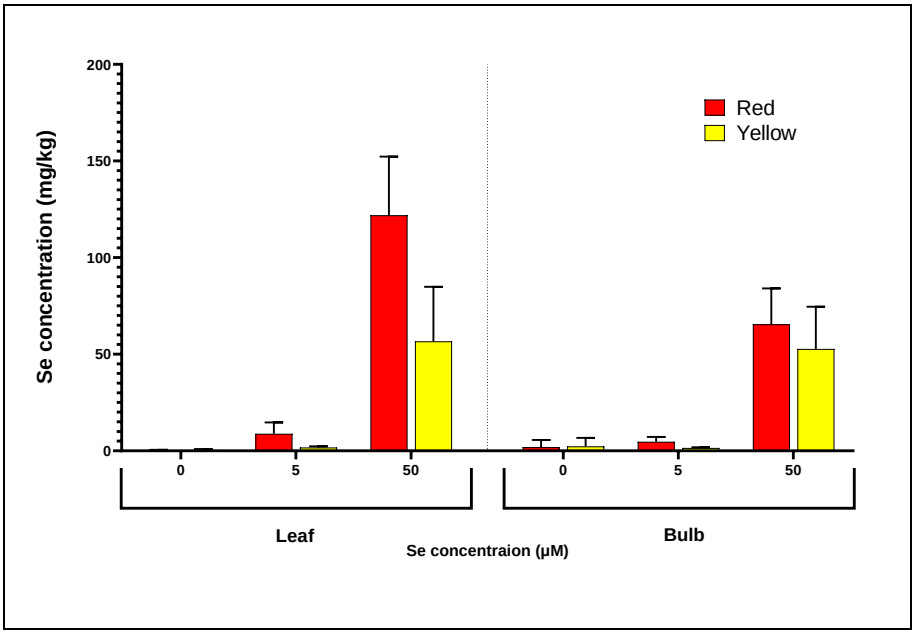

Analysis of variance

Variate: Selenium_concentration

Source of variation	d.f.	s.s.	m.s.	v.r.	F pr.
Onion_Variety	1	5717601.	5717601.	1.95	0.175
Tissue	1	67444209.	67444209.	23.01	<.001
Se_Levels	2	15103336.	7551668.	2.58	0.097
Onion_Variety.Tissue	1	5888498.	5888498.	2.01	0.169
Onion_Variety.Se_Levels	2	12716723.	6358361.	2.17	0.136
Tissue.Se_Levels	2	3547330.	1773665.	0.61	0.554
Onion_Variety.Tissue.Se_Levels	2	13455629.	6727814.	2.30	0.122
Residual	24	70350772.	2931282.		
Total 35	194224097.				

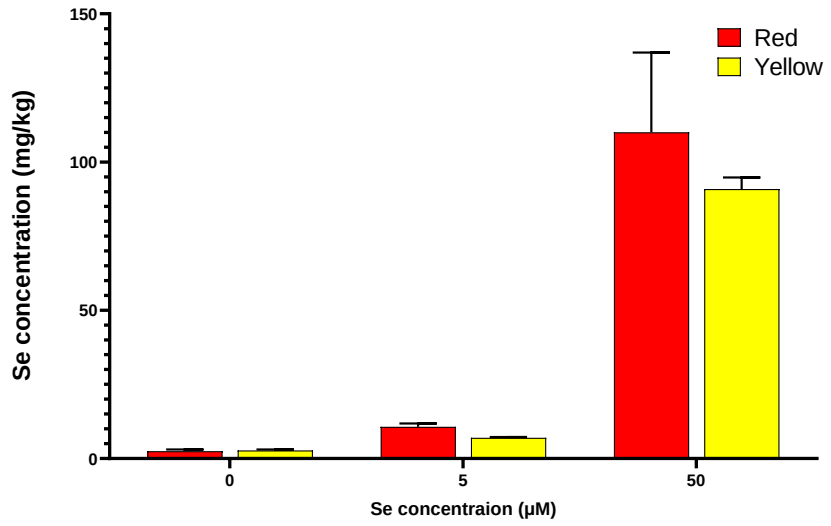

Source of Variation	*SS*	*df*	*MS*	*F*	*P-value*	*F crit*
Se_Levels	48589.51	2	24294.76	42.33776	1.56E-07	3.554557
Onion_Variety	164.9302	1	164.9302	0.287419	0.598443	4.413873
Interaction	238.7226	2	119.3613	0.208007	0.814126	3.554557
Within	10328.97	18	573.8318			
Total	59322.14	23				

Figure 28: Bars and ANOVA analysis which show effect of selenium treatments on the Se content in the leaf and bulb of two onion varieties grew hydroponically for 77 and on just bulbs for 140 days (A and B respectively). Bars show Mean ± SD. n=4

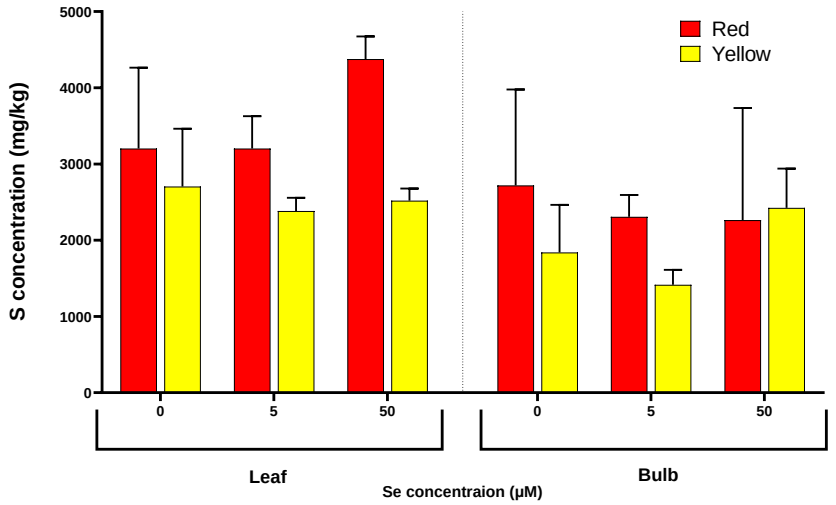

Analysis of variance

Variate: S_Cnocentration

Source of variation	d.f.	s.s.	m.s.	v.r.	F pr.
Onion_Variety	1	7439261.	7439261.	19.78	<.001
Tisuue	1	5372751.	5372751.	14.28	<.001
Se_Levels	2	3568492.	1784246.	4.74	0.018
Onion_Variety.Tisuue	1	151552.	151552.	0.40	0.532
Onion_Variety.Se_Levels	2	443356.	221678.	0.59	0.563
Tisuue.Se_Levels	2	83841.	41921.	0.11	0.895
Onion_Variety.Tisuue.Se_Levels	2	1223775.	611887.	1.63	0.218
Residual	24	9028553.	376190.		
Total 35		27311580.			

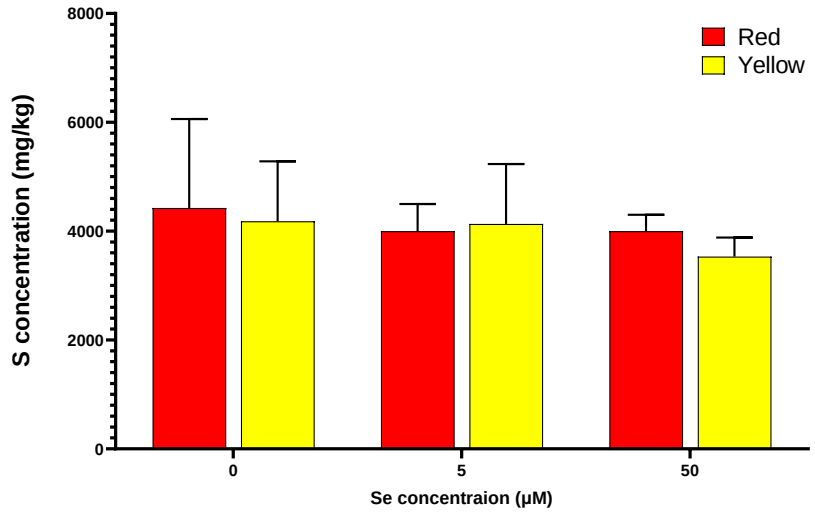

ANOVA S

Source of Variation	*SS*	*df*	*MS*	*F*	*P-value*	*F crit*
Se_Levels	1168945	2	584472.5	0.360707	0.702109	3.554557
Onion_Variety	212189.2	1	212189.2	0.130953	0.72166	4.413873
Interaction	621689.1	2	310844.6	0.191838	0.827107	3.554557
Within	29166333	18	1620352			
Total	31169157	23				

Figure 29: Bars and ANOVA analysis which show effect of selenium treatments on the S content in the leaf and bulb of two onion varieties grew hydroponically for 77 days and on just bulbs for 140 days (A and B respectively). Bars show Mean ± SD. n=4

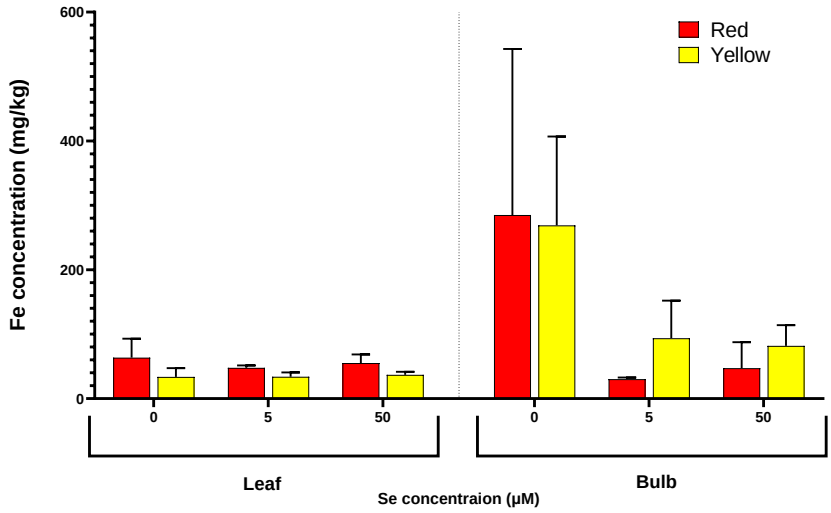

Analysis of variance

Variate: Fe_Concentration

Source of variation	d.f.	s.s.	m.s.	v.r.	F pr.
Onion_Variety	1	459.	459.	0.06	0.810
Tissue	1	71691.	71691.	9.25	0.006
Se_Levels	2	96763.	48382.	6.24	0.007
Onion_Variety.Tissue	1	5305.	5305.	0.68	0.416
Onion_Variety.Se_Levels	2	3349.	1675.	0.22	0.807
Tissue.Se_Levels	2	91067.	45534.	5.88	0.008
Onion_Variety.Tissue.Se_Levels	2	2014.	1007.	0.13	0.879
Residual	24	185943.	7748.		
Total 35	456593.				

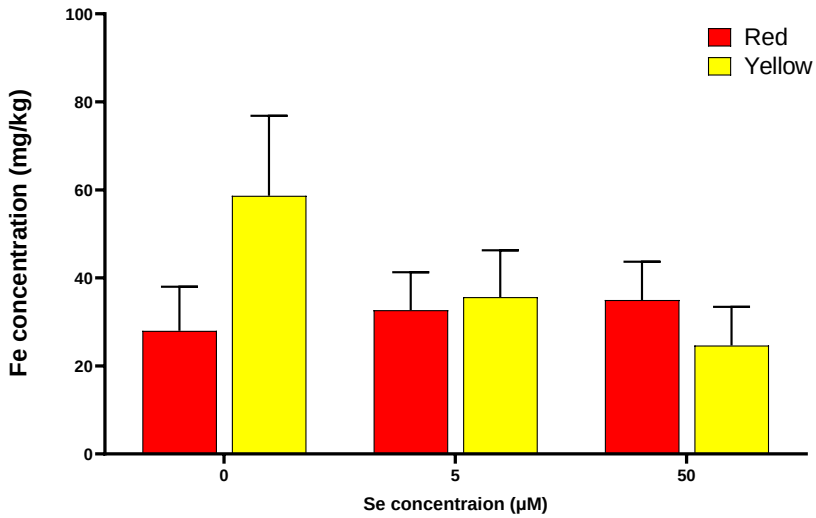

ANOVA Fe

Source of Variation	*SS*	*df*	*MS*	*F*	*P-value*	*F crit*
Se_Levels	1456.89	2	728.4448	3.547384	0.050258	3.554557
Onion_Variety	117.549	1	117.549	0.572441	0.45908	4.413873
Interaction	1069.173	2	534.5863	2.603331	0.10161	3.554557
Within	3696.247	18	205.347			
Total	6339.858	23				

Figure 30: Bars and ANOVA analysis which show effect of selenium treatments on the Fe content in the leaf and bulb of two onion varieties grew hydroponically for 77 and on just bulbs for 140 days (A and B respectively). Bars show Mean ± SD. n=4

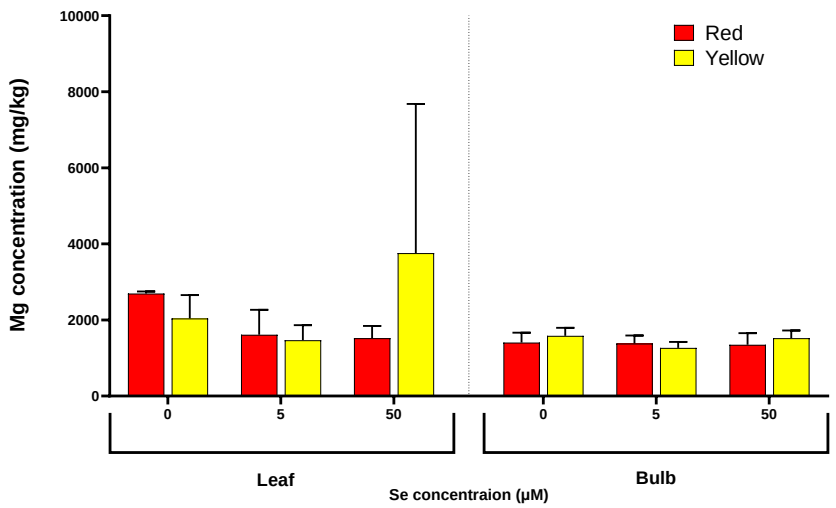

Analysis of variance

Variate: Mg_Concentration

Source of variation	d.f.	s.s.	m.s.	v.r.	F pr.
Onion_Variety	1	76967.	76967.	0.50	0.485
Tissue	1	6443457.	6443457.	42.13	<.001
Se_Levels	2	323513.	161757.	1.06	0.363
Onion_Variety.Tissue	1	226969.	226969.	1.48	0.235
Onion_Variety.Se_Levels	2	804688.	402344.	2.63	0.093
Tissue.Se_Levels	2	285328.	142664.	0.93	0.407
Onion_Variety.Tissue.Se_Levels	2	428467.	214233.	1.40	0.266
Residual	24	3670213.	152926.		
Total	35	12259602.			

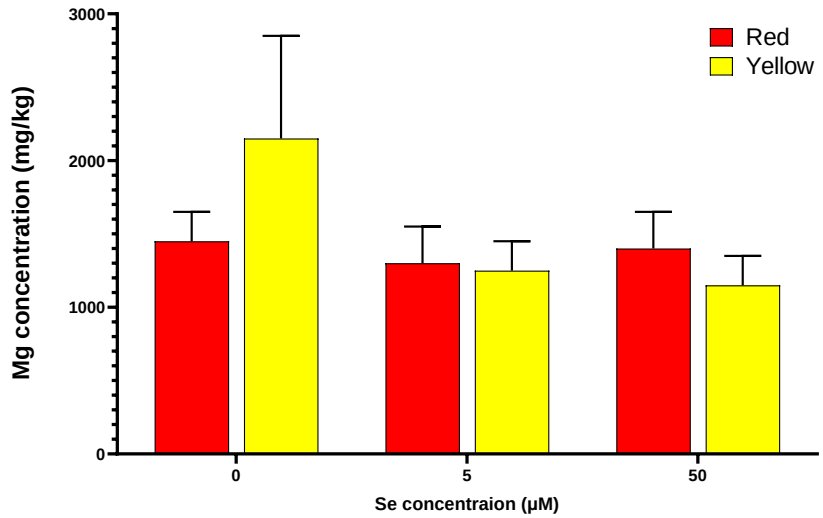

ANOVA Mg

Source of Variation	*SS*	*df*	*MS*	*F*	*P-value*	*F crit*
Se_Levels	1516240	2	758120.1	4.620921	0.024006	3.554557
Onion_Variety	785.5247	1	785.5247	0.004788	0.945597	4.413873
Interaction	1287372	2	643686	3.923418	0.038529	3.554557
Within	2953126	18	164062.6			
Total	5757524	23				

Figure 31: Bars and ANOVA analysis which shows the effect of selenium treatments on the Mg content in the leaf and bulb of two onion varieties grew hydroponically for 77 and on just bulbs for 140 days (A and B respectively). Bars show Mean ± SD. n=4

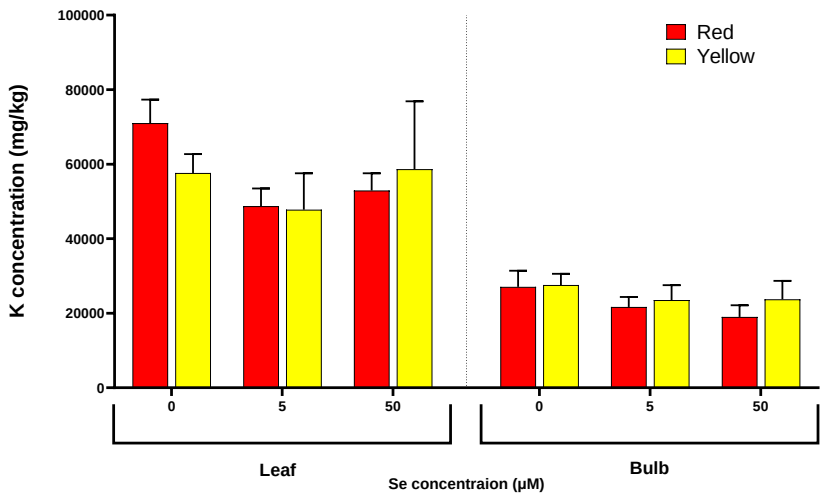

Analysis of variance

Variate: K_Concentration

Source of variation	d.f.	s.s.	m.s.	v.r.	F pr.
Onion_Variety	1	2.587E+06	2.587E+06	0.05	0.824
Tissue	1	9.000E+09	9.000E+09	176.29	<.001
Se_Levels	2	8.014E+08	4.007E+08	7.85	0.002
Onion_Variety.Tissue	1	1.168E+08	1.168E+08	2.29	0.143
Onion_Variety.Se_Levels	2	1.682E+08	8.411E+07	1.65	0.214
Tissue.Se_Levels	2	1.714E+08	8.568E+07	1.68	0.208
Onion_Variety.Tissue.Se_Levels	2	5.001E+07	2.501E+07	0.49	0.619
Residual	24	1.225E+09	5.105E+07		
Total	35	1.154E+10			

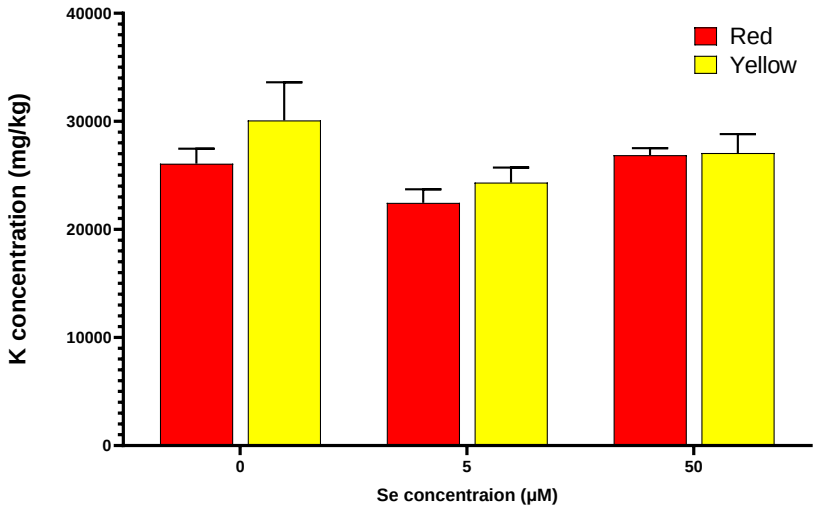

ANOVA K

Source of Variation	*SS*	*df*	*MS*	*F*	*P-value*	*F crit*
Se_Levels	53748719	2	26874359	0.89409	0.426383	3.554557
Onion_Variety	7998253	1	7998253	0.266096	0.612241	4.413873
Interaction	20751449	2	10375724	0.345193	0.71267	3.554557
Within	5.41E+08	18	30057784			
Total	6.24E+08	23				

Figure 32: Bars and ANOVA analysis which show the effect of selenium treatments on the K content in the leaf and bulb of two onion varieties grew hydroponically for 77 and on just bulbs for 140 days (A and B respectively). Bars show Mean ± SD. n=4

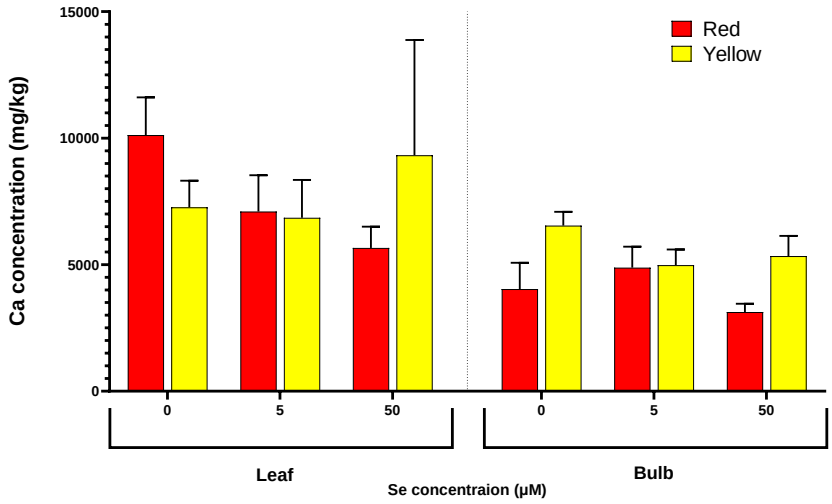

Analysis of variance

Variate: Ca_Concentration

Source of variation	d.f.	s.s.	m.s.	v.r.	F pr.
Onion_Variety	1	5717604.	5717604.	1.95	0.175
Tissue	1	67444204.	67444204.	23.01	<.001
Se_Levels	2	15103332.	7551666.	2.58	0.097
Onion_Variety.Tissue	1	5888496.	5888496.	2.01	0.169
Onion_Variety.Se_Levels	2	12716719.	6358360.	2.17	0.136
Tissue.Se_Levels	2	3547327.	1773663.	0.61	0.554
Onion_Variety.Tissue.Se_Levels	2	13455624.	6727812.	2.30	0.122
Residual	24	70350762.	2931282.		
Total 35	194224067.				

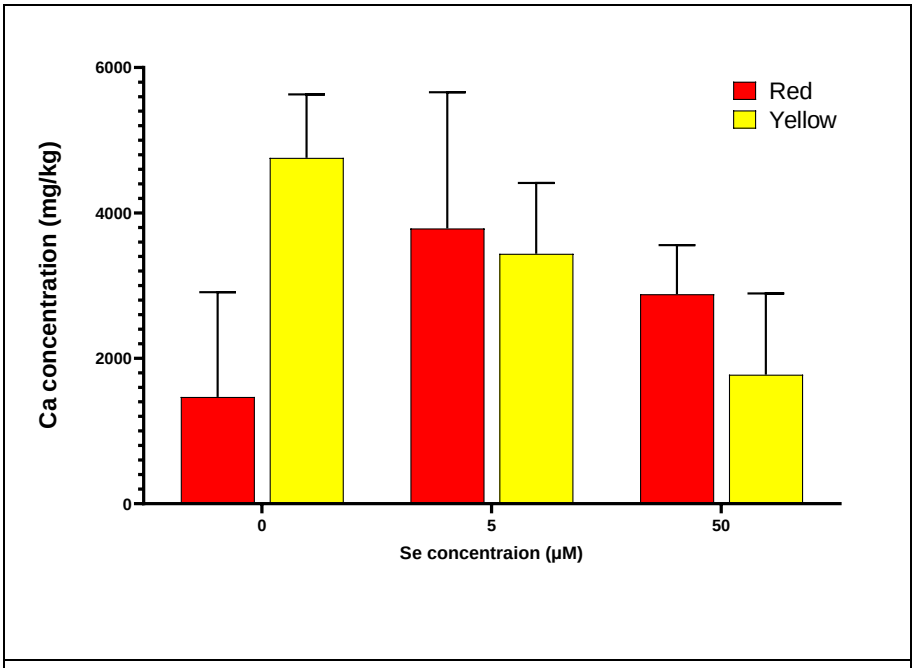

ANOVA Ca

Source of Variation	*SS*	*df*	*MS*	*F*	*P-value*	*F crit*
Se_Levels	8237535	2	4118767	2.579068	0.103543	3.554557
Onion_Variety	1381708	1	1381708	0.865191	0.364598	4.413873
Interaction	9213616	2	4606808	2.884667	0.081903	3.554557
Within	28745970	18	1596998			
Total	47578829	23				

Figure 33: Bars and Anova which show effect of selenium treatments on the Ca content in the leaf and bulb of two onion varieties grew hydroponically for 77 and on just bulbs for 140 days (A and B respectively). Bars show Mean ± SD. n=4

2.3.2 Effect of Selenium on Stored Onion bulbs:

To assess the impact of Selenium on onion bulb quality during storage, fresh onion bulbs from two varieties, subjected to various Se treatments, were stored in a cold, dark environment for three months. Their weights were recorded weekly throughout the storage period. The resulting data were analysed using Excel and GenStat (ANOVA). Additionally, after the storage period, the onion bulbs were dried using

freeze-dryers and subsequently stored in a freezer for further analysis. This subsequent evaluation aimed to determine whether Selenium presence influenced the mineral content of the onions after storage compared to their composition at harvest.

All onion bulbs experienced weight loss due to water loss during storage. However, some bulbs exhibited weight gain later in the storage period due to germination. Based on the gradual weight change over three months, the Se5 treatment had the most favourable impact on stored red and yellow bulbs, with yellow bulbs showing less weight alteration compared to red bulbs. This indicates that yellow bulbs maintained higher quality during storage (Figure 34).

ANOVA analysis revealed that all P-values for the two factors (Se levels and tissue type) and their interaction were below 0.05 ($P = 0.001$), indicating a significant difference between the factors and their interaction. These findings suggest that Selenium positively influences onion bulb storage quality, with Se5 demonstrating the most beneficial effect according to bar graph results.

Furthermore, Selenium concentrations in both varieties (Red: 120.3657 mg kg^{-1} DW, Yellow: 162.3345 mg kg^{-1} DW) increased significantly with Se50 compared to Se5 and control treatments (Figure 35). Despite the higher Selenium absorption at Se50, Se5 remains the most effective treatment for maintaining onion storage quality, as it best preserved bulb weight after three months.

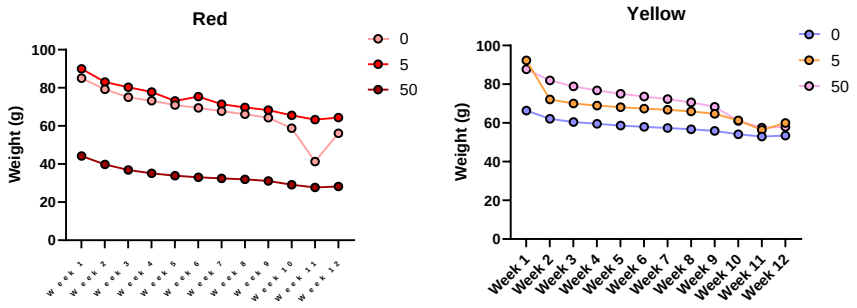

Analysis of variance

Variate: Weight

Source of variation	d.f.	s.s.	m.s.	v.r.	F pr.
Onion_Variety	1	1075.71	1075.71	15.95	<.001
Se_Levels	2	3874.43	1937.21	28.73	<.001
Onion_Variety.Se_Levels	2	8385.81	4192.90	62.18	<.001
Residual	66	4450.41	67.43		
Total 71 17786.35					

Figure 34: Graphs showing the weights of onion bulbs over time in weeks at different concentrations of selenium treatments, for red onions and yellow onions respectively. Plotted points indicate Mn, n=4.

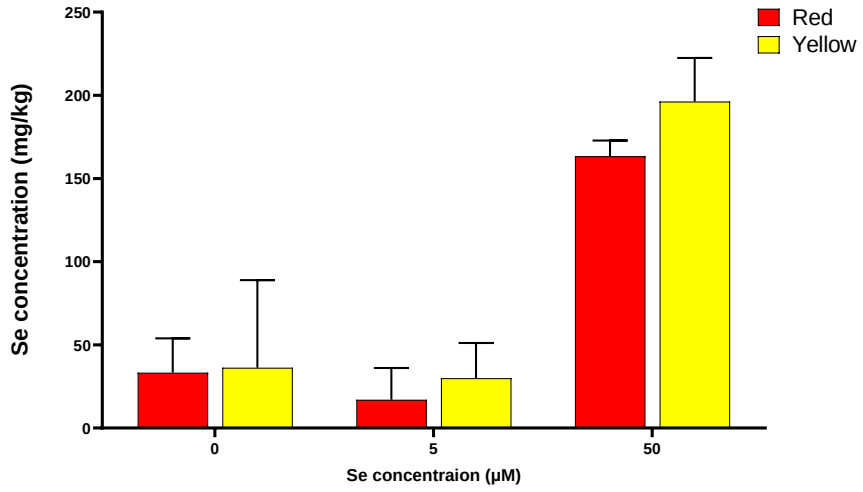

Figure 35: Effect of selenium treatments on the Se content of bulb of two onion varieties grew Hydroponically and stored for three months. Bars show Mean ± SD. n=4

Experiment 3 (Rijnsburger, Bedfordshire Champion onion and Spring Onion - White Lisbon Varieties):

In comparison to onion varieties, spring onions demonstrated a higher capacity for selenium (Se) absorption as Se concentration increased. Notably, red onions exhibited greater absorption abilities than yellow onions. Across all types, both spring onions and onion varieties displayed an upward trend in Se absorption with increasing Se levels. The highest Se content was observed in the Se50 treatment: red onion (6.2714 mg kg^{-1} DW), yellow onion (2.5056 mg kg^{-1} DW), and spring onion (19.6958 mg kg^{-1} DW). Conversely, the lowest Se content was recorded in the control group: red onion (0.1361 mg kg^{-1} DW), yellow onion (0.0977 mg kg^{-1} DW), and spring onion (0.115 mg kg^{-1} DW) (Figure 36). ANOVA results indicated no significant differences between factors or their interactions, as all P values were greater than 0.05.

An antagonistic correlation between Se levels and sulfur (S) content was observed in spring onions, while results varied among onion varieties. In spring onions, Se and S appear to have a reciprocal relationship in the uptake pathway, where increased Se absorption results in decreased S absorption, and vice versa.

The lowest S content in spring onions was recorded in Se0 (2366.7436 mg kg^{-1} DW) and the highest in Se50 (1888.1218 mg kg^{-1} DW). Conversely, onion varieties demonstrated an opposing trend, with the highest S content found in control red onions (1899.1899 mg kg^{-1} DW) and the lowest in control yellow onions (1676.8892 mg kg^{-1}

DW) (Figure 37). ANOVA results showed no significant differences, as all P values were greater than 0.05.

Both onion varieties and spring onions exhibited increasing iron (Fe) content with rising Se levels, with a more pronounced trend in red onions. All control samples exhibited the lowest Fe content (Figure 38). ANOVA results showed a significant difference in the Plant_Type factor ($P = 0.03 < 0.05$). However, other factors and their interactions were not significant ($P > 0.05$).

For magnesium (Mg), red onions displayed a positive correlation between Se levels and Mg uptake, with the lowest Mg content in the control (451.5243 mg kg^{-1} DW) and the highest in Se50 (760.3826 mg kg^{-1} DW). In contrast, yellow onions and spring onions exhibited fluctuating trends, with the lowest Mg content recorded in Se5 (632.6058 mg kg^{-1} DW for yellow onions and 1081.0587 mg kg^{-1} DW for spring onions) (Figure 39). ANOVA analysis revealed a significant difference for the Plant Type factor ($P = 0.015 < 0.05$), but no significant differences were found for other factors or their interactions ($P > 0.05$).

Regarding potassium (K) absorption, red and yellow onions showed a consistent upward trend with increasing Se levels, whereas spring onions displayed a variable pattern. The lowest K content in spring onions was recorded at Se5 (12773.5999 mg kg^{-1} DW) (Figure 40). ANOVA results indicated a significant difference for the Plant Type factor ($P = 0.004 < 0.05$), while other factors and interactions were not significant ($P > 0.05$).

In terms of calcium (Ca) absorption, yellow onions and spring onions exhibited opposing fluctuating trends, with the highest Ca content recorded in spring onions and the lowest in yellow onions, both at

Se5. In contrast, red onions displayed a positive correlation between Se levels and Ca absorption (Figure 41). ANOVA analysis showed no significant differences for all factors and their interactions, as all P values were greater than 0.05.

In summary, Se absorption trends vary considerably between onion varieties and spring onions. While red onions generally exhibit a positive correlation between Se levels and element uptake, yellow onions and spring onions show more complex or fluctuating patterns. Significant differences were primarily observed in the Plant Type factor for Fe, Mg, and K absorption, highlighting potential physiological differences in nutrient absorption mechanisms among the onion types.

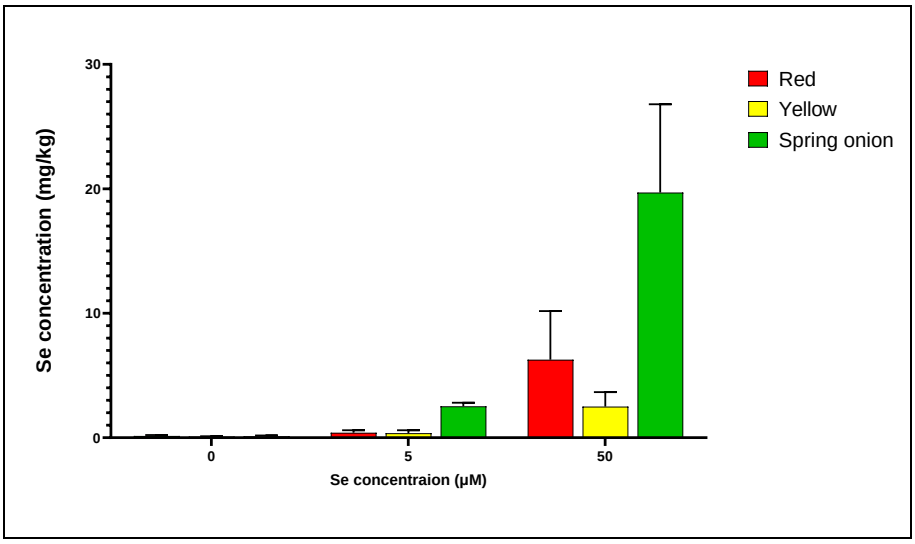

Source of Variation	SS	df	MS	F	P-value	F crit
Se_Levels	637.242754	2	318.6213772	42.7507	4.293E-09	3.3541
Plant_Type	280.249244	2	140.1246219	18.8011	7.675E-06	3.3541
Interaction	385.124493	4	96.28112334	12.9184	5.295E-06	2.7278
Within	201.23133	27	7.453012239			
Total	1503.84782	35				

Figure 36: Bars and ANOVA analysis which show effect of selenium treatments on Se content on bulb of two onion varieties and spring onion grown hydroponically, harvest time. Bars show Mean ± SD. n=4

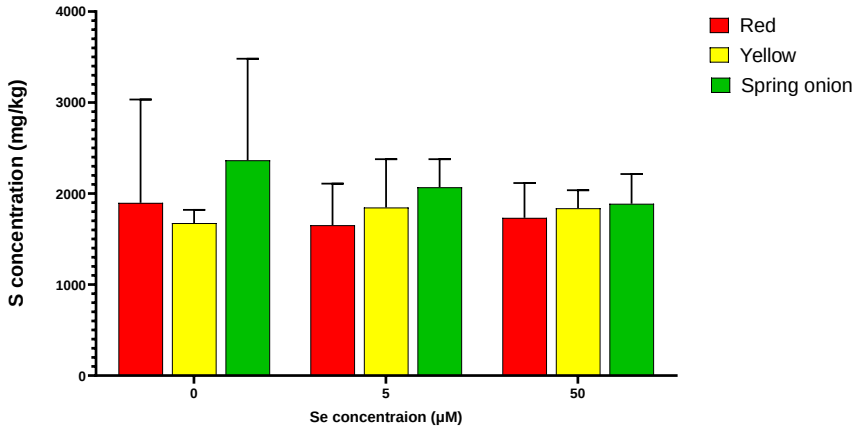

ANOVA S

Source of Variation	SS	df	MS	F	P-value	F crit
Se_Levels	74350.93	2	37175.46	0.103776	0.901785	3.354131
Plant_Type	419854.8	2	209927.4	0.586014	0.563464	3.354131
Interaction	368579.9	4	92144.99	0.257223	0.902682	2.727765
Within	9672197	27	358229.5			
Total	10534983	35				

Figure 37: Bars and ANOVA analysis which show effect of selenium treatments on S content on bulb of two onion varieties and spring onion grown hydroponically, harvest time. Bars show Mean ± SD. n=4

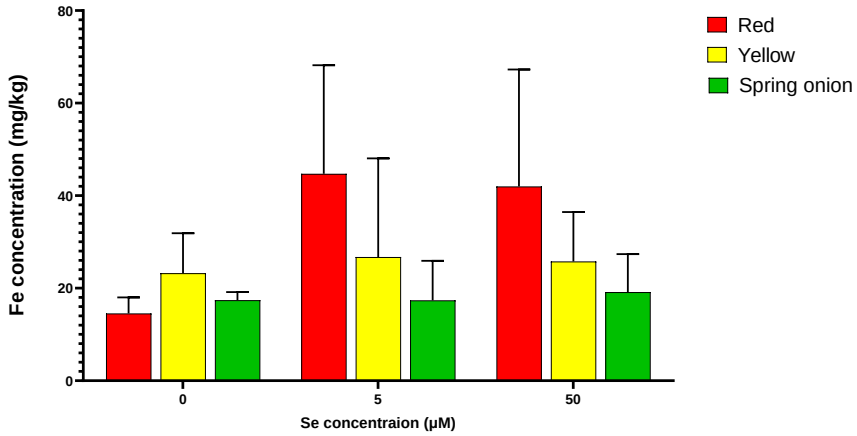

ANOVA Fe

Source of Variation	*SS*	*df*	*MS*	*F*	*P-value*	*F crit*
Se_Levels	920.2191	2	460.1095	2.265472	0.123158	3.354131
Plant_Type	1534.807	2	767.4033	3.778515	0.035741	3.354131
Interaction	1464.299	4	366.0747	1.802467	0.157501	2.727765
Within	5483.607	27	203.0966			
Total	9402.932	35				

Figure 38: Bars and ANOVA analysis which show effect of selenium treatments on Fe content on bulb of two onion varieties and spring onion grown hydroponically, harvest time. Bars show Mean ± SD. n=4

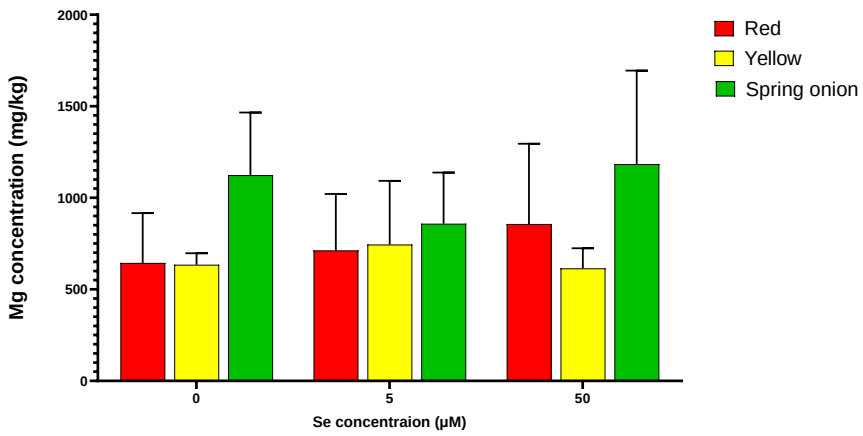

ANOVA Mg

Source of Variation	*SS*	*df*	*MS*	*F*	*P-value*	*F crit*
Se_Levels	82588.85	2	41294.42	0.390085	0.680753	3.354131
Plant_Type	1034025	2	517012.3	4.883928	0.015474	3.354131
Interaction	288982.6	4	72245.65	0.682465	0.610208	2.727765
Within	2858218	27	105859.9			
Total	4263814	35				

Figure 39: Bars and ANOVA analysis which show effect of selenium treatments on Mg content on bulb of two onion varieties and spring onion grown hydroponically, harvest time. Bars show Mean ± SD. n=4.

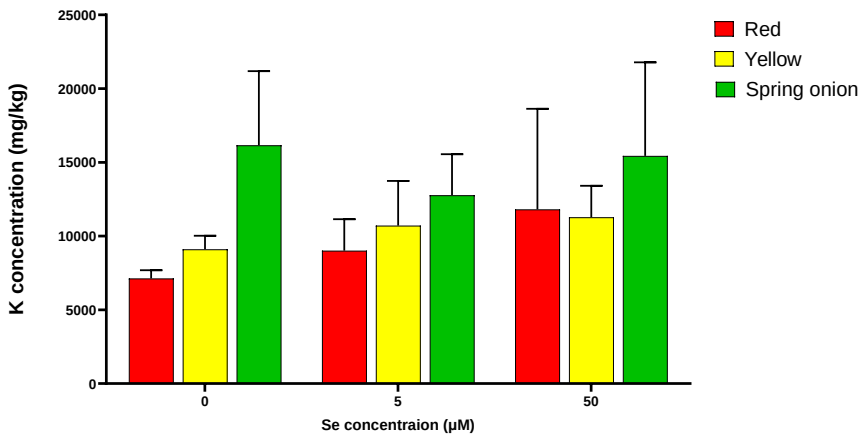

ANOVA K

Source of Variation	*SS*	*df*	*MS*	*F*	*P-value*	*F crit*
Se_Levels	32457672	2	16228836	1.051398	0.363322	3.354131
Plant_Type	2.01E+08	2	1E+08	6.498956	0.004965	3.354131
Interaction	46174089	4	11543522	0.747856	0.568035	2.727765
Within	4.17E+08	27	15435484			
Total	6.96E+08	35				

Figure 40: Bars and ANOVA analysis which show effect of selenium treatments on K content on bulb of two onion varieties and spring onion grown hydroponically, harvest time. Bars show Mean ± SD. n=4.

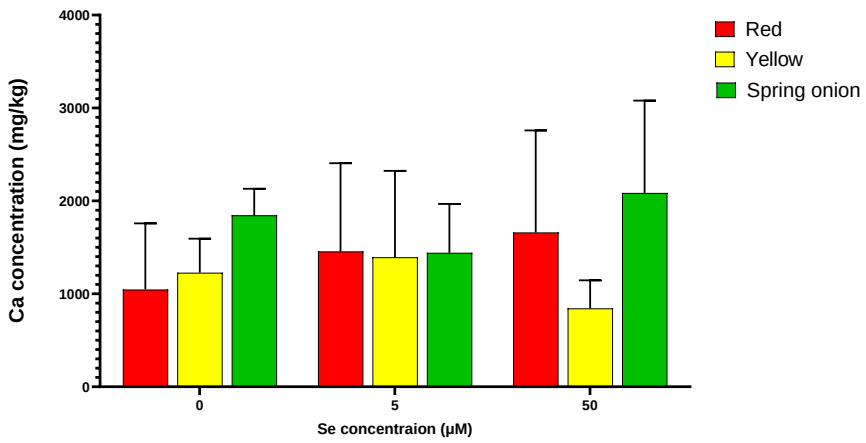

ANOVA Ca

Source of Variation	*SS*	*df*	*MS*	*F*	*P-value*	*F crit*
Se_Levels	150855.6	2	75427.81	0.134452	0.874776	3.354131
Plant_Type	2488213	2	1244107	2.217654	0.128313	3.354131
Interaction	2113189	4	528297.2	0.941704	0.454992	2.727765
Within	15147036	27	561001.3			
Total	19899294	35				

Figure 41: Bars and ANOVA analysis which show effect of selenium treatments on Ca content on bulb of two onion varieties and spring onion grown hydroponically, harvest time. Bars show Mean ± SD. n=4.

Comparison of all experiments:

Elemental Interactions

Selenium biofortification demonstrated varied interactions with different elements across all experiments, reflecting both synergistic and antagonistic effects depending on tissue type, selenium concentration, and growth stage.

- **Sulfur (S):**

Selenium treatments positively correlated with sulfur uptake in leaves, indicating a synergistic interaction where selenium likely facilitates or complements sulfur metabolism. However, in bulbs, higher selenium

concentrations, especially during later growth stages, led to a decline in sulfur content. This reduction is likely attributed to metabolic trade-offs or reallocation processes, where sulfur is redirected to other tissues or utilized in physiological processes essential for maturation.

- **Iron (Fe):**

An antagonistic relationship between selenium and iron was most evident at intermediate selenium levels (Se5) in Experiment 1, where iron uptake decreased significantly. However, this inhibitory effect was not observed at higher selenium concentrations (Se50), suggesting a threshold beyond which selenium no longer impairs iron assimilation. Experiments 2 and 3 exhibited a less pronounced antagonistic effect, indicating that varietal and species-specific differences influence iron-selenium interactions.

- **Calcium (Ca):**

Selenium treatments generally promoted calcium accumulation in leaves during early growth stages across all experiments. In contrast, bulbs exhibited reduced calcium levels with increasing selenium concentrations, underscoring a tissue-specific response. This inverse relationship suggests that selenium may influence calcium transport or storage mechanisms differently in leaves and bulbs.

Species and Variety Comparisons

The three experiments highlighted both commonalities and differences in selenium biofortification across various onion species and varieties.

1. **Experiment 1 vs. Experiment 2:**

Both experiments demonstrated consistent selenium uptake patterns, with leaves consistently accumulating more selenium than bulbs. The inclusion of the Bedfordshire Champion variety in Experiment 2

revealed only minor varietal differences, as both varieties responded similarly to selenium treatments. These findings suggest that selenium biofortification strategies are broadly applicable across different onion varieties.

2. Experiment 1 and 2 vs. Experiment 3:

In Experiment 3, spring onions exhibited selenium uptake patterns comparable to bulb onions, despite receiving only a single selenium treatment. Unlike bulb onions, spring onions did not exhibit a decline in selenium levels during maturation, likely due to their shorter growth cycle and differing metabolic demands. This highlights the suitability of spring onions for rapid biofortification under limited treatment conditions.

Key Trends and Implications

1. Tissue-Specific Selenium Storage:

Across all experiments, leaves consistently accumulated more selenium than bulbs, establishing them as the primary sites for selenium storage. This trend was evident regardless of species, variety, or selenium treatment applied, indicating a generalizable pattern in selenium uptake and accumulation.

2. Growth Stage Influence:

Selenium levels in bulbs decreased during maturation in Experiments 1 and 2, whereas leaf selenium concentrations remained stable or increased throughout all experiments. In Experiment 3, the shorter growth cycle of spring onions effectively prevented this decline, highlighting their potential for rapid biofortification compared to longer-cycle bulb onions.

3. Storage and Quality:

Experiment 2 demonstrated improved post-harvest storage quality in selenium-enriched bulbs, suggesting selenium's antioxidant properties may confer protective effects during storage. This enhancement in quality supports the broader applicability of selenium biofortification for improving both nutritional value and shelf life.

4. Species and Genetic Factors:

Despite minor varietal differences, genetic and species-specific disparities were minimal across experiments. Both Allium cepa (onions) and Allium fistulosum (spring onions) effectively absorbed selenium, demonstrating the robustness of selenium biofortification strategies across different onion types.

Conclusion

Selenium biofortification proved effective across all experiments, with consistent selenium uptake patterns observed in both leaves and bulbs. Despite differences in species and varieties, the experiments demonstrated a generally predictable response to selenium treatments, with leaves consistently accumulating higher selenium levels than bulbs. Spring onions, due to their shorter growth cycle, displayed particular promise for rapid biofortification under limited treatment conditions. Elemental interactions, while influenced by selenium levels, generally followed predictable trends, emphasizing selenium’s role in enhancing nutrient dynamics. These findings support the feasibility of selenium biofortification as a practical strategy for improving nutrient content and storage quality across diverse onion systems.

2.4 Discussion:

An investigation of the effect of selenium biofortification on other elements uptake was conducted in this study in onion and spring onion plants using an NFT system. Furthermore, a comparison was conducted between onion varieties and different tissues in terms of their ability to accumulate elements. Thus, the outcomes indicate through biofortification technique, selenium can be taken up in the NFT system and affects other elements' absorption. The accumulation of selenium and other elements differs between onion varieties and tissue types (leaves and bulbs). As compared to the bulb, the leaf is more capable of accumulating elements, and the red variety accumulated elements at a higher rate than the white variety. Based on these results, genetics may play an important factor in onion uptake and the difference between varieties, and this could be used in the evaluation of gene functions in onion.

Plants may first demonstrate Se presence through a change in their concentration of specific elements (Pazurkiewicz – Kocot et al., 2003). The mobility of other elements or their assimilation has been altered by Se (Djanaguiraman et al., 2005). The elements S and Se are in the same group of the periodic table, the chalcogens, and studies have shown that plants absorb and assimilate these elements in the same way. As selenate, Se (VI) can be absorbed via S transporters that reside in the root plasma membrane (Terry et al., 2000). Previous research has shown that Se and S have an antagonistic interaction when it comes to uptake (Ferrari and Renosto, 1992; Leggett and Epstein, 1956; Mikkelsen et al. 1989), the similar result was obtained in yellow variety leaf and spring onion in our experiments clearly, indicating that Se and S have an antagonistic connection. Nevertheless, there was a variable relationship between Se

concentration and S concentration in yellow bulbs and red bulbs, with some experiments showing that when selenium concentrations were high, onion S content increased significantly compared to the control, while in others the trend was the opposite. This differences in results of experiments and from previous studies could be due to plant species or developmental stage.

Even though selenium treatments did not have any overall influence on Fe content in either variety's leaves or spring onion, the relationship between selenium and Fe content in each variety's bulbs was antagonistic, resulting in higher Fe contents at selenium control levels. In 2006, Faragsova et al. discovered that rising Se levels prevent elements like Fe from absorbing. Plant tissues are protected from Se through Mg as a Se tolerance mechanism (Wilkinson et al., 1990). In tomato leaves (Schiavon et al., 2013) and maize plants (Hawrylak & Nowak, 2008), Se treatments had no significant effect on Mg levels. Interestingly, in this study, the graphs for the two kinds of leaves were opposite, indicating that elevating Se levels led to lower Mg levels in the red leaves but higher levels in the yellow leaves. A comparison of elevated Se levels to two other Se levels showed little effect on Mg concentration in red bulbs, however Se5 compared to control had a significant negative effect on Mg concentration in yellow bulbs and spring onions.

The shoots and roots of corn plants treated with Se in nutritional solution decreased in K content and increased in Ca (Hawrylak – Nowak, 2008). K and Ca in this study indicated a variable correlation with increasing Se in the experiments with Allium species. According to Gupta (1991), leaf tissue of a variety of forage and vegetable crops contained the highest concentration of Se. In this experiment, both onion varieties showed the same results. Furthermore, the red cultivar

had higher Se contents in both tissues than the yellow variety, indicating the red cultivar is better at accumulating the mineral.

The study also investigated whether the selenium concentration increases have a positive effect on stored onion bulbs. Se5 gets preference for onion storage quality because it is the most effective at changing onion weight after three months, even though bulbs absorb the maximum selenium at Se50. In onion storage process, there are different ways in which moisture can be lost, depending on the temperature of storage, such as desiccation, respiration and sprouting (Sharma and Lee, 2016).

In conclusion, red onion varieties are more capable of accumulating nutrients than yellow varieties, and their leaf tissues accumulate more nutrients than the bulbs.

Chapter 3: Impact of selenium-enrichment on agronomic parameters and bioactivity in spring onions

3.1 Introduction

Spring onions (*Allium fistulosum L.),* belong to the *Liliaceae* family, and they are known as scallions, Welsh onions, or Japanese bunching onions. Originally from China, they are used as a medication in traditional Chinese medicine for treating headaches, influenza, cardiovascular disease, and colds. (Kayat et al., 2021). They also possess antifungal and antibacterial properties. Spring onions are rich in vitamin C, A, and B6, thiamine, folate, rhamnose, galactose, glucose, arabinose, and xylose (Kayat et al., 2021). In addition to being inexpensive, spring onions are rich sources of antioxidants. Spring onion leaves are beneficial to both vegetarian and nonvegetarian diets since they are medicinally beneficial and nutritious. A number of biologically active compounds in spring onions inhibit cyclooxygenase-2 (COX-2) and nitric oxide synthase (iNOS), and impede different cellular markers involved in tumour apoptosis, proliferation, blood vessel development and invasion (El-Ghorab et al., 2017). Spring onions work through a variety of processes, including altering enzymes, obstructing mutagenesis, removing free radicals, promoting apoptosis, and in many ways influencing cell proliferation and the growth of tumours. They also act as defence mechanisms for breast cancer cells by facilitating the movement of reductase proteins, which are recognised for

their capacity to deactivate cytotoxic cancer-causing substances. (Izawa et al., 2008; Rose et al., 2005; Munday and Munday., 2004; Rodgers and Grant., 1998).

The chemical process of oxidation involves the acceptance of electrons from the initial molecule by an oxidising agent. Free radicals, which are highly reactive substances created during oxidation processes and have one or more unpaired electrons in their outermost shell, are well known for being able to do this. In order to prevent the next step in the oxidation cycle from occurring, antioxidants remove free radical mediators produced during the chemical process and oxidise themselves.

Numerous human diseases are caused by oxidative stress, including liver disease, cardiovascular diseases, aging, cancer, Parkinson's disease, Alzheimer's disease, muscular dystrophy, and neurovascular diseases. Based on where they come from, antioxidants are divided into two types: synthetic and natural. In stark contrast to natural antioxidants, synthetic antioxidants, which are oil-based, may result in unfavourable impacts on individuals. They require more metabolic energy, are only used to stabilise oil, do not offer a variety of products, have no antioxidant impact on human tissue, and are non-nutritional. Natural antioxidants have numerous health benefits: they are more readily utilised by the body, and are formed in a variety of plants, and have an antioxidant effect on human tissue.

Natural antioxidants are classified into three groups: phytochemicals, vitamins, and enzymes. Natural antioxidants can either be produced by the human body through metabolic

processes or supplemented from natural sources. Enzyme antioxidants come from proteins and minerals, and examples like superoxide dismutase, glutathione peroxidase, and catalases are produced by the human body. A phytochemical is a natural antioxidant that plants produce to prevent free radical damage. As part of our daily diets, we eat proteins and minerals, which contain antioxidant vitamins, including vitamins A, C, E, folic acid and beta-carotene (Kulisic et al., 2004). It is being emphasised that using plant antioxidants is a crucial strategy for stopping molecular oxidation and disarming free radicals. The significance of selenium as a chemopreventive was established in a study published in 1969. Cancer death rates were found to be negatively linked with the distribution of selenium in foraged crops (Shamberger and Frost, 1969). The only option to obtain items with high Se and antioxidant content is through biofortification because most agricultural crops and herbs aren't Se accumulators (Pilon–Smits, 2019; White, 2016).

This study used a biofortification technique to enrich spring onion plants with selenium. Spring onion was chosen as the subject of study as it has similar properties to onion and comes from the same family – in addition, there are relatively few studies on spring onions so this was an opportunity to fill this gap. Firstly, selenium was evaluated in terms of agronomic parameters on plants, as well as its ability to affect the uptake of other elements in the plants. The biofortified plants were then assessed for their biological properties, including how they inhibit cancer cell proliferation and scavenge free radicals.

The aims and objectives of this study were:

1. Does selenium biofortification affect agronomic parameters in spring onion?
2. Does selenium biofortification affect the uptake of other elements?
3. Identifying the selenium concentration and application method most effective for scavenging free radicals.
4. Is selenium-enriched spring onion a chemopreventive agent against cancer cell growth?

3.2 Materials and Methods

3.2.1 Spring onion growth conditions

Spring onions (*Allium fistulosum* L., variety White Lisbon) were cultivated under controlled environmental conditions. Initially, seeds were sown in June 2022 in 5 cm diameter seedling pots containing a sterile potting mix composed of peat, perlite, and vermiculite in a 2:1:1 ratio. The potting mix was sterilized before use to prevent contamination. Germination was conducted under a 16-hour light/8-hour dark photoperiod, with daytime and night-time temperatures maintained at 22 ± 2°C and 18 ± 2°C, respectively, and a relative humidity of 60% (Figure 42). Light intensity was set at 250 μmol m-2 s-1 using cool white fluorescent lamps. Seedlings were watered with deionized water as needed to maintain consistent soil moisture.

Once seedlings reached the two-leaf stage after approximately two weeks, they were thinned to one plant per pot and transplanted into 12 cm diameter pots containing the same sterile potting mix. The plants

were then grown under identical controlled conditions until the four-leaf stage before selenium biofortification treatments were applied.

3.2.2 Selenium biofortification process

Selenium biofortification was conducted using sodium selenate (Na_2SeO_4) via two application methods: foliar spraying and soil soaking. Treatments were administered biweekly throughout the plant's developmental stage (Figure 43) as follows:

- Foliar Spraying: Solutions of 5 µM and 50 µM Na_2SeO_4 were prepared in deionized water. Each plant received 50 ml of the solution, ensuring even foliar coverage. Applications were conducted early in the morning to minimize evaporation losses.
- Soil Soaking: The same selenium concentrations (5 µM and 50 µM) were applied directly to the soil at two-week intervals, with each pot receiving 50 ml of the solution for uniform soil saturation.

The spring onions were harvested two months after the initial treatment, and agronomic parameters were measured, including leaf area, leaf length, leaf width, wet weight, dry weight, width-to-length ratio, chlorophyll content (measured using a SPAD meter), and yield (kg/ha). Leaf area measurements were conducted using a LI-3100C Leaf Area Meter (LICOR Biosciences, USA). To prevent residual selenium from affecting ICP-MS analysis, plants treated with foliar spraying were washed three times with Milli-Q water.

The yield was calculated using the equation:

$$Yield\ (kg\ per\ ha) = \frac{Plant\ weight\ (kg)}{Pot\ area\ (m^2)} \times 10000$$

Where the pot area was consistent across all plants at 0.0113m^2 (calculated using area = πr^2 where r = radius and radius was 6cm). Plant weight was calculated by measuring the wet weight of the plants in each pot in grams and diving it by 1,000 to cover to kg. Plant weight/pot area was multiplied by 10,000 to calculate the plant weight per hectare.

3.2.3 Leaf area measurement using computational approaches

Leaf area measurements were performed using a leaf area meter. In cases where leaves were too large or irregularly shaped, they were scanned and analysed using ImageJ software (NIH, USA). The procedure was as follows:

- Leaf Scanning: Individual leaves were placed flat on a high-resolution flatbed scanner at 300 dpi, ensuring no folds or overlaps. Images were saved in TIFF format to preserve quality.
- Image Analysis in ImageJ: The scanned images were imported into ImageJ, where a ruler (used as a reference object of known dimensions) was used to establish a scale. Leaf areas were then outlined either manually or through automated thresholding techniques. The software calculated the area in pixels, which was converted to cm^2 using the pre-set scale.

3.2.4 ICP-MS Micronutrient Analysis

Post-harvest, spring onions were freeze-dried using a VirTis Freezemobile 25ES (SP Industries, USA) and stored at -70°C.

Samples were ground into a fine powder using liquid nitrogen and digested using the Hot Plate Acid Digestion method (Chapter 2). Selenium and other micronutrients, including sulfur (S), iron (Fe), magnesium (Mg), potassium (K), and calcium (Ca), were quantified using an ICP-MS (Agilent 7900, Agilent Technologies, USA). Data were analysed using ANOVA in GenStat software (version 19.1, VSN International Ltd., UK).

3.2.5 Extraction of spring onion samples

Twenty-seven samples from selenium-treated spring onions were processed for extraction. Each sample (100 mg) was mixed with 1 ml of sterile deionized water and homogenized using a Tissuelyser II (Qiagen, Germany) at 30 Hz for 15 seconds. The homogenate was incubated at room temperature for 30 minutes, centrifuged at 3000 rpm for 3 minutes (Eppendorf 5810R centrifuge), and the supernatant was stored at -20°C until further use.

3.2.6 Cell culture preparation

HepG2 cells were sourced from the University of Nottingham's cell culture facility and maintained in Dulbecco's Modified Eagle Medium (DMEM, Gibco, USA) supplemented with 10% foetal bovine serum (FBS, Sigma-Aldrich, USA) and 1% penicillin-streptomycin (Sigma-Aldrich, USA). Cells were cultured in T75 flasks (Thermo Fisher Scientific, USA) at 37°C with 5% CO2. Subculturing was performed using 0.25% trypsin-EDTA (Gibco, USA) following PBS washes. After centrifugation at 1500 rpm for 5 minutes, cells were resuspended in fresh medium and seeded into 96-well plates for viability assays.

3.2.7 Crystal Violet Viability Test

The crystal violet viability test was conducted following selenium-enriched extract treatments. Cells were fixed with 4% paraformaldehyde, stained with 0.5% crystal violet for 10 minutes, washed with deionized water, and solubilized in 200 µl of 100% methanol. Absorbance was measured at a 550 nm wavelength using a FluoStar Omega plate reader (BMG Labtech, Germany) (Feoktistova et al., 2016).

3.2.8 Antioxidant Assays (ABTS and DPPH)

Two antioxidant assays were performed to evaluate the free radical scavenging activity of the spring onion extracts:

- ABTS Assay: The ABTS assay, based on 2,2′-azino-bis(3-ethylbenzothiazoline-6-sulfonic acid), was used to determine the antioxidant capacity of the extracts. A volume of 10 µL of the extract was added to 190 µL of ABTS solution in a 96-well plate, followed by a 3-minute incubation. Absorbance was then recorded at 734 nm using the FluoStar Omega plate reader.

- DPPH Assay: The DPPH assay, utilizing 2,2-diphenyl-1-picrylhydrazyl, was used to assess the free radical scavenging potential of the extracts. A mixture of 10 µL of extract and 290 µL of DPPH solution was incubated for 5 minutes, after which absorbance was measured at 517 nm. Each assay was performed in triplicate for all concentrations, and the results were subjected to statistical analysis using ANOVA.

3.2.1 ICP-MS micronutrients analysis

Plants were placed in the freeze-dryer, and then kept in the -70C freezer for further experiments. Spring onion samples were digested by being ground with liquid nitrogen and weighed. The experiment was continued with an ICP-MS analysis of Hot Plate Acid Digestion as per chapter 2. The results of ICP-MS analysis were used to determine how selenium affects the uptake of other elements and results were statistically analysed using ANOVA in GenStat software. Some samples were chosen from foliar spray and soil-soaked applications to evaluate the biological characteristics of biofortified spring onions, alongside samples from the previous experiment employing the NFT method.

Figure 42: The spring onions were grown in pots and treated with selenium using foliar spray (yellow labels) and soil (red labels) application. (A) Early stage

growing after germination. (B) Plants by transferred to the pots. (C and D) Plants were labelled depending on selenium application methods. (E) The spring onions were treated with selenium by foliar spray method in developmental phase. (F) The spring onion soak soil application method in developmental phase. (G) The plants by foliar method in last stage of growth phase. (H) The plants by soak soil application in final growth stage.

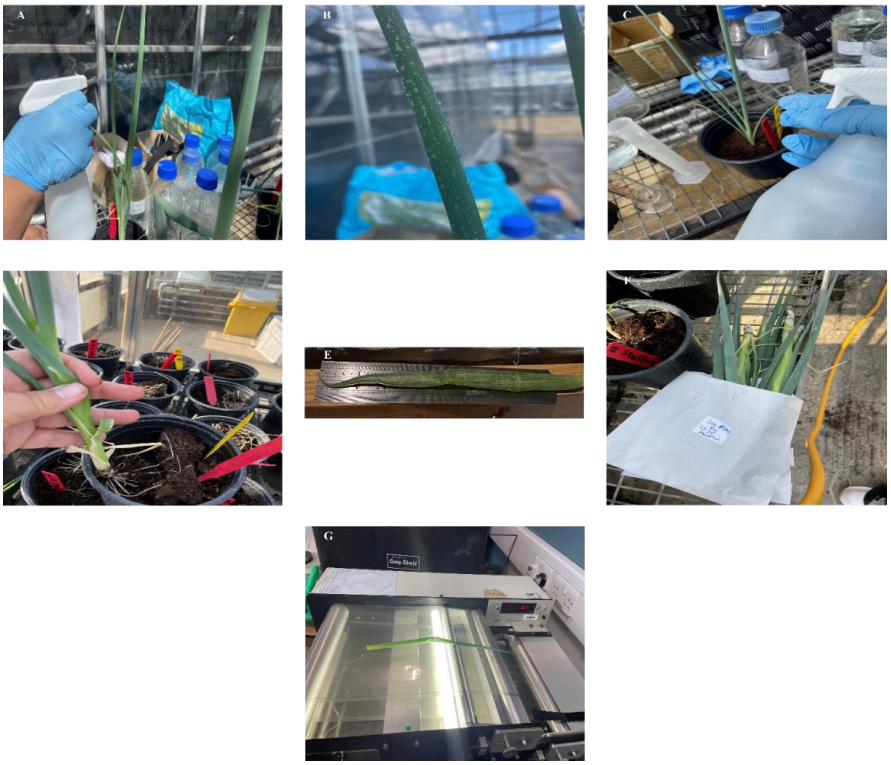

Figure 43: Spring onion plants measurements. (A, B, C) Selenium foliar spray application. (D) Harvesting. (E) Measuring width and length leaf. (F) Sample collecting. (G) Estimating leaf area.

3.2.2 Biological activity of plant extracts experiments:

In order to explore how selenium-enrichment of spring onions via biofortification affects cancer cell viability and scavenges free radicals as an antioxidant, 27 samples (Figure 45A) of spring onion from all application methods (foliar spray, soil soaked, NFT) with selenium levels (0, 5 µM, 50 µM) were extracted.

3.2.2.1 Extraction of Spring Onion Samples

To analyse the bioactive compounds and evaluate the antioxidant properties of selenium-enriched spring onions, an extraction procedure was conducted on plant tissues. The process consisted of the following steps:

1. Sample Preparation:

Fresh spring onion leaves were harvested and immediately freeze-dried using to preserve the integrity of bioactive compounds. The dried plant material was then finely ground using liquid nitrogen to prevent heat-induced degradation.

2. Extraction Process:

A total of 100 mg of the powdered spring onion sample was accurately weighed and placed into a 2 mL microcentrifuge tube. To extract bioactive compounds, 1 mL of sterile deionized water was added as the extraction solvent. Water was chosen to simulate physiological conditions and ensure compatibility with subsequent biological assays.

The mixture was homogenized using a Tissuelyser II (Qiagen, Germany) at 30 Hz for 15 seconds to effectively disrupt plant cells and enhance the release of bioactive compounds. Following homogenization, the samples were left at room temperature for 30 minutes to optimize the extraction of soluble compounds.

Centrifugation and Collection:

The homogenized samples were centrifuged at 3000 rpm using a Yellowline TTS 2 centrifuge (as shown in the image) for 3 minutes

using an Eppendorf 5810R centrifuge to separate plant debris from the liquid extract. The supernatant, containing the extracted bioactive compounds, was then carefully transferred to a clean microcentrifuge tube using a pipette, ensuring minimal disturbance of the plant debris pellet.

Storage:

The collected extracts were stored at -20°C until further analysis to prevent degradation of sensitive bioactive compounds. These extracts were later utilized for cell culture assays, antioxidant tests, and other biochemical analyses.

This extraction method facilitated the efficient recovery of bioactive compounds from selenium-enriched spring onion tissues, enabling their subsequent evaluation for biological activity and antioxidant potential.

3.2.2.1 Cell culture preparation:

HepG2 cells were cultured in T75 flasks using Dulbecco's Modified Eagle Medium (DMEM, Gibco, USA), supplemented with 10% fetal bovine serum (FBS, Sigma-Aldrich, USA) and 1% penicillin-streptomycin (Sigma-Aldrich, USA). The cells were maintained in an incubator at 37°C with 5% CO2 to provide optimal growth conditions.

Once the cells reached approximately 80-90% confluence, they were ready for passaging. The culture medium was aspirated with a pipette to remove any waste products and dead cells. The monolayer of HepG2 cells attached to the bottom of the flask was then washed with 5 mL of phosphate-buffered saline (PBS, Sigma-Aldrich, USA) to eliminate residual FBS, which could interfere with trypsin activity.

Next, 2 mL of 0.25% trypsin-EDTA (Gibco, USA) was added to the flask to detach the cells. The flask was gently tilted to ensure that the trypsin solution covered the entire surface. The flask was then incubated for 2-3 minutes at 37°C to allow trypsin to enzymatically break down the proteins that anchor the cells to the surface.

When the cells began to round up and detach, the flask was gently tapped or agitated to help dislodge any remaining attached cells. If necessary, this mechanical dislodging process was repeated to ensure full detachment of the cells.

Mechanical dislodging process:

• Tapping the Flask: The T75 flask was held securely and gently but firmly tapped against the palm of the hand. This action was typically done by tapping the flask two to three times on each side.

• Observation: Immediately after tapping, the flask was examined under a microscope to ensure that the majority of the cells had detached from the surface. Detached cells appear as rounded, free-floating cells in the medium, as opposed to flattened and adherent cells still attached to the flask surface.

To neutralize the trypsin and halt its enzymatic activity, 8 mL of fresh complete DMEM medium was added to the flask. The cell suspension was then transferred to a 15 mL or 50 mL universal tube, depending on the volume, and centrifuged at 1500 rpm for 5 minutes to pellet the cells.

After centrifugation, the supernatant was carefully discarded, and the cell pellet was resuspended in 10 mL of fresh complete DMEM

medium. Approximately 1/10th of the suspension was transferred to a new T75 flask containing 13 mL of fresh medium to continue cell culture growth. The remaining suspension was used for seeding other experimental setups. The cells were incubated overnight at 37°C with 5% CO2 and were used for treatment the following day.

HepG2 Cell Line Source

The HepG2 cells, a human liver cancer cell line, were obtained from the Bioscience North labs at the University of Nottingham. These cells were selected for their relevance in cancer research and their use in evaluating the effects of bioactive compounds on cell viability.

Reagents

- Fetal Bovine Serum (FBS): Sourced from Sigma-Aldrich (USA), FBS is an essential component of the cell culture medium, providing necessary growth factors, hormones, and nutrients for cell proliferation and survival. It was heat-inactivated at 56°C for 30 minutes before use to eliminate any complement proteins that could interfere with cell growth.

- Phosphate-Buffered Saline (PBS): The PBS solution, purchased from Sigma-Aldrich (USA), was used for washing cells, diluting substances, and maintaining pH balance during experimental procedures. The 1X PBS solution had a pH of 7.4, ensuring isotonic conditions that are gentle on cells.

These reagents were essential for maintaining the optimal condition of HepG2 cells, ensuring the reliability and reproducibility of the experimental results.

Samples were cultured with three of each selenium concentration treatment (0, 5 μM, 50 μM). This equated to nine of foliar sprays, nine of soil soaks, and nine of NFTs (previous experiment). The medium consisting of 10% FBS and 1% penicillin was used for cell culture. This study used HepG2 cells, which were cultured every Monday, Wednesday, and Friday (Picture 3A). Cell flasks were maintained in a humidified incubator consisting of 37 ˚C and 5% CO2. Every time cells were cultured, medium was removed using a 10 ml pipette from the bottom corner of an old flask (T75 flask). The cell surface was then washed with PBS using a 10 ml pipette. The PBS was removed and trypsin was added. The minimum amount of trypsin (2ml) was used to avoid damaging the cells. The trypsin was rolled around the flask to ensure it covered all of the cell surfaced prior to incubation.

The flask was hit mechanically before being viewed under the microscope to observe flowing cells. A further 8 ml of trypsin was added to the flask for neutralisation. The liquid was removed from the flask and centrifuged for 5 minutes – white cells settled at the bottom after centrifugation (picture 3B).

10 ml of fresh medium was added to the flask. 1ml of this sample was transferred to a new flask to continue the culture and topped up with 13ml of medium. It was labelled with the date, name, 1:10 ratio and passage number and stored in the incubator.

Cell count was calculated by measuring the number of cells in the corner of a square and extrapolating for the whole flask. Below is an example of one of the cell count calculations in this study using a haemocytometer for the seeding process in the 96-well plate:

620/4 = 155 cell numbers per corner of square

155 × 10000 = 1550000

1550000× 10 = 15500000 cells numbers in 10 ml

15500000/10000 = 1550 cells numbers in µl

100 µl × 110 = 11000 liquid per plate = 11 ml

10000 × 110 = 1100000 cells per plate

1100000/1550 = 709.677 µl cells = 0.709 ml cells per plate

11 ml – 0.709 ml cells = 10.291 ml medium per plate

Immediately following seeding (Picture 3C), well plates were put in the incubator for one night, with treatment taking place the next day. The treatment process began with removal of the medium. The well plates were washed with PBS, then spring onion treatment was added (Picture 3D), before being incubated 24 hours. A dilution of the samples was the first step of the treatment. In this study five drug concentrations (0, 6 mg/ml, 12 mg/ml, 25 mg/ml, 50 mg/ml) were tested on cancer cells to determine viability and cytotoxicity of the cells. Originally, the samples were concentrated at 100 mg/ml and were diluted to 50 mg/ml by mixing them with medium without FBS. An example for making 50 mg/ml concentration for 6 wells is given below.

50 µl× 6 = 350 µl medium (50 µl more for pipetting air)

\+ = 700 µl mixture

50 µl× 6 = 350 µl samples (50 µl more for pipetting air)

Table 4: An example of how dilution samples can be used to treatment process.				
	Treatment Concentration (Se50 Spray)	**R1**	**R2**	**R3**
A	0	100 µl just medium	100 µl just medium	100 µl just medium
B	6 mg/ml	100 µl from C + 100 µl medium = 100 µl to waste	100 µl from C + 100 µl medium = 100 µl to waste	100 µl from C + 100 µl medium = 100 µl to waste
C	12 mg/ml	100 µl from D + 100 µl medium	100 µl from D + 100 µl medium	100 µl from D + 100 µl medium
D	25 mg/ml	100 µl dilution sample + 100 µl medium	100 µl dilution sample + 100 µl medium	100 µl dilution sample + 100 µl medium
E	50 mg/ml	100 µl just dilution sample	100 µl just dilution sample	100 µl just dilution sample

To check the effectiveness of drug treatment on cancer cells, the well plates were evaluated under a microscope (Picture 3E). A viability test using crystal violet was carried out to prepare the well plates for plate reading (Picture 3F). This process is described below.

Treatment: 100 mg/ml onion extracts were diluted down to 0, 6, 12, 25 and 50 mg/ml samples in medium without FBS and added to cells in 96 well plates (Figure 44D) after seeding.

Viability test:

The crystal violet viability test is a cell viability assay that uses crystal violet dye to stain cells and assess their proliferation and viability. Crystal violet binds to DNA and proteins in the cell, primarily staining adherent cells that remain on the plate following washing steps. Cells are then lysed, and the dye is solubilised for quantification, typically using a spectrophotometer to measure absorbance at a wavelength of around 540-590 nm.

This test was used to prepare the well plates for plate reading. Liquid was removed from the wells and 20 µl of crystal violet was added for 10 minutes. The plates were washed with sterile water to leave only the dye bound to viable cells and 200 µl of methanol was added for 20 minutes to solubilise the dye (Figure 44F). The plates were then read at 550nm using the plate reader (FluoStar Optima).

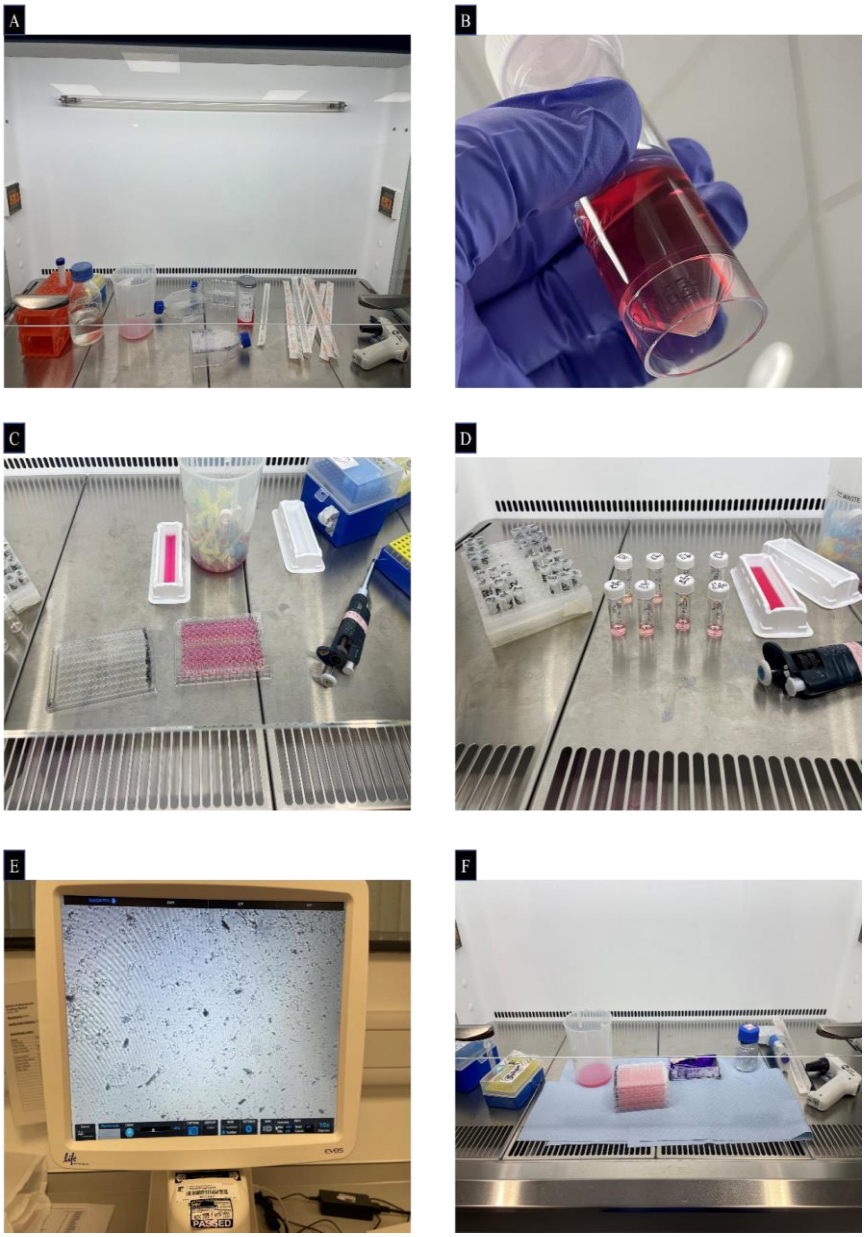

Figure 44: Cell culture stages. (A) Culturing HepG2 cells. (B) Cancer cells as white cells after centrifuging. (C) Seeding the well plates. (D) Treatment process like dilution samples and treating the cells. (E) Looking the plates under the microscope after treatment. (F) Crystal violet viability assay.

3.2.2.3 Antioxidant assays:

The ABTS (2,2'-azino-bis(3-ethylbenzothiazoline-6-sulfonic acid)) and DPPH (2,2-diphenyl-1-picrylhydrazyl) assays were used to measure the antioxidant activity of the treatments used. These assays are commonly used to assess the antioxidant ability of compounds by behaving like a free radical that changes colours when interacting with antioxidants.

The ABTS assay involves the generation of a blue-green ABTS radical cation which absorbs light at a wavelength of 734nm. The donation of electrons to this radical by antioxidants results in its neutralisation and a decrease in its colour intensity. The DDPH assay works similarly, using a DPPH free radical with a violet colour – it absorbs light at 517nm and changes colour to yellow when it receives hydrogen atoms from antioxidants. ABTS scavenging activity was determined by method which described by Re et al (1999). And DPPH assay was evaluated by using method according to Chang et al (2001).

ABTS

7mM of ABTS salt was dissolved in water. The solution was then mixed with 2.45 mM of potassium persulfate. The mixture was left in the dark for 14 hours overnight at room temperature to form the radical. The next day, the solution was diluted with ethanol and repeated measured with the plate reader at 734nm wavelength until the absorbance reached 0.68-0.72. 10 µl of sample solution was mixed with 190 µl of ABTS solution in a 96-well plate. The mixture was incubated at room temperature for 3 minutes, before being read by the plate reader (FluoStar Optima) at 734nm.

DPPH

0.1mM of DPPH was dissolved in methanol on the days of the experiments. 10 µl of sample solution was added to 290 µl of DPPH in a 96 well plate and incubated at room temperature for 5 minutes in the dark, before being read by the plate reader (FluoStar Optima) at 517nm.

Calculation

The percentage of radical scavenging activity was calculated using the following formulas:

$$\mathrm{ABTS} + \ \mathrm{scavenage\%} \ = \ (\mathrm{E1} - \mathrm{E2/E1}) \ \times \ 100$$

%RSA = (Abs control – Abs sample/Abs control) × 100

Table 5: An example of how dilution samples can be used to antioxidant assays.

	Antioxidant Concentration (Se50 Spray)	**R1**	**R2**	**R3**
A	0	100 µl just ethanol	100 µl just ethanol	100 µl just ethanol
B	6 mg/ml	100 µl from C + 100 µl ethanol = 100 µl to waste	100 µl from C + 100 µl ethanol = 100 µl to waste	100 µl from C + 100 µl ethanol = 100 µl to waste
C	12 mg/ml	100 µl from D + 100 µl ethanol	100 µl from D + 100 µl ethanol	100 µl from D + 100 µl ethanol
D	25 mg/ml	100 µl from E + 100 µl ethanol	100 µl from E + 100 µl ethanol	100 µl from E + 100 µl ethanol
E	50 mg/ml	100 µl sample + 100 µl ethanol	100 µl sample + 100 µl ethanol	100 µl sample + 100 µl ethanol

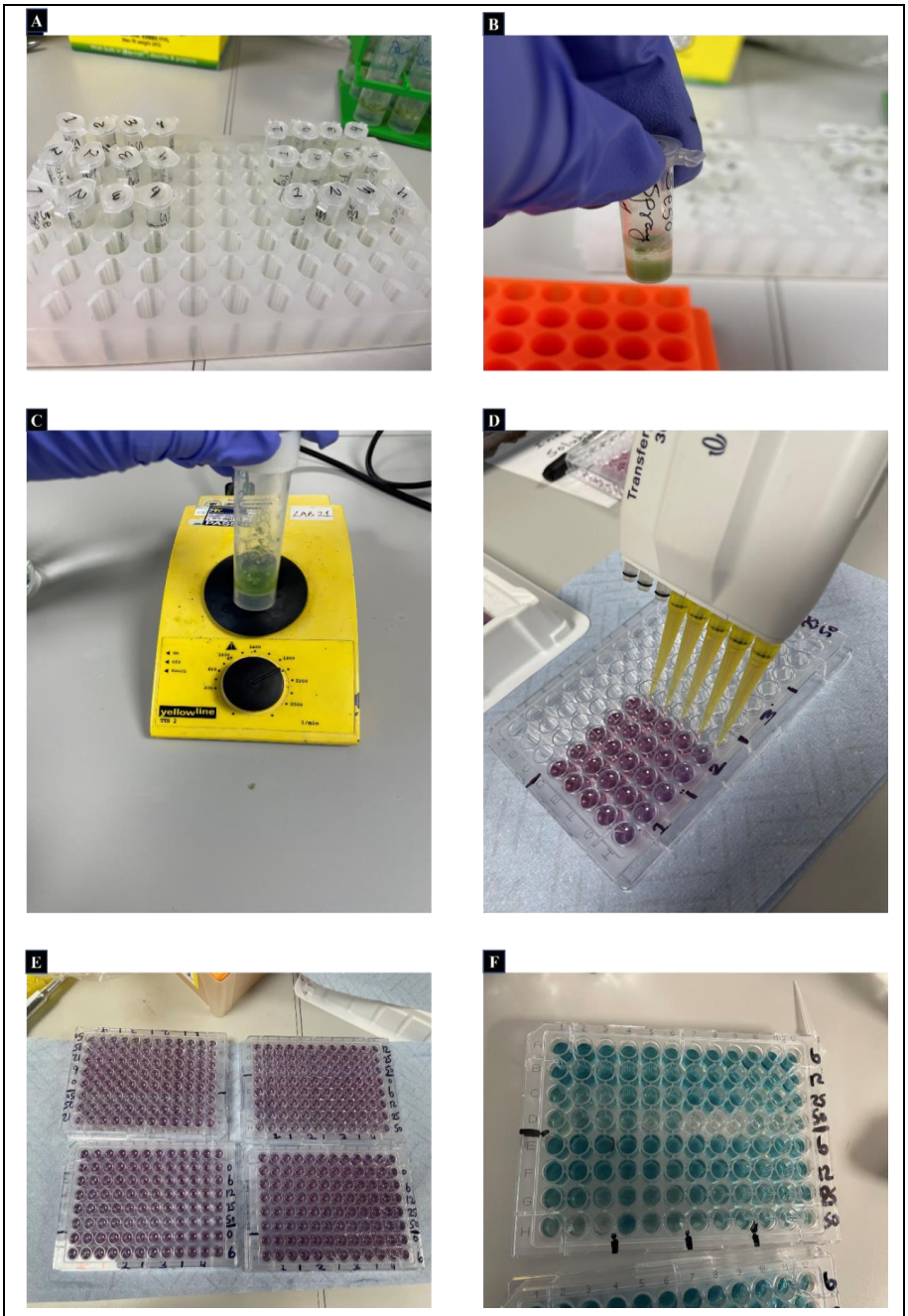

Figure 45: Antioxidant assays. (A) Spring onion samples. (B) Sample mixed with water. (C) Mixer machine. (D) Pipetting the samples with DPPH solution. (E) Samples ready to plate reader at 517 nm in DPPH assay. (F) Samples ready to read by plate reader at 734 nm in ABTS assay.

3.3 Results

3.3.1 Effect of selenium on spring onion agronomic parameters

The effects of selenium (Se) concentration and application methods on agronomic traits (leaf area, leaf length, leaf width, leaf width-to-length ratio, chlorophyll content, and yield) were statistically analysed using analysis of variance (ANOVA). Each treatment was applied to a group of 30 plants (n=30), and mean values for each trait were compared across treatment groups. The significance level was set at $\alpha = 0.05$, with p-values greater than 0.05 indicating no statistically significant difference among the treatments.

For each agronomic trait measured, standard deviations (SD). When ANOVA results indicated no significant effects ($p > 0.05$), differences in agronomic traits between selenium-treated and control plants were considered statistically nonsignificant.

ANOVA was also used to examine interactions between Se concentration and application method for certain traits, such as the width-to-length ratio and yield. Significant interactions were indicated for these parameters with p-values below 0.05 -- specifically width-to-length ratio, where interaction between Se concentration and application method was significant ($P = 0.002$), and yield, where a significant interaction effect was observed ($P = 0.03$).

Agronomic traits were not significantly affected by selenium concentrations or application methods, so there was no significant change in these traits.

In foliar spray method, treatment 5 µM Se increased leaf area, length and yield by 45.19±1.83, 45.72±0.77 and 33162.83±6065.65 compared to control plants (41.69±2.32, 45.33±1.06 and

31884.07±5746.32 respectively) but these increases were not significant. In contrast, the highest Se treatment 50 µM caused an increase in all agronomic parameters (leaf area, leaf length, leaf width, ratio of leaf width to length, chlorophyll, and yield) compared to control plants was not statistically significant, as indicated by p-values greater than 0.05 in the ANOVA results.

A soil application of 5µM selenium led to higher leaf areas, leaf lengths, leaf widths, chlorophyll levels, and yields when compared to the controls.

Conversely, when highest concentrations of selenium (50 µM) were used, leaf area by 40.03±1.53, ratio of width to length by 0.033±0.0001 and yield 30121.82±4637.53 were reduced in comparison to control plants (44.11±0.85, 0.033±0.0002 and31884 ±5746.32 (kg/ha) respectively). These results were also not statistically significant based on p-values above 0.05.

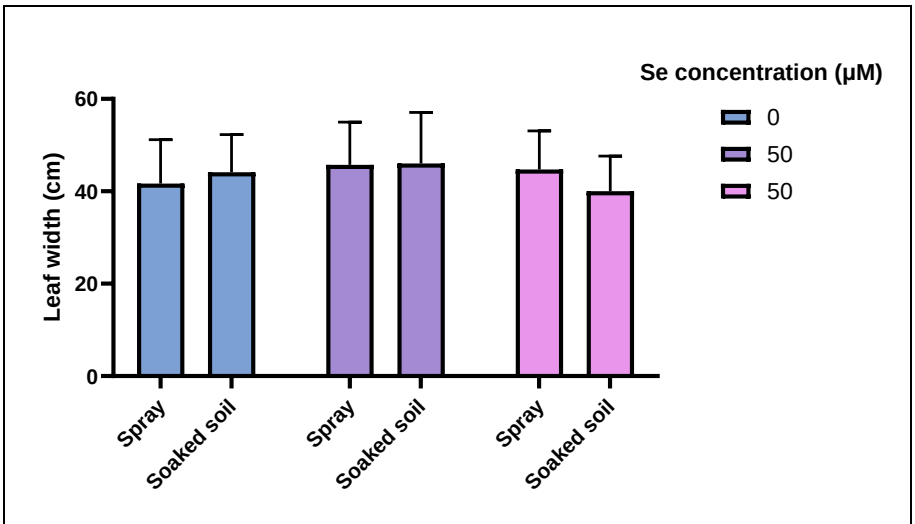

Figure 46: Effect of selenium on the spring onion lea area (cm²). ANOVA shows Selenium does not affect leaf area, based on the p value > 0.05. Bars indicate SD (n=30)

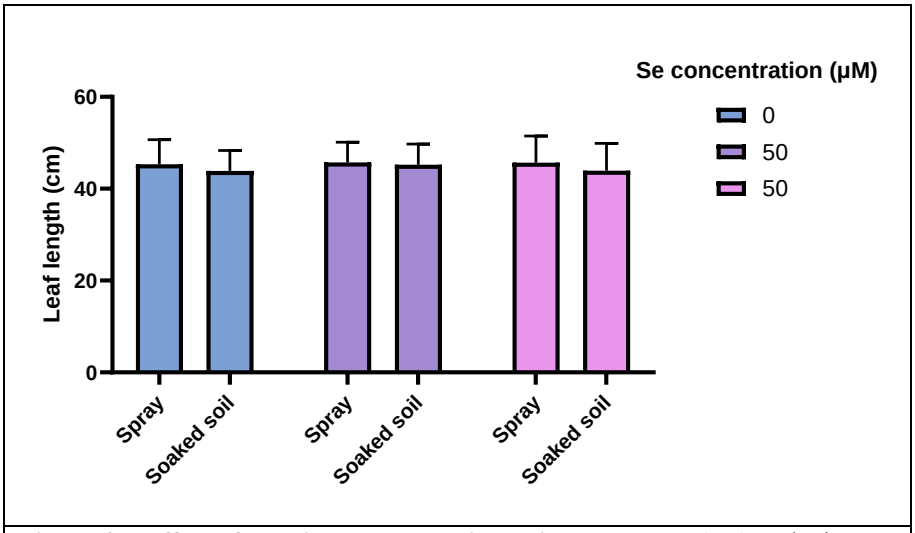

Figure 47: Effect of selenium on the spring onion lea length (cm). Selenium has no impact on leaf area, according to the p value > 0.05. Bars indicate SD (n=30).

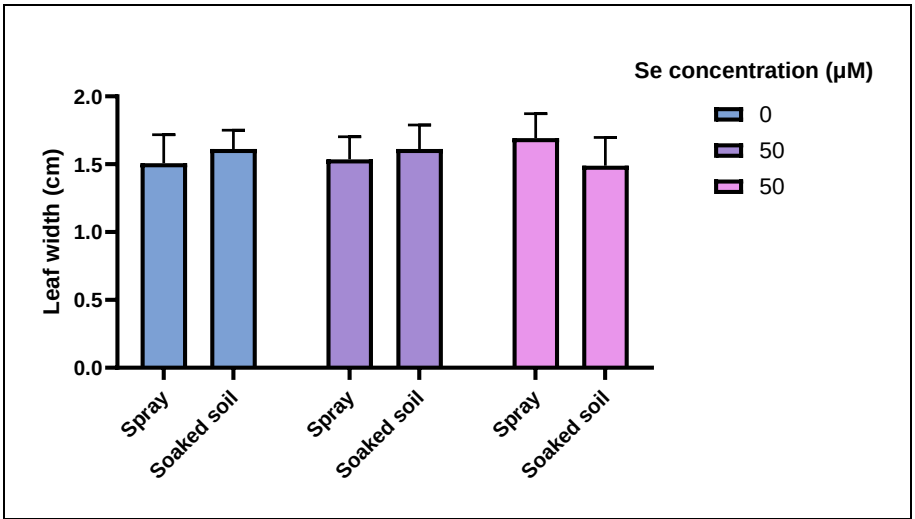

Figure 48: Effect of selenium on the spring onion width (cm). According to the p value > 0.05, selenium has virtually no impact on leaf area**.** Bars indicate SD (n=30).

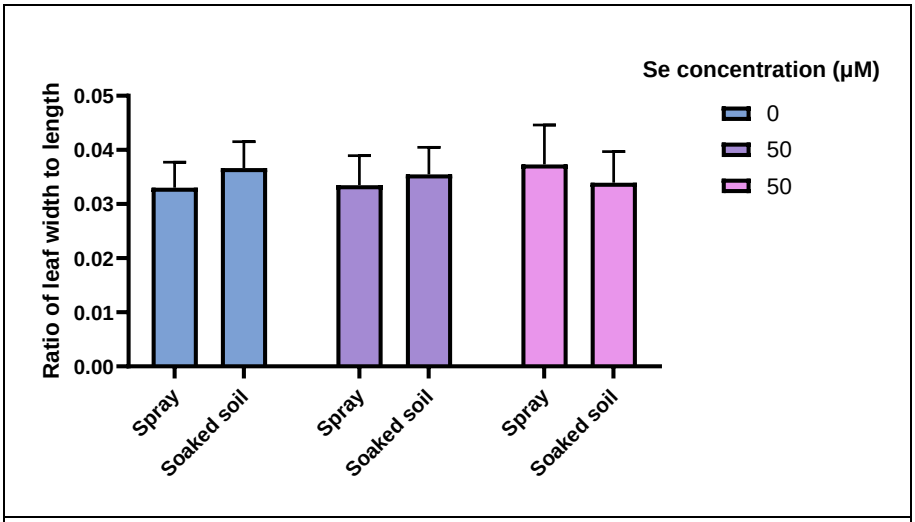

Figure 49: Effect of selenium on the spring onion Ration leaf width to length. The p value indicates that only the interaction between Se concentration and application (P = 0.002) is significant. Bars indicate SD (n=30).

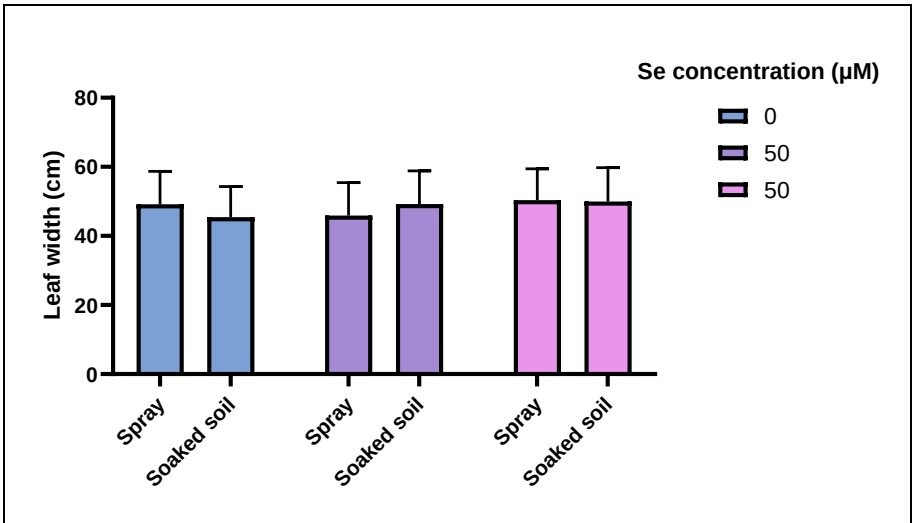

Figure 50: Effect of selenium on the spring onion Ration chlorophyl. Considering the p value > 0.05, selenium has practically no effect on leaf area. Bars indicate SD (n=30).

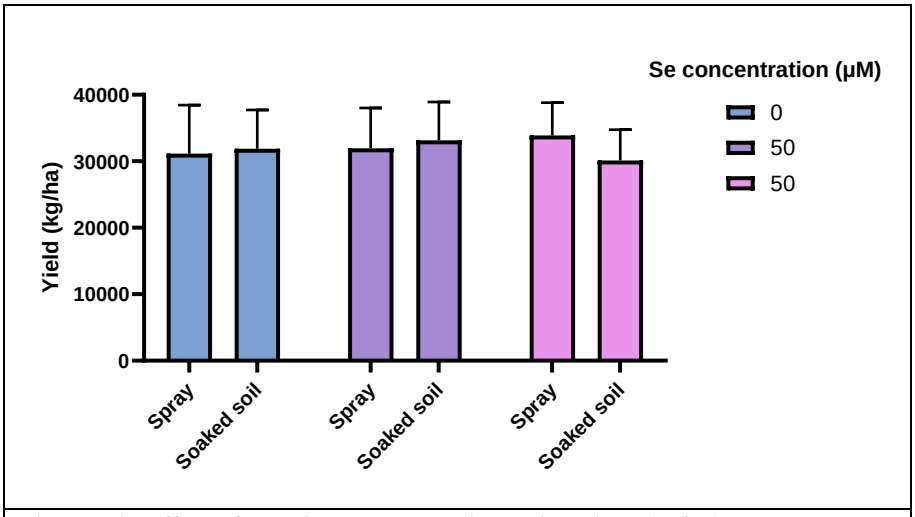

Figure 51: Effect of selenium on the spring onion yield (kg/ha). Se concentration and application only interact significantly (P = 0.03), as indicated by the p value. Bars indicate SD (n=30).

3.3.2 Impact of selenium tissue micronutrient levels

To determine the impact of selenium (Se) concentration and application methods (foliar spray vs. soaked soil) on the uptake of various micronutrients—Se, S, Fe, Mg, K, and Ca—in spring onion plants, analysis of variance (ANOVA) was applied. Each treatment was replicated across 30 plants (n=30), and mean values, along with standard deviations (SD), are represented as error bars in Figures 52 through 57. Statistical significance was set at a level of $\alpha = 0.05$, with P-values above 0.05 indicating no significant effect.

The ANOVA results revealed that the effects of Se concentration and application method differed across micronutrients. For sulfur (S), a significant effect was observed with concentration and application interaction, indicating that selenium levels and application methods together influenced sulfur uptake. Although no significant effect was found for iron (Fe) uptake ($P > 0.05$), the data suggest that soaking may be detrimental to iron uptake, especially at higher selenium concentrations. This outcome could be due to factors related to how soil conditions and plant physiology interact under soaked conditions.

When soil is soaked, it can become anaerobic, reducing oxygen availability around the roots. Iron uptake relies on active transport mechanisms that are often less efficient in low-oxygen environments. Additionally, high selenium levels may alter soil pH, making iron less soluble and therefore less accessible for plant roots. Selenium and iron may also compete for similar uptake pathways; high selenium concentrations could inhibit iron transporters, further limiting absorption. Selenium-induced oxidative stress could be another factor. Under soil-soaking conditions, where roots are constantly exposed to high selenium levels, the plant may prioritize managing stress over nutrient absorption, further impacting iron uptake.

For magnesium (Mg), significant differences were noted based on the application methods, with soil soaking showing reduced Mg uptake compared to foliar application ($P = 0.001$). Potassium (K) content was significantly influenced by both application method and Se concentration. The highest K uptake was observed at 5 µM Se with foliar spray, while the lowest uptake occurred at 50 µM Se (27521.76 gr/Kg DW and 25180.02 gr/Kg DW respectively, $P = 0.0001$).

Calcium (Ca) exhibited an antagonistic relationship with Se, with Ca uptake decreasing as Se concentration increased.

Interactions between Se concentration and application methods were assessed for micronutrients that displayed variable responses. Significant interactions were observed for sulfur ($P = 0.003$) and potassium ($P = 0.0001$), suggesting that soil soaking generally enhances selenium uptake compared to foliar spray.

The ANOVA results offer additional insights. Although higher concentrations of selenium (50 µM) increased Se uptake, these changes were not statistically significant, with P-values above 0.05.

For sulfur (S), contrary to our initial hypothesis that Se would inhibit S uptake, results showed an increase in sulfur content with higher Se concentration, particularly in soil-soaked applications. Iron (Fe) content showed no significant change with increasing Se concentration, suggesting minimal impact of Se on Fe uptake. Magnesium (Mg) and calcium (Ca) demonstrated an antagonistic relationship with Se, as both Mg and Ca contents decreased with increasing Se concentration. Potassium (K) content was significantly influenced by both the method of application and Se concentration, with foliar application at 5 µM Se yielding the highest K uptake and 50 µM Se resulting in the lowest K uptake.

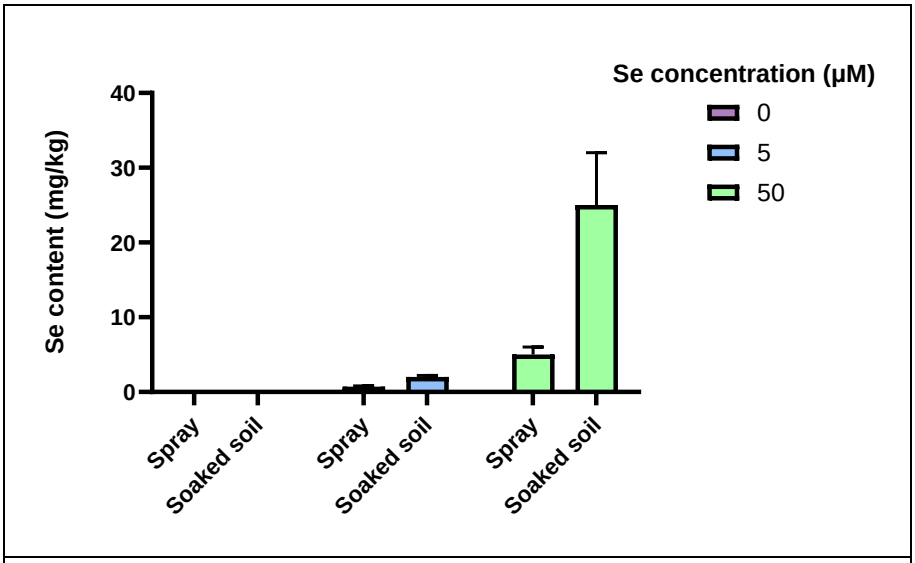

Figure 52: Effect of selenium on uptake of selenium element. Based on all p value > 0.05, the ANOVA shows Selenium has no effect on selenium content. Bars indicate Mn±SD. (n=30).

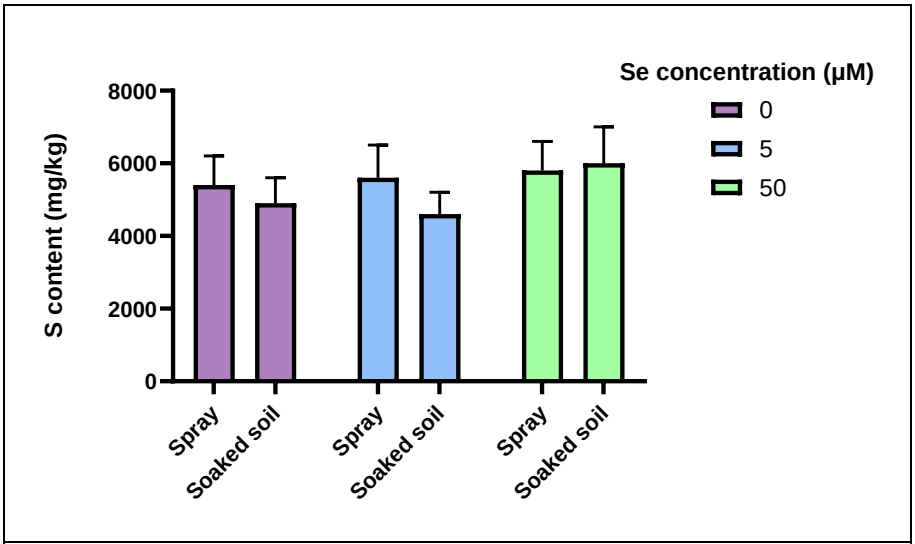

Figure 53: Effect of selenium on uptake sulfur element. In terms of ANOVA, application methods and concentration-application interaction differ significantly when P values are lower than 0.05 (0.03 and 0.003 respectively). Bars indicate Mn±*SD* (n=30).

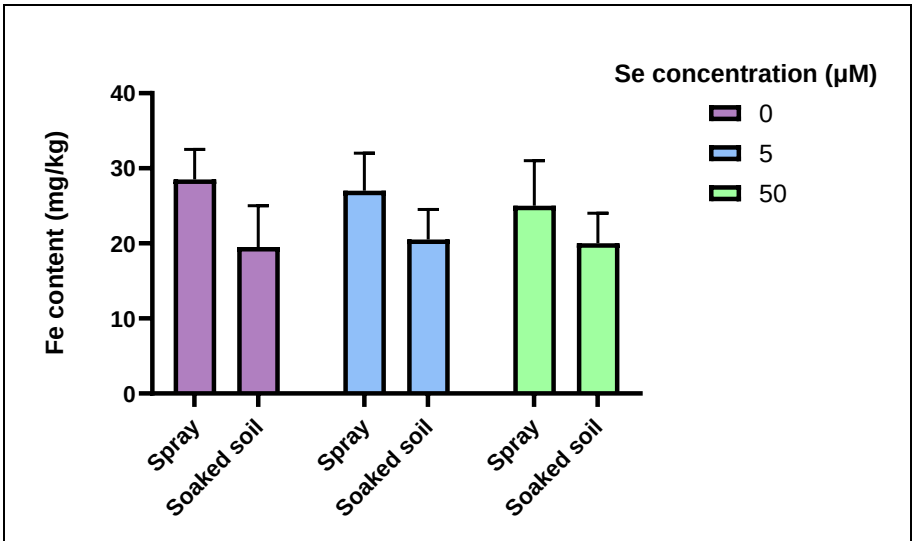

Figure 54: Effect of selenium on uptake Fe element. The ANOVA demonstrates that selenium has no influence on selenium content due to all the p value > 0.05. Bars indicate Mn±*SD*. (n=30).

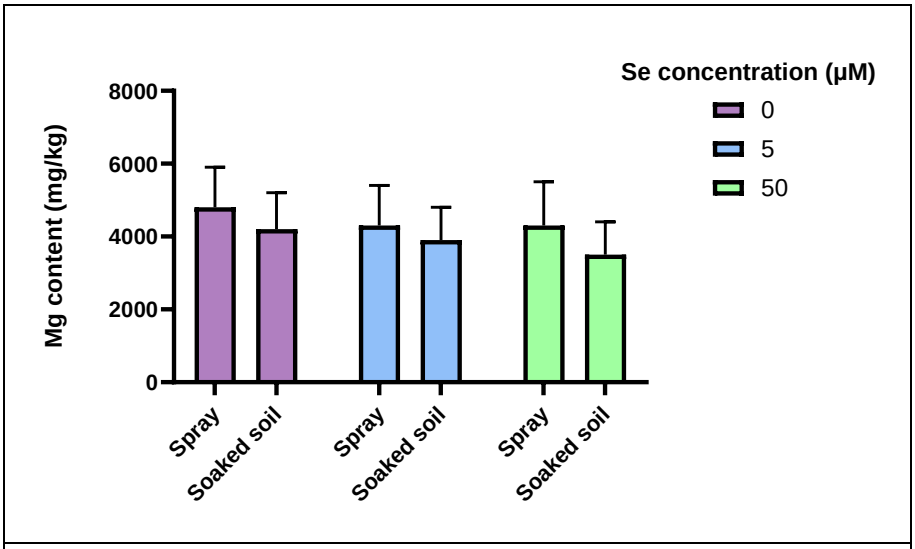

Figure 55: Effect of selenium on uptake Mg element. Based on p = 0.001 in ANOVA, application methods approach indicates significant differences. Bars indicate Mn±*SD*. (n=30).

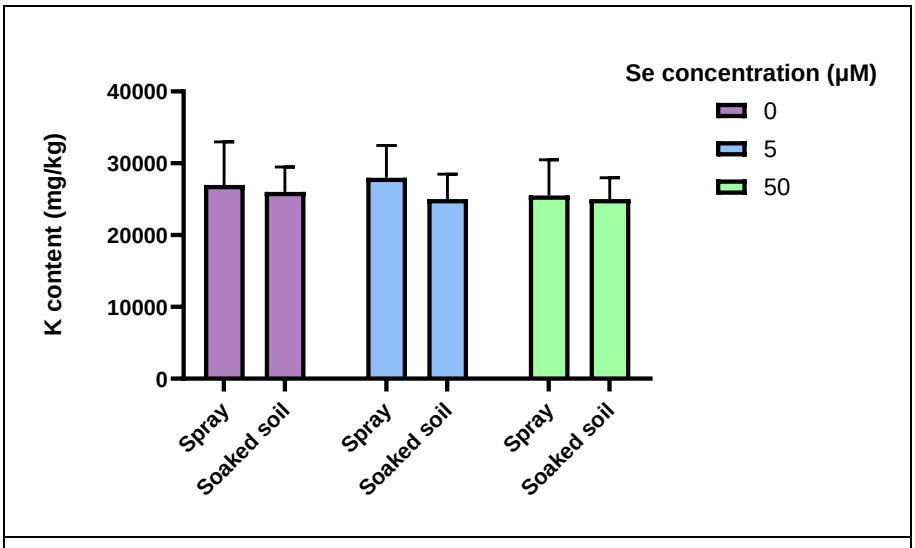

Figure 56: Effect of selenium on uptake K element. As indicated by p = 0.005 in the ANOVA, significant differences are observed in the application methods approach. Bars indicate mn±*SD*. (n=30).

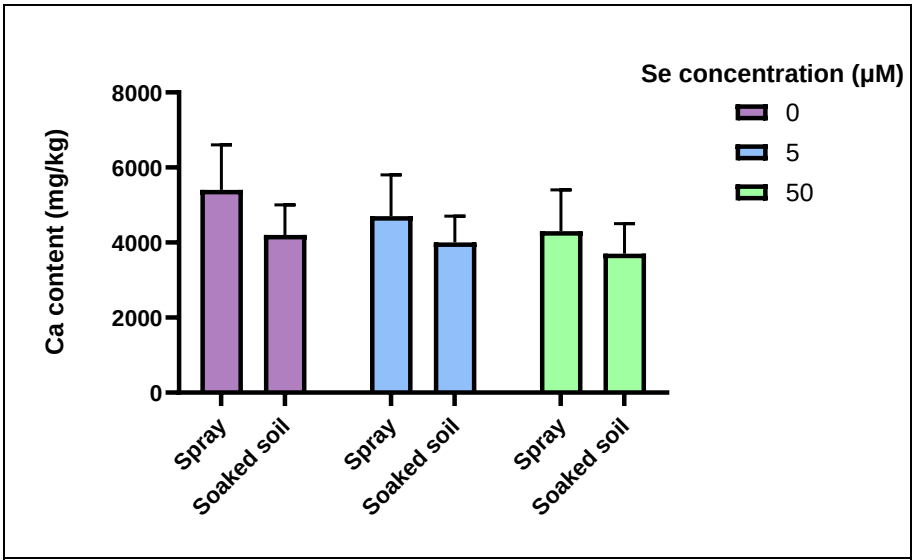

Figure 57: Effect of selenium on uptake K element. The selenium concentrations differ significantly in ANOVA with p = 0. 0001. Bars indicate mn±*SD*. (n=30).

3.3.3 Effect of selenium biofortified spring onion on HepG2 cells

Cell morphological changes were observed by microscopy (Figures 58 – 60) by exposing HepG2 cells to 0, 6, 12, 25, 50 mg/ml of selenium biofortified spring onion extracts. Untreated HepG2 cells have epithelial-like shapes (Figures 58A, 59A, 60A), However, selenium treatment causes the cells to shrivel and explode by stimulating morphological changes associated with apoptosis depending on extract concentration. Spring onion extracts should be toxic enough to collapse cancer cells and reduce the viability of cancer cells after treatment. The morphological pictures of the cells and the viability results of cancerous cells were shown to meet this expectation. Based on the viability graph (figure 63), it is evident that the viability of cancerous cells decreased with increasing extract concentration, and 50 mg/ml of Se5 µM by spray and Se50 µM applied via foliar spray, soaked soil or NFT method shows the lowest viability on HepG2, indicating these doses of extract have the best effect on inducing cell

death in cancer cells. Se50 by soaked soil also indicates the lowest viability percent of HepG2 cells in all drug concentrations, as a result, this application method, in conjunction with a higher concentration of selenium, had the most effective results against cancerous cells (Figure 60).

In the control (Se0) samples of this study, where no additional selenium was applied, any observed effects on cancer cell viability could be attributed to compounds naturally present in spring onions, as taken up from the compost. These include selenium, but not at extra levels. Spring onions are known to contain various bioactive compounds, such as antioxidants, sulfur-containing compounds (like allicin), and flavonoids, which have shown anti-cancer and anti-inflammatory properties.

The presence of these naturally occurring compounds in spring onions can contribute to cytotoxic effects on cancer cells, even without added selenium. These compounds may help induce apoptosis or inhibit cell proliferation, which could account for the baseline level of effectiveness observed in the control (Se0) samples.

In contrast, selenium biofortification likely enhances these effects due to selenium's known role in promoting apoptosis and acting as an antioxidant. The Se50 soaked soil treatment, with the lowest IC50, indicates that additional selenium amplifies the cytotoxic effect, making the spring onion extract more potent against cancer cells at lower concentrations. This suggests that while naturally occurring compounds in spring onion have a beneficial effect, selenium enrichment further strengthens the anti-cancer potential of the extracts.

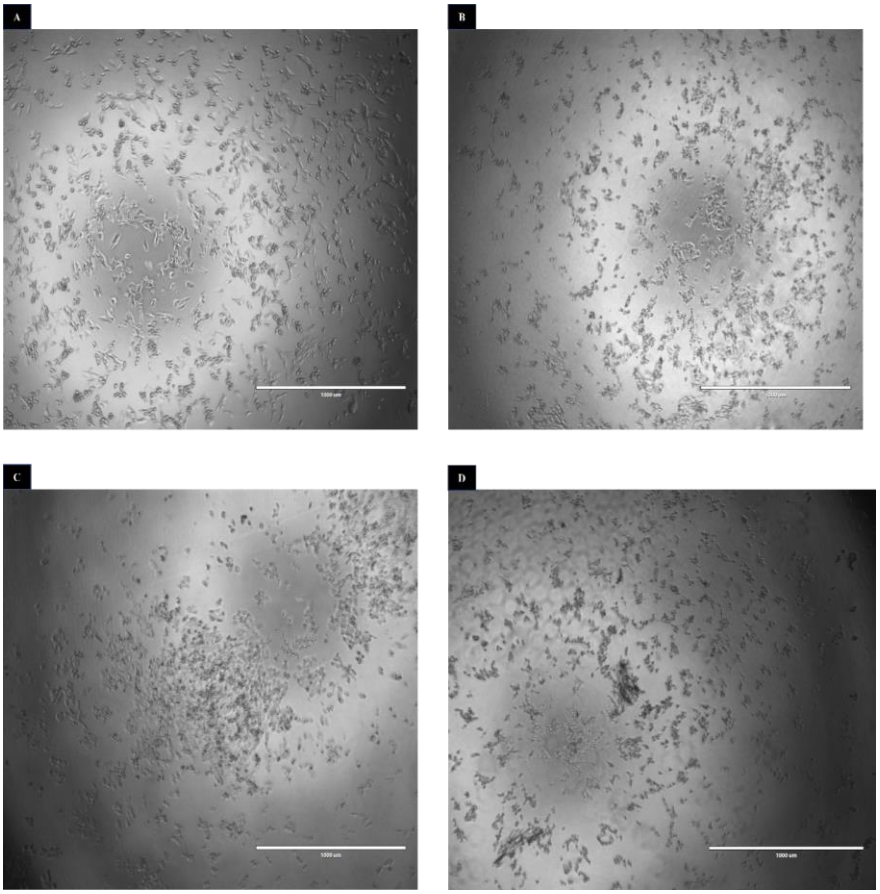

Figure 58: Images of HepG2 cells. (A, B) After seeding and before treatment. (A) Control. (B) Se0 NFT with extract concentration 50mg/ml. (C) Se5 NFT with extract concentration 50 mg/ml. (D) Se50 NFT with extract concentration 50 mg/ml. Scale bar = 1000 µm.

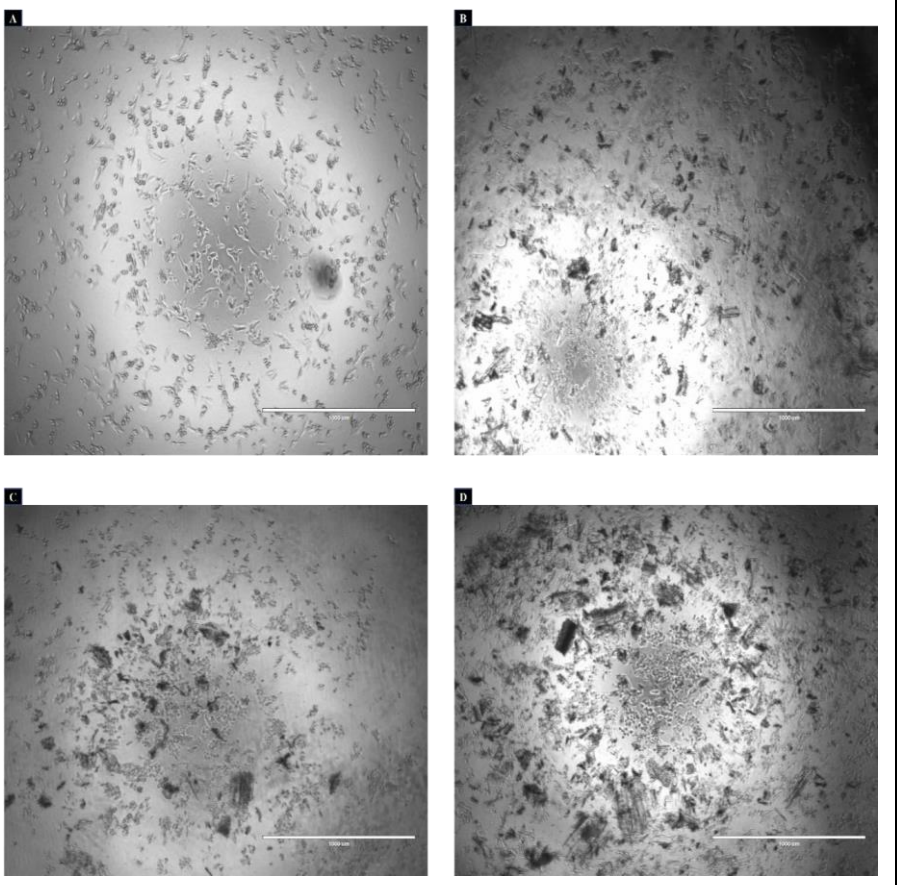

Figure 59: Images of HepG2 cells. (A) Control. (B) Se0 Spray with extract concentration 50mg/ml. (C) Se5 Spray with extract concentration 50 mg/ml. (D) Se50 Spray with extract concentration 50mg/ml. Scale. bar = 1000 µm.

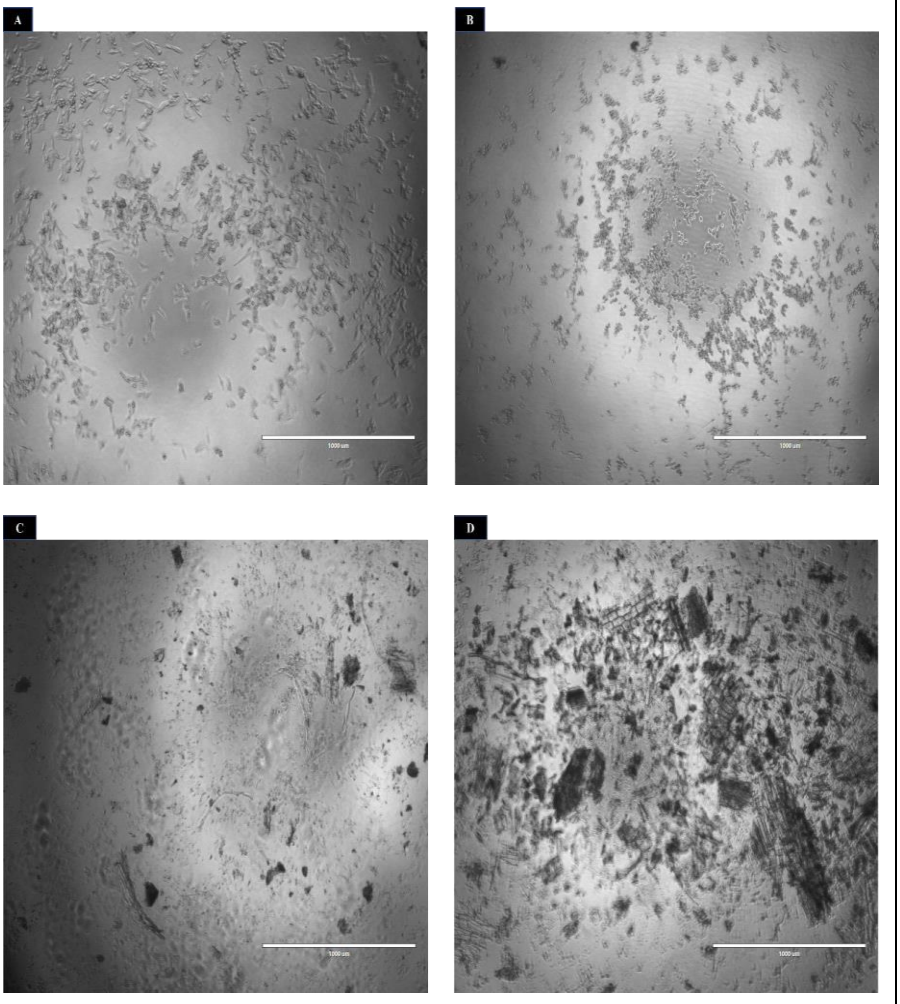

Figure 60: Images of HepG2 cells. (A) Control. (B) Se0 Soil with extract concentration 50mg/ml. (C) Se5 Soil with extract concentration 50 mg/ml. (D) Se50 Soil with extract concentration 50 mg/ml. Scale. bar = 1000 µm.

3.3.3.1 IC50:

The efficacy of a drug can be effectively measured by its half-maximal inhibitory concentration (IC50). The IC50 value represents the concentration of a drug required to inhibit the activity of a target molecule by 50%, thereby demonstrating the concentration necessary to reduce a population by half compared to a control group (Hoetelmans, 2017). This metric allows for the comparison of different drugs based on their efficiency against a specific target.

Drug-dose response graphs are commonly used to evaluate the relationship between a drug's inhibitory effects and its concentration. Variations in cell growth observed during these studies may be attributed to reduced cell proliferation, increased cell death, or a combination of both. Notably, drugs with low IC50 values are highly potent even at low concentrations, resulting in reduced systemic toxicity when administered to patients. For cells exposed to cytotoxic agents, the extent of cell death is largely determined by the amount of drug absorbed, which must exceed a specific threshold to be effective. Consequently, comparing IC50 values provides a useful method for assessing the potency of different drugs, with lower IC50 values indicating greater effectiveness at lower concentrations (Yu et al., 2015; Tallarida, 2011; Chevereau & Bollenbach, 2015).

The results presented in Table 6 demonstrate that Se50-soaked soil exhibits a significantly lower IC50 of 36.57. This suggests that this extract is particularly effective at inducing apoptosis in cancer cells at low concentrations. Since cytotoxic drugs target rapidly dividing cells, including both cancerous and normal cells, a drug effective at low concentrations is generally less harmful to the body. Therefore, the Se50-soaked soil extract displays a desirable characteristic of high potency coupled with potentially lower toxicity compared to other extracts.

In this study, IC50 values for various extracts were determined using the following formula derived from the regression of viability percentage graphs (Figures 60–62):

$Y = MX + C$

Solving for IC50:

X= IC50 = (Y−C)/MX

The results, presented in Table 6 and illustrated in Graph 61B, reveal that the Se50-soaked soil extract exhibits a lower IC50, indicating superior efficacy in inducing apoptosis at lower concentrations. This characteristic is advantageous since drugs with high potency at low concentrations are less likely to cause systemic toxicity, making Se50-soaked soil extract a particularly promising candidate for further development.

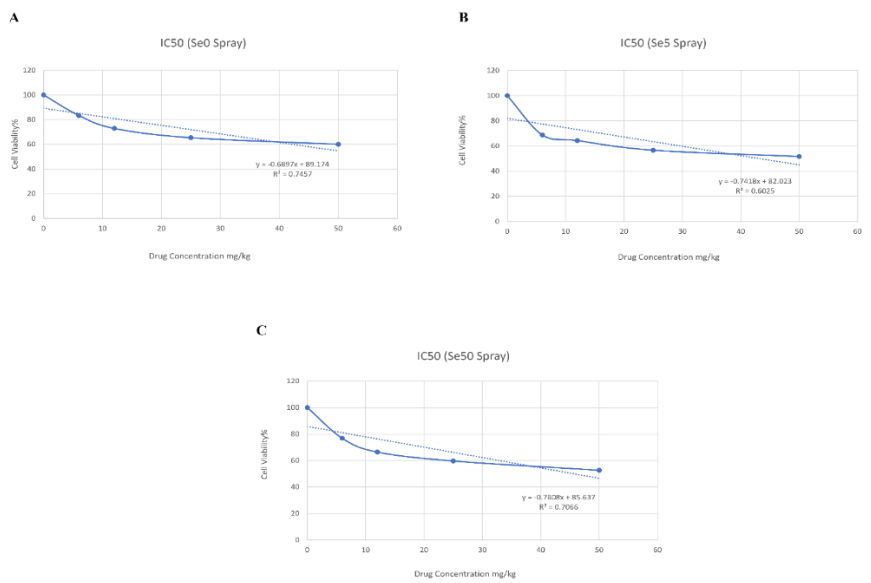

Figure 60: IC50 drug (Selenium biofortified spring onion) with Spray application method. (A) IC50 drug with Se0 concentration. (B) IC50 drug with Se5 concentration. (C) IC50 drug with Se50 concentration.

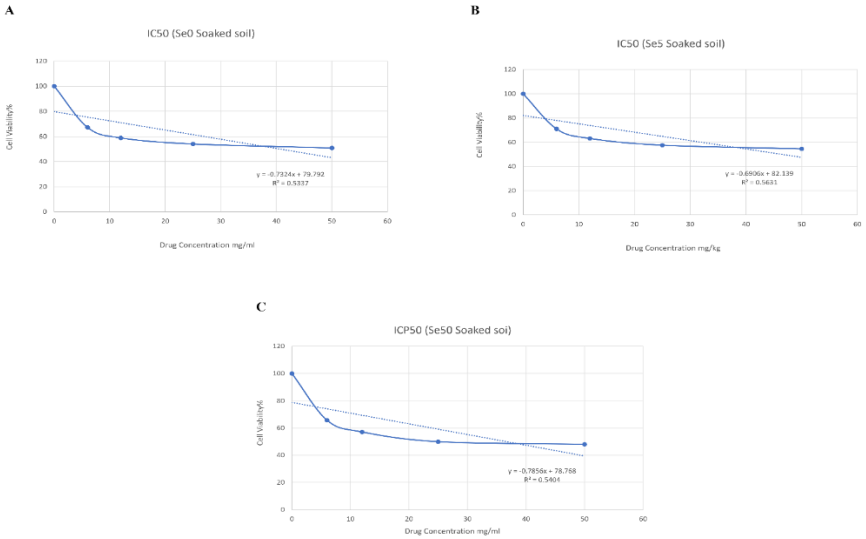

Figure 61: IC50 drug (Selenium biofortified spring onion) with Soaked soil application method. (A) IC50 drug with Se0 concentration. (B) IC50 drug with Se5 concentration. (C) IC50 drug with Se50 concentration.

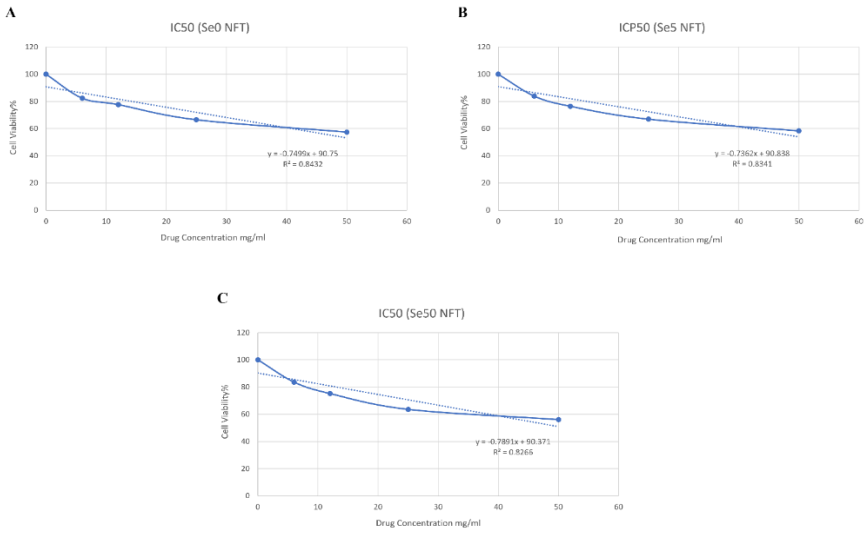

Figure 62: IC50 drug (Selenium biofortified spring onion) with NFT method. (A) IC50 drug with Se0 concentration. (B) IC50 drug with Se5 concentration. (C) IC50 drug with Se50 concentration.

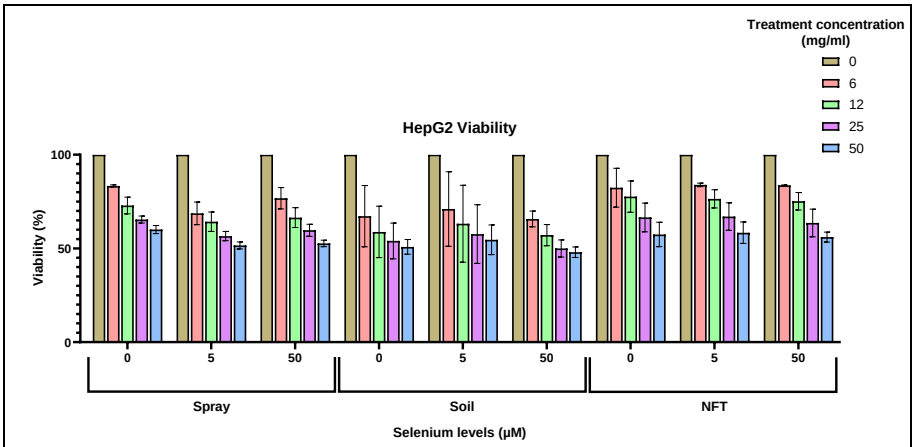

Figure 63: Viability% of HepG2 cells after treatment with selenium biofortified extractions. Bars indicate Mn+SD (n=12).

Table 6: Inhibition of HepG2 cells proliferation table. This table shows IC50 of 9 spring onion extracts which used as drug for treating on liver cancer cells (HepG2).

Spring onion extracts	Se0 Spray	Se5 Spray	Se50 Spray	Se0 Soil	Se5 Soil	Se50 Soil	Se0 NFT	Se5 NFT	Se50 NFT
IC50	56.79	43.16	45.64	40.62	46.53	36.57	54.34	55.47	51.16

3.3.4 Analysing the antioxidant and anti-free radical properties of biofortified spring onions with selenium

To evaluate the antioxidants activity of biofortified spring onions with selenium, and how antioxidants scavenge the free radicals on solutions, ABTS (2,2′-azino-bis(3ethylbenzohiazoline-6-sulfonic acid) and DPPH (2,2-diphenyl-1-picrylhdrazyl) antioxidative assays were performed. In the ABTS assay, as the antioxidants in the extract scavenge free radicals, the solution changes from blue-green to colourless, with a more significant colour change indicating higher antioxidant activity. Similarly, in the DPPH assay, antioxidants reduce the DPPH radical, causing the solution to shift from red to yellow. The

intensity of the colour change in both assays corresponds to the amount of antioxidant present in the extracts—the greater the antioxidant activity, the more pronounced the color change.

In accordance with expectations, the antioxidant activity of spring onion extracts increased with increasing extracts concentrations as measured via ABTS (Figure 64A).

This result aligns with expectations, as higher concentrations of selenium-enriched extracts generally produced stronger antioxidant effects. All extracts displayed the highest radical scavenging percentages at 50 mg/nl concentrations and this trend shifted downward with a decrease in extract concentrations. The foliar spray method at Se50 µM demonstrated the highest ability to scavenge free radicals, at 83.82 %. Se50 µM used in soak soil application showed only slightly greater antioxidant activity than control at the highest extract concentration (70.21% and 69.79% respectively) (Figure 64A).

In contrast, the DPPH assay did not show a consistent increase in antioxidant activity with higher extract concentrations at all. Instead, the scavenging activity fluctuated across concentrations, with the highest observed activity in the soil-soaked Se50 µM treatment, which reached a radical scavenging rate of 14.10%. This variation suggests that the compounds within the spring onion extracts might interact differently with DPPH compared to ABTS, potentially due to the distinct properties of the two radicals and the specific antioxidants present in the extracts.

Overall, the ABTS assay results were more predictable, while the DPPH assay indicated an inconsistent trend, likely due to different antioxidant components being more reactive with ABTS than with DPPH. This difference suggests that the two assays may capture

different aspects of antioxidant capacity, which reflects the complex nature of the bioactive compounds in selenium-biofortified spring onions. Therefore, a direct correlation between ABTS and DPPH antioxidant activities was not evident, highlighting how antioxidant capacity measurements can vary depending on the assay used.

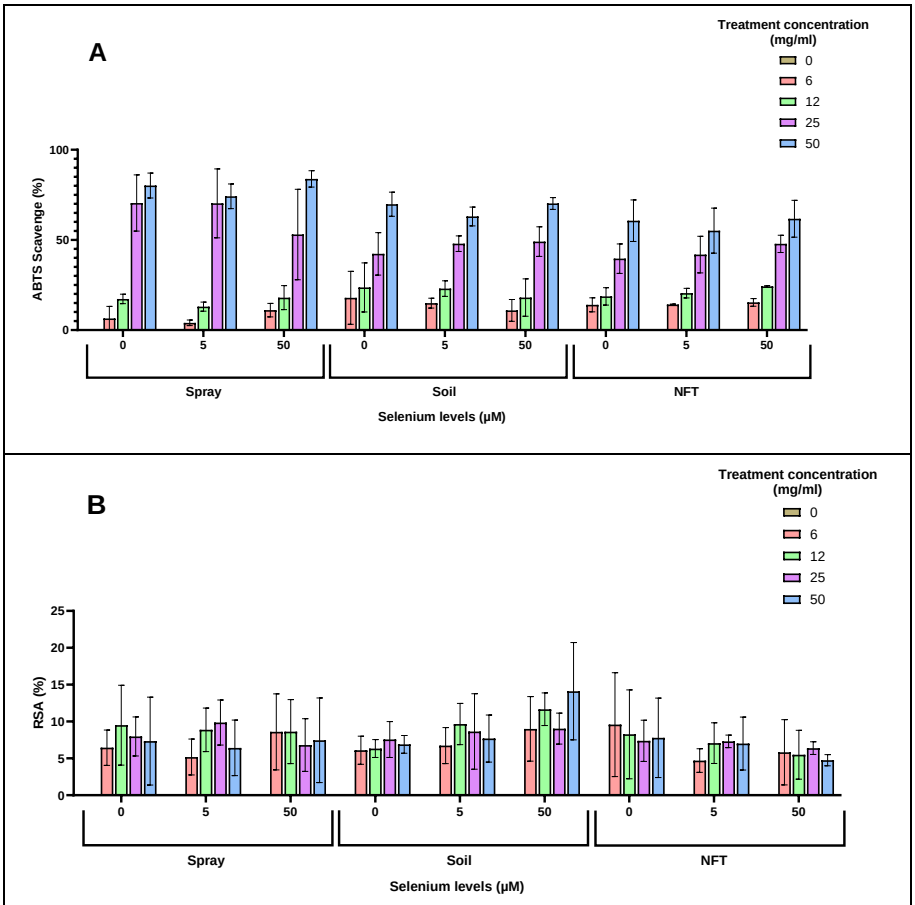

Figure 64: These bars show the radical scavenge% in ABTS (A) and DPPH (B) assays. For the control (0 mg/ml) these percentages are zero due to no antioxidant's activity in them (just free radicals + ethanol). In others, the results depends on the level of antioxidants and the ability to scavenge free radicals. Bars indicate mn$\pm SD$. (n=3).

3.4 Discussion

Two selenium application methods were used in this study to enrich spring onions via biofortification, these being foliar spraying and soil application. The results show the spring onion plants absorbed more selenium through soaked soil application as compared with foliar spray application. Similarly, other researchers have observed that when Se was applied via soil, it accumulated higher in leaf, root, and whole plant tissue than when applied via foliar application (da Silva et al., 2020). Despite that, foliar sprays have some advantages, including being less likely to cause contaminants in the environment and disturbing soil chemistry and resulting in microbiological effects (Alfthan et al., 2015; Ibrahimi et al., 2019).

When comparing the high Se levels to the control levels, there was not a significant impact on the crop agronomic parameters. In terms of results, Se5 soaked applications increased chlorophyll levels in spring onion plant which indicates similarity with other studies showing chlorophyll production can be increased by applying selenium at low concentrations during the photosynthetic process (Ashraf et al., 2018; Hemmati et al., 2019; Seliem et al., 2020). There was a slight increase in yield with increasing selenium concentration, particularly with foliar sprays, a result that was similar to other studies; there are numerous studies that suggest that plants which are foliar fertilized with selenium element have enhanced growth (Germ et al., 2007, Ozbolt et al., 2008), also El-Bassiony (2020) showed that mineral selenium spraying resulted in positive effects on onion plant growth and yield characteristics (El-Bassiony et al., 2020). This experiment shows that selenium has no significant effect on other elements' uptake, where a non-significant effect is seen, it is only slight and can be either positive or negative. In others it showed that Se presence in

plants is likely to be detected by changes in the concentrations of specific elements (Pazurkiewicz - Kocot et al., 2003). According to earlier studies, Se and S are antagonistic when it comes to uptake (Ferrari and Renosto, 19772; Leggett and Epstein, 1956; Mikkelsen et al. 1989). However, in our experiment, a positive correlation was observed between increasing selenium concentration and S contents in spring onion tissues; the highest concentration of selenium significantly increased S contents compared to the control. Similarly, another study found that higher amounts of selenate treatment increased the S content of lettuce shoots produced hydroponically (Hawrylak-Nowak, 2013).

Fargsova et al. (2006) found that increasing levels of Se inhibited the absorption of element Fe, similarly this study shows a slight antagonistic relationship between Fe content with increasing Se concentration in foliar spray. Although some studies have found no significant effect of Se treatments on Mg in corn (Hawrylak – Nowak, 2008) and tomato (Schiavon et al., 2013), this study revealed an antagonistic relationship between Se and Mg and Ca – with increasing Se concentrations, both Mg and Ca content decreased. Poldma et al. (2013) also reported a decrease in Ca content in onions grown with foliar sprays and an increase in Mg content by selenium biofortification. Different plant species and different stages of plant growth may contribute to different results.

Se biofortification was evaluated with other elements, all of which are vital for human health. There is concern that Se biofortification may alter the absorption of other essential elements. However, this study indicates that generally increasing Se does not negatively impact the absorption of other elements.

In this research, selenium was found to be effective at scavenging free radicals – in particular, ABTS assays strongly supported this conclusion. Some studies show similar results, Allium sativum extract combined with Selenium nanoparticles demonstrated relatively strong ABTS radical scavenging capability (Jay and Shafkat, 2017). Furthermore, it is known that selenium compounds can induce apoptosis in tumour cells, which is an effective cancer treatment agent. In this study, higher Se doses hindered the proliferation of cancer cells. The growth of cancer cells is inhibited by higher dosages of Se according to numerous studies, supporting our data (Thompson et al., 1994; Ronai et al., 1995; Sinha and Medina, 1997; Gopee et al., 2004; Hu et al., 2005). Due to its nutritional importance and the fact that Se can be integrated into several vital enzymes, including glutathione peroxidase, Se compounds may have chemopreventive qualities (Rotruck et al., 1973).

Selenium bioactivity results in this study indicate that selenium can have strong antioxidant properties and induce cell death in cancer cells, especially at high concentrations and via soak soil application methods.

Chapter 4: Identification of genes involved in selenium uptake using associative transcriptomics

4.1 Introduction

The majority of agricultural and evolutionary features are intricate and depend on a variety of genetic loci, environmental conditions, and how those factors interact with one another (Mackay, Stone, & Ayroles, 2009). The initial influx of association mapping studies on model agricultural and plant species was stimulated by developments in genomic technology and techniques in addition to the need to analyse variations in attributes across various genetic backgrounds.

Genome-wide association studies (GWAS) have been possible as a result of developing sequencing technology and concerted community-based initiatives (Michael & Jackson, 2013). It is essential to understand the genetic structure of complicated characteristics for agricultural and evolutionary goals. GWAS have identified genetic regions associated with a wide range of agronomic, physiological, and physical development behaviours, including flowering duration, kernel number, resilience to stress, and grain yield in *Arabidopsis* (Ersoz et al., 2007; Gupta, Kulwal, & Jaiswal, 2019; Liu & Yan, 2019; Sukumaran & Yu, 2014). As GWAS techniques began to develop in the 1990s, the first GWAS publications emerged in the early 2000s (Lander, 1996; Lander & Kruglyak, 1995), As late as 2005, *Arabidopsis* became the first plant on which a genome-wide association study was conducted in an area other than human medical genetics (Aranzana et al., 2005). The bulk of the phenotypes of plant species have intricate features controlled by numerous genes and their

interactions, making GWAS valuable for genetic research of plant phenotypes. Based on the extensive genetic variation data of *Arabidopsis thaliana*, it is now possible to map chromosomal interactions with multifaceted features with high levels of precision (Lee, 2020). `

Genetic analysis of complicated traits has become possible with the invention of associative transcriptomics (AT), an advanced technique that combines association mapping with transcriptome analysis to uncover gene-trait associations in crops and model species (Bazakos et al., 2017). This approach utilizes RNA-seq data to map high-resolution loci associated with quantitative traits, facilitating a deeper understanding of gene function beyond the capabilities of traditional GWAS (Harper et al., 2020). Unlike GWAS, which relies solely on genomic DNA, AT integrates gene expression data, making it more effective for detecting both single-nucleotide polymorphisms (SNPs) and gene expression markers (GEMs) that influence complex traits (Alcock et al., 2017).

AT has proven highly advantageous in agricultural genomics, providing precise mapping of candidate genes linked to various traits (Lee, 2020). Its high-resolution mapping capabilities enable researchers to pinpoint loci with greater accuracy, enhancing genetic analysis and trait selection (Koprivova et al., 2014). The combination of GEMs and SNPs improves marker development, thereby supporting more efficient breeding strategies by correlating traits with specific genetic markers (Alcock et al., 2017). Additionally, AT is particularly effective for polyploid crops such as oilseed rape (*Brassica* napus) and wheat, facilitating accurate mapping of homoeologous gene reads and aiding in the identification of potential candidate genes (Bazakos et al., 2017; Harper et al., 2020). AT has

resulted in the discovery of a number of genes in allopolyploid crops. The equilibrium of nitrate, phosphate, and sulphate anions, the accumulation of calcium and magnesium, and the nutritional value of the leaves were just a few of the complexities in rapeseed that were characterised using the AT platform (Koprivova et al., 2014; Alcock et al., 2017).

Comprehensive transcriptomic analyses, including RNA sequencing (RNA-seq), play a crucial role in revealing genetic diversity and identifying loci that govern significant agricultural traits (Rai et al., 2022). The rapid progress in RNA-seq technology has greatly contributed to advances in marker discovery, differential gene expression studies, and understanding the genomic structure in various plant species (Michael & Jackson, 2013). Integrating AT techniques allows for an in-depth exploration of complex traits, identifying specific markers and their associated genes with high precision (Mackay et al., 2009).

AT's ability to quantify gene expression and detect SNPs using high-quality references enhances its utility for accurate mapping and identification of candidate genes involved in specific traits (Alcock et al., 2017). This is especially beneficial for crops within the *Brassica* genus, due to the diversity within the genus and its wider significance for agriculture and horticulture. These include B. rapa, B. oleracea, and B. juncea, which have been studied for traits like nutrient uptake and anion balance (Koprivova et al., 2014; Harper et al., 2020). The implementation of AT has also advanced the identification of agronomically significant genes in these species, promoting its use in breeding programs (Alcock et al., 2017).

Since its inception, *Brassica* RNA-Seq has advanced quickly, offering important insights into the development of markers, diversity, and differential gene expression, as well as genomic structure and diversity research (Rai et al., 2022). With AT techniques, we might be able to find markers that match features with a high degree of precision and granularity, allowing for a more refined analysis of intricate traits. The discovery of SNPs and gene expression quantification in polyploids are also based on high quality references, as they enable more accurate mapping of homoeologous reads to the appropriate genome and make it easier to identify candidate genes.

An associative transcriptomics analysis of SNPs and gene expression markers (GEMs) was done in this study to determine the target genes which regulate selenium uptake in *Brassica* napus and *Arabidopsis thaliana*.

The aim and objective of this study is to:

To identify genes which may be involved in the regulation of selenium accumulation in *Brassica* napus and *Arabidopsis thaliana*.

Hypothesis:

Genes identified through associative transcriptomics analysis are involved in selenium regulation and contribute to selenium uptake in *Brassica napus* and *Arabidopsis thaliana*.

4.2 Materials and methods:

Associative transcriptomics analysis

This study repurposed data from a previous investigation into the mineral diversity of a *Brassica* napus population (Thomas et al. 2016)

to explore new targets for selenium (Se) accumulation. In that earlier work, inbred lines of *Brassica* napus L. were selected from a core panel of 387 genotypes representing a wide range of crop types—including winter, spring, semi winter oilseed rape, swede, winter fodder, and exotic forms. Two distinct cultivation systems were used: one to evaluate seedling root traits using a 'pouch and wick' hydroponic system, and another to assess leaf and seed mineral traits in plants grown in compost within a polytunnel.

Seedling Root Phenotyping

In the hydroponic system, growth pouches were constructed by combining germination paper with an overlay of black polythene. These pouches were suspended over plastic drip trays filled with a 25 % strength Hoagland's solution, ensuring that the substrate was fully saturated (for at least 4 hours) before sowing. A single seed was carefully sown near the top edge of each pouch, with seed size effects minimized by selecting seeds that spanned a range of sizes for each genotype (yielding an average seed diameter of ~1.8 mm). Seeds were pre-sorted using meshes of various diameters (1.4, 1.7, 2.0, and 2.36 mm) so that each size category represented 25 % of the seed lot; if a category was underrepresented, the next smallest size was used.

Fourteen days after sowing (DAS), the polythene layers were removed and digital images of the roots were captured using a DSLR camera (Canon EOS 1100D with a 35 mm lens at a fixed height of 75 cm). The images were then batch-renamed to incorporate unique experimental details, cropped to remove extraneous background, and analysed using RootReader2D. This software processed each image by applying automated thresholding, skeletonization, and segment building, after which the primary root length (PRL) was determined

by marking the base and tip of the primary root. In addition, lateral root length (LRL) and lateral root number (LRN) were quantified, allowing the calculation of derived traits such as total root length (TRL = PRL + LRL), mean lateral root length (MLRL = LRL/LRN), and lateral root density (LRD = LRN/PRL). A custom database, developed using a Python script, integrated these measurements with the experimental design details encoded in the image filenames.

Within the core panel, 354 genotypes were screened (including 156 winter, 124 spring, seven semi-winter OSR, 14 winter fodder, 33 swede, and 20 exotic/unspecified types) along with two additional reference winter OSR lines per run. Each experimental run included 32 genotypes with 24 individuals per genotype, totalling 11,176 potential images across 16 runs. Images were excluded if the seed failed to germinate, if the seed rolled off the paper (preventing shoot emergence), if the seedling was stunted (radicle < 3 cm), or if the radicle was deformed (e.g., twisted around the seed). Overall, 29 % of the images were removed from the analysis (see Additional file 1: Table S2). Variance components for the root traits were estimated using a REML (Residual Maximum Likelihood) model incorporating factors such as run, frame, column, tray, paper-side, crop habit, seed size, and genotype—with genotype later treated as a fixed factor to calculate genotype means.

Leaf and Seed Mineral Composition Analysis

For assessing mineral composition, seeds from all genotypes were sown directly into a fine-grade (< 3 mm) compost-based medium (Levington Seed & Modular + Sand -F2S) in modular propagation trays (650 plants m^{-2}, with an internal diameter of 2.5 cm and a module volume of 55 cm^3). Sowing took place between 22 and 29

October 2013. Following sowing, the compost was covered with perlite and transferred to a glasshouse maintained at 15 °C (controlled by a TomTech μClimate system), with supplementary lighting (Philips Master GreenPower SON-T 400 W bulbs controlled by a Grasslin Uni 45 timer) to provide a 12-hour photoperiod. Watering was conducted daily by hand until transplantation.

Between the 16th and 29th of January 2014, five plants per genotype were transplanted into individual 5 L pots (internal diameter 22.5 cm, height 18 cm) containing Levington C2 compost. The pots were arranged in a randomized block design within two single-skinned polytunnels (using Visqueen Luminance Skin) at the Sutton Bonington Campus of the University of Nottingham (52°49'58.9" N, 1°14'59.2" W). Each replicate block contained 432 units, which included one instance of each of the 387 core genotypes, 16 reference genotypes for normalization, and an additional 29 genotypes to fill gaps. In cases of poor germination, empty, compost-filled pots were used as placeholders.

Irrigation in the polytunnels was automated using a Hunter Irrigation Controller (with water distributed from a header tank via a DAB Active JI112M pump) so that each pot received 133 mL of water at 08:00, 12:00, and 16:00 daily through a low-density polyethylene (LDPE) system fitted with compensated, non-leaking drippers (4 L h^{-1} capacity); each dripper served four pots via a four-tipped manifold. Additionally, a Dosatron D3GL-2 feed injector was used to deliver Kristalon Red NPK fertiliser (Yara) from 24 March to 22 May 2014, diluting a stock solution (100 g fertiliser per litre water) at a ratio of 1:100. Once inflorescences appeared, plants were enclosed in 380 × 900 mm microperforated pollination bags to prevent cross-pollination, with any emerging side shoots subsequently removed. A

total of 2160 experimental units were established. Harvesting was conducted between 14 and 17 July 2014; stems were cut just above the bottom of the pollination bags, which were then tied securely and placed in 1 m^3 ventilated crates for storage before being transported to Elsoms Seeds (Spalding, Lincolnshire) for threshing using an SRC single plant thresher and cleaning with a Selecta seed cleaner. Thousand seed weight was determined for each plant using a Contador seed counter.

Leaf Sample Preparation and Elemental Analysis

Leaf samples were collected at the rosette stage (typically when 6–8 true leaves were visible) from 5 to 11 March 2014. For each plant, a minimum of three fully expanded leaves were excised, weighed, and photographed immediately. The leaves were then stored in labeled paper bags at –20 °C before being freeze-dried (using a CHRIST Alpha 2-4 LD freeze dryer) for 48–60 hours and re-weighed. The dried tissue was homogenized in liquid nitrogen with a pestle and mortar and kept frozen until analysis.

Approximately 0.20 g of dry leaf material was digested using a microwave digestion system (Multiwave 3000 platform with a 48-vessel MF50 rotor; digestion vessels featured PFA liners and PEEK pressure jackets). The digestion mixture consisted of 2 mL of 70 % Trace Analysis Grade HNO_3, 1 mL of Milli-Q water (18.2 MΩ cm), and 1 mL of H_2O_2. The microwave was set to 1400 W power, 140 °C, and 2 MPa pressure for 45 minutes. Two operational blanks were included in each run, and duplicate samples of a certified reference material (Tomato SRM 1573a, NIST) were processed approximately every fourth run; a laboratory reference material (LRM) from pooled freeze-dried *Brassica* napus leaves was used in later digests. After

digestion, samples were diluted to a final volume of 15 mL by adding 11 mL of Milli-Q water, transferred to 25 mL tubes, and stored at room temperature. Prior to analysis, leaf digestates were further diluted 1:5. Elemental concentrations for 28 elements (including Ag, Al, As, B, Ba, Ca, Cd, Cr, Co, Cs, Cu, Fe, K, Mg, Mn, Mo, Na, Ni, P, Pb, Rb, S, Se, Sr, Ti, U, V, and Zn) were determined using inductively coupled plasma-mass spectrometry (ICP-MS; Thermo Fisher Scientific iCAPQ). Three operational modes were used: a helium collision cell (He-cell) with kinetic energy discrimination, standard mode (STD) with an evacuated collision cell, and a hydrogen collision cell (H_2-cell). Samples were introduced via an autosampler with an ASXpress™ rapid uptake module and a PEEK nebulizer. Internal standards (Sc at 20 μg L^{-1}, Rh at 10 μg L^{-1}, Ge at 10 μg L^{-1}, and Ir at 5 μg L^{-1}) were added in 2 % HNO_3. External calibration was performed using multi-element standards (Claritas-PPT grade CLMS-2) and a bespoke calibration solution (PlasmaCAL) for Ca, K, Mg, and Na. In-house standards were used for boron, phosphorus, and sulfur. In-sample switching allowed for the measurement of B and P in STD mode and Se in H_2-cell mode, while other elements were measured in He-cell mode. A total of 2096 samples were analyzed over 14 ICP-MS runs using Qtegra™ software for data processing.

Seed Sample Preparation and Elemental Analysis

Dry seeds (three per tube, with occasional adjustments for very small seeds) were placed in Pyrex test tubes (16 × 100 mm) and weighed. The remaining seed masses were estimated using the method described by Danku et al. Seeds were left overnight to pre-digest in 1.16 mL of trace metal grade HNO_3 (spiked with an indium internal standard) along with 1.2 mL of H_2O_2. The pre-digested samples were then heated in dry block heaters (DigiPREP MS) at 115 °C for 4 hours.

After digestion, seed samples were diluted to 11.5 mL with Milli-Q water and transferred to 96-well deep well plates using an adjustable multichannel pipette. Elemental analysis was conducted using an ICP-MS (PerkinElmer NexION 300D with an Elemental Scientific autosampler and Apex HF sample introduction system) in standard mode, monitoring 20 elements (including Li, B, Na, Mg, P, S, K, Ca, Mn, Fe, Co, Ni, Cu, Zn, As, Se, Rb, Sr, Mo, and Cd). A liquid reference material prepared from pooled seed digests was run alongside the samples to correct for instrumental variation. Concentrations were determined via external calibration using standards prepared from single-element solutions. In total, 1986 seed samples were analysed across four ICP-MS runs.

Data Processing for Mineral Composition

For each sample, the mean operational blank value (specific to each element) from the ICP-MS run was subtracted from the measured concentration. The corrected value was then multiplied by the initial sample volume, divided by the original dry mass, and expressed as mg element per kg of dry material. Element-specific limits of detection (LODs) were defined as three times the standard deviation of the blank values (assuming starting dry weights of 0.200 g for leaves and 0.015 g for seeds; see Additional file 1: Table S3). For leaf samples, recoveries from certified reference materials ranged from 68 % to 134 % for 18 elements (Additional file 1: Table S4). Seven elements (Ag, Co, Cr, Ni, Pb, U, V) were excluded from the leaf analysis because their mean concentrations were at or near the LOD (Additional file 1: Table S5), and similarly, seven elements (As, Co, Cr, Fe, Ni, Pb, Se) were omitted from the seed analysis (Additional file 1: Table S6). For the remaining elements, values below the LOD were replaced with half the LOD value, and data points exceeding five

standard deviations above the global mean were removed to avoid using contaminated samples (125 out of 58,688 values for leaves and 107 out of 42,504 for seeds).

Genotypic and non-genotypic variance components for leaf and seed composition were calculated using a REML procedure in GenStat. The model incorporated random factors for crop habit, genotype, and experimental design factors (polytunnel, replicate within polytunnel, and sub-block within replicate) [habit + genotype + polytunnel + polytunnel/replicate + polytunnel/replicate/sub-block]. For leaf composition traits, an additional model including replicate and genotype interactions [replicate + (replicate/subblock) + genotype + (replicate/genotype)] was used, with genotype subsequently treated as a fixed factor to derive genotype means. For seed composition, arithmetic means per genotype were used.

Multivariate Analyses

A comprehensive correlation analysis was performed on all 945 possible pairwise combinations among the 44 variate sets derived from root, leaf, and seed traits (using genotype means). Additionally, five stepwise discriminant analyses were conducted in GenStat: one each for the root morphology (6 variates), leaf mineral composition (21 variates), seed mineral composition (15 variates), and seed weight (2 variates) datasets, as well as one analysis combining all traits. Genotypes were grouped based on crop habit. A Wilks' Lambda forward selection algorithm was employed to sequentially add the trait variate that best explained the between-group variation, with specificity plots illustrating the proportion of correctly classified genotypes and discrimination plots providing a two-dimensional visualization of group separation. All statistical analyses were

performed using GenStat 15th Edition (VSN International Ltd, Hemel Hempstead, UK).

Association Transcriptomics for Selenium Accumulation

The selenium data from the *Brassica* napus mineral diversity study were reanalysed to uncover new targets for Se accumulation. AT, utilizing mRNA sequencing data, was used to identify high-resolution loci quantitatively associated with the traits of interest. This approach benefits from the use of RNA sequences to develop markers—both single-nucleotide polymorphisms (SNPs) and gene expression markers (GEMs)—which offer practical advantages over DNA-based markers. The analysis was carried out with the GAPIT package in R 3.2.0 using SNP and Q-matrix data. A fixed-effect linear model was applied to assess the relationship between RPKM values and Q-matrices as predictors of trait variation. Prior to generating Manhattan plots using R's graphing functions, SNPs with low secondary allele frequencies were excluded from the dataset. Statistical significance was determined at $P < 0.05$, following adjustments for false discovery rates and Bonferroni corrections, in line with the phenotypic growth trial and analysis performed by Alcock (2016). In total, 355,537 SNPs and 53,890 GEMs were plotted from the two *Brassica* genomes—B. rapa (A genome) and B. oleracea (C genome). Subsequently, *Arabidopsis* homologs of the selenium uptake and translocation genes were identified, facilitating further studies using *Arabidopsis* gene knockouts. The resulting files were sorted based on their $-\log_{10} P$ values, with the markers showing the strongest associations positioned at the top.

The significance level was set at $P < 0.05$ by adjusting false discovery rates and Bonferroni corrections using the phenotypic growth trial and analysis performed by Alcock 2016.

The data utilized in this study originated from a prior analysis of the mineral composition in the *Brassica* napus diversity population (Thomas et al., 2016). This study specifically analysed selenium (Se) data to identify novel targets for Se accumulation (Alcock et al., 2017). Association transcriptomics, which leverages transcribed sequences (mRNA-seq), was employed to identify high-resolution loci quantitatively related to traits (Lipka et al., 2012). In these association studies, RNA sequences offer the advantage of developing markers through both single-nucleotide polymorphisms (SNPs) and gene expression markers (GEMs), providing more convenience compared to DNA sequences (Alcock et al., 2017).

The association transcriptomics analysis was conducted using the GAPIT R package in R version 3.2.0, incorporating both SNP and Q-matrix data (Lipka et al., 2012; R Core Team, 2013). For examining the relationships between gene expression markers (GEMs) and traits, a fixed-effect linear model was applied in R, using RPKM values and Q-matrices as explicating factors and trait values as responses (R Core Team, 2013). SNPs with low secondary allele frequencies—that is, those with a minor allele frequency (MAF) below 0.05 (5%)—were excluded from the dataset prior to creating Manhattan plots with R's graphical functions to ensure robustness and reduce noise from rare alleles (Alcock et al., 2017). Significance was maintained at $P < 0.05$, with adjustments made using both false discovery rate (FDR) and Bonferroni corrections (Benjamini & Hochberg, 1995; Dunn, 1961). A total of 355,537 SNPs and 53,890 GEMs were plotted, derived from two *Brassica* genomes: B. rapa (A genome) and B. oleracea (C

genome) (Chalhoub et al., 2014; Alcock et al., 2017). Subsequently, *Arabidopsis* gene equivalents associated with selenium uptake and translocation were identified, facilitating the study of gene knockouts in *Arabidopsis* (Schranz et al., 2006).

The analysis outputs were sorted by $-\log_{10}P$ values, ensuring that markers with the highest association were prioritized at the top (Yang et al., 2011). The computational analysis involved specific R packages such as GAPIT for association transcriptomics, base R functions including p.adjust() for multiple testing corrections, and custom scripts for GEM associations (Lipka et al., 2012; R Core Team, 2013; Alcock et al., 2017). The False Discovery Rate (FDR) is a statistical approach used to control for the expected proportion of false positives among results declared significant (Benjamini & Hochberg, 1995) and, unlike the Bonferroni correction which controls the Family-Wise Error Rate (FWER), FDR is less stringent and more suitable for high-throughput data such as that generated by genome-wide studies (Storey & Tibshirani, 2003). Higher statistical power is achieved using the FDR approach compared to the Bonferroni method, which is particularly advantageous for studies involving thousands of tests and reduces the risk of false negatives (Benjamini & Hochberg, 1995; Storey & Tibshirani, 2003), and the Benjamini–Hochberg (BH) procedure—the most widely used method for FDR calculation—involves ranking p-values and adjusting them based on their rank and the total number of tests (Benjamini & Hochberg, 1995; Benjamini & Yekutieli, 2001), which can be implemented in R using the p.adjust() function with the method set to "fdr" (R Core Team, 2013). The Bonferroni correction adjusts the significance threshold by dividing the desired alpha level (e.g., 0.05) by the number of comparisons, thereby ensuring strict control over Type I errors (Dunn, 1961),

although it can be overly conservative when applied to data with a large number of tests, potentially increasing the risk of Type II errors (Bland & Altman, 1995), and is particularly useful when the cost of a false positive is high (Dunn, 1961; Shaffer, 1995), but in genome-wide studies its stringency may result in the failure to identify true associations due to an elevated risk of false negatives (Perneger, 1998).

The $-\log_{10}$ transformation of p-values is used for visual representation in Manhattan plots, enhancing the interpretability of very small p-values (Manolio, 2010); for example, a p-value of 1×10^{-5} transforms to $-\log_{10}(1 \times 10^{-5}) = 5$, facilitating clearer visualization (Pe'er et al., 2006), and a typical threshold such as $-\log_{10}P > 5.7$ indicates a significant association, corresponding to an unadjusted p-value of approximately 2×10^{-6} (Yang et al., 2011). The GAPIT R package was employed as a comprehensive tool for genome-wide association and associative transcriptomics analyses, applying multiple models for the detection of significant loci (Lipka et al., 2012), with base R and supporting packages utilized, including functions like p.adjust() for multiple testing corrections using both FDR and Bonferroni methods (R Core Team, 2013), and custom scripts developed for GEM associations automated the processing and analysis of the data (Alcock et al., 2017).

The analysis also utilized two reference genomes, B. rapa (A genome) and B. oleracea (C genome), which represent the two sub-genomes of the allotetraploid *Brassica* napus (Chalhoub et al., 2014). Incorporating both genomes was essential for accurately identifying SNPs and GEMs as well as for distinguishing homoeologous genes within the polyploid species (Parkin et al., 2014; Snowdon et al., 2015). This dual-genome approach enabled a comprehensive

understanding of the genetic structure and interactions that influence traits such as selenium accumulation (Harper et al., 2012; Edwards et al., 2017). Identifying *Arabidopsis* orthologs of selenium uptake and translocation genes facilitated comparative analyses and validation studies using *Arabidopsis* gene knockouts (Schranz et al., 2006; Wang et al., 2011), thereby allowing for high-resolution mapping and robust cross-species comparisons in association transcriptomics studies (Chalhoub et al., 2014; Harper et al., 2012).

4.2.1 Identification of targets

The identification of candidate genes associated with selenium accumulation was achieved through associative transcriptomics analysis, an approach that integrates Single Nucleotide Polymorphisms (SNPs) and Gene Expression Markers (GEMs) to detect genetic regions linked to selenium accumulation traits. This study leveraged data from a previous *Brassica* napus diversity population analysis (Thomas et al., 2016), employing mRNA-seq to generate high-resolution datasets that map genomic regions influencing selenium accumulation. The expressed sequences were aligned to the reference genomes of B. rapa (A genome) and B. oleracea (C genome).

Associative transcriptomics was conducted using the GAPIT R package (version 3.2.0) with a fixed-effect linear model to examine the relationships between genetic variation (in the form of SNPs and GEMs) and selenium accumulation traits. The analysis encompassed 355,537 SNPs and 53,890 GEMs across the two genomes. To enhance accuracy, SNPs with low minor allele frequencies were excluded, reducing noise and potential false positives. Statistical significance was established at $P < 0.05$, with additional adjustments made using

Bonferroni corrections and False Discovery Rate (FDR) adjustments to minimize Type I errors.

Significant associations were identified across multiple chromosomes, including A01, A03, A05, A08, A09, A10, C01, C04, C05, and C09. Notably, the strongest associations involving GEMs were localized on chromosome C03. To determine which genes were associated with these regions, orthologous genes in *Arabidopsis thaliana* were identified using the ENSEMBL database, revealing 16 SNPs and 378 GEMs related to selenium accumulation based on their genomic location and functional annotation.

Candidate genes were prioritized based on their location, statistical significance (log10P value), and FDR-adjusted P-value, with stringent thresholds set at log10P > 5.7 and FDR-adjusted P-value < 0.05. Experimental validation was performed through PCR analysis and Inductively Coupled Plasma Mass Spectrometry (ICP-MS), confirming the relevance of several identified genes.

Among these, AT3G07090, a member of the PPPDE thiol peptidase family, emerged as a particularly promising candidate. This gene was found to significantly influence selenium accumulation without affecting the uptake of other elements, highlighting its potential as a target for enhancing selenium accumulation in *Brassica* species. Its similarity to known *Arabidopsis thaliana* genes further strengthens its candidacy for targeted breeding or genetic engineering aimed at improving selenium biofortification.

Further investigation involved assessing genes surrounding the significant markers to identify additional potential targets. Given that some marker locations differed from those recorded in databases, gene markers with log10P values > 2 were also examined within GEMs.

Linkage Disequilibrium (LD) decay was evaluated with thresholds of $0.05 < R^2 < 0.1$ to enhance precision.

Subsequent analysis identified orthologous genes of interest in *Arabidopsis thaliana* using the TAIR database, following the same process of statistical filtration and annotation. Seven distinctive genes were selected for further validation using mutant *Arabidopsis thaliana* seeds obtained from the Nottingham *Arabidopsis* Stock Centre (NASC).

Primers were designed to amplify regions surrounding each gene insertion using Primer3 (https://primer3.ut.ee/). By pasting flanking sequences from TAIR into BLAST and ENSEMBL, precise gene locations were confirmed. Complete genomic sequences surrounding the identified regions (approximately 12kb) were downloaded, and PCR primers were designed to produce a 900 bp product. The PCR size of potential target genes was determined by measuring the length from the left border to the insert (bp) and the right border to the insert (bp).

This comprehensive approach successfully pinpointed AT3G07090 as a key candidate for enhancing selenium accumulation. Its specific influence on selenium uptake, independent of other elements, makes it a valuable target for further genetic improvement efforts in *Brassica* species.

Table 7: Designed left and right primers in potential target *Arabidopsis* genes.

Number	*Arabidopsis* genes	NASC STOCK CODE	Primers

1	AT2G35800.1	N613885	LEFT PRIMER 431 20 58.83 50.00 0.00 0.00 0.00 CCATTGACTGTTGCGGTGAT RIGHT PRIMER 1043 20 59.13 50.00 0.00 0.00 0.00 TTTCCGACTCACAAATGCCG
2	AT2G41170.1	N613794	LEFT PRIMER 161 20 58.79 50.00 0.00 0.00 0.00 GAGTTCGAGGTTTGTTGCGA RIGHT PRIMER 770 20 59.07 55.00 6.95 0.00 0.00 GTTCGTCGCCATTGGATCTC
3	AT3G04950.1	N582534	LEFT PRIMER 127 20 58.17 50.00 0.00 0.00 0.00 AATTCCCGGCTCAAGAACAG RIGHT PRIMER 636 20 57.44 45.00 0.00 0.00 0.00 TCCGCAACATCTTCAAGGAA
4	AT3G07090.1	N577739	LEFT PRIMER 103 20 58.63 55.00 0.00 0.00 0.00 GCCAGCTCTCACAATCACTC RIGHT PRIMER 781 20 58.85 50.00 0.00 0.00 0.00 GCTGCTTCACTTGCTCGTAA
5	AT4G12120.1	N555233	LEFT PRIMER 241 20 58.97 55.00 0.00 0.00 0.00 CGGTTCTAGGACGAGCATCT RIGHT PRIMER 772 21 59.03 47.62 0.00 0.00 0.00 AGCAACCCCGTTAGTTAGTCA

The primers designed for the potential target genes in *Arabidopsis* were systematically restructured to enhance clarity and detail. Each gene was assigned left and right primers with their specific sequences, GC content, melting temperature (Tm), primer length, and the size of the resulting PCR product. For instance, the primers for AT2G35800.1 included a left primer sequence of CCATTGACTGTTGCGGTGAT with a GC content of 58.83%, a Tm of 50°C, and a length of 20 base pairs (bp), producing a product size of 431 bp. Similarly, the right primer sequence was TTTCCGACTCACAAATGCCG with a GC content of 59.13%, the same Tm of 50°C, and a length of 20 bp, yielding a product size of 1043 bp. This systematic approach was applied across all genes, such as AT2G41170.1, AT3G04950.1, AT3G07090.1, and AT4G12120.1, with detailed attributes presented for each primer. These comprehensive details ensure precision and reproducibility in PCR experiments, facilitating targeted gene amplification in *Arabidopsis*.

Table 8: PCR Product Size in *Arabidopsis* target genes.

GENE	The PCR product size (Left border to insert) bp	The PCR product size (Insert to Right border) bp
AT2G35800	421 – 721 ~ 300	721 – 1021 ~ 300
AT2G41170	121 – 241 ~ 120	241 – 721 ~ 480
AT4G12120	241 – 661 ~ 420	661 – 721 ~ 60
AT3G07090	61 – 421 ~ 360	421 – 721 ~ 300

AT3G04950	121 – 481 ~ 360	481 – 601 ~ 120

4.2.2 Identification of homozygous lines

PCR was used to determine whether the insert was present and whether it was heterozygous or homozygous. A total of five *Arabidopsis* genotype lines were provided by NASC. On 14/12/2021, 15 plants of each line were potted. The tissues (1 cm of each tissue) were collected on 15/02/2022, straight frozen in liquid nitrogen, and stored in a -80 freezer until processing.

4.2.2.1 DNA Extraction:

Fresh *Arabidopsis* thaliana tissue (~100 mg per sample) was harvested and immediately frozen in liquid nitrogen to preserve DNA integrity; the frozen tissue was then ground into a fine powder using either a ball mill (30 Hz for 1 minute) or a pestle and mortar while maintaining immersion in liquid nitrogen to ensure efficient disruption of cellular structures. A fresh extraction buffer was prepared containing 100 mM Tris-HCl (pH 8.0) as a buffering agent, 50 mM EDTA to chelate divalent cations and prevent nuclease activity, 500 mM NaCl to aid in solubilizing nucleic acids by disrupting protein-DNA interactions, and 1% SDS to lyse cell membranes and denature proteins, with an optional addition of 1% β-mercaptoethanol to reduce disulfide bonds in proteins when working with tissues high in phenolic compounds.

Approximately 1 mL of this extraction buffer was added to every 100 mg of powdered tissue in sterile microcentrifuge tubes, and the mixture was vortexed briefly for 10 seconds to ensure even mixing. The samples were then centrifuged at 13000 rpm g for 10 minutes at 4°C, and the supernatant containing the solubilized DNA was

carefully transferred to fresh tubes without disturbing the pellet. To the collected supernatant, an equal volume of ice-cold isopropanol was added, and the tubes were gently inverted 5–7 times to mix thoroughly, thereby facilitating the precipitation of DNA by reducing its solubility in aqueous solutions. The mixture was centrifuged at 13000 rpm for 10 minutes at 4°C, resulting in a visible white DNA pellet at the bottom of the tube; the supernatant was carefully decanted, ensuring that the pellet remained undisturbed.

The DNA pellet was subsequently washed with 500 µl of 70% ethanol to remove residual salts and contaminants, gently vortexed, and centrifuged at 10,000 x g for 5 minutes at 4°C. After discarding the ethanol, the pellet was allowed to air-dry for 5–10 minutes to evaporate any remaining ethanol. Finally, the dried DNA pellet was resuspended in 50–100 µl of nuclease-free water or TE buffer (10 mM Tris, 1 mM EDTA, pH 8.0), the tubes were briefly vortexed and incubated at room temperature for 5–10 minutes to ensure complete dissolution of the DNA. The quality and purity of the extracted DNA were then assessed by measuring concentration and purity using a NanoDrop spectrophotometer (examining the 260/280 and 260/230 ratios), and the DNA integrity was evaluated via electrophoresis on a 1% agarose gel; the extracted DNA was stored at –20°C for short-term use or –80°C for long-term storage.

4.2.2.2 PCR Analysis:

Five PCR mixes were made with different primers for each gene, containing:

1. Left (gene primer) + Right (gene primer)

2. Left (gene primer) + SALK A (TDNA border line)

3. Left (gene primer) + SALK B (TDNA border line)

4. Right (gene primer) + SALK A (TDNA border line)

5. Right (gene primer) + SALK B (TDNA border line)

Table 9: Primers Used for Gene Amplification and Expression Analysis in *Arabidopsis* gene targets.

Gene Name	Primer Type	Primer Sequence	GC Content (%)	Melting Temperature (Tm, ÂºC)	Primer Length (bp)	Product Size (bp)
AT2G35800.1	LEFT	CCATTGACTGTTGCGGTGAT	58.83	50	20	431
AT2G35800.1	RIGHT	TTTCCGACTCACAAATGCCG	59.13	50	20	1043
AT2G41170.1	LEFT	GAGTTCGAGGTTTGTTGCGA	58.79	50	20	161
AT2G41170.1	RIGHT	GTTCGTCGCCATTGGATCTC	59.07	55	20	770
AT3G04950.1	LEFT	AATTCCCGGCTCAAGAACAG	58.17	50	20	127
AT3G04950.1	RIGHT	TCCGCAACATCTTCAAGGAA	57.44	45	20	636
AT3G07090.1	LEFT	GCCAGCTCTCACAATCACTC	58.63	55	20	103
AT3G07090.1	RIGHT	GCTGCTTCACTTGCTCGTAA	58.85	50	20	781
AT4G12120.1	LEFT	CGGTTCTAGGACGAGCATCT	58.97	55	20	241
AT4G12120.1	RIGHT	AGCAACCCCGTTAGTTAGTCA	59.03	47.62	21	772

PCR mix was made up of 5 µl Green 5x Buffer, 2 µl MgCl2, 0.5 µl dNTP, 1.25 µl Primer1 and 1.25 µl Primer2, 0.12 µl Taq DNA Polymerase, and 13.9 µl water for adding to 1µl DNA, then was put in the PCR machine. Finally, Agarose gel electrophoresis was utilised to detect homozygous lines. To make gel, 0.8 gram of Agarose was added to 100 ml of "TRIS - BORATE - EDTA - BUFFER" and microwaved for one minute. After cooling a bit, 2 µl of Ethidium Bromide was added to gel tank and kept under hood for 30 minutes. Upon putting the gel tank into Gel Electrophoresis and covering it with "TRIS - BORATE - EDTA - BUFFER" first put the 4 µl marker on and continued with 10 µl samples, followed by turning on the Gel Electrophoresis machine for 30-40 minutes at 100 (V, mV). The gel tank was then placed in a documentation system to analyse and print the results.

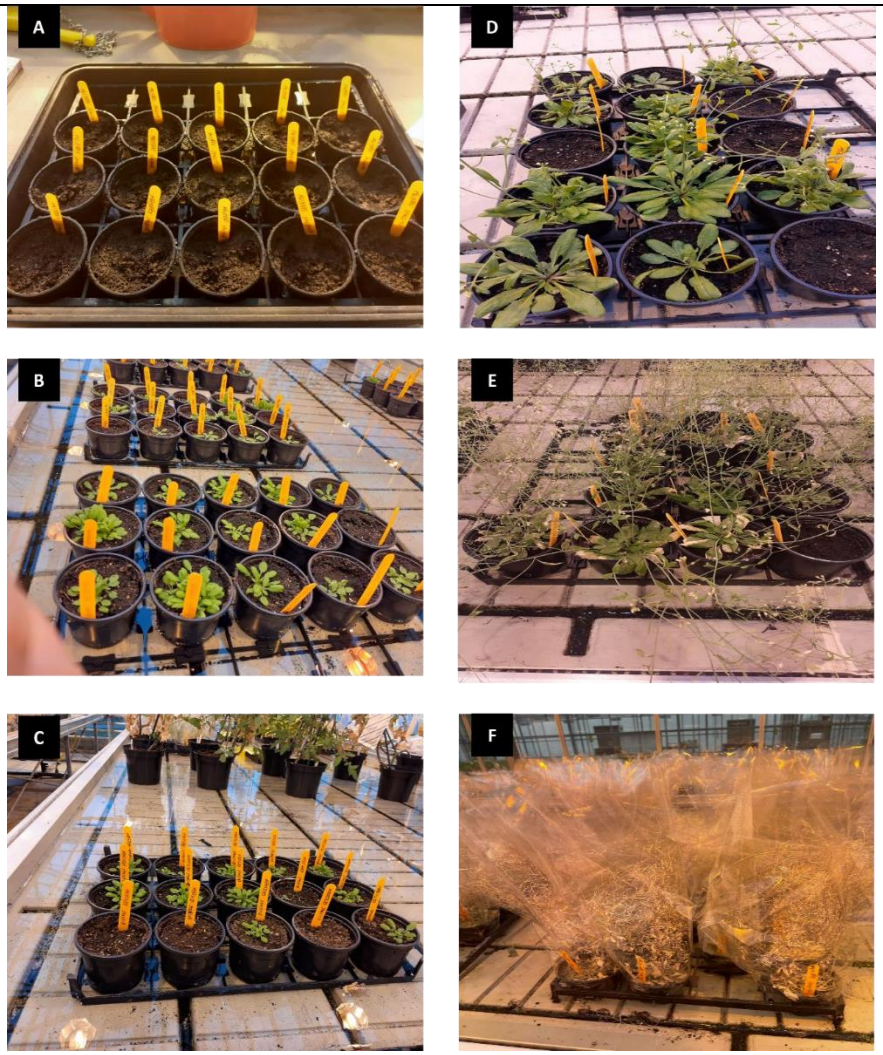

Figure 65: Phases of *Arabidopsis* growth. (A) Sowing of seeds. (B) Growing phase. (C) Using an automatic irrigation system. (D) Developmental phase. (E) Flowering. (F). Harvest time.

4.2.3 Phenotyping lines

A total of 40 plants of each line (Homozygous and Wild type lines) were planted (16/11/2022). 20 plants consuming selenium naturally from compost, 20 plants taking additional selenium, and 40 plants of Colombia wild type as controls were used to test the efficiency of each gene. A transgenic space in a glasshouse was set up for all the pots,

and every other week Se5 μM (50 ml per plant) was applied to the plants that needed selenium. An ICP-MS analysis of sample *Arabidopsis* plants was performed to assess whether the gene knockout affected its phenotype (selenium uptake). 9 plants of homozygous and wild type lines were collected on 06/02/2023 (This indicates that the plants were 82 days old (approximately 11.7 weeks) at the time of collection), and the results were plotted on bar graphs and analysed statistically using Two-factor ANOVA in GenStat software. As for the other plants, they continued to grow until the seeds were harvested on 03/03/2023.

The Hot Plate Acid Digestion method for preparing *Arabidopsis* samples for ICP-MS analysis involved several key steps. First, *Arabidopsis* tissues are harvested and dried, typically using a freeze dryer to ensure complete moisture removal. The dried samples are then ground into a fine powder, often with the aid of liquid nitrogen to facilitate grinding without structural loss. A precise weight of the powdered sample, usually between 0.2 and 0.5 g, is transferred into a digestion vessel, such as a Teflon-coated or glass digestion tube. Concentrated nitric acid (HNO_3) is added to initiate digestion, and the vessels are placed on a hot plate at a controlled temperature, typically between 120 and 140°C, where they are maintained for several hours until the organic material is fully dissolved. To ensure complete oxidation of residual organic compounds, a small amount of hydrogen peroxide (H_2O_2) may occasionally be added. After digestion, the samples are cooled to room temperature before being diluted with deionized water to a specific final volume, such as 50 mL, to prepare them for ICP-MS analysis. Finally, the prepared samples undergo ICP-MS analysis to quantify elemental concentrations, including selenium and other micronutrients, within the plant tissues.

4.3 Results

Analysis of the Manhattan plots reveals that genomic loci associated with the highest selenium accumulation are represented by prominent peaks in the plots. As a consequence of low allele frequencies, some markers could not be visualised using the Manhattan plots. In GAPIT Manhattan plot, association peaks were observed on chromosomes A01, A03, A08, A10, C01, C04, C05, C06, C09, although the A01 and A03 peak were the most clearly defined (Figure 66). Additionally, Manhattan plot indicated GEM peaks on chromosomes A05, A09, C03, and C04 (Figure 67).

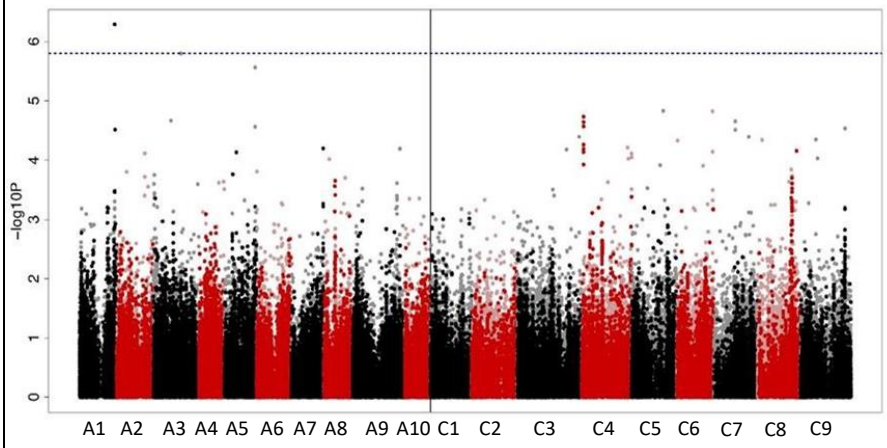

Figure 66: GAPIT Manhattan plot. An orderly list of markers in the *B. napus* pan-transcriptome that are associated with Selenium accumulation in terms of their -log10P values. A Bonferroni correct significance threshold is indicated by the dashed line (Alcock et al., 2017). 'A' represents genome in *B.rapa* (A genome) and 'C' represents genome in *B.oleracea.*

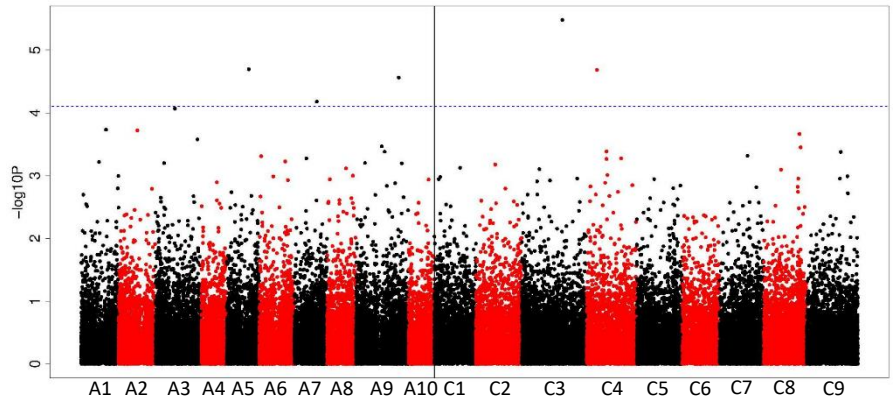

Figure 67: Regress Manhattan Plot. The GEMs markers are associated with Selenium accumulation to *B.napus* pan-transcriptome (Alcock et al., 2017). 'A' represents genome in *B.rapa* (A genome) and 'C' represents genome (C genome) in *B.oleracea.*

4.3.1 Identification of *Brassica* and *Arabidopsis* gene targets

In this study, we examined the association between SNPs and GEMs with selenium accumulation in *Brassica napus*. These associations were analysed using *Brassica* pan-transcriptomes and ENSEMBL gene annotations, with the findings presented below. Our analysis includes linkage disequilibrium (LD) plots, the identification of potential genes within significant genomic regions, and an exploration of genetic variation at these loci. Additionally, gene expression versus selenium accumulation plots were generated to assess potential positive or negative correlations for GEM markers.

SNP and GEM Associations

We identified several significant SNP markers associated with selenium accumulation in *Brassica napu*s, with $\log_{10}$P values exceeding 5.7 and false discovery rate (FDR)-adjusted p-values below 0.05. These SNP markers correspond to genes involved in essential physiological processes such as sulfur assimilation, protein modification, and transport. The following SNPs were linked to their respective *Brassica* and *Arabidopsis* orthologs, selected for their involvement in protein modification, cell signalling, sulfate transport, and protein translocation—mechanisms that may regulate selenium transport and accumulation in *Brassica* plants.

Linkage Disequilibrium (LD) and Genetic Variation

To better understand the genetic variation at these loci, we generated LD plots for the SNPs associated with selenium accumulation, identifying strong genetic linkage in chromosomes 1, 2, 3, and 5. The observed LD decay (R^2) provides insights into how tightly these SNPs are linked, suggesting the presence of gene clusters that regulate selenium uptake. Furthermore, quantification of genes within these linked regions revealed clusters of genes that may act together in selenium metabolism. Analysis of allele segregation at these loci demonstrated clear population-level segregation patterns, indicating that certain SNPs could serve as effective genetic markers for breeding programs aimed at enhancing selenium accumulation in *Brassica* napus.

Gene Expression Markers (GEMs) and Their Relationship with Selenium Accumulation

For the GEM markers, we assessed the correlation between gene expression levels and selenium accumulation. Gene expression versus selenium content plots were created to identify genes whose

expression correlates with increased selenium levels. Key findings include:

- **Bo3g028560.1 (AT2G35800.1):** This gene exhibited a positive correlation with selenium accumulation, suggesting that higher expression of this mitochondrial substrate family protein (SAMTL) is linked to increased selenium uptake in *Brassica* plants.

- **Bo9g094130.1 (AT4G12120.1):** This gene showed a negative correlation, implying that high expression of the Sec1/munc18-like protein could inhibit selenium accumulation, potentially due to competition with other metal transport pathways.

Our analysis confirmed that genes involved in metal transport, sulfate assimilation, and antioxidant defence significantly correlate with selenium levels in *Brassica*. These findings align with studies conducted by the Bancroft lab (Bancroft et al., 2011), which also identified key genes regulating metal homeostasis and sulfur metabolism that influence selenium uptake.

Table 10: Potential Genes target in B. napus and *A. thaliana* orthologous via *Brassica* pantranscriptomes and ENSMBL.

Numbers	*Brassica* Gene ID	*Arabidopsis* Gene ID	Loci	NASC Code	Growth Conditions	Function
1	Cab046650.1	AT3G07090.1	A03	N577739	22°C,16/8h light/dark	PPDE putative thiol peptidase family protein
2	Bo4g013000.1	AT2G41170.1	A02	N613794	22°C,16/8h light/dark	F-box family protein
3	Bo9g094130.1	AT4G12120.1	A04	N555233	22°C,16/8h light/dark	Sec1/munc18-like (SM) proteins superfamily

4	Bo3g028560.1	AT2G35800.1	A02	N613885	22°C,16/8h light/dark	Mitochondrial substrate family protein (SAMTL)
5	Bo3g058750.1	AT3G04950.1	A03	N582534	22°C,16/8h light/dark	Protein translocase subunit SecA

4.3.2 Isolation of homozygous knockout lines

Gel electrophoresis was conducted on 10 to 16 plant PCR extracts for each gene line, and the results (Figure 68 A – F as samples) are described below. The gel images were carefully analysed to confirm the successful amplification of target genes, with band patterns corresponding to expected product sizes for each gene line. The intensity and clarity of the bands were assessed to evaluate the quality of PCR amplification, ensuring that the DNA was of sufficient quantity and integrity for downstream analysis. Variations in band intensities were also examined, which provided insights into the efficiency and consistency of PCR amplification across different plant lines. These results were critical for validating the presence of specific alleles or genetic variants, guiding subsequent steps such as sequencing, genotyping, or further molecular analysis.

Gel electrophoresis was conducted on 10 to 16 plant PCR extracts for each gene line, and the results (Figure 68 A – F as samples) are described below.

If either the left or right gene primer, along with a T-DNA border primer, produces a band, it indicates the presence of the T-DNA insert. Therefore, when no bands are observed with either primer, the plant is homozygous for the insert—meaning both copies of the gene contain the insertion. In contrast, the presence of a band suggests heterozygosity, indicating that only one copy of the gene carries the

insert. It is noteworthy that the line is wild type if it has no bands for TDNA border primers but has bands for gene primers. Thus, the results of homozygous, heterozygous, and wild types of lines were summarised as tables (tables: 11 - 15).

AT2G35800.1 gene: PCR was performed on 13 plants and results showed that plants number 11 and 12 were homozygous and wildtype, respectively. The rest of the plants were heterozygous.

AT3G04950.1 gene: In the 11 plants that were analysed by PCR, only plant number 5 is a wildtype. No homozygous lines were detected.

AT3G07090.1 gene: PCR results showed homozygous lines in 5 plants (number: 7, 3, 15, 12 and 10). One plant showed wild type (plant number 16), while the rest indicated heterozygosity.

AT4G12120.1 gene: Of the 12 plants, 2 were homozygous (number: 2, 4) and 2 were wild type; the remaining plants were heterozygous.

AT2G41170.1 gene: A PCR analysis of 10 plants revealed no homozygous lines, that is, only one plant was wildtype while the rest were heterozygous.

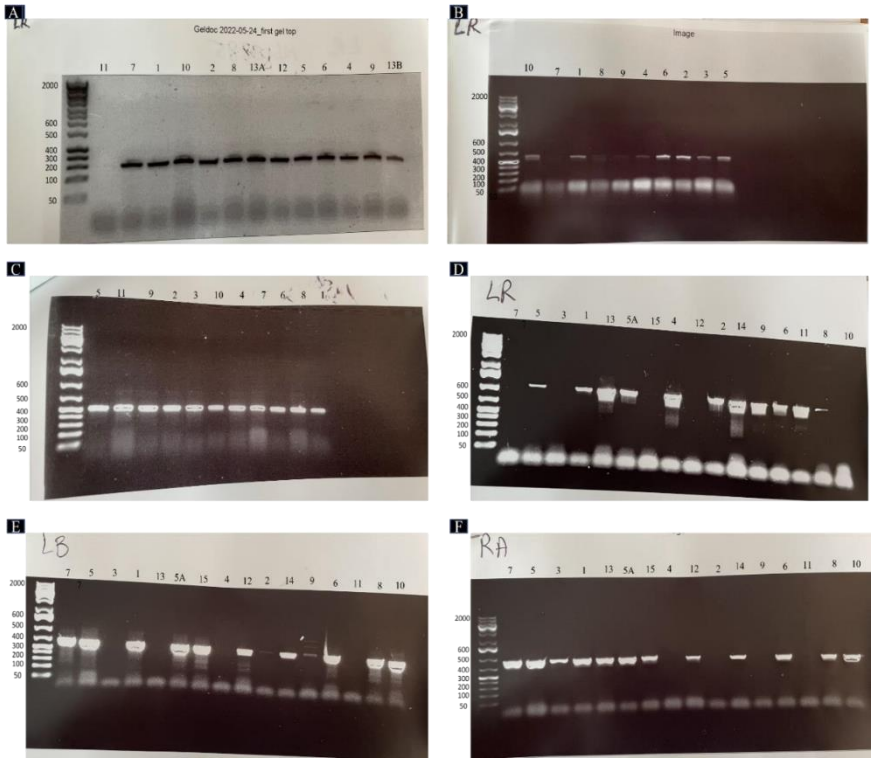

Figure 68: Gel electropherosis result: (A) Right+Left primers of *AT2G35800.*1 gene. (B) Right+Left primers of *AT2G41170.1* gene. (C) Right+Left primers of *AT3G04950.1* gene. (D) Right+Left primers of *AT3G07090.1* gene. (E) Left+SALK B primers of *AT3G07090.1* gene. (F) Right+SALK A primers of *AT3G07090.1* gene. Each line was represented by a plant number based on the PCR results.

Table 11: The *AT2G35800.1* gene was analysed by PCR to determine whether each plant had a homo or hetero type and wild type line. LR: Right+Left genes primers. LA: Left gene primer+SalkA primer, LB: Left gene primer+SalkB primer, RA: Right gene primer+SalkA primer, RB: Right gene primer+SalkB primer.

Line AT2G35800 Plant numbers	LR	LA	LB	RA	RB	Line type

11	_	+	+	+	+	**Homozygous**
7	+	+	+	+	+	**Heterozygous**
1	+	+	+	+	+	**Heterozygous**
10	+	_	+	_	_	**Heterozygous**
2	+	_	+	+	+	**Heterozygous**
8	+	_	+	+	+	**Heterozygous**
13A	+	+	+	+	+	**Heterozygous**
12	+	_	_	_	_	**Wild type**
5	+	+	+	+	+	**Heterozygous**
6	+	_	+	+	+	**Heterozygous**
4	+	+	+	+	+	**Heterozygous**
9	+	_	_	+	+	**Heterozygous**
13B	+	+	+	+	+	**Heterozygous**

Table 12: A PCR analysis of the *AT3G04950.1* gene was performed to determine whether each plant was homozygous or heterozygous, and to identify the wild type representative of each plant. . LR: Right+Left genes primers. LA: Left gene primer+SalkA primer, LB: Left gene primer+SalkB primer, RA: Right gene priemr+SalkA primer, RB: Right gene primer+SalkB primer.

Line *AT3G04950* Plant numbers	LR	LA	LB	RA	RB	Line type

5	+	+	+	_	_	**Heterozygous**
11	+	_	_	_	_	**Wild type**
9	+	+	+	_	+	**Heterozygous**
2	+	+	+	_	+	**Heterozygous**
3	+	+	+	_	+	**Heterozygous**
10	+	+	+	_	_	**Heterozygous**
4	+	+	+	_	+	**Heterozygous**
7	+	+	+	_	+	**Heterozygous**
6	+	_	+	_	+	**Heterozygous**
8	+	+	+	_	_	**Heterozygous**
1	+	_	+	_	_	**Heterozygous**

Table 13: To identify whether each plant had a homo, hetero, or wild type line, the *AT3G07090.1* gene was evaluated by PCR analysis. . LR: Right+Left genes primers. LA: Left gene primer+SalkA primer, LB: Left gene primer+SalkB primer, RA: Right gene priemr+SalkA primer, RB: Right gene primer+SalkB primer.

Line *AT3G07090* Plant numbers	LR	LA	LB	RA	RB	Line type

7	−	+	+	+	+	**Homozygous**
5	+	+	+	+	+	**Heterozygous**
3	_	+	_	+	+	**Homozygous**
1	+	+	+	+	+	**Heterozygous**
13	+	+	_	+	_	**Heterozygous**
5A	+	+	+	+	+	**Heterozygous**
15	_	+	+	+	+	**Homozygous**
4	+	_	_	_	_	**Wild type**
12	_	_	+	+	_	**Homozygous**
2	+	+	+	_	_	**Heterozygous**
14	+	+	+	+	+	**Heterozygous**
9	+	_	+	_	_	**Heterozygous**
6	+	+	+	+	+	**Heterozygous**
11	+	_	_	_	+	**Heterozygous**
8	+	+	+	+	_	**Heterozygous**
10	_	+	+	+	+	**Homozygous**

Table 14: Analysing the *AT4G12120.1* gene by PCR helped identify whether each plant was homozygous, heterozygous, or wild type.

Line AT4G12120 Plant numbers	LR	LA	LB	RA	RB	Line type
1	+	+	+	+	+	**Heterozygous**
7	+	_	_	_	_	**Wild type**
9	+	_	_	+	_	**Heterozygous**
8	+	_	+	_	_	**Heterozygous**
2	_	+	+	_	_	**Homozygous**
12	+	_	+	+	_	**Heterozygous**
3	+	+	+	_	_	**Heterozygous**
10	+	_	+	_	_	**Heterozygous**
11	+	_	_	_	_	**Wild type**
5	+	_	_	_	+	**Heterozygous**
4	_	_	+	_	_	**Homozygous**
*9	+	_	+	+	+	**Heterozygous**

Table 15: Through PCR analysis, the *AT2G41170.1* gene was evaluated for each plant to determine whether it was homo, hetero, or wild type. primer, RA: Right gene primer+SalkA primer, RB: Right gene primer+SalkB primer.

Line AT2G41170 Plant numbers	LR	LA	LB	RA	RB	Line type
10	+	+	+	+	+	**Heterozygous**
7	+	+	+	+	+	**Heterozygous**
1	+	_	_	_	_	**Wild type**
8	+	+	+	+	+	**Heterozygous**
9	+	+	_	_	+	**Heterozygous**
4	+	+	_	_	_	**Heterozygous**
6	+	+	+	+	+	**Heterozygous**
2	+	+	+	_	+	**Heterozygous**
3	+	+	+	+	_	**Heterozygous**
5	+	+	+	+	_	**Heterozygous**

4.3.3 Phenotyping of homozygous lines:

Following the characterisation and confirmation of the gene targets in *Arabidopsis* plants, ICP-MS analysis was used to assess Se

accumulation in *Arabidopsis* plants. As shown in Figure 69 to 76, the Se content analysis is presented with error bars to illustrate variability in data and measurement precision. In untreated *Arabidopsis* plants, we demonstrated that the AT3G07090.1 gene is involved in regulating Se uptake due to the effect of this gene knockout on the phenotype of Se uptake (Figure 69), as compared to the Colombia wildtype. Indeed, uptake was two-fold lower in gene knockouts viz. 3.7932 mg/kg and 1.5627 mg/kg respectively. The phenotype is seen in two separate lines. It is noteworthy that this identified gene's locus is in the A03 loci, which has previously been shown one of the highest associations with the GAPIT Manhattan plots (See Figure 66). The other lines tested were not significantly different to Columbia wild type plants.

In comparison, the differences between homozygous lines (7.56 mg/kg, 6.76 mg/kg and 6.68 mg/kg) and control (7 mg/kg) were not significant in selenium-treated trials, just plant number 3 of AT3G07090 (5.94 mg/kg) indicated a slightly decrease in selenium accumulation compared to cotrol. Since it is the same homozygous gene line (AT3G07090 plant 3) in plants not treated with selenium, it seems external selenium caused this gene knockout to show the effect of this phenotype as clearly as untreated selenium.

Additionally, the untreated *Arabidopsis* plants were compared with a control (Colombia wildtype) for the effect on uptake of other elements, but no significant differences were noted even with identified gene AT3G07090.1, which is a promising selenium accumulation regulator (Figure 71 – 76). It thus appears that this newly discovered gene does not contribute to the regulation of any other elements (S, Fe, Mg, K, Ca) in *Arabidopsis* and may be specific to Se.

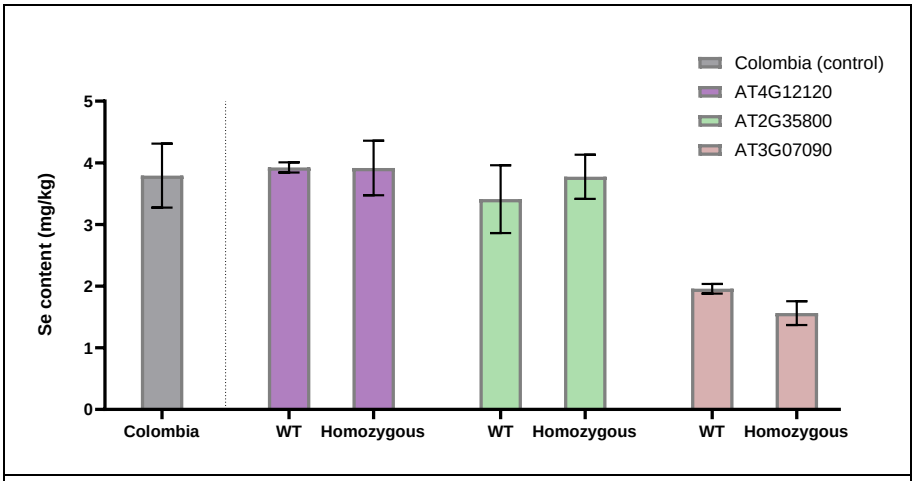

Figure 69: Seleium uptake in untreated *Arabidopsis* plants. An untreated selenium basis trial showed 2 homozygous lines (*AT3G07090* plants 3, 7) exhibited accumulation phenotypes as gene knock out mutants compared with Colombia wild type control. Bars indicate Mn± SD. (n=3).

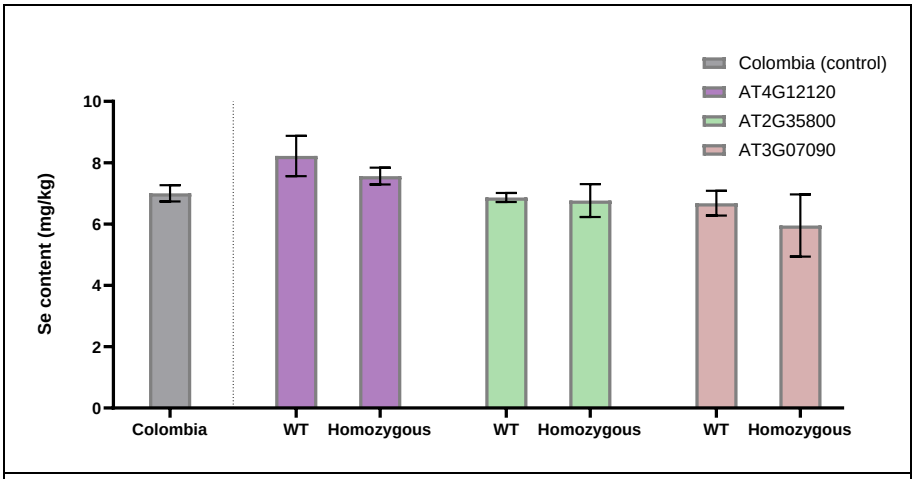

Figure 70: Selenium uptake in treated *Arabidopsis* plants. The selenium treated trial showed no significant differences between the homozygous line and the Colombia wildtype control in terms of accumulation phenotypes. Bars indicate Mn± SD. (n=3).

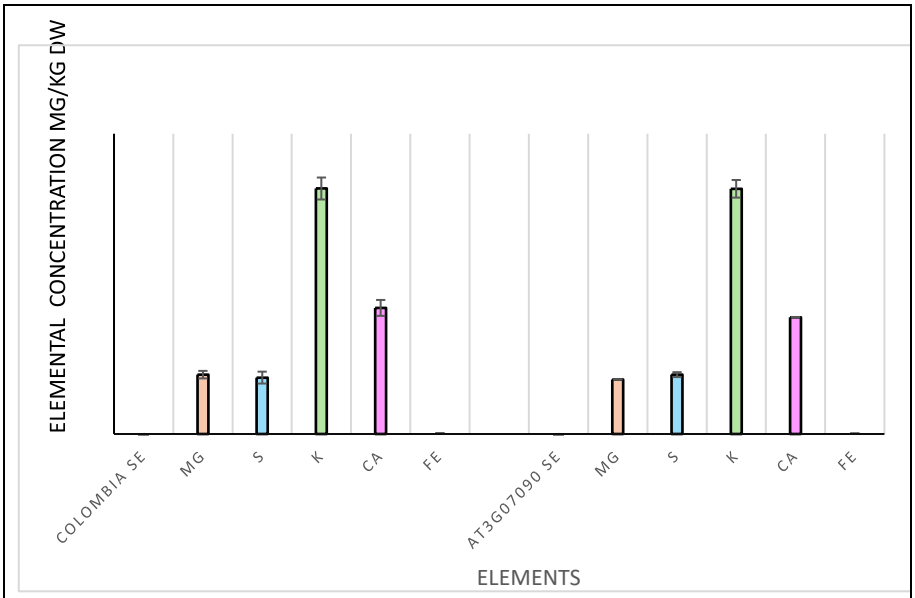

Figure 71: Elemental uptake in untreated *AT3G07090* homozygous and Colombia wild type lines. The homozygous line does not differ from the control line in terms of uptake of other elements. Bars indicate Mn± SD. (n=3).

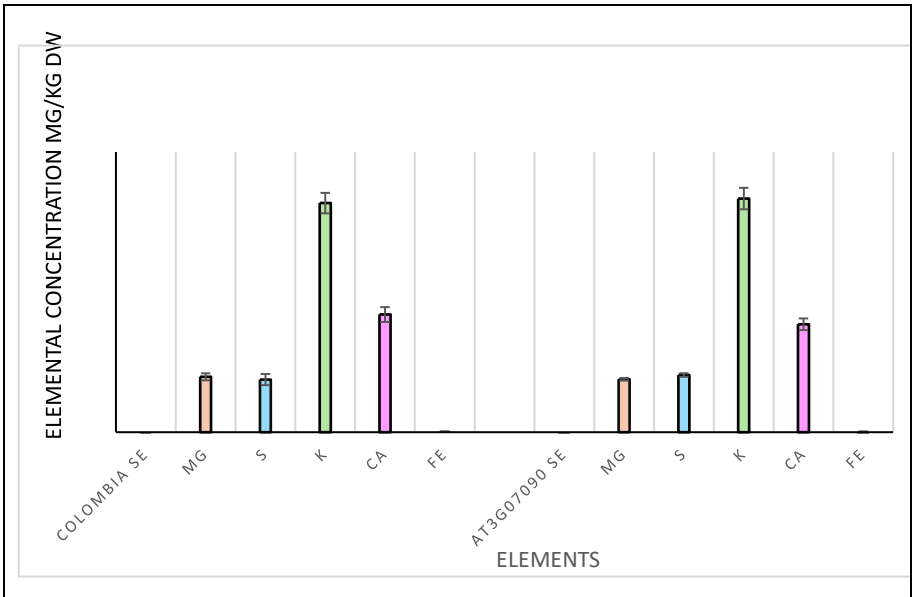

Figure 72: Elemental uptake in untreated *AT3G07090* homozygous and Colombia wild type lines. No difference was observed between the

homozygous line and control in the uptake of other elements. Bars indicate Mn± SD. (n=3).

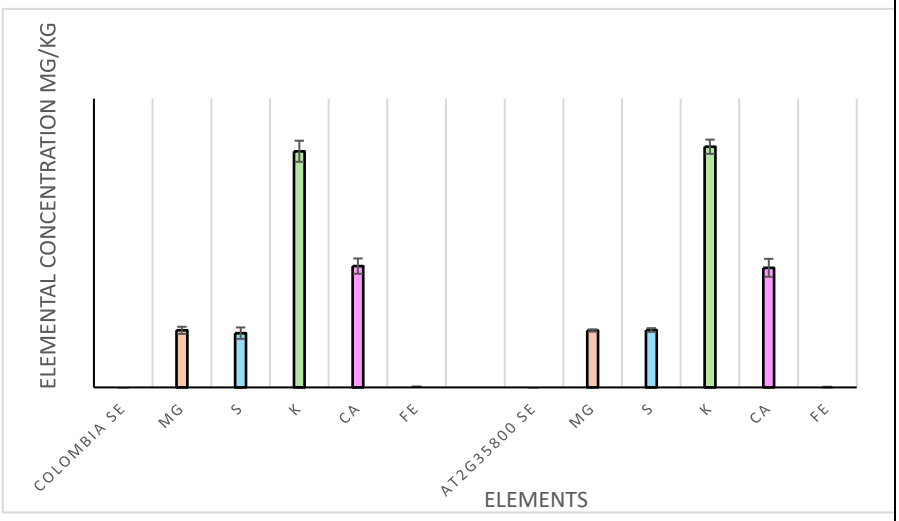

Figure 73: Elemental uptake in untreated *AT2G35800* homozygous and Colombia wild type lines. No difference was observed between the homozygous line and control in the uptake of other elements. Bars indicate Mn± SD. (n=3).

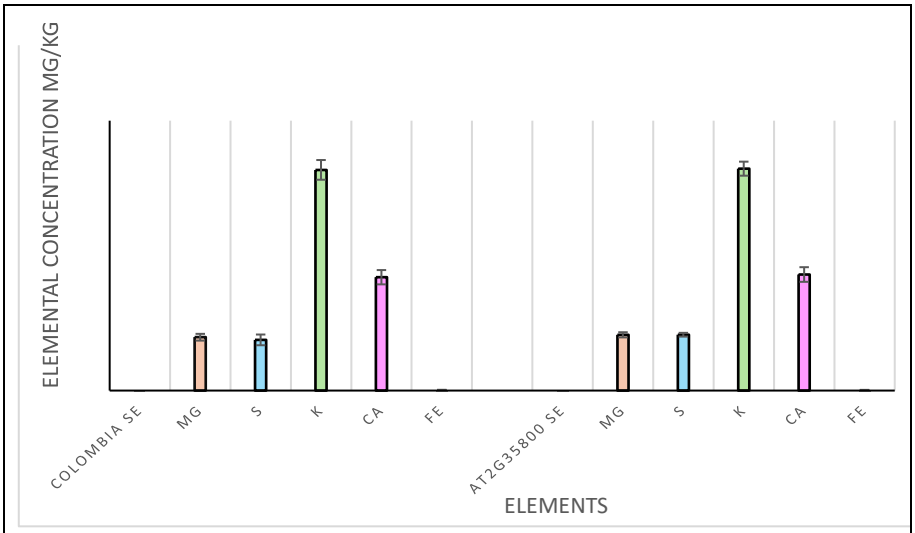

Figure 74: Elemental uptake in untreated *AT2G35800* wild type and Colombia wild type lines. There were no observed differences in accumulation of other elements between this line and the Colombia control. Bars indicate Mn± SD. (n=3).

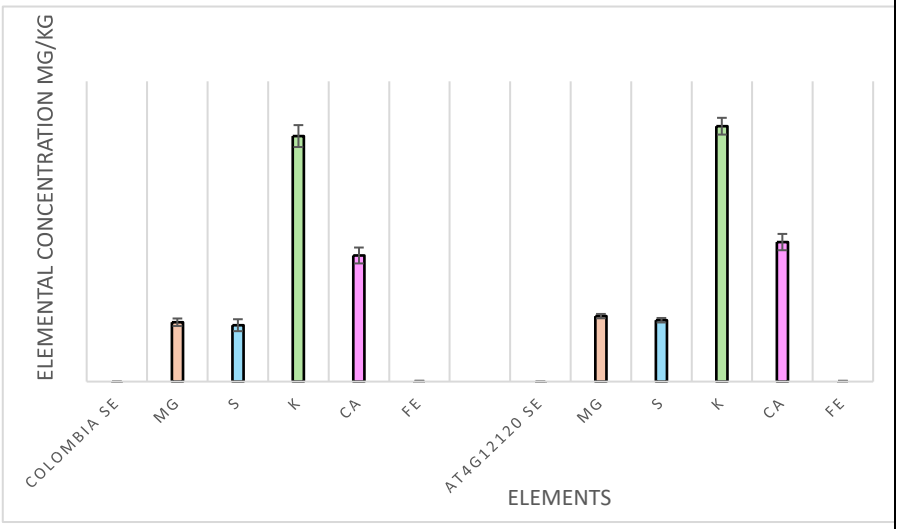

Figure 75: Elemental uptake in untreated *AT4G12120* homozygous and Colombia wild type lines. In terms of accumulation of other elements, we found no difference between this line and the Colombia control. Bars indicate Mn± SD. (n=3).

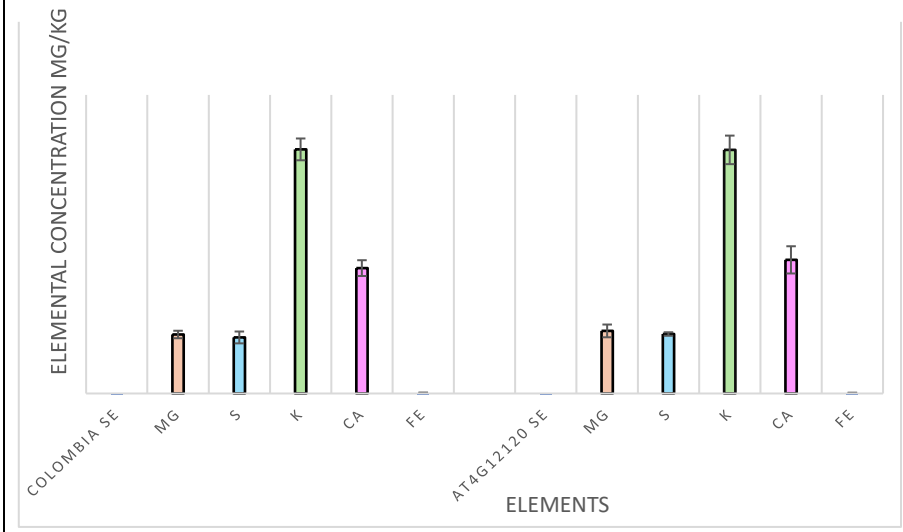

Figure 76: Elemental uptake in untreated *AT4G12120* wild type and Colombia wild type lines**.** There is no difference between this line and the Colombia control in regard to the accumulation of other elements. Bars indicate Mn± SD. (n=3).

4.4 Discussion

Our understanding of genetic expression has been transformed by transcriptomics.

Brassica pan-transcriptomes were investigated for potential genes with linkage disequilibrium (LD) of SNPs. LD occurs when alleles are not randomly associated at different loci. There is a strong tendency for genes located close to each other to inherit together, so they are often in very strong LD (Thomas, 2016). A factor of particular importance when employing associative transcriptomics is LD decay in B. napus. The LD decay in B. napus reduces the number of possible options when searching for candidate genes (Alcock et al., 2017). Interestingly, that only genes whose expression levels are connected to

variation are indicated by GEM correlations with a trait; they do not indicate the causative polymorphism (Alcock et al., 2017). This study evaluated SNPs and GEMs gene markers to identify selenium accumulation regulatory genes. Based on Manhattan plots evaluation, Se concentrations were strongly correlated with loci on chromosomes A01, A03, A05, A08, A09, A10, C01, C04, C05, and C09 (Figure 66, 67). The SNPs for Se with the strongest association was located on chromosomes A01 and A03 (Figure 66). The GEMs for Se exhibiting the strongest association is located on chromosome C03 (Figure 67). In primary identification of B. napus and A. *thaliana* orthologs via *Brassica* pan-transcriptomes, 16 SNPs and 378 GEMs markers were associated with selenium accumulation based on LD decay and P value, and among them 7 genes were identified as significant targets of selenium accumulation based on gene location and gene function in ENSEMBL PLANTS. It was subsequently determined through PCR process and ICPMS results that just one *Arabidopsis* gene identified participated in selenium accumulation which is AT3G07090 (Figure 77). Table 12 shows that this gene type is protein coding that is classified as a member of the PPPDE thiol peptidase family. *Arabidopsis* plants T-DNA knockout mutants containing this gene were significantly reduced in absorbing Se when grown at untreated external Se concentration compared to control as revealed by ICP-MS of *Arabidopsis*. Conversely, when the plants were grown at higher external Se concentrations it was unaffected or slightly affected. In light of this result, it indicates this gene to be a promising gene for controlling Se accumulation in A. *thaliana* and probably in B. napus due to its genome similarity (Genome lineage) with *Arabidopsis* (Table 12). The ICP-MS results indicate that this gene does not participate in regulating other elements in this research, since the other elements contents in both homozygous lines and controls are similar,

and homozygous lines do not show a reduction of other elements observed. However, selenium content was reduced significantly in homozygous lines carrying the AT3G07090 gene, which indicates this gene plays a specific role in regulating selenium accumulation.

Table 16: Gene summary in the National Library of Medicine.

Gene symbol	AT3G07090
Gene description	PPPDE putative thiol peptidase family protein. Interacts with C3H59 via its WD40 domain and C-terminal region, respectively, in the nucleus.
Locus tag	AT3G07090
Gene type	protein coding
Organism	*Arabidopsis thaliana*
Lineage	Eukaryota; Viridiplantae; Streptophyta; Embryophyta; Tracheophyta; Spermatophyta; Magnoliopsida; eudicotyledons; Gunneridae; Pentapetalae; rosids; malvids; *Brassica*les; *Brassica*ceae; Camelineae; *Arabidopsis*

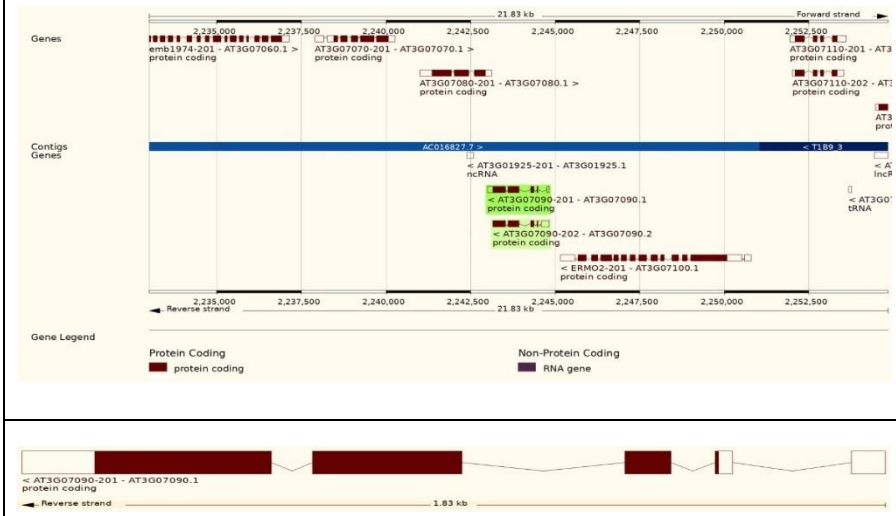

Figure 77: *AT3G07090.1* loci in *Arabidopsis thaliana* in ENSEMBL PLANTS. In databases, this gene contains Exons: 5, Coding exons: 4, Transcript length: 1,054 bps, Translation length: 265 residues, and is a protein coding. (Figure from ENSEMBL Plants)

The noted selenium regulating gene (AT3G07090) is called *desi1* and was previously identified as a SUMO protease (Table 17) in *Arabidopsis* by Orosa et al. (2018).

Table 17: Identification of SUMO proteases in yeast and *Arabidopsis*, with their known names, TAIR accession numbers, cysteine protease classification, and tissues expressed (Table from Morrell and Sadanandom, 2019).

Species	Name	Cysteine protease clan	Cysteine protease family	TAIR accession	Tissue expression
Saccharomyces cerevisiae	ULP1	CE	C48	NA	NA
	ULP2	CE	C48	NA	NA
Arabidopsis thaliana	OTS1 (ULP1d)	CE	C48	At1g60220	Root tissue, shoot vasculature of seedlings, developing flowers, wounding sites
	OTS2 (ULP1c)	CE	C48	At1g10570	Root tissue, shoot vasculature of seedlings, petioles, filaments, wounding sites
	ESD4	CE	C48	At4g15880	Seedlings, leaves, shoots, flowers and roots
	ELS1 (ULP1a)	CE	C48	At3g06910	Ubiquitously high levels in root vasculature tissue and flowers
	ELS2 (ULP1b)	CE	C48	At4g00690	Uncharacterized
	FUG1	CE	C48	AT3G48480	Uncharacterized
	SPF1/ASP1/ULP2like2	CE	C48	At1g09730	Ubiquitous in seedlings newly developing leaves and the tips of the roots. Also present in embryo sacs, inflorescences, anthers, and developing seed with intermediate expression levels in stems and rosette leaves
	SPF2/ULP2like1	CE	C48	At4g33620	Leaves, vasculature, inflorescences and maternal floral tissues, stems, cauline leaves, rosette leaves, and middle-length siliques
	Desi 1	CP	C97	At3g07090	Uncharacterized
	Desi 2A	CP	C97	At4g25660	Uncharacterized
	Desi 2B	CP	C97	At4g25680	Uncharacterized
	Desi 3A	CP	C97	At1g47740	Not known
	Desi 3B	CP	C97	At2g25190	Uncharacterized
	Desi 3C	CP	C97	At5g25170	Uncharacterized
	Desi 4A	CP	C97	At4g17486	Uncharacterized
	Desi 4B	CP	C97	At5g47310	Uncharacterized

All eukaryotes including yeast, mammals, and plants rely on the small ubiquitin-like modifier (SUMO) protein for their normal cellular functions (Novatchkova et al., 2004). The SUMO protein family covalently attaches to and detaches from other proteins in cells to alter their function (SUMOylation). Apoptosis, protein stability, stress response, nuclear-cytosolic transport, transcriptional control, and cell

cycle progression are just a few of the diverse functions that these proteins play in cellular processes (Hay, 2005). Computer mapping has revealed that the 11-kDa SUMO protein has one isoform in yeast and eight in A. *thaliana* (Novatchkova et al., 2004). SUMO1 and SUMO2 are the only two SUMOs that *Arabidopsis* expresses at high levels out of the total four that are expressed. At SUMO1 and 2 are orthologs of human SUMO2/3 and have 83% of the same amino acid sequence, according to sequence similarity. Sequence similarity suggests that the roles and susceptibility to stress of human SUMO2/3 and At SUMO1/2, respectively (Benlloch and Lois, 2018; Castaño-Miquel et al., 2011). The SUMOylation process involves switching from conjugated to non-conjugated forms of SUMO, as SUMO conjugates and deconjugates protein substrates, the SUMO cycle shares the same biochemical steps as ubiquitin (Kerscher et al., 2006).

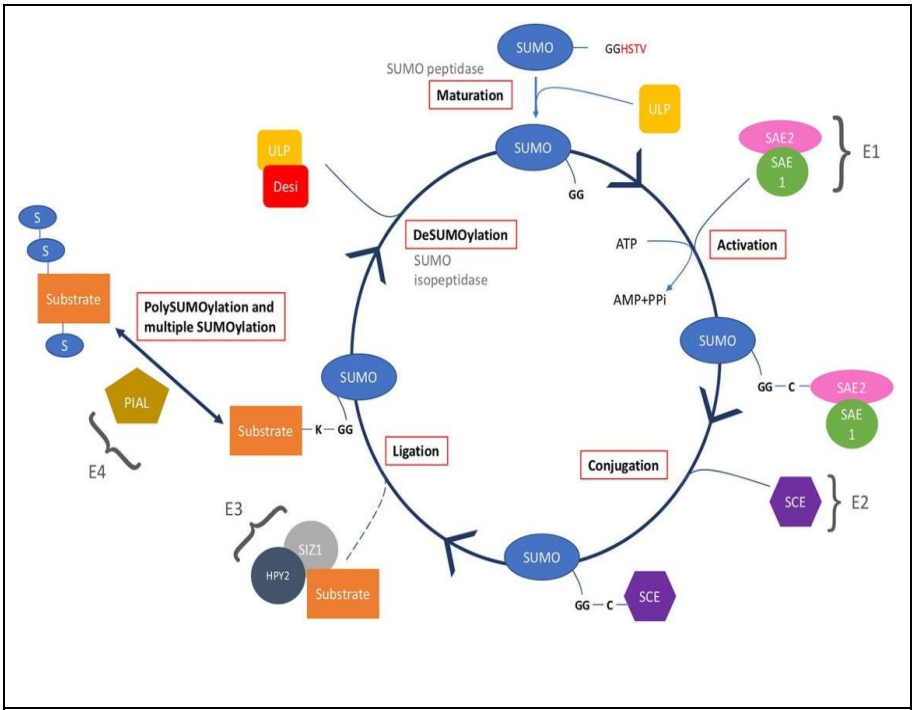

Figure 78: As the SUMO cycle proceeds, immature SUMO is first maturated by cleaving off the C-terminus with a SUMO peptidase. In a conjugation step, mature SUMOs are activated by ATP and a heterodimer of SAE1 and SAE2, then SUMOylated on the substrate with SUMO ligases where it can form polySUMO chains. To generate free SUMO, SUMO isopeptidases remove SUMO from the substrate in the deSUMOylation step (Figure from Morrell and Sadanandom, 2019).

The process of SUMOylation is cyclical (Figure 78) because of SUMO proteases. SUMO becomes liberated after being split off from the target substrates, making it a reversible alteration. By cleaving a c-terminal peptide from the immature SUMOs, newly synthesised SUMOs are hence matured (Johnson, 2004). It has been determined that all identified SUMO proteases are cysteine proteases within one of four types of proteases in plants, such as cysteine-, serine-, aspartate-, and metalloproteases, as well as with the protease superfamily (Hou et al., 2018). Founded on the similarity between SUMO proteases and yeast ULP1/2 proteases, SUMO proteases have

previously been grouped together into the same protein superfamily, the ULP superfamily (Mukhopadhyay and Dasso, 2007; Hickey et al., 2012). Today, eight *Arabidopsis* ULPs have been predicted, six of them are known as SUMO proteases.

There have been two new types of SUMO proteases discovered, *Desi1* (deSUMOylating isopeptidase 1) and DeSI2 in mouse, which were different from ULP enzymes and lacked sequence similarity, and are SUMO proteases (Shin et al., 2012). Eight putative DeSI proteases were identified in *Arabidopsis* based on sequence similarity to human *Desi1*/2 and functionally characterized one protein, DeSI3a (Orosa et al., 2018). As one of the C97 cysteine proteases, these DeSI proteases belong to the CP clan, which has a catalytic dyad of histidine and cysteine. The histidine ring of the DeSI active site does not require the orientation of the third residue (Suh et al., 2012). It was once thought that a PPPDE (peptidase-permuted papain fold peptidase) was a DeSI peptidase that functioned as a deubiquitinating peptidase, but no activity has been seen. *Desi1* can cleave polymeric SUMO2/3 from its targets in a mouse model, in accordance with research (Shin et al., 2012, Suh et al., 2012). Based on the mammalian *Desi1* active site, eight potential *Arabidopsis* DeSI proteins were identified (Orosa et al. ,2018). DeSI proteins, in contrast to other SUMO proteased proteins, are smaller proteins with a longer active site, which is around 140 amino acids in length (Table 18). The active site is also situated more closely to the N terminus (Hickey et al., 2012). The active sites are situated between a helix and a beta barrel and point towards the groove on the surface of this *Desi1* homodimer (Suh et al., 2012).

Table 18: A map showing the location and length of the active sites of several different SUMO proteases: the orange box represents the SIM site in ULP1, the blue oval depicts the active site for C48, the green oval represents C97, and the purple oval represents C98. (Table from Morrell and Sadanandom, 2019).

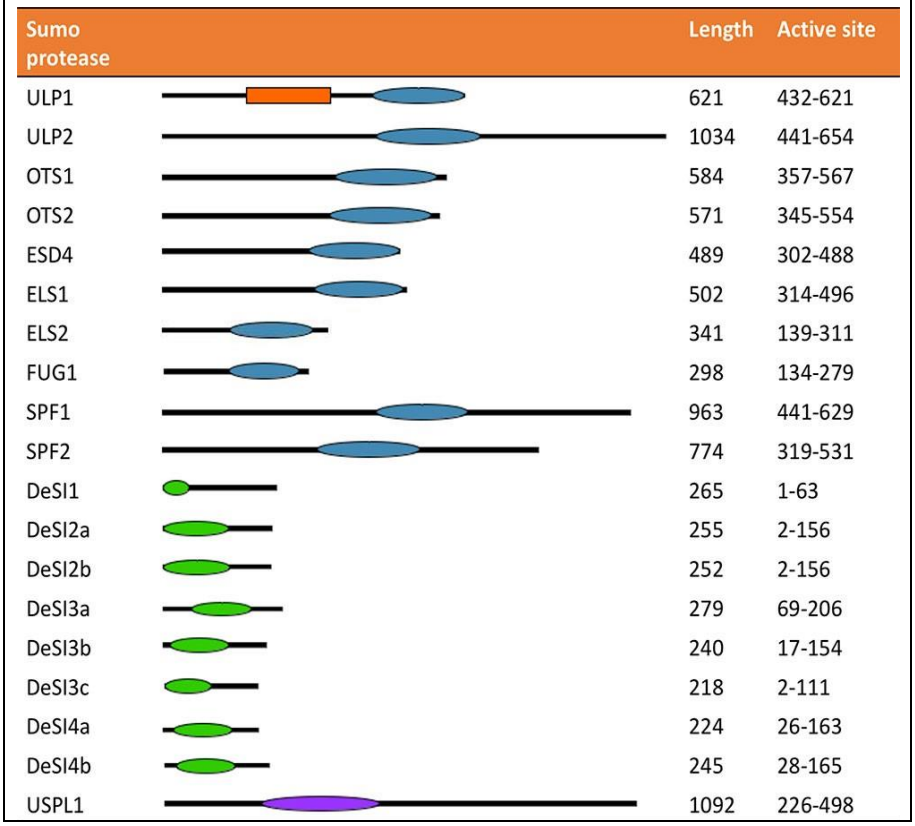

Sumo protease	Length	Active site
ULP1	621	432-621
ULP2	1034	441-654
OTS1	584	357-567
OTS2	571	345-554
ESD4	489	302-488
ELS1	502	314-496
ELS2	341	139-311
FUG1	298	134-279
SPF1	963	441-629
SPF2	774	319-531
DeSI1	265	1-63
DeSI2a	255	2-156
DeSI2b	252	2-156
DeSI3a	279	69-206
DeSI3b	240	17-154
DeSI3c	218	2-111
DeSI4a	224	26-163
DeSI4b	245	28-165
USPL1	1092	226-498

When plants encounter biotic and abiotic stressors, the SUMO proteases play a significant role. Therefore, plant immunity and stress response are SUMO proteases' fundamental roles. However, numerous SUMO proteases have been discovered by bioinformatics, but genetic, biomedical and physiological approaches have not been able to properly characterise their roles. The uncharacterized SUMO proteases are DeSI proteases except Desi3a, as well as two ULP proteases, FUG1 and ELS2.

Understanding these proteases and their molecular targets and localization may help illuminate the multitude of pathways in which SUMO is involved (Morrell and Sadanandom, 2019).

Although my research shows *Desi1* as a potential selenium regulator, *Desi1* is one of some SUMO proteases that require further research in order to understand more about its characteristics.

Chapter 5: Discussion

Malnutrition, defined by the World Health Organisation (WHO) as "deficiencies, excesses or imbalances in a person's intake of energy and/or nutrients" is one of the most pressing global health issues affecting mankind today. Malnutrition covers both the consequences of caloric overconsumption and undernutrition and is thus related to the development of a large number of noncommunicable diseases.

An important type of undernutrition is micronutrient deficiency/insufficiency, caused either by undereating or an imbalanced diet lacking appropriate levels of essential nutrients. This leads to a variety of physiological consequences and is an important cause of ill-health and mortality worldwide. It is thus important to not only focus on resolving food scarcity when speaking about malnutrition, but to also devise plans to ensure that available food can provide the necessary amounts of nutrients required to sustain a healthy state.

An example of an essential nutrient is the element Selenium (Se). Se is an important component of the 21st amino acid selenocysteine, which is used to construct a number of antioxidant proteins. Se deficiency has been associated with increased mortality, impaired immune function, cardiovascular disease, thyroid dysfunction and cancer. Despite these risks, approximately 1 billion people are deficient in Se worldwide, suggesting that our strategies for targeting Se deficiency need to be improved.

As per the WHO guidelines, individuals should take 55 µg of Se each day (Institute of Medicine, 2000). One method of Se intake is through

the consumption of plants, and raising the nutritional value of these plants can be a valuable way of tackling Se deficiency.

Furthermore, direct association between cancer incidence/fatality risk and Se deficiency fuelled studies into Se as a potential anti-cancer element. These reported cancer cell cytotoxicity at supranutritional levels of Se in some cancers, but not others. Raising Se consumption beyond the required minimum may thus be therapeutically useful.

This study focused on the ways through which we can raise the Se content of plants without compromising on other essential nutrients. This was done in two ways: identifying the effects of genetic mutations on Se uptake and assessing the usefulness of varying biofortification techniques in enriching plants with Se.

Selenium biofortification can be a great way to combat selenium deficiency. Two methods were used to assess the effect of selenium on the uptake of other elements: hydroponics and pots. In the pot experiment, two methods of applying selenium were used: foliar spray and soaked soil (the results of which were discussed in chapter 2 and 3). This study compares the effects of selenium enrichment through soil-based biofortification and soilless biofortification on the uptake of several important elements. As shown in chapter 2, several experiments were conducted on onion and spring onion using the NFT system, as well as one spring onion experiment in pots. The effects of selenium on other elements were evaluated via ICP-MS. The results of 120 all experiments, whether conducted in NFT or pot, demonstrated that increasing selenium treatment raised selenium uptake in onion and spring onion, suggesting that biofortification is a successful strategy for increasing Se levels in these plants. Extracts taken from these plants were used as Se treatment on HepG2 cells. Extracts from

plants biofortified with higher Se concentrations resulted in high levels of HepG2 cell death, showing that these extracts are active. The next stage is to understand whether consumption of these plants would result in higher Se levels and would therefore be a useful way of tackling malnutrition in humans.

Hydroponics is the best method of selenium biofortification in glasshouse plants. A particular worry with biofortification is that enrichment with one nutrient may cause reductions in the uptake of other essential nutrients by the plant, particularly if the elements display an antagonistic relationship. Such relationship was expected between selenium and sulfur, as previous studies had established that they share the same transfer route in plants, through which they compete with each other for uptake. This effect was, however, only observed in the NFT system experiments in spring onion. Pot experiments did not show an antagonistic relationship between the two elements. The enrichment of onion using the NFT system showed a mixture of both negative and positive correlations between the uptake of Se and S in different experiments. The varied outcomes do not support a clear rival relationship between selenium and sulfur.

However, whilst pots were a preferable method of preventing antagonism between Se and S specifically, spring onion in pots slightly exhibit antagonistic trends for Fe, Mg, K, and Ca uptake with Se, while NFT experiments in spring onion and onion indicated varying results. Different growth phases of plants, genetic differences, and the method of biofortification used may have led to these varying results but no significant relationship was identified.

Thus, in accordance with this study's results, the most effective method of selenium biofortification in glasshouse plants is

hydroponics, as there is less risk of depleting other important nutrients. In the NFT system the nutrients are better controlled than in pots.

Soil application results in higher selenium uptake than foliar spray. Not all plants can be grown using a hydroponic system. It is thus important to establish the most optimal method of selenium biofortification in a soil-based system. In this study, soil application of Se resulted in a higher Se uptake by spring onion than foliar spray in pots, which translated to greater antioxidant ability and a greater cytotoxic effect on HepG2 cells. Despite this, foliar spray is probably a better biofortification method for Se in farms, as previous research in farms have reported rival interactions between Se and other elements (Alfthan et al. 2015, Ebrahimi et al. 2019). Furthermore, foliar spray application is less likely to cause contamination of the environment and reduce soil chemistry and microbiology effects.

Selenium biofortified plants kill cancer cells with low associated toxicity. A biofortification technique was used to evaluate the bioactivity of selenium. In accordance with chapter 3 outcomes, it strongly seems that selenium is a free radical scavenger, especially at high selenium concentrations. In cell culture images and IC50 analysis, Se50 μM soaked soil showed the greatest viability inhibition of cancer cells, and this extract can kill cancer cells with low toxicity compared to other extracts. This suggests that selenium-biofortified plants can result in increased cancer cell death whilst being associated with low toxicity. There was no significant difference in the levels of other elements in biofortified plants and controls, suggesting that selenium was the responsible element for observed differences. These findings show that selenium possesses biological properties that merit

further study, especially in view of its potentially powerful impact in combating cancer.

The AT3G07090.1 gene was discovered via gene mapping analysis as potentially important for Se uptake:

As well as biofortification, another method of enriching plants with nutrients is optimising uptake through genetic modification. For this to be possible, genetic regulators of uptake have to be identified. B. napus associated transcriptomics together with a T-DNA knockout in A. *thaliana* was used to identify target genes candidates thought to potentially be involved in selenium uptake. In the plant A. *thaliana*, the AT3G07090.1 gene was discovered to be a selenium uptake regulator. This gene, called *Desi1*, codes for a SUMO protease that is functionally uncharacterised. The loci of this gene is in chromosome A03. Since A. *thaliana* and B. napus have similar phylogenies (Thomas, 2016), it can be assumed that this newly discovered gene will have similar effects in B. napus. There is a good chance that more research on genotypes with alleles of genes which control selenium uptake in plants may result to generate the higher selenium-accumulating lines and a reduction of selenium deficiency. The next step is to understand the behaviour of this gene, from expression patterns across tissues and developmental stages to cellular localisation through fusion with GFP. As loss of function in this gene was associated with a reduction in plant Se, it may be worth investigating whether overexpression of the WT gene results in higher Se uptake. For the future, alleles of this gene in *Brassica* lines with high Se content (taken from the population) can be identified. They can also be explored in other species, with their respective proteins and effect on Se uptake analysed. The goal is to find alleles which

result in the highest Se uptake, which could be used in the future as a strategy to tackle Se deficiency (for example, through CRISPR).

For the future, alleles of selenium uptake-related genes in Brassica lines with naturally high Se content can be identified through genome-wide association studies and transcriptomics approaches, helping to pinpoint genetic variants responsible for enhanced Se accumulation (Alcock et al., 2017). These alleles can be further investigated in other species, with analysis of their respective proteins and their effects on Se uptake pathways (Pilon-Smits et al., 1999). The primary objective is to isolate and utilize alleles that result in the highest Se uptake efficiency, which can then be applied in biofortification strategies to combat Se deficiency in humans (Broadley et al., 2006).

These strategies could include the use of CRISPR/Cas9 to insert beneficial alleles into commercial varieties, overexpression of Se transporters such as SULTR1;2 or enzymes like ATP sulfurylase, or pyramiding multiple high-uptake alleles into a single genotype to enhance Se uptake and translocation (El Kassis et al., 2007; Leustek et al., 2000).

Additionally, it is crucial to consider where selenium accumulates in the plant; studies have shown that Se tends to accumulate more in leaves than in roots or bulbs, suggesting that leafy vegetable crops like kale, cabbage, broccoli, and pak choi within the Brassica genus are particularly suitable for biofortification (Zayed et al., 1998; Gupta, 1991). Breeding such crops for high Se content ensures that the biofortified nutrient is concentrated in the edible portion, improving its dietary impact (White and Broadley, 2009). Functional studies of candidate genes, such as gene knockout or overexpression experiments in model organisms like Arabidopsis thaliana, can help

validate the role of these alleles in selenium metabolism and uptake pathways (Ng and Anderson, 1978; Alcock et al., 2017). Ultimately, integrating these genetic approaches with conventional breeding and agronomic practices holds great promise for developing sustainable solutions to global selenium deficiency.

In summary, this thesis demonstrates the effectiveness of Se biofortification in enhancing the nutritional value and health-promoting properties of Allium crops, particularly onions and spring onions, using both hydroponic and soil-based methods. The research highlights how Se accumulation varies by tissue type, plant variety, and biofortification technique, with leaves generally showing higher Se uptake and red onion varieties outperforming yellow ones. Importantly, Se-enriched extracts exhibited significant antioxidant activity and anticancer effects against HepG2 liver cancer cells, suggesting potential functional food applications. Additionally, transcriptomics analysis identified key genes, such as Desi1, involved in Se uptake, offering valuable targets for future genetic improvement. Overall, the findings support Se biofortification as a sustainable strategy to address global micronutrient deficiencies and enhance public health through plant-based nutrition.

Bibliography

1. A.N.Rai, M.Rao, N.C.Gupta. 2022. Transcriptomics Research and Resources in *Brassica* spp. The *Brassica* juncea Genome pp 295 – 322.
2. Abdulah, R., Farjed, A., Kobayashi, K., Yamazaki, C., Suradi, E.W., Ito, K., Suzuki, K., Murakami., Kuwano, H. & Koyama, H.: (2009): Selenium enrichment of broccoli sprout extract increases chemosensitivity and apoptosis of LNCaP prostate cancer cells, BMC Cancer, 9: 414–426.
3. Ahmed, N., Khan, G., & Tabassum, A. (2017) . Bioactive compounds of Allium vegetables as anticancer agents. Asian Pacific Journal of Cancer Prevention, 18(4), 1057-1061.
4. Akl MA, Ismael DS, El-Asmy AA. Precipitate flotation-separation, speciation, and hydride generation atomic absorption spectrometric determination of selenium (IV) in food stuffs. Microchem J. 2006; 83:61– 69. 8.
5. Alcock, T.D., Havlickova, L., He, Z., Bancroft, I., White, P.J., Broadley, M.R., & Graham, N.S. (2017) . Identification of candidate genes for calcium and magnesium accumulation in *Brassica* napus L. by association genetics. Frontiers in Plant Science, 8.
6. Alfthan, G.; Eurola, M.; Ekholm, P.; Venäläinen, E.-R.; Root, T.; Korkalainen, K.; Hartikainen, H.; Salminen, P.; Hietaniemi, V.; Aspila, P.; et al. Effects of nationwide addition of selenium to fertilizers on foods, and animal and human health in Finland: From deficiency to optimal selenium status of the population. J. Trace Elem. Med. Biol. 2015, 31, 142–147.

7. Allan, B.C.; Lacourciere, G.M.; Stadtman, T.C. Responsiveness of selenoproteins to dietary selenium. Annu. Rev. Nutr. 1999, 19, 1-6.
8. Anderson JW. De Kok LJ .1993. Selenium interactions in sulfur metabolism nutrition and assimilation in higher plants – regulatory, agricultural and environmental aspects. SPB Academic, the Netherland, pp
9. Antioxidant activity of extracts from Acacia confusa bark and heartwood. Agric Food Chem
10. *Arabidopsis* Genome Initiative, 2000 Analysis of the genome sequence of the flowering plant *Arabidopsis thaliana*. Nature 408: 796–815.
11. Arner, E.S. Focus on mammalian thioredoxin reductases—Important selenoproteins with versatile functions. Biochim. Biophys. Acta 2009, 1790, 495–526.
12. Ashraf, M. Y., et al. (2018) . Selenium supplementation improves photosynthesis and productivity in spring wheat under drought. Photosynthetica, 56(3), 773-778.
13. Ashraf, M.A., Akbar, A., Parveen, A., Rasheed, R., Hussain, I., Iqbal, M., 2018. Phenological application of selenium differentially improves growth, oxidative defense and ion homeostasis in maize under salinity stress. Plant Physiol. Biochem. 123, 268–280.
14. Augmentation of Signals. National Library of Medicine. PMID: 33175379.
15. Avissar, N., Kerl, E. A., Baker, S. S. & Cohen, H. Extracellular glutathione peroxidase mRNA and protein in human cell lines. Arch. Biochem. Biophys. 309, 239–246 (1994).

16. B. Halliwell, J. M. C. Gutteridge. Free Radicals in Biology and Medicine. Oxford University Press, Oxford (1999).
17. Banuelos, G.S., & Meek, D.W. (1990) . "Accumulation of Selenium in Plants Grown on Selenium-Treated Soil." Journal of Environmental Quality, 19(3), 727-733.
18. Ban˜uelos G, Terry N, LeDuc DL, Pilon-Smits EAH, Mackey B. 2005b. Field trial of transgenic Indian mustard plants shows enhanced phytoremediation of selenium-contaminated sediment. Environmental Science and Technology 39: 1771–1777.
19. Barberon M, Berthomieu P, Clairotte M, Shibagaki N, Davidian J-C, Gosti F. 2008. Unequal functional redundancy between the two *Arabidopsis thaliana* high-affinity sulphate transporters SULTR1; 1 and SULTR1;2. New Phytologist 180: 608–619.
20. Bazakos, C., Hanemian, M., Trontin, C., Jiménez-Gómez, J.M., & Loudet, O. (2017) . New strategies and tools in quantitative genetics: How to go from the phenotype to the genotype. Annual Review of Plant Biology, 68, 435–455.
21. Bañuelos, G.S.; Ajwa, H.A.; Wu, L.; Guo, X.; Akohoue, S.; Zambrzuski, S. Selenium-induced growth reduction in *Brassica* land races considered for phytoremediation. Ecotoxicol. Environ. Saf. 1997, 36, 282–287.
22. Bell PF, Parker DR, Page AL. 1992. Contrasting selenate–sulfate interactions in selenium-accumulating and nonaccumulating plant species. Soil Science Society of America Journal 56: 1818–1824.
23. Benjamini, Y., & Hochberg, Y. (1995) . Controlling the false discovery rate: A practical and powerful approach to multiple

testing. Journal of the Royal Statistical Society: Series B (Methodological), 57(1), 289–300.

24. Benjamini, Y., & Yekutieli, D. (2001) . The control of the false discovery rate in multiple testing under dependency. Annals of Statistics, 29(4), 1165–1188.
25. Benlloch, R., Lois, L. M. (2018) . Sumoylation in plants: mechanistic insights and its role in drought stress. J. Exp. Bot. 69, 4539–4554. doi:
26. Benton J and Jones Jr (1982) . Hydroponics: History and use in plant nutrition studies. Journal of plant nutrition. 5(8).
27. Benton J and Jones Jr (2005) . Hydroponics: A Practical guide for soilless grower. CRC Press 2nd Edition. 1-28.
28. Birringer M, Pilawa S, Flohe´ L. 2002. Trends in selenium biochemistry. Natural Product Reports 19: 693–718.
29. Birringer, P C, M., Block, E., Kotrebai, M., Tyson, J.F., Uden, P.C., Lisk & D.J.: (2000) : chemical speciation influences comparative activity of selenium-enriched garlic and yeast in mammary cancer prevention j. Agric. Food Chem., 48: 2062–2070.
30. Bjelakovic, G., M. Nikolova, J. Gluud, et al. 2007. “Antioxidant Supplements for Preventing Mortality in Healthy Participants and Patients with Various Diseases.” Cochrane Database of Systematic Reviews 2007 (2): CD007176.
31. Bland, J. M., & Altman, D. G. (1995) . Multiple significance tests: the Bonferroni method. BMJ, 310(6973), 170.
32. Bodnar M., Konieczka P., Namiesnik J. (2012) . The properties, functions, and use of selenium compounds in living organisms. J. Environ. Sci. Health Part C 30, 225–252.
33. Bonifacio, E., et al. (2018) . "Genetic engineering for selenium biofortification in crops." Frontiers in Plant Science, 9, 774.

34. Bouis, H. E., et al. (2011) . "Biofortification: A new tool to reduce micronutrient malnutrition." Food and Nutrition Bulletin, 32(1_suppl1), S31-S40.
35. Bouis, H.E., C. Hotz, B. McClafferty, J.V. Meenakshi, andW.H.Pfeiffer.2011.“Biofortification: A new tool to reduce micronutrient malnutrition”. Food and Nutrition Bulletin 32 (Supplement 1): 31S40S.
36. Boyd, R., 2011. Selenium stories. Nat. Chem. 3, 570
37. Brezezinska-Slebodzinska E, Slebodzinski AB, Pietras B, Wieczorek G. Antioxidant effect of vitamin E and glutathione on lipid peroxidation in boar semen plasma. Biol Trace Elem Res. 1995; 47(1–3):69–74.
38. Brigelius-Flohe, R. Glutathione peroxidases and redox-regulated transcription factors. Biol. Chem. 387, 1329–1335 (2006).
39. Broadley, M.R.; Alcock, J.; Alford, J.; Cartwright, P.; Foot, I.;
40. Broadley, M. R., White, P. J., Bryson, R. J., Meacham, M. C., Bowen, H. C., Johnson, S. E.; Tucker, M. (2006). Biofortification of UK food crops with selenium. Proceedings of the Nutrition Society, 65(2), 169-181. Buchner P, Parmar S, Kriegel A, Carpentier M, Hawkesford MJ. 2010. The sulfate transporter family in wheat: tissue-specific gene expression in relation to nutrition. Molecular Plant 3: 374–389.
41. Buchner P, Stuiver CEE, Westermann S, et al. 2004. Regulation of sulfate uptake and expression of sulfate transporter genes in *Brassica* oleracea L. as affected by atmospheric H2S and pedospheric sulphate nutrition. Plant Physiology 136: 3396–3408.
42. Burau, R.G., 1985. Environmental chemistry of selenium. Calif. Agric., 39: 16-18.

43. Burke, KE, Combs, GF, Gross, EG, Bhuyan, KC & Abu-Libdeh, H (1992
44. Buttke, T.M.; Sandstrom, P.A. Oxidative stress as a mediator of apoptosis. Immunol. Today 1994, 15, 7–10.
45. Cabannes E, Buchner P, Broadley MR, Hawkesford MJ. 2011. A comparison of sulfate and selenium accumulation in relation to the expression of sulfate transporter genes in Astragalusspecies. Plant Physiology 157: 2227–2239.
46. Cakmak, I., et al. (2010) . "Biofortification of cereals with zinc and iron." Plant and Soil, 335, 161-174.
47. Cao MJ, Wang Z, Wirtz M, Hell R, Oliver DJ, Xiang CB. 2013. SULTR3;1 is a chloroplast-localized sulphate transporter in *Arabidopsis thaliana*. The Plant Journal 73: 607–616.
48. Cappa JJ, Cappa PJ, El Mehdawi AF, McAleer JM, Simmons MP, PilonSmits EAH. 2014. Characterization of selenium and sulfur accumulation across the genus Stanleya (*Brassica*ceae): a field survey and common-garden experiment. American Journal of Botany 101: 830–839.
49. Carey, A. M., Scheckel, K. G., Lombi, E., Newville, M., Choi, Y., Norton, G. J., et al. (2012) . Grain accumulation of selenium species in rice (Oryza sativa L.). Environ. Sci. Technol. 46, 5557–5564.
50. Cartes, P., Jara, A. A., Pinilla, L., Rosas, A., and Mora, M. L. (2010) . Selenium improves the antioxidant ability against aluminium-induced oxidative stress in ryegrass roots. Ann. Appl. Biol. 156, 297–307. doi:
51. Castaño-Miquel, L., Seguí, J., Lois, L. M. (2011) . Distinctive properties of *Arabidopsis* SUMO paralogues support the in

vivo predominant role of AtSUMO1/2 isoforms. Biochem. J. 436:581–590. doi:

52. Chasteen, T.G.; Bentley, R. Biomethylation of selenium and tellurium: Microorganisms and plants. Chem. Rev. 2003, 103, 1–26.
53. Chatterjee M, Saluja R, Kanneganti S, et al. Biochemical and molecular evaluation of neutrophil NOS in spontaneously hypertensive rats. Cell Mol. Biol. 2007; 33: 84 – 93.
54. Chelsea D Specht, Nhu H. Nguyen, Heather E. Driscoll. A Molecular phylogeny of the Wild Onions (Allium; Alliaceae) with a focus on the Western North American Centre of diversity 2007; Molecular Phylogentics and Evolution: 47: 1157-1172.
55. Cheng, W.H.; Ho, Y.S.; Ross, D.A.; Valentine, B.A.; Combs, G.F.; Lei, X.G. Cellular glutathione peroxidase knockout mice express normal levels of selenium-dependent plasma and phospholipid hydroperoxide glutathione peroxidases in various tissues. J. Nutr. 1997, 127, 1445–1450.
56. Chevereau G, Bollenbach T," Systematic discovery of drug interaction mechanisms", Mol Syst Biol. 11(4):807, 2015
57. Chevereau, G., & Bollenbach, T. (2015) . Systematic discovery of drug interaction mechanisms. Molecular Systems Biology, 11(4), 807.
58. Chilimba, A.D.; Young, S.D.; Black, C.R.; Meacham, M.C.; Lammel, J.; Broadley, M.R. Agronomic biofortification of maize with selenium (Se) in Malawi. Field Crop. Res. 2012, 125, 118–128.
59. Choudhuri Supratim. 2014. Bioinofrmatics for Beginners.

60. Christensen, M. J. & Burgener, K. W. Dietary selenium stabilizes glutathione peroxidase mRNA in rat liver. J. Nutr. 122, 1620–1626 (1992).
61. Chu, J., Yao, X., and Zhang, Z. (2010) . Responses of wheat seedlings to exogenous selenium supply under cold stress. Biol. Trace Elem. Res. 136, 355–363.
62. Cold Spring Harbor Laboratory Press, Cold Spring Harbor, NY.
63. Combs GF & Gray WP (1998) Chemopreventive agents: selenium. Pharmacol Ther 79, 179–192.
64. Combs GF Jr (2001) Selenium in global food systems. British Journal of Nutrition 85, 517–547.
65. Combs, G. F. (2001). Selenium in Global Food Systems. British Journal of Nutrition 85 (5): 227-230.
66. Combs, G.F., Jr. Current evidence and research needs to support a health claim for selenium and cancer prevention. J. Nutr. 2005, 135, 343-347.
67. Combs, G.F., Jr. Status of selenium in prostate cancer prevention. Br. J. Cancer 2004, 91, 195-199.
68. Comp. Biochem. Phys. C 129, 163-173 (2001).
69. Compounds in Living Organisms, Journal of Environmental Science and
70. D.L., 1990: Magnesium in plants: Uptake, distribution, function, and utilization by man and animals. In: Sigel, H., Sigel, A. (eds.), Metal Ions in Biological System, 56. Marcel Dekker, Inc.
71. DJANAGUIRAMAN, M., DEVI, D.D., SHANKER, A.K., SHEEBA, J.A., BANGARUSAMY, U., 2005: Selenium – an antioxidative protectant in soybean during senescence. Plant Soil. 272, 77-86. DOI 10.1007/ s11104-004-4039-1.

72. Da Silva, D.F.; Cipriano, P.E.; de Souza, R.R.; Júnior, M.S.; Faquin, V.; de Souza Silva, M.L.; Guilherme, L.R.G. Biofortification with selenium and implications in the absorption of macronutrients in Raphanus sativus L. J. Food Compos. Anal. 2020, 86, 103382.
73. Dagnell, M.; Schmidt, E.E.; Arner, E.S.J. The A to Z of modulated cell patterning by mammalian thioredoxin reductases. Free Radic. Biol. Med. 2018, 115, 484–496.
74. De Souza MP, Pilon-Smits EAH, Lytle CM, Hwang S, Tai JC, Honma TSU, Yeh L, Terry N (1998) Rate-limiting steps in selenium volatilization by *brassica* juncea. Plant Physiol 117:1487–1494.
75. DeTar RA, Alford E´ R, Pilon-Smits EAH. 2015. Molybdenum accumulation, tolerance and molybdenum–selenium–sulfur interactions in Astragalus selenium hyperaccumulator and nonaccumulator species. Journal of Plant Physiology 183: 32–40.
76. Dhillon, K.S., & Dhillon, S.K. (2003) . "Distribution and Management of Selenium in Soils and Crops." Pedosphere, 13(2), 173-185.
77. Diamond AM, Dale P, MurrayJL, et aL The inhibition of radiationinduced nlutagenesis by the combined effects of selenium and the aminothiol WP.-l (165. Muter P-.es t 996; 356: i 47-54.
78. Dudoit, S., Shaffer, J. P., & Boldrick, J. C. (2003) . Multiple hypothesis testing in microarray experiments. Statistical Science, 18(1), 71–103.
79. Duncan, E., Maher, W., Jagtap, R., Krikowa, F., Roper, M. M., and O'Sullivan, C. A. (2017) . Selenium speciation in wheat

grain varies in the presence of nitrogen and sulphur fertilisers. Environ. Geochem. Health 39, 955–966.

80. Dunn, O. J. (1961) . Multiple comparisons among means. Journal of the American Statistical Association, 56(293), 52–64.
81. EAH (2006b) spatial imaging, speciation and quantification of selenium in
82. Ebrahimi, N.; Stoddard, F.L.; Hartikainen, H.; Seppänen, M.M. Plant species and growing season weather influence the efficiency of selenium biofortification. Nutr. Cycl. Agroecosystems 2019, 114, 111–124.
83. Eiche E.; Nothstein A. K.; Göttlicher J.; Steininger R.; Dhillon K. S.; Neumann T. The behaviour of irrigation induced Se in the groundwatersoil-plant system in Punjab, India. Environ. Sci. Process. Impacts 2019, 21 (6), 957–969. 10.1039/C9EM00009G.
84. El Kassis E, Cathala N, Rouached H, et al. 2007. Characterization of a selenate-resistant *Arabidopsis* mutant. Root growth as a potential target for selenate toxicity. Plant Physiology 143: 1231–1241.
85. El-Bassiony, A. M.1, S. H. Mahmoud1, S. M. El-Sawy1 and Shaymaa I
86. El-Ghorab, Ahmed, Zainab Aslam, Saeed Akhtar, Muhammed Imran, Muhammad Nadeem, Syed Amir Gilani, Elnashar, Magdy. Antioxidant activity, Anti-inflammatory activites, Anticancer and Chemical Composition of Spring Onion Extracts 2017; ISSN: 0975-8585: RJPBCS 8(2): 1880-1890.
87. Emoto K, Umeda M, Nakagawa Y. Failure of the expression of

88. Ersoz, E. S., Yu, J., & Buckler, E. S. (2007) . Applications of linkage disequilibrium and association mapping in crop plants. In R. K. Varshney, & R. Tuberosa (Eds.), Genomics-assisted crop improvement (pp. 97– 119). *Dordrecht, Netherlands: Springer, 1*, -40206295-7_5.
89. Esworthy, R.S.; Aranda, R.; Martin, M.G.; Doroshow, J.H.; Binder, S.W.; Chu, F.F. Mice with combined disruption of Gpx1 and Gpx2 genes have colitis. Am. J. Physiol. Gastrointest. Liver Physiol. 2001, 281, G848– G855.
90. FARGAŠOVÁ, A., PASTIEROVÁ, J., SVETKOVÁ, K., 2006: Effect of Se-metal pair combinations (Cd, Zn, Cu, Pb) on photosynthetic pigments produc-tion and metal accumulation in Sinapis Alba L. seedlings. Plant Soil Env. 52, 8-15.
91. Fabiana F, Islam Yassir and Pfeiffer Wolfgang H. 2103. Biofortification:
92. Fairweather – Tait, S.J.; Bao, Y.; Broadley, M.R.; Collings, R.; Ford, D.; Hesketh, J.E.; Hurst, R. Selenium in human health and disease. Antioxid. Redox signal. 2011, 14, 1337 – 1383.
93. Fairweather-Tait, S.J.; Hart, D.J.; Hurst, R.; Knott, P.; McGrath, S.P.; et al. Selenium biofortification of high-yielding winter wheat (Triticum aestivum L.) by liquid or granular Se fertilisation. Plant Soil 2010, 332, 5– 18.
94. Feist LJ, Parker DR. 2001. Ecotypic variation in selenium accumulation among populations of Stanleya pinnata. New Phytologist 149: 61–69.
95. Ferrari, G., and F. Renosto. 1992. Regulation of sulfate uptake by excised barely roots in the presence of selenate. Plant physio. 49: 114 – 116.

96. Freeman JL, Tamaoki M, Stushnoff C, et al. 2010. Molecular mechanisms of selenium tolerance and hyperaccumulation in Stanleya pinnata. Plant Physiology 153: 1630–1652.
97. Freeman JL, Zhang LH, Marcus MA, Fakra S, McGrath SP, Pilon-Smits
98. G., Hoekstra W. G. (1973) . Selenium: biochemical role as a component of glutathione peroxidase. Science 179, 588–590.
99. Galeas ML, Zhang LH, Freeman JL, Wegner M, Pilon-Smits EAH (2007) Seasonal fl uctuations of selenium and sulfur accumulation in selenium hyperaccumulators and related non-accumulators. New Phytol 173:517– 525.
100. Galeas ML, Zhang LH, Freeman JL, Wegner M, Pilon-Smits EAH. 2007. Seasonal fluctuations of selenium and sulfur accumulation in selenium hyperaccumulators and related nonaccumulators. New Phytologist 173: 517–525.
101. Galeas, M.L., et al. (2007) . "Differential Selenium Accumulation Among Populations of Stanleya pinnata." New Phytologist, 173(3), 517-525.
102. Galton VA. Targeted disruption of the type 2 selenodeiodinase gene (DIO2) results in a phenotype of pituitary resistance to T4. Mol Endocrinol. 2001; 15:2137–2148.
103. Genetics, 10, 565– 577.
104. Germ M, Kreft I, Stibilj V, Urbanc-Berčič O. 2007. Combined effects of selenium and drought on photosynthesis and mitochondrial respiration in potato, Plant Physiol. and Biochem. (Paris) 45: 162-167
105. Gigolashvili T, Kopriva S. 2014. Transporters in plant sulphur metabolism. Frontiers in Plant Science 5: 422.

106. Gladyshev, V. N. 2007. “Selenoprotein Gene Families and Selenocysteine Synthesis.” Biochimica et Biophysica Acta (BBA) - Molecular Cell Research 1773 (9): 1233-1245.
107. Gupta, P. K., Kulwal, P. L., & Jaiswal, V. (2019) . Chapter Two— Association mapping in plants in the post-GWAS genomics era. In D.
108. Gupta, P.K., Kulwal, P.L., & Jaiswal, V. (2019) . Association mapping in plants in the post-GWAS genomics era. In D. Kumar (Ed.), Advances in Genetics (Vol. 104, pp. 75–154). Academic Press.
109. Gupta, S., Singh, B., & Kapoor, D. (2016) . Selenium supplementation in the prevention of cancer: a review of clinical trials. Journal of Cancer Research and Clinical Oncology, 142(1), 35-42.
110. Gupta, U. C. 1991. Boron, molybdenum, and selenium status in different plants parts in legumes and vegetable crops. J. plant Nutr. 14: 613 – 621.
111. HAWRYLAK-NOWAK, B., 2008: Effect of selenium on selected macronutrients in maize plants. J. Elem. 13, 513-519.
112. Halliwell, B. 2007. “Biochemistry of Oxidative Stress.” Biochemical Society Transactions 35 (5): 1147-1150.
113. Hama, H., Yamanoshita, O., Chiba, M., Takeda, I. & Nakajima, T.: (2008) : selenium-enriched japanese radish sprouts influence glutathioneperoxidase and glutathione s-transferase in an organspecific manner in rats j. Occup. Health, 50: 147–154.
114. Hansen, J., T. Bond, B. Cairns, H. Gaeggler, B. Liepert, T. Novakov, and B. Schichtel, 2004: Carbonaceous

aerosols in the industrial era. Eos Trans. Amer. Geophys. Union, 85, no. 25, 241, 245.

115. Hanson S, et al. (2003) Tetracycline-aptamer-mediated translational regulation in yeast. Mol Microbiol 49(6):1627-37.

116. Hariharan Sneha, Dharmaraj Selvakumar. 2020. Selenium and selenoproteins: it's role in regulation of inflammation.

117. Harper Andrea L, He Zhesi, Langer Swen, Havlickova Lenka, Wang

118. Harper, A.L., He, Z., Langer, S., Havlickova, L., Wang, L., Fellgett, A., Gupta, V., Pradhan, A.K., & Bancroft, I. (2020) . Validation of an Associative Transcriptomics platform in the polyploid crop species *Brassica* juncea by dissection of the genetic architecture of agronomic and quality traits. Plant Journal, 103, 1885–1893.

119. Harris J, Schneberg KA, Pilon-Smits EAH. 2014. Sulfur–selenium– molybdenum interactions distinguish selenium hyperaccumulator Stanleya pinnata from non-hyperaccumulator *Brassica* juncea (*Brassica*ceae). Planta 239: 479–491.

120. Hartikainen H and Xue T 1999 The promotive effect of selenium on plant growth as triggered by ultraviolet irradiation. J. Environm. Qual. 28, 1372–1375.

121. Hasanuzzaman, M., Hossain, M. A., and Fujita, M. (2011) . Seleniuminduced up-regulation of the antioxidant defense and methylglyoxal detoxification system reduces salinity induced damage in rapeseed seedlings. Biol. Trace Elem. Res. 43, 1704–1721.

122. Hatfield, D. L. & Gladyshev, V. N. How selenium has altered our understanding of the genetic code. Mol. Cell Biol. 22, 3565–3576 (2002).
123. Hawrylak-Nowak, B. (2013) . Comparative effects of selenite and selenate on growth and selenium accumulation in lettuce plants under hydroponic conditions. Plant. Growth Regul. 70, 149–157.
124. Hawrylak-Nowak, B. (2013) . Selenium in higher plants: Physiological role, antioxidant activity, and influence on the uptake of other elements. Acta Physiologiae Plantarum, 35(8), 2131-2142.
125. Hay RT (April 2005). *Molecular Cell*, *18*, (1): 1–12.
126. Hay, R. T. (2005) . SUMO: a history of modification. Mol. Cell 18, 1–12.
127. Health, Part C: Environmental Carcinogenesis and Ecotoxicology
128. Hemmati, M., Delkhosh, B., Rad, A.H.S., Mohammadi, G.N., 2019. Effect of the application of foliar selenium on canola cultivars as influenced by different irrigation regimes. J. Agric. Sci. 25 (3), 309–318.
129. Hickey, C. M., Wilson, N. R., Hochstrasser, M. (2012) . Function and regulation of SUMO proteases. Nat. Rev. Mol. Cell Biol. 13, 755–766. doi:
130. Hill, K. E., Lloyd, R. S., Yang, J. G., Read, R. & Burk, R. F. The cDNA for rat selenoprotein P contains 10 TGA codons in the open reading frame. J. Biol. Chem. 266, 10050–10053 (1991).
131. Ho, Y.S.; Magnenat, J.L.; Bronson, R.T.; Cao, J.; Gargano, M.; Sugawara, M.; Funk, C.D. Mice deficient in cellular glutathione peroxidase develop normally and show no

increased sensitivity to hyperoxia. J. Biol. Chem. 1997, 272, 16644–16651.

132. Hoetelmans RM. "IC50 versus EC50". PK-PD relationships for antiretroviral drugs. Amsterdam: Slotervaart Hospital. Archived from the original on 2017-05-28 – via U.S. Food and Drug Administration. 97. Hotz C. 2013. Biofortification as a Strategy to Address Global Micronutrient Deficiencies. Encyclopedia of Human Nutrition (Third Edition).

133. Hoetelmans, R. M. W. (2017) . Pharmacokinetics of anticancer drugs in relation to their efficacy and toxicity. Expert Opinion on Pharmacotherapy, 18(7), 711-723.

134. Hou, S., Jamieson, P., He, P. (2018) . The cloak, dagger, and shield:

135. Hsu F-C, Wirtz M, Heppel SC, et al. 2011. Generation of Se-fortified broccoli as functional food: impact of Se fertilization on S metabolism.

136. Huang, Z., Zhang, L., Chen, B., & Liu, Y. (2021) . Application of ICP-MS in Trace Element Analysis and Its Recent Progress in Environmental Analysis. Analytical Chemistry, 93(6), 2475–2486.

137. Imai H, Suzuki K, Ishizaka K, Ichinose S, Oshima H, Okayasu I,

138. Ingold, I. et al. Selenium utilization by GPX4 is required to prevent hydroperoxide-induced ferroptosis. Cell 172, 409–422. e421 (2018).

139. Inostroza-Blancheteau C, Reyes-Dı´az M, Alberdi M, et al. 2013. Influence of selenite on selenium uptake, differential antioxidant performance and gene expression of

sulfate transporters in wheat genotypes. Plant and Soil 369: 47–59.

140. Institute of Medicine. Dietary Reference Intakes for Vitamin C, Vitamin E, Selenium, and Carotenoids; The National Academies Press:

141. Ip, C. Lessons from basic research in selenium and cancer prevention. J. Nutr. 1998, 128, 1845- 1854.

142. Leustek, T., Martin, M. N., Bick, J. A., & Davies, J. P. (2000). Pathways and regulation of sulfur metabolism revealed through molecular and genetic studies. Annual Review of Plant Biology, 51(1), 141-165.

143. J. L. Avanzo, A. De Mendonça; S. M. Piccoli,; M. De Cerqueira.

144. Jarvis, K. E., & Gray, A. L. (1989) . Applications of Inductively Coupled Plasma Mass Spectrometry in the Environmental Sciences. Journal of Analytical Atomic Spectrometry, 4(5), 743–749.

145. Jay, J. M., & Shafkat, A. (2017) . ABTS radical scavenging capability of Allium sativum extract combined with selenium nanoparticles. International Journal of Pharmacy and Pharmaceutical Sciences, 9(7), 42-46.

146. Jeff Gauthier, Antony T. Vincent, Steve J. Charette and Nicolas Derome. A brief history of bioinformatics. Briefings in Bioinformatics, 2018, 1–16.

147. Johnson, E. S. (2004) . Protein modification by SUMO. Annu. Rev.

148. Johnson, S.E., Hawkesford, M.J., McGrath, S.P., Zhao, F-J, Breward, N., Harriman, M. & Tucker, M. (2006) : biofortification of un food crops with selenium proceed. Nutr. Soc., 65: 169–181

149. Jones J B J 1997 A Guide for the Hydroponics & Soilless Grower, First Edit (Delray Beach: St. Lucie Press)
150. Jones, J. B., & Case, V. W. (1990) . Soil Testing and Plant Analysis (3rd ed.). American Society of Agronomy.
151. Joy EJM, Ander EL, Young SD, Black CR, Watts MJ, Chilimba ADC, Chilima B, Siyame EWP, Kalimbira AA, Hurst R, Fairweather-Tait SJ, Stein AJ, Gibson RS, White PJ, Broadley MR (2014) Dietary mineral supplies in africa. Physiol Plant 151:208–229.
152. Kabata-Pendias A, Mukherjee AB (2007) Trace elements from soil to human. Springer, Berlin/ Heidelberg/New York
153. Kagan V., Nohl H., Quinn P., Cadenas E., Packer L. Handbook of Antioxidants. Marcel Dekker; New York, NY, USA: 2002.
154. Kang Donghyun, Lee Jeeyeon, Wu3 Cuiyan, Guo3 Xiong, Jae Lee2 Byeong, Jang-Soo Chun5 and Jin-Hong Kim. 2020. The role of selenium metabolism and
155. Karunasinghe N., Ryan J., Tuckey J., Master J., Jamieson M., Clarke L. C., Marshall J. R., Ferguson L. R. (2004) . DNA stability and serum selenium levels in a high-risk group for prostate cancer. Cancer Epidemiol.
156. Kataoka T, Hayashi N, Yamaya T, Takahashi H. 2004a. Root-to-shoot transport of sulfate in *Arabidopsis*. Evidence for the role of SULTR3;5 as a component of low-affinity sulfate transport system in the root vasculature. Plant Physiology 136: 4198–4204.
157. Kayat Fatimah, Mohammed Arifallah, Ibrahim Ahmed Mahmood.

158. Kennedy, G., G.Nantel and P. Shetty. 2003. The scourge of “hidden hunger”:Global dimensions of micronnutrient deficiencies. Food Nutr.Agric. 32:8-16.

159. Kerscher, O., Felberbaum, R., Hochstrasser, M. (2006) . Modification of proteins by ubiquitin and ubiquitin-like proteins. Annu. Rev. Cell Dev.

160. Kikkert, J., and Berkelaar, E. (2013) . Plant uptake and translocation of inorganic and organic forms of selenium. Arch. Environ. Contam. Toxicol.

161. Kingston, H. M., & Haswell, S. J. (1997) . Microwave-Enhanced Chemistry: Fundamentals, Sample Preparation, and Applications. American Chemical Society.

162. Kise Y, Yamamura M, Kogata M. et ah Inhibition by se leniunl ofnltrahepafic cholan~ocarclnonla hlducdon ill Syrian golden hamsters by N'-nitrosohis(2 oxopropyl) amine. Nutr Cancer I991; 16:153-64.

163. Koprivova, A., Harper, A.L., Trick, M., Bancroft, I., & Kopriva, S. (2014) . Dissection of the control of anion homeostasis by associative transcriptomics in *Brassica* napus. Plant Physiology, 166(1), 442–450.

164. Kubachka KM, Meija J, LeDuc DL, Terry N, Caruso JA (2007) Environ Sci Technol 41:1863–1869.

165. Kumar (Ed.), Advances in Genetics (pp. 75–154). Cambridge, MA:

166. Kumar, M., Bijo, A. J., Baghel, R. S., Reddy, C. R. K., and Jha, B. (2012) . Selenium and spermine alleviates cadmium induced toxicity in the red seaweed Gracilaria dura by regulating antioxidant system and DNA methylation. Plant Physiol. Biochem. 51, 129–138. doi:

167. Labunskyy, V. M., H. R. M. Gladyshev, and V. N. 2014. “Selenoproteins and Selenium.” Annual Review of Nutrition 34: 219-237.

168. Lee Tak, Lee Insuk. 2021. Genome-Wide Association Studies in

169. Lee, R.R.Q., & Chae, E. (2020) . Variation patterns of NLR clusters in *Arabidopsis thaliana* genomes. Plant Communications, 1(4), 100089.

170. Lee, S., Woodard, H. J., and Doolittle, J. J. (2011) . Effect of phosphate and sulfate fertilizers on selenium uptake by wheat (Triticum aestivum). Soil Sci. Plant Nutri. 57, 696–704.

171. Leggett, J. E., and E. Epstein. 1956. Kinestics of sulfate absorption by barely roots. Plant physiol. 31: 222 – 226.

172. Li H-F, McGrath SP, Zhao F-J. 2008. Selenium uptake, translocation and speciation in wheat supplied with selenate or selenite. New Phytologist 178: 92–102.

173. Li, H.-F., McGrath, S. P., and Zhao, F.-J. (2008) . Selenium uptake, translocation and speciation in wheat supplied with selenate or selenite.

174. Liang, Y. K., Su, Y., Li, L., Huang, X., Panhwar, F. H., Zheng, T. D., et al. (2019) . Quick selenium accumulation in the selenium-rich rice and its physiological responses in changing selenium environments. BMC Plant Biol. 19:559.

175. Liang, Y. et al. Effect of selenium on selenoprotein expression in the adipose tissue of chickens. Biol. Trace Elem. Res. 160, 41–48 (2014).

176. Lihong, Fellogett Alison, Gupta Vibha, Pradham Akshay kumar, Bancroft Ian. 2020. Validation of an Associative Transcriptomics platform in the polyploid crop

species *Brassica* juncea by dissection of the genetic architecture of agronomic and quality traits. The Plant Journal 103(5).

177. Lin, T.; Zhu, G.; Zhang, J.; Xu, X.; Yu, Q.; Zheng, Z.; Zhang, Z.; Lun, Y.; Li, S.; Wang, X.; et al. Genomic analyses provide insights into the history of tomato breeding. Nat. Genet. 2014, 46, 1220–1226.

178. Lipka, A. E., Tian, F., Wang, Q., Peiffer, J., Li, M., Bradbury, P. J., ... & Zhang, Z. (2012) . GAPIT: genome association and prediction integrated tool. Bioinformatics, 28(18), 2397–2399.

179. Liu, H. J., & Yan, J. (2019) . Crop genome-wide association study: A harvest of biological relevance. The Plant Journal, 97, 8–18. https:

180. Liu, M., Yang, Y., Liang, T., Hou, F., Zhang, M., He, S., Liu, P., Zou, C., Ma, L., Pan, G., & Shen, Y. (2019) . Dynamic transcriptome and GWAS uncover that a hydroxyproline-rich glycoprotein suppresses Agrobacterium-mediated transformation in maize. Molecular Plant. Advance online publication.

181. Liu, X., Wang, Q., Hu, C., Zhao, X., Duan, B., and Zhao, Z. (2016a). Regulatory effects of sulfur on oilseed rape (*Brassica* napus L.) response to selenite. Soil Sci. Plant Nutr. 62, 247–253. doi:

182. Liu, X., Zhao, Z., Duan, B., Hu, C., Zhao, X., and Guo, Z. (2015) . Effect of applied sulphur on the uptake by wheat of selenium applied as selenite. Plant Soil 386, 35–45.

183. Longchamp M.; Angeli N.; Castrec-Rouelle M. Selenium uptake in Zea mays supplied with selenate or

selenite under hydroponic conditions. Plant Soil 2013, 362 (1–2), 107–117. 10.1007/s11104-0121259-7.

184. Lu, J.; Holmgren, A. The thioredoxin antioxidant system. Free Radic. Biol. Med. 2013.

185. M. Valko, C. J. Rhodes, J.; Moncol, M. Izakovic, M., Mazur. Chem.Biol. Interact. 160, 1-40 (2006).

186. MALGORZATA BODNAR , PIOTR KONIECZKA & JACEK

187. Mackay, T. F. C., Stone, E. A., & Ayroles, J. F. (2009) . The genetics of quantitative traits: Challenges and prospects. Nature Reviews

188. Mackay, T. F. C., Stone, E. A., & Ayroles, J. F. (2009) . The genetics of quantitative traits: Challenges and prospects. Nature Reviews Genetics, 10, 565–577.

189. Mackay, T.F.C., Stone, E.A., & Ayroles, J.F. (2009) . The genetics of quantitative traits: challenges and prospects. Nature Reviews Genetics, 10(8), 565–577.

190. Manolio, T. A. (2010) . Genomewide association studies and assessment of the risk of disease. New England Journal of Medicine, 363(2), 166–176.

191. Matusiewicz, H., & Barnes, R. M. (1985) . Comparison of Various Sample Introduction Systems for ICP-MS Analysis of Aqueous Solutions. Spectrochimica Acta Part B: Atomic Spectroscopy, 40(4–6), 403–413.

192. Meetu Gupta, Shikha Gupta. 2017. An Overview of Selenium Uptake, Metabolism, and Toxicity in Plants. Frontiers in Plant Science 7. DOI:

193. Michael, T. P., & Jackson, S. (2013) . The first 50 plant genomes. The Plant Genome, 6, 1– 7.

194. Michael, T. P., & Jackson, S. (2013) . The first 50 plant genomes. The Plant Genome, 6, 1–7. 0001in.

195. Michael, T.P., & Jackson, S. (2013) . The first 50 plant genomes. The Plant Genome, 6, plantgenome2013.03.0001in.

196. Mihara H, Esaki N (2002) Bacterial cysteine desulfurases: their function and mechanisms. Appl Microbiol Biotechnol 60:12–23.

197. Mikkelsen, R. L., A. L. Page, and F. T. Bingham. 1989. Factors affecting selenium accumulation by agricultural crops, P. 65 – 94. In: L.

198. Molecular Medicine. doi.org/10.1038/s12276-020-0408-y 144. Moreno SG, Laux G, Brielmeier M, Bornkamm GW, Conrad M. Testis-specific expression of the nuclear form of phospholipid hydroperoxide glutathione peroxidase (PHGPx) Biol Chem.

199. Morrell, R., Sadanandom, A. Dealing with stress: A Review of Plant SUMO Proteases. 2019. Front. Plant Sci. Volume 10 – 2019.

200. Moustafa ME, Kumaraswamy E, Zhong N, Rao M, Carlson BA, Hatfield DL. Models for assessing the role of selenoproteins in health. J Nutr. 2003; 133:2494S–2496S.

201. Mukhopadhyay, D., Dasso, M. (2007) . Modification in reverse: the SUMO proteases. Trends Biochem. Sci. 32, 286–295. doi:

202. Muller, M.F.; Florian, S.; Pommer, S.; Osterhoff, M.; Esworthy, R.S.; Chu, F.F.; Brigelius-Flohe, R.; Kipp, A.P. Deletion of glutathione peroxidase-2 inhibits azoxymethane-induced colon cancer development. PLoS ONE 2013, 8, e72055.

203. NAMIESNIK (2012) The Properties, Functions, and Use of Selenium
204. Neoplasia 2000, 2, 291-299.
205. Neuhierl B, Thanbichler M, Lottspeich F, Bo¨ck A (1999) A family of s-methylmethionine dependent thiol/selenol methyltransferases. Role in selenium tolerance and evolutionary relation. J Biol Chem 274:5407–5414.
206. New Phytol. 178, 92–102.
207. Ng, B. H., & Anderson, J. W. (1978). Assimilation of selenate and selenite by Cucurbita pepo. Plant Physiology, 61(6), 122-127.
208. Novatchkova, B., Yates, G., Verma, V., Srivastava, A. K., Srivastava, M., Campanaro, A., et al. (2018) . SUMO conjugation to the pattern recognition receptor FLS2 triggers intracellular signalling in plant innate immunity. Nat. Commun. 9 (1), 5185.
209. Novatchkova, M., Budhiraja, R., Coupland, G., Eisenhaber, F., Bachmair, A. (2004) . SUMO conjugation in plants. Planta 220, 1–8. doi:
210. ODS. Selenium: Dietary Supplement Fact Sheet. Health Information. US Department of Health and Human Services, National Institutes of Health; Office of Dietary Supplements: Washington, DC, USA, 2016.
211. Ofori Prince Danso, Bismark Asante-Badu, Zezhou Zhang, Jiaping Song, Zhangmin Wang, Xuebin Yin and Renbin Zhu. 2023. Selenium Biofortification: Strategies, Progress and Challenges. DOI:
212. Ogra Y, Anan Y. 2012. Selenometabolomics explored by speciation. Biological and Pharmaceutical Bulletin 35: 1863–1869.

213. Ožbolt L, Kreft S, Kreft I, Germ M, Stibilj V. 2008. Distribution of selenium and phenolics in buckwheat plants grown from seeds soaked in Se solution and under different levels of UV-B radiation, Food Chemistry, 110: 691 - 696.

214. PAZURKIEWICZ-Kocot, K., Galas, W., Kita, A., 2003: The effect of sele-nium on the accumulation of some metals in Zea mays L. plants treated with indole-3-acetic acid. Cell Mol. Biol. Lett. 8, 97-104.

215. PC Raich, J Lu, HJ Thompson, GF Combs Jr 2001 Cancer Invest 19:540.

216. Packer, L., M. S. R. L. B. M. R. 2017. "The Role of Antioxidants in the Prevention and Treatment of Oxidative Stress-Related Diseases." Free Radical Biology and Medicine 123: 75-85.

217. Pandey, C., and M. (2015) . Selenium and auxin mitigate arsenic stress in rice (Oryza sativa L.) by combining the role of stress indicators, modulators and genotoxicity assays. J. Hazard. Mater. 287, 384–391. doi:

218. Papp, L.V.; Lu, J.; Holmgren, A.; Khanna, K.K. From selenium to selenoproteins: Synthesis, identity, and their role in human health.

219. Paul S, Datta SK, Datta K. 2015. MiRNA regulation of nutrient homeostasis in plants. Frontiers in Plant Science 6: 232.

220. Pe'er, I., Yelensky, R., Altshuler, D., & Daly, M. J. (2006) . Estimation of the multiple testing burden for genomewide association studies of nearly all common variants. Genetic Epidemiology, 31(4), 383–395.

221. Pence, BC, Pelier, E & Dunn, CG (1994) Effects of dietary selenium on uvb-induced skin carcinogenesis and epidermal antioxidant status. J Invest Dermatol 102, 759–761.

222. Penney, R., et al. (2012) . "Calcium biofortification of leafy vegetables: Genetic and agronomic strategies." Journal of Agricultural and Food Chemistry, 60(28), 7067-7076.

223. Peooas A., Zoidis E., Surai P., Zervas G. Selenoproteins and material nutrition. Comp. Biochem. Physiol. B. 2008; 151: 361 – 372.

224. Perchellet, JP, Abney, NL, Thomas, RM, Guislan, YL & Perchellet, EM (1987) Effects of combined treatments with selenium, glutathione and vitamin e on glutathione peroxidase activity, ornithine decarboxylase induction and complete and multistage carcinogenesis in mouse skin. Cancer Res 47, 477–485.

225. Perneger, T. V. (1998) . What's wrong with Bonferroni adjustments. BMJ, 316(7139), 1236–1238.

226. Pilon M, Owen JD, Garifullina GF, Kurihara T, Mihara H, Esaki N, Pilon-Smits EAH (2003) Enhanced selenium tolerance and accumulation in transgenic *arabidopsis thaliana* expressing a mouse selenocysteine lyase. Plant Physiol 131:1250–1257.

227. Pilon M, Pilon-Smits EAH (2007) The *arabidopsis* cysteine desulfurase cpnifs is essential for maturation of iron-sulfur cluster proteins, photosynthesis, and chloroplast development. Proc Natl Acad Sci USA 104:5686–5691.

228. Pilon-Smits, E. A. H., Hwang, S., Lytle, C. M., Zhu, Y. L., Tai, J., Bravo, R. C.; Terry, N. (1999). Overexpression of ATP sulfurylase in Indian mustard leads to increased selenate

uptake, reduction, and tolerance. Plant Physiology, 119(1), 123-132.

229. Pilon-Smits EAH, LeDuc DL. 2009. Phytoremediation of selenium using transgenic plants. Current Opinion in Biotechnology 20: 207–212.

230. Pilon-Smits, E.A.H., & Quinn, C.F. (2010) . "Selenium Metabolism in Plants." In Cell Biology of Metals and Nutrients (pp. 225-241). Springer.

231. Pilon-Smitws Elizabeth AH, Quinn Colin, 2010. Selenium Metabolism in Plants. Plants cell Monographs.

232. Pilon–Smits, E.A.H. On the Ecology of Selenium Accumulation in Plants. Plants, 2019, 8(7), article 197;

233. Pitts, M. W. & Hoffmann, P. R. Endoplasmic reticulum-resident selenoproteins as regulators of calcium signaling and homeostasis. Cell Calcium 70, 76–86 (2018).

234. Plant Biotechnol. J. 16, 1582– 1594.

235. Plant Signalling & Behaviour. 2013;8: e22681.

236. Plant, Cell and Environment 34: 192–207.

237. Poblaciones, M.J.; Rodrigo, S.; Santamaria, O.; Chen, Y.; McGrath, S.P. Selenium accumulation and speciation in biofortified chickpea (Cicer arietinum L.) under Mediterranean Plant Soil conditions. J. Sci. Food Agric. 2014, 94, 1101–1106.

238. Pommerrenig B, Diehn TA, Bienert GP. 2015. Metalloido-porins: essentiality of Nodulin 26-like intrinsic proteins in metalloid transport. Plant Science 238: 212–227.

239. Premarathna, L.; McLaughlin, M.J.; Kirby, J.K.; Hettiarachchi, G.M.; Stacey, S.; Chittleborough, D.J. Selenate-enriched urea granules are a highly Effective fertilizer for selenium biofortification of paddy rice grain. J. Agric. Food Chem. 2012, 60, 6037–6044.

240. Price, R. A., J. D. Palmer, and I. A. Al-Shehbaz, 1994 Sytematic relationships of *Arabidopsis*: a molecular and orphological perspective, pp.
241. Proc Natl Acad Sci USA 92:9373–9377.
242. Progress toward a more nourishing future. Global Food Security. DOI:
243. Pucci, B.; Kasten, M.; Giordano, A. Cell cycle and apoptosis.
244. Pukacka, S., Ratajczak, E., and Kalemba, E. (2011) . The protective role of selenium in recalcitrant Acer saccharium L. seeds subjected to desiccation. J. Plant Physiol. 168, 220–225. doi:
245. Põldma, P., Tõnutare, T., Viitak, A., Luik, A., and Moor, U. (2011) . Effect of selenium treatment on mineral nutrition, bulb size, and antioxidant properties of garlic (Allium sativum L.). J. Agric. Food Chem. 59, 5498–5503.
246. Qian J., Combs G. F., Jr, Morris J. S. (2005) . Prostate cancer risk and DNA damage:
247. R Core Team (2013) . R: A language and environment for statistical computing. R Foundation for Statistical Computing, Vienna, Austria.
248. Rai, A.N., Rao, M., & Gupta, N.C. (2022) . Transcriptomics research and resources in *Brassica* spp. In C. Kole & T. Mohapatra (Eds.), The *Brassica* juncea Genome (pp. 295–322). Springer. Compendium of Plant Genomes.
249. Ramos, S.J.; Faquin, V.; Guilherme, L.R.G.; Castro, E.M.; Avila, F.W.; Carvalho, G.S.; Bastos, C.E.A.; Oliveira, C. Selenium biofortification and antioxidant activity in lettuce plants fed with selenate and selenite. Plant Soil Environ. 2010, 56, 584–588.

250. Rayman M. P. (2000) . The importance of selenium to human health. Lancet. 356, 233–241. 10.1016/S0140-6736(00)02490-9

251. Rayman, M. P. (2008) . Selenium in cancer prevention: a review of the evidence and mechanisms. Cancer Causes & Control, 19(2), 229-249.

252. Rayman, M. P. 2012. “Selenium and Human Health.” The Lancet 379 (9822): 1256-1268.

253. Rayman, M.P. Selenium in cancer prevention: a review of the evidence and mechanism of action. Proc. Nutr. Soc. 2005, 64, 527-542.

254. Re Roberta, Pellegrini Nicoletta, Anna Proteggente, Ananth Pannala, Min Yang, and Catherine Rice-evans. 1999. Antioxidant activity applying an improved abts radical cation decolorization assay. Free Radical Biology & Medicine, Vol. 26, Nos. 9/10, pp. 1231–1237.

255. Rebecca Bailey,2008-07-25 at the Retrieved on July 22, 2008

256. Rederstorff M, Krol A, Lescure A. Understanding the importance of selenium and selenoproteins in muscle function. Cell Mol Life Sci. 2006; 63:52–59.

257. Renkema, H., Koopmans, A., Kersbergen, L., Kikkert, J., Hale, B., and Berkelaar, E. (2012) . The effect of transpiration on selenium uptake and mobility in durum wheat and spring canola. Plant Soil 354, 239–250. doi:

258. Reviews, 30:3, 225-252,

259. Rhee, S.G. Overview on Peroxiredoxin. Mol. Cells 2016, 39, 1–5.

260. Rosenfeld I, Beath OA. 1964. Selenium: geobotany, biochemistry, toxicity, and nutrition. New York: Academic Press.

261. Rotruck J. T., Pope A. L., Ganther H. E., Swanson A. B., Hafeman D.

262. Rouached H, Wirtz M, Alary R, et al. 2008. Differential regulation of the expression of two high-affinity sulfate transporters, SULTR1.1 and SULTR1.2, in *Arabidopsis*. Plant Physiology 147: 897–911.

263. Rouached H. Recent developments in plant zinc homeostasis and the path toward improved biofortification and phytoremediation programs.

264. Saaid M F, Yahya N A M, Noor M Z H and Ali M S A M 2013 A development of an automatic microcontroller system for Deep Water Culture (DWC) Proc. - 2013 IEEE 9th Int. Colloq. Signal Process. its Appl. CSPA 2013 328–332.

265. Saltzman Amy, Birol Ekin, Bouis Howarth E, Boy Erick, Demoura

266. Saltzman, A.; Birol, E.; Bouis, H.E.; Boy, E.; De Moura, F.F.; Islam, Y.; Pfeiffer, W.H. Biofortification: Progress toward a more nourishing future. Glob. Food Secur. 2013, 2, 9–17.

267. Schiavon M, Pilon M, Malagoli M, Pilon-Smits EAH. 2015. Exploring the importance of sulphate transporters and ATPsulphurylases for selenium hyperaccumulation – comparison of Stanleya pinnata and *Brassica* juncea (*Brassica*ceae). Frontiers in Plant Science 6: 2.

268. Schiavon M., Dall'acqua S., Mietto A., Pilon-Smits E. A., Sambo P., Masi A., et al. (2013) . Selenium fertilization alters the chemical composition and antioxidant constituents of

tomato (Solanum lycopersicon L.). J. Agric. Food Chem. 61, 10542–10554.

269. Schiavon, M.; dall'Acqua, S.; Mietto, A.; Pilon-Smits, E.A.H.; Sambo, P.; Masi, A.; Malagoli, M. Impact of selenium fertilization on chemical composition and Antioxidant constituents of tomato (Solanum lycopersicon L.). J. Agric. Food Chem. 2013, 61, 10542–10554.

270. Schmidt, H. H. H. W., M. J. F. L. E. L. H. 2016. "Oxidative Stress and Aging: The Role of the Antioxidant System." Free Radical Research 50 (9): 935-940.

271. Schneider MJ, Fiering SN, Pallud SE, Parlow AF, St Germain DL,

272. Schomburg L, Schweizer U, Holtmann B, Flohe L, Sendtner M, Kohrle J. Gene disruption discloses role of selenoprotein P in selenium delivery to target tissues. Biochem J. 2003; 370:397–402.

273. Schrauzer, G.N.; Rhead, W.J. Interpretation of the methylene blue reduction test of human plasma and the possible cancer-protecting effect of selenium. Experientia 1971, 27, 1069-1071.

274. Schwarz K, Foltz CM. Selenium as an integral part of factor 3 against dietary necrotic liver degeneration. J Am Chem Soc. 1957; 79:3292–3293. selenoproteins in cartilage homeostasis and arthropathies. Experimental &

275. Seliem, M.K., Hafez, Y., El-Ramady, H., 2020. Using of nano - selenium in reducing the negative effects of high temperature stress on Chrysanthemum morifolium ramat. J. Sustain. Agric. Sci. doi.org/10.21608/jsas.2020.23905.1203.

276. Seo, Y. R., Sweeney, C. and Smith, M. L. (2002) Selenomethionine induction of dna repair response in human fibroblasts. Oncogene, 21, 3663–3669.

277. Seppänen M, Turakainen M, Hartikainen H (2003) Selenium effects on oxidative stress in potato. Plant Sci 165:311–319.

278. Shaffer, J. P. (1995) . Multiple hypothesis testing. Annual Review of Psychology, 46(1), 561–584.

279. Shamberger, R. J., & Frost, D. V. (1969) . Possible protective effect of selenium against human cancer. Canadian Medical Association Journal, 100(14), 682-687.

280. Shamberger, R.J.; Frost, D.V. Possible protective effect of selenium against human cancer. Can. Med. Assoc. J. 1969, 100, 682.

281. Sharma K, Lee YR (2016) . Effect of different storage temperature on chemical composition of onion (Allium cepa L.) and its enzymes. Journal of Food Science and Technology 53(3):1620-1632.

282. Shedeed. 2020. Stimulation of Growth and Productivity of Onion Plants by Selenium and Growth Active Substances. Middle East Journal of Agriculture Research. Volume: 09 | Issue: 03| Pages: 637-645.

283. Sheetal Gupta and Tamuna Prakash. Study on Indian green leafy vegetables for their antioxidant activity, Plant Food for Human nutrition, March 2009; Volume 64: Issue 1: 39-45.

284. Shibagaki N, Rose A, McDermott JP, et al. 2002. Selenate-resistant mutants of *Arabidopsis thaliana* identify Sultr1; 2, a sulfate transporter required for efficient transport of sulfate into roots. The Plant Journal 29:

285. Shin, E. J., Shin, H. M., Nam, E., Kim, W. S., Kim, J. H., Oh, B. H., et al. (2012) . DeSUMOylating isopeptidase: a second class of SUMO protease. EMBO Rep. 13, 339–346.

286. Shinmachi F, Buchner P, Stroud JL, et al. 2010. Influence of sulfur deficiency on the expression of specific sulfate transporters and the distribution of sulfur, selenium, and molybdenum in wheat. Plant Physiology 153: 327–336.

287. Sies, H. (1993) . Strategies of antioxidant defense. European Journal of Biochemistry, 215(2), 213–219. https://doi.org/ 10.1111 /j.1432-1033. 1993.tb18025.x

288. Sies, H. 2015. “Oxidative Stress: A Concept in Redox Biology and Medicine.” Redox Biology 4: 180-183.

289. Smith FW, Ealing PM, Hawkesford MJ, Clarkson DT (1995) Plant members of a family of sulfate transporters reveal functional subtypes.

290. Smith-Rose RL (1926) Mr. J. L. Baird. Nature 158, 88–89. Taylor EW (1995) Selenium and cellular immunity. Evidence that selenoproteins may be coded in the þ1 reading frame overlapping the human CD4, CD8 and HLA-DR genes. Biol Trace Elem Res 49, 85–95.

291. Sors TG, Ellis DR, Na GN, et al. 2005a. Analysis of sulfur and selenium assimilation in Astragalus plants with varying capacities to accumulate selenium. The Plant Journal 42: 785–797.

292. Sors TG, Ellis DR, Salt DE (2005) Selenium uptake, translocation, assimilation, and metabolic fate in plants. Photosynth Res 86:373–389.

293. Sors TG, Ellis DR, Salt DE. 2005b. Selenium uptake, translocation, assimilation, and metabolic fate in plants. Photosynthesis Research 86: 373–389.

294. Sreelatha, A. et al. Protein AMPylation by an evolutionarily conserved pseudokinase. Cell 175, 809–821 e819 (2018).

295. Stoffaneller, R.; Morse, N.L. A review of dietary selenium intake and selenium status in Europe and the Middle East. Nutrients, 2015, 7(3), 1494-1537.

296. Storey, J. D., & Tibshirani, R. (2003) . Statistical significance for genomewide studies. Proceedings of the National Academy of Sciences, 100(16), 9440–9445.

297. Suh, H. Y., Kim, J. H., Woo, J. S., Ku, B., Shin, E. J., Yun, Y., et al. (2012) . Crystal structure of DeSI-1, a novel deSUMOylase belonging to a putative isopeptidase superfamily. Proteins 80, 2099–2104. doi:

298. Sukumaran, S., & Yu, J. (2014) . Association mapping of genetic resources: Achievements and future perspectives. In R. Tuberosa, A. Graner, & E. Frison (Eds.), Genomics of plant genetic resources (pp. 207– 235). *Dordrecht, Netherlands: Springer*, *978*, -94007-7572-5_9.

299. Surai P.F. Vitamin e in Avian Reproduction. FAO; Rome, Italy: 1999

300. Surai, P.F. Selenium in Nutrition and Health; Nottingham University Press: Nottingham, UK, 2006.

301. Takahashi H, Buchner P, Yoshimoto N, Hawkesford MJ, Shiu S-H. 2012. Evolutionary relationships and functional diversity of plant sulfate transporters. Frontiers in Plant Science 2: 119

302. Takahashi H, Watanabe-Takahashi A, Smith FW, Blake-Kalff M, Hawkesford MJ, Saito K. 2000. The roles of three functional sulphate transporters involved in uptake and

translocation of sulphate in *Arabidopsis thaliana*. Plant Journal 23: 171–182.

303. Takebe, G.; Yarimizu, J.; Saito, Y.; Hayashi, T.; Nakamura, H.; Yodoi, J.; Nagasawa, S.; Takahashi, K. A comparative study on the hydroperoxide and thiol specificity of the glutathione peroxidase family and selenoprotein P. J. Biol. Chem. 2002, 277, 41254–41258.

304. Tallarida RJ," Quantitative methods for assessing drug synergism", Genes Cancer, 2(11):1003-8, 2011.

305. Tallarida, R. J. (2011) . Quantitative methods for assessing drug synergism. Genes & Cancer, 2(11), 1003-1008.

306. Tegeder M. 2012. Transporters for amino acids in plant cells: some functions and many unknowns. Current Opinion in Plant Biology 15: 315– 321.

307. Terry N, Zayed AM, de Souza MP, Tarun AS (2000) Selenium in higher plants. Ann Rev Plant Physiol Plant Mol Biol 51:401–432.

308. Terry N, Zayed AM, de Souza MP, Tarun AS. 2000. Selenium in higher plants. Annual Review of Plant Physiology and Plant Molecular Biology 51: 401–432.

309. Terry, N., et al. (2000) . "Phytoremediation of Selenium-Contaminated Soils and Waters: Fundamentals and Future Prospects." Journal of Environmental Quality, 29(4), 1153-1167.

310. Thomas, C. et al. (2017) . [Title of the study/article]. Journal Name, volume(issue), pages.

311. Thomas, R. (2004) . Practical Guide to ICP-MS: A Tutorial for Beginners. CRC Press.

312. Thomson, C. D. (2004) . Selenium and health: a review. Clinical Nutrition, 23(3), 473-486.

313. Tinggi, U., 2003. Essentiality and toxicity of selenium and its status in Australia: a review. Toxicol. Lett. 137, 193 – 110.

314. Toppo, S.; Flohe, L.; Ursini, F.; Vanin, S.; Maiorino, M. Catalytic mechanisms, and specificities of glutathione peroxidases: Variations of a basic scheme. Biochim. Biophys. Acta 2009, 1790, 1486–1500.

315. Valko M, Rhodes CJ, Moncol J, Izakovic M, et al. Free radicals, metals and antioxidants in oxidative stress – induced cancer. Mini – review. Chem. Biol. Interact. 2006; 160: 1 – 40.

316. Van Hoewyk D, Abdel-Ghany SE, Cohu C, Herbert S, Kugrens P,

317. Van Hoewyk D, Garifullina GF, Ackley AR, Abdel-Ghany SE, Marcus MA, Fakra S, Ishiyama K, Inoue E, Pilon M, Takahashi H, Pilon-Smits EAH (2005) Overexpression of atcpnifs enhances selenium tolerance and accumulation in *arabidopsis*. Plant Physiol 139:1518–1528. 234. Van Hoewyk D, Garifullina GF, Ackley AR, et al. 2005. Overexpression of AtCpNifS enhances selenium tolerance and accumulation in *Arabidopsis*. Plant Physiology 139: 1518–1528. 235. Van Hoewyk D, Garifullina GF, Ackley AR, et al. 2005. Overexpression of AtCpNifS enhances selenium tolerance and accumulation in *Arabidopsis*. Plant Physiology 139: 1518–1528.

318. Van Huysen T, Terry N, Pilon-Smits EAH. 2004. Exploring the selenium phytoremediation potential of transgenic *Brassica* juncea overexpressing ATP sulfurylase or cystathionine-c-synthase. International Journal of Phytoremediation 6: 111–118.

319. Vinceti, M.; Filippini, T.; Del Giovane, C.; Dennert, G.; Zwahlen, M.; Brinkman, M.; Zeegers, M.P.; Horneber, M.; D'Amico, R.; Crespi, C.M. Selenium for preventing cancer. Cochrane Database Syst. Rev. 2018, 1, Cd005195.

320. W. Jacobs(ed). Selenium in agriculture and the environment. Amer. Soc. Agron – Soil Sci. Soc. Amer., Madison, Wis.

321. WILKINSON, S.R., WELCH, R.M., MAYLAND, H.F., GRUNES,

322. Wang, J., Cappa, J. J., Harris, J. P., Edger, P. P., Zhou, W., Pires, J. C., et al. (2018) . Transcriptome-wide comparison of selenium hyperaccumulator and non-accumulator Stanleya species provides new insight into key processes mediating the hyperaccumulation syndrome.

323. Washington, DC, USA, 2000; p. 528.

324. Waters D. J., Shen S., Glickman L. T., Cooley D. M., Bostwick D. G.,

325. Watts DL. The nutritional relationships of selenium. J Orthomol Med. 1994; 9:111–117.

326. Whanger, P.D. Selenium, and its relationship to cancer: an update. Br. J. Nutr. 2004, 91, 11-28.

327. White PJ, Bowen HC, Parmaguru P, et al. 2004. Interactions between selenium and sulphur nutrition in *Arabidopsis thaliana*. Journal of Experimental Botany 55: 1927–1937.

328. White PJ, Broadley MR, Bowen HC, Johnson SE. 2007b. Selenium and its relationship with sufur. In: MJ Hawkesford, LJ de Kok, eds. Sulfur in plants – an ecological perspective. Dordrecht: Springer, 225–252.

329. White PJ, Broadley MR. 2009. Biofortification of crops with seven mineral elements often lacking in human diets – iron, zinc, copper, calcium, magnesium, selenium and iodine. New Phytologist 182: 49–8. 246. White, F.J. Selenium accumulation by plants. Annals of Botany, 2016, 117 (2), 217–235;

330. White Philip J. 2016. Selenium accumulation by plants. Annals of botany 117: 217 – 235.

331. White, P. J. (2018) . Selenium metabolism in plant. Biochim. Biophys.

332. White, P. J., & Broadley, M. R. (2009) . Biofortification of crops with selenium. Agriculture, 2(3), 1-15.

333. White, P. J., et al. (2004) . "Selenium biofortification of wheat: A promising approach to improving selenium intake." Journal of the Science of Food and Agriculture, 84(7), 850-856.

334. White, P.J., & Broadley, M.R. (2009) . "Biofortification of Crops with Seven Mineral Elements Often Lacking in Human Diets – Iron, Zinc, Copper, Calcium, Magnesium, Selenium, and Iodine." New Phytologist, 182(1), 49-84.

335. Wilson LG, Bandurski RS (1958) . Enzymatic reactions involving sulfate, sulfite, selenate and molybdate. J Biol Chem 233:975–981.

336. Winkel, L. H. E., Vriens, B., Jones, G. D., Schneider, L. S., PilonSmits, E., and Bañuelos, G. S. (2015) . Selenium cycling across soil-plantatmosphere interfaces: a critical review. Nutrients 7, 4199–4239. doi:

337. Xime´nez-Embu´n P, Alonso I, Madrid-Albarran Y, Camara C. 2004. Establishment of selenium uptake and species distribution in lupine, Indian mustard, and sunflower plants. Journal of Agricultural and Food Chemistry 52: 832–838.

338. Xinbin Zhou1, Jing Yang1 , Herbert J. Kronzucker2 and Weiming Shi3. Selenium Biofortification and Interaction with Other Elements in Plants: A Review. 2020. Frontiers in Plant Science 11. DOI:

339. Yang, J., Lee, S. H., Goddard, M. E., & Visscher, P. M. (2011) . GCTA: A tool for genome-wide complex trait analysis. American Journal of Human Genetics, 88(1), 76–82.

340. Yoshida, T., et al. (2014) . "Biofortification of rice with iron through genetic modification." Rice Science, 21(2), 94-102.

341. Yu D, Kahen E, Cubitt C, McGuire J, Kreahling J, Lee J, Altiok S, et al.” Identification of Synergistic, Clinically Achievable, Combination Therapies for Osteosarcoma”, Scientific Reports 5:16991, 2015

342. Yu, C., Liu, S. L., Qin, X., & He, X. (2015) . Dose-response analysis of anti-cancer drugs and combination drugs. Bioinformatics, 31(1), 18-21.

343. Yu-chin Chen, K.sandeep Prabhu, Andrea M.Mastro. Is Selenium a Potential Treatment for Cancer? 2013. Nutriants. 5 (4), 1149 – 1168.

344. Zayed A, Lytle CM, Terry N (1998) Accumulation and volatilization of different chemical species of selenium by plants. Planta 206, 284-292.

345. Zeng Huawei. Selenium as an Essential Micronutrient: Role in Cell Cycle and Apoptosis. Molecules 2009, 14, 1263-1278; doi:

346. Zeng, H.; Combs, G.F., Jr. Selenium as an anticancer nutrient: roles in cell proliferation and tumor cell invasion. J. Nutr. Biochem. 2008, 19, 1-7.

347. Zhang L, Hu B, Li W, et al. 2014. OsPT2, a phosphate transporter, is involved in the active uptake of selenite in rice. New Phytologist 201: 1183–119.

348. Zhang L-H, Abdel-Ghany SE, Freeman JL, Ackley AR, Schiavon M, PilonSmits EAH. 2006a. Investigation of selenium tolerance mechanisms in *Arabidopsis thaliana*. Physiologia Plantarum 128: 212–223.

349. Zhang, H., et al. (2021) . "Iron biofortification of rice: Advances and challenges." Plant Science, 308, 110946.

350. Zhang, J., W. Wang, L. Zhang, and L. Zhang. 2016. “Selenium and Cancer Prevention: A Comprehensive Review.” Current Opinion in Clinical Nutrition and Metabolic Care 19 (4): 318-324.

351. Zhao XQ, Mitani N, Yamaji N, Shen RF, Ma JF. 2010. Involvement of silicon influx transporter OsNIP2; 1 in selenite uptake in rice. Plant Physiology 153: 1871–1877.

352. Zhao, J.; Sauvage, C.; Zhao, J.; Bitton, F.; Bauchet, G.; Liu, D.; Huang, S.; Tieman, D.M.; Klee, H.J.; Causse, M. Meta-analysis of genome-wide association studies provides insights into genetic control of tomato flavor. Nat. Commun. 2019, 10, 1534.

353. Zhoue Xinbin, Yang Jing, Kronzucker Herbert J. and Shi Weiming. 2020. Selenium Biofortification and Interaction

with Other Elements in Plants: A Review. Frontiers in Plant Science: 2020.586421.

354. Zhu, C., Gore, M. A., Buckler, E. S., & Yu, J. (2008) . Status and prospects of association mapping in plants. The Plant Genome, 1, 5– 20.

Appendices

Appendix 1

Table 1: A summary of the fundamental functions of the elements.

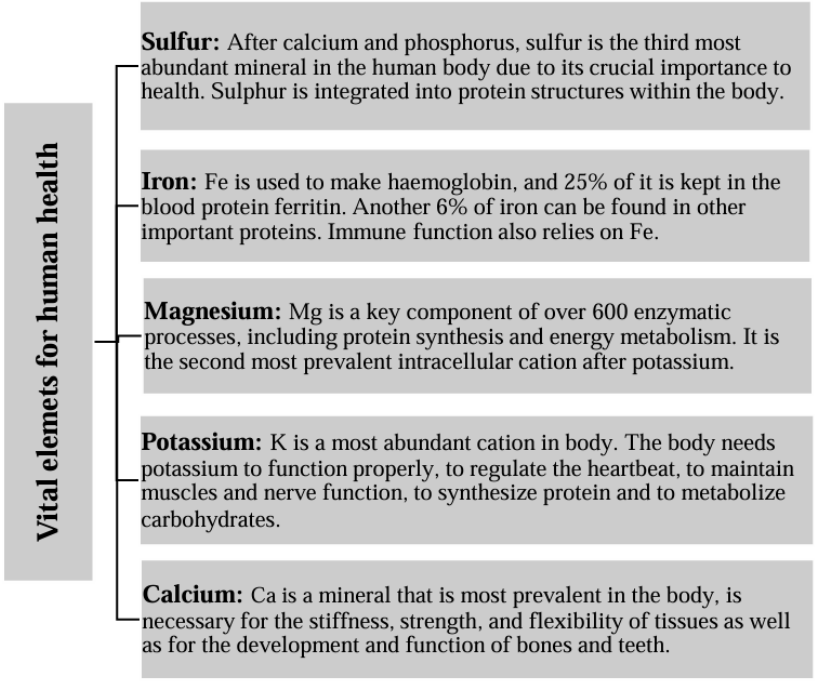

Appendix 2

Table 2: SNPs candidate targets for selenium accumulation in *Brassica napus* and *Arabidopsis thaliana.*

Candid marker	FDR_Adjusted_P-values	log10P	LDdecay(KB)	Loc	Chr	Marker function	Lead marker	TAIR_id	TAIR_description	Surrounding marker genes	Function
[illegible]	[illegible]	[illegible]	[illegible]	[illegible]	[illegible]	[illegible] ISOPROPYLMALATE ISOMERASE LARGE SUBUNIT 1; 4 iron, 4 sulfur cluster binding / hydro-lyase / lyase.	[illegible]	[illegible]	isopropyl malate isomerase large subunit 1		
[illegible]	[illegible]	[illegible]	[illegible]	[illegible]	C08	The function of absorbing and responding to electromagnetic radiation with a wavelength of approximately 400-700 nm.	[illegible]	[illegible]	cryptochrome 2	[illegible]	Oxidoreductase activity
[illegible]	[illegible]	[illegible]	[illegible]	[illegible]	C09	Nucleotide binding, Catalytic activity, Hydrolase activity, Bis (5'-adenosyl)-triphosphatase activity.	[illegible]	[illegible]	FRAGILE HISTIDINE TRIAD	[illegible]	Histone-binding protein MSI 1-like
[illegible]	[illegible]	[illegible]	[illegible]	[illegible]	[illegible]	Deamidating isopeptidase.	[illegible]	[illegible]	PPPDE putative thiol peptidase family protein	[illegible]	Transport protein Sec24-like [illegible] function: Sec23/Sec24 protein transport family protein [illegible]
[illegible]	[illegible]	[illegible]	[illegible]	[illegible]	C01	Mediator-associated protein 1-like.	[illegible]	[illegible]	DNA-binding storekeeper protein-related transcriptional.	[illegible]	Putative glycerol-3-phosphate transporter 2
[illegible]	[illegible]	[illegible]	[illegible]	[illegible]	C03	Uncharacterized Protein.	[illegible]	[illegible]	Tubulin alpha-6 chain.		
[illegible]	[illegible]	[illegible]	[illegible]	[illegible]	C03	Uncharacterized Protein.	[illegible]	[illegible]	Tubulin alpha-6 chain.		
[illegible]	[illegible]	[illegible]	[illegible]	[illegible]	C03	Inactive GDSL esterase/lipase-like protein 25	[illegible]	[illegible]	GDSL-like Lipase/Acylhydrolase superfamily protein		
[illegible]	[illegible]	[illegible]	[illegible]	[illegible]	C03	Inactive GDSL esterase/lipase-like protein 25	[illegible]	[illegible]	GDSL-like Lipase/Acylhydrolase superfamily protein		
[illegible]	[illegible]	[illegible]	[illegible]	[illegible]	C05	Magnesium ion binding, inorganic diphosphatase activity, hydrolase activity metal ion binding.	[illegible]	[illegible]	pyrophosphorylase 1	[illegible]	Endonuclease homolog 1, transcript variant X1
[illegible]	[illegible]	[illegible]	[illegible]	[illegible]	C05	Nucleic acid binding, RNA binding.	[illegible]	[illegible]	RNA-binding (RRM/RBD/RNP motifs) family protein		
[illegible]	[illegible]	[illegible]	[illegible]	[illegible]	C06	???	[illegible]	[illegible]	TIFY domain/Divergent CCT motif family protein		
[illegible]	[illegible]	[illegible]	[illegible]	[illegible]	C01	Protein KAKU4, transcript variant X2.	[illegible]	[illegible]	Flocculation protein.	[illegible]	Zinc finger protein 62
[illegible]	[illegible]	[illegible]	[illegible]	[illegible]	[illegible]	Uncharacterized Protein.	[illegible]	[illegible]	Transmembrane protein.	[illegible]	Cell wall / vacuolar inhibitor of fructosidase 1-like
[illegible]	[illegible]	[illegible]	[illegible]	[illegible]	A10	Mediator RNA polymerase II transcription subunit 33e, ATP binding.	[illegible]	[illegible]	heat shock cognate protein 70-1	[illegible]	Transcription factor-like protein DPA
[illegible]	[illegible]	[illegible]	[illegible]	[illegible]	C04	F-box protein	[illegible]	[illegible]	F-box family protein		

Appendix 3

Table 3: The GEMs candidate genes markers for selenium accumulation in *Brassica napus* and *Arabidopsis thaliana*.

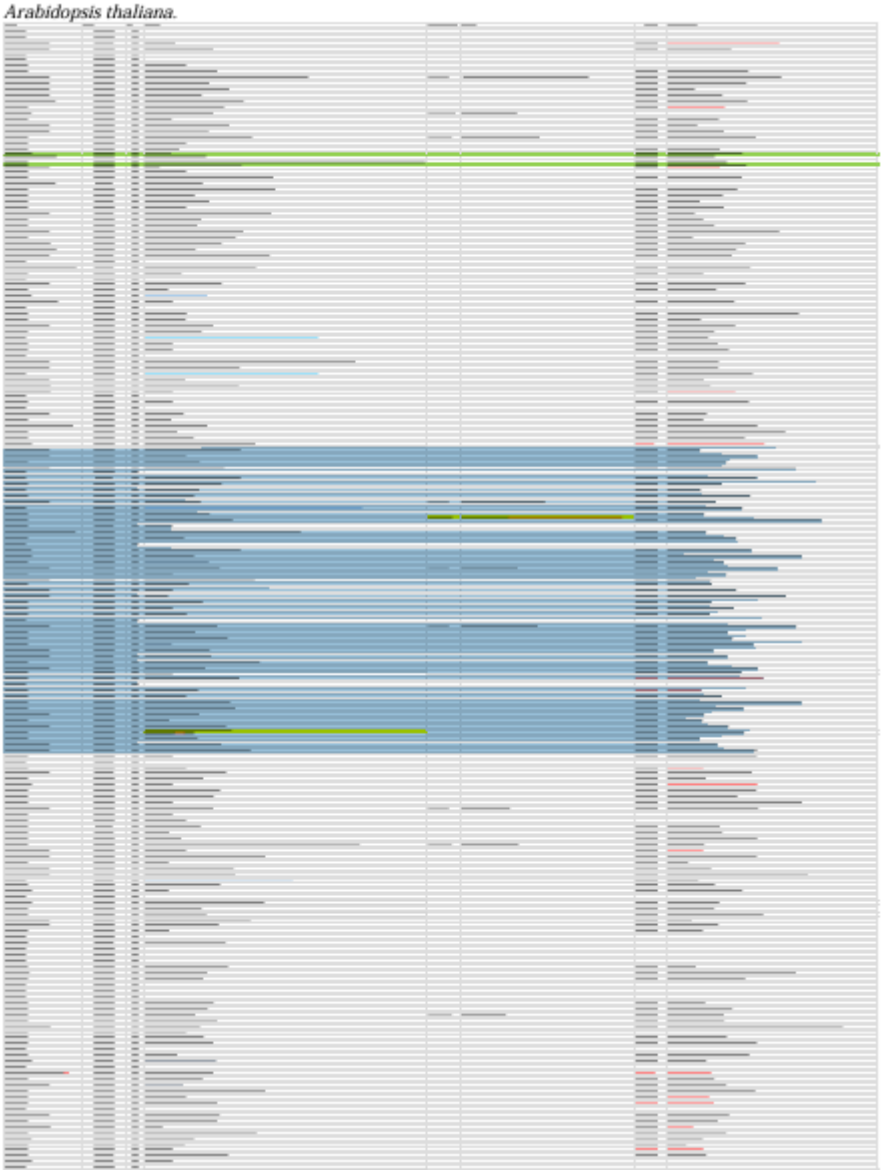

Index